KU Leuven
Biomedical Sciences Group
Faculty of Medicine
Department of Development and Regeneration

&

University of Porto
Faculty of Engeneering of the University of Porto

IN VIVO MODELS AND *IN SILICO* SIMULATIONS OF MESH AUGMENTED PROLAPSE REPAIR

Rita RYNKEVIC

Promoter: Prof. Jan Deprest
Promoter: Prof. Antonio Augusto Fernandes
Co-promoter: Dr. Nele Famaey
Co-promoter: Dr. Pedro Alexandre Lopes de Sousa Martins
Co-promoter: Dr. Marco Paulo Lages Parente
Chair: Prof. Sophie Debrock
Secretary: Prof. Frank Van der Aa
Jury members: Prof. Frank Van der Aa
Prof. Hans Van Oosterwyck
Prof. Renato Natal Jorge
Prof. Julius Griškevičius
Prof. Ladislav Krofta
Dr. Baptiste Pierrat

Dissertation presented in partial fulfilment of the requirements for the degree of Doctor in Biomedical Sciences and for the degree of Doctor in Occupational Safety and Health

June, 2019

This thesis was submitted as partial fulfillment of the requirements for the degrees to be awarded by the two institutions:

By the KU Leuven: “Doctor of biomedical science”
By the University of Porto: “Doctor in Occupational Safety and Health”

ISBN: 9789082637670

The picture on the cover represents 3D model of the sheep pelvis, reconstructed from magnetic resonance images. Cover designed by Rita Rynkevic

Identification: RYNKEVIC, Rita, *In vivo* models and *in silico* simulations of mesh augmented prolapse repair, Leuven, Belgium, 2019, 227 pages, doctoral thesis, KU Leuven, Biomedical Sciences, Department of development and regeneration and University of Porto, Faculty of Engineering of the University of Porto, promoter Prof. Jan Deprest MD and Prof. Antonio Augusto Fernandes.

Keywords: meshes, animal models, sheep, soft tissues, biomechanics

In Leuven, 27.06.2019 Rita Rynkevic

PDF version could be downloaded:

TABLE OF CONTENTS

LIST OF ABBREVIATIONS 6
CHAPTER 1 8
INTRODUCTION 8
SPECIFIC STUDY AIMS AND HYPOTESIS 20
CHAPTER 2 26
IN VITRO STUDY OF THE MECHANICAL PERFORMANCE OF HERNIA MESH UNDER CYCLIC LOADING 26
CHAPTER 3 38
IN VITRO SIMULATION OF *IN VIVO* DEGRADATION AND CYCLIC LOADING OF NOVEL DEGRADABLE ELECTROSPUN MESHES FOR PROLAPSE REPAIR 38
CHAPTER 4 58
ASSESSMENT OF ELECTROSPUN AND ULTRA-LIGHT-WEIGHT POLYPROPYLENE MESHES IN THE SHEEP MODEL FOR VAGINAL SURGERY 58
CHAPTER 5 80
BIOMECHANICAL AND MORPHOLOGICAL PROPERTIES OF THE MULTIPAROUS OVINE VAGINA AND EFFECT OF SUBSEQUENT PREGNANCY 80
CHAPTER 6 96
THE EFFECT OF CONSECUTIVE PREGNANCIES ON THE OVINE PELVIC SOFT TISSUES: LINK BETWEEN BIOMECHANICAL AND HISTOLOGICAL COMPONENTS 96
CHAPTER 7 110
LINKING HYPERELASTIC THEORETICAL MODELS AND EXPERIMENTAL DATA OF VAGINAL TISSUE THROUGH HISTOLOGICAL DATA 110
CHAPTER 8 128
HISTOLOGICALLY-DRIVEN SIMULATIONS OF VAGINAL TISSUE: APPLICATION TO BALL BURST TESTING 128
CHAPTER 9 142
CREATION OF AN OVINE PELVIC FLOOR THREE-DIMENSIONAL 142
MODEL USING MAGNETIC RESONANCE 142
CHAPTER 10 150
GENERAL DISCUSSION 150
FUTURE PERSPECTIVES 156
SUPPLEMENTARY MATERIAL 1 162
PHYSIOLOGIC MUSCULOFASCIAL COMPLIANCE FOLLOWING REINFORCEMENT WITH ELECTROSPUN POLYCAPROLACTONE-UREIDOPYRIMIDINONE MESH IN A RAT MODEL 162
SUPPLEMENTARY MATERIAL 2 184
EXPERIMENTAL RECONSTRUCTION OF AN ABDOMINAL WALL DEFECT WITH ELECTROSPUN POLYCAPROLACTONE UREIDOPYRIMIDINONE MESH CONSERVES COMPLIANCE YET MAY HAVE INSUFFICIENT STRENGTH 184
CHAPTER 11 206
SUMMARY 206
SAMENVATTING 210

RESUMO 214
CURRICULUM VITAE 218
THESIS RELATED PUBLICATION ACTIVITY 220
PERSONAL ACKNOWLEDGEMENT 224
PERSONAL CONTRIBUTION AND CONFLICT OF INTEREST 226

LIST OF ABBREVIATIONS

3D	three-dimensional
α-SMA	smooth muscle actin α
ACM	acellular collagen matrix
ANOVA	analysis of variance
BIP-UPY	Bioactive Implantable Polymers based on Ureido-Pyrimidinone
BMI	body mass index
CD	cluster of differentiation
EAS	external anal sphincter
ECM	extracellular matrix
EDA	epidural analgesia
FBGC	foreign body giant cells
FDA	food and drug administration
FEM	finite element method
FEA	finite element analysis
GA	genetic algorithms
GPC	gel permeation chromatography
GRCs	graft related complications
H&E	hematoxylin & eosin
HGO	Holzapfel-Gasser-Ogden
HM	Histologically-Motivated
i.e	id est
IRC	Implant Related Complications
ICS	international continence society
IUGA	international urogynecological association
KHP	Potassium Hydrogen Phthalate
LAM	levator ani muscle
M1	macrophage type 1
M2	macrophage type 2
Mn	the number average molecular weight
mN	milinewton
MPa	megapascal
MR	magnetic resonance
Mw	the weight average molecular weight
N	Newton
NTR	native tissue repair
PBS	Phosphate Buffer Saline
PC	polycarbonate
PCL	polycaprolactone
PCR	polymerase chain reaction
PFD	pelvic floor disorders
POP	pelvic organ prolapse
PP	polypropylene
PU	polyurethane
PVDF	polyvinylidenefluoride
SCENIHR	Scientific Committee on Emerging and Newly Identified Health Risks
SEF	Strain-energy function
±SEM	±standard error of the mean

SEM	scanning electron microscope
SGA	simple genetic algorithm
SMC	smooth muscle cells
SUI	stress urinary incontinence
TF	thicker fiber
TM	thicker mesh
UI	urinary incontinence
UPy	Ureido-pyrimidinone
UPy-PC	Ureidopyrimidinone- Polycarbonate
UPY-PCL	Ureidopyrimidinone-Polycaprolactone

CHAPTER 1

INTRODUCTION

1. Pelvic organ prolapse

Pelvic organ prolapse (POP) is a common condition that can have a substantial negative impact on a woman's quality of life. POP occurs when the tissue and muscles of the pelvic floor no longer support the pelvic organs adequately, resulting in the protrusion (prolapse) of the pelvic organs from their normal position [1] (Fig. 1). Many women are asymptomatic or feel minimal disturbance, 12% of women diagnosed with pelvic floor dysfunction (PFD) have to cope with physical and emotional distress [2]. The close anatomical relationship between the vaginal wall, bladder and rectum often contribute to the emergence of dysfunctions in the adjacent organs, mainly including urinary incontinence (UI), anal incontinence yet also defection problems, and dyspareunia, which in the most severe cases will require medical or surgical treatment [3]. For instance, the overall lifetime risk for primary surgery for UI or POP today is 20% by the age of 80 years. In 2005, the number (rate) of admissions for POP surgery in Germany, France and England was 102,492 (1.05 per 1000 women) with a substantial cost (308,335,289 euro) [4].

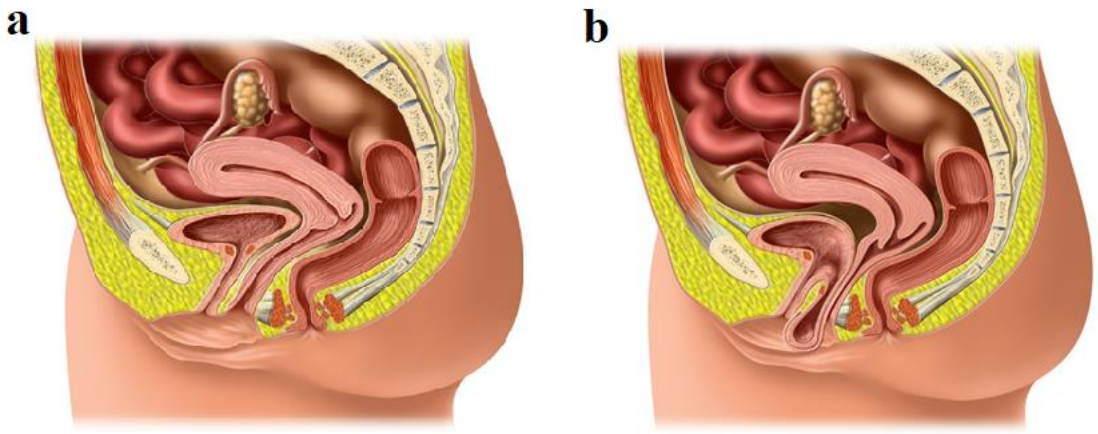

Fig. 1 Female pelvic floor, **a**- normal pelvic floor, **b**- cystocele. Reproduced with permission from the UZ Leuven; drawing made by Dream Team, Leuven, Belgium.

DeLancey graphically summarized the likely causal factors in a "life-span model" [5] (Fig. 2). Rarely there are some genetic problems that predispose to early presentation or more severe forms of prolapse, e.g. due to problems in the connective tissue – like Marfan syndrome, to name only one example. The next important factors are pregnancy and delivery. During pregnancy, the vaginal wall and pelvic floor organs adapt to the imminent delivery. The largest contributor of both is vaginal delivery [6]. It causes direct trauma to the pelvic floor, as recently reviewed by Callewaert et al [7]. Epidemiologic

studies show that many women fail to recover completely from this event [8]. The number of vaginal deliveries has an impact on the later occurrence of UI and more so on POP [9] [10]. Later in life, age and menopause may add to the onset or exacerbation of PFD, and additional interfering pathologies may contribute as well.

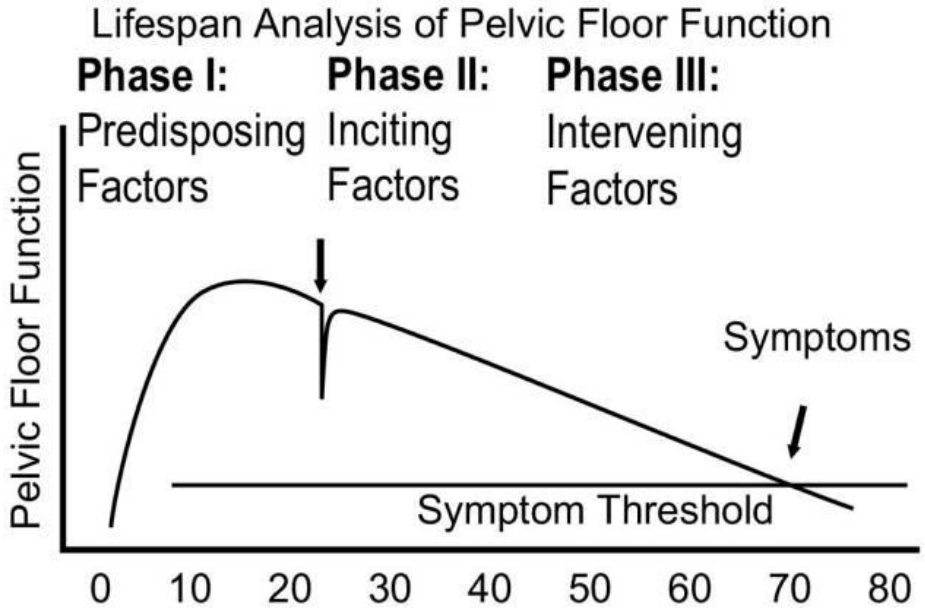

Fig. 2 Integrated life span analysis of pelvic floor function [5]. Reproduced with permission from Elsevier.

The treatment of POP is complex because of the complexity of the disorder itself. Overall one can start with lifestyle recommendations (weight loss, avoiding heavy lifting or coughing and physiotherapy), yet nor the therapeutic neither its preventive effect of have been properly studied. Another conservative option is the use of a pessary, which provides mechanical support to the descending pelvic organs [11]. The mainstay of therapy for the POP remains however surgical correction [12].

2. Surgical treatment of POP and implants

The overall lifetime risk for primary surgery for PFD including POP and stress urinary incontinence (SUI) is 20% by the age of 80 years [13]. There is a multitude of surgeries for pelvic floor repair.

They can be primarily divided based on the approach, i.e. vaginal or abdominal (either by open abdomen or by laparoscopy) repair (Fig. 3). Repairs can also be divided in the way the defects are repaired, using either native tissue or in case of the use of mesh, whether these are used to reinforce or substitute the support (Fig. 4). There are also more palliative or obliterative procedures such as colpocleisis and colpectomy.

However, surgery has a relatively high failure rate, either presenting as recurrence or the development of PFD in other compartments [14]. This can be addressed by a new operation, which may then make use of a surgically inserted implant or prosthesis [15]. A prosthesis is a fabricated substitute to assist a damaged body part or to augment or stabilize a hypoplastic structure. A mesh is a specific type of prosthesis, network fabric

or structure with open spaces or interstices between the strands of the net. It is typically made of synthetic materials. If any tissue or organ is used instead of synthetic material, this implant is then called graft, all this nomenclature according to the standardization committee of International Urogynecological Association (IUGA) and International Continence Society (ICS) [15]. Hernia surgeons use the term mesh and implant interchangeably [16].

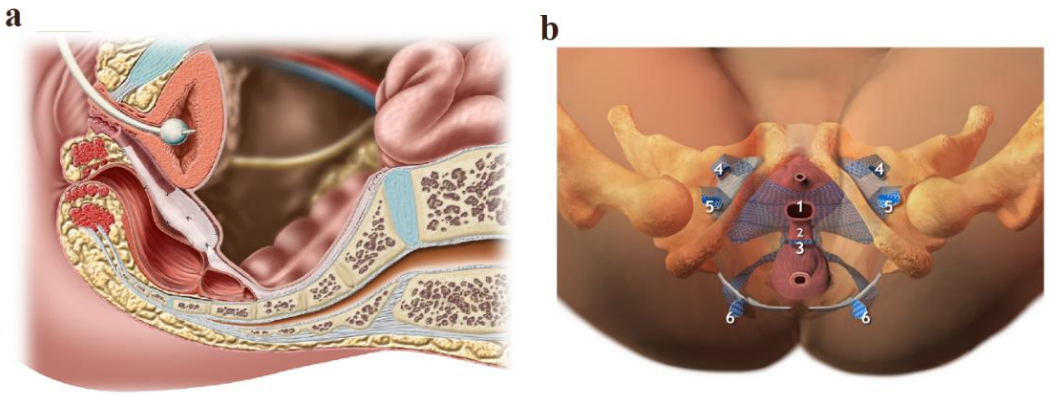

Fig. 3 Surgical treatment of the POP using implants: **a**- by laparoscopy (sacrocolpopexy), **b**- vaginal (mesh reinforcement). Reproduced with permission from UZ Leuven; drawing Dream Team, Leuven, Belgium.

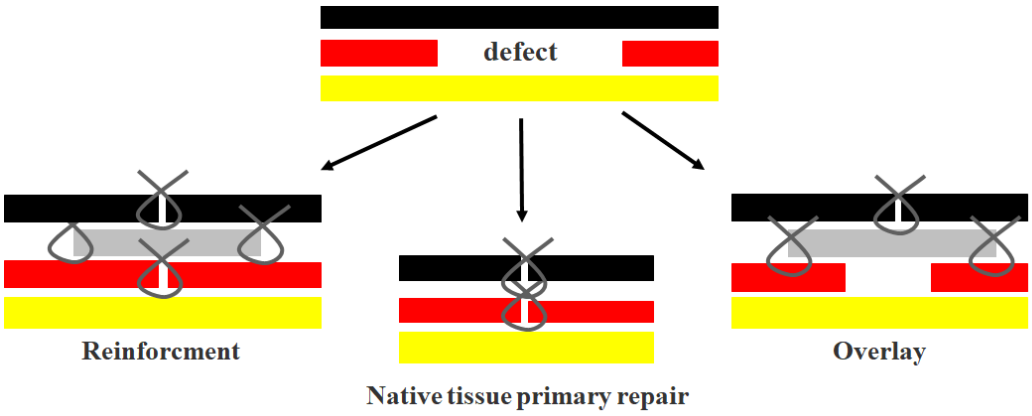

Fig. 4 Schematic drawing of surgical repair techniques; black- skin, red-muscle tissue, yellow- organs, gray- mesh implant.

The first implant type that became popular in the treatment of PFD, were the so-called sub-urethral slings, which are small devices made with synthetic tapes, for the treatment of urinary incontinence. Larger devices are used to treat prolapse (Fig. 3). Almost all synthetic meshes are currently manufactured from four main polymers: polypropylene (PP), polyethylene terephthalate (PET), polytetrafluoroethylene (PTFE), and polyvinylidenefluoride (PVDF). Surgical meshes can be designed as mono- or multifilament. Meshes with monofilament yarns are stiffer; while multifilament are softer, however they have a higher contact surface area and they form by definition very

small pores between the individual fibers [17]. Most surgical meshes are knitted, consisting of continuous filaments, wrapped around other threads in the loop. Due to the production method, implants can have very different mechanical properties in the longitudinal and transverse directions [18].

There is a number of classifications that cover the meshes previously and currently used. The eldest classification is the one by Amid, based on porosity, which was pointing to the concept of how the host interacts with the mesh, mainly in terms of tissue ingrowth and the ability of host defense cells to infiltrate into the pores [19]. Later on another classification was suggested by Coda which is based on weight [20]. Very recently Klinge and Klosterhalfen proposed a classification they described as being "clinically relevant" and covering the wide spectrum of the implants available on the market (Table 1) [21]. There is currently no consensus on what classification is to be used.

Table1. Classification of surgical meshes for hernia repair by Klinge and Klosterhalfen [21]

C/ Classification by Klinge		**Sub-division or characterization**	**Example of mesh**
Class I:	Large pore meshes (characterized by a textile porosity of >60% or an effective porosity of >0%)	Ia) Monofilament Ib) Multifilament Ic) Mixed structure or polymer (e.g. absorbable + non- absorbable, or different non-absorbable)	Vypro Ultrapro Ti-mesh Mersilene
Class II:	Small pore meshes (characterized by a textile porosity of <60% and without any effective porosity)	Ia) Monofilament IIb) Multifilament IIc) Mixed structure or polymer.	Marlex Prolene Atrium Surgipro
Class III:	Meshes with special features	Porous meshes with special features, e.g. to prevent adhesions	Sepramesh
Class IV:	Meshes with films	Film-like meshes without porosity, submicronic pore size or secondarily excised pores	ePTFE
Class V:	3D meshes	Pre-shaped, pre-formed, or 3D devices	Electrospun (PCL, PU)
Class VI:	Biologicals	VIa) Non-cross-linked VIb) Cross-linked VIc) Special features	Surgisis
All implant materials above can be absorbable or non-absorbable			

Over the past decade, a huge number of new implants and ancillary devices have been introduced to the market, but their wide adoption has not been substantiated by robust preclinical data. At least 10% of local complications occur, which may be due to insufficient biocompatibility and inappropriate biomechanical properties of the implants, next to patient and surgeon factors [22]. These so-called graft-related complications (GRCs) are related to a variety of factors, including foreign body reaction, mesh shrinkage (called contraction), infection and pain, vaginal mesh exposure or migration into adjacent structures (called erosion), etc. [23]. After implantation, the mesh becomes part of the muscle-fascial complex. Besides covering the defect, it should function together with the

muscles and fascia. Therefore, the complications arising after implantation may have a mechanical origin. Complications can be linked with the mismatch of the mechanical properties of the mesh and the acting loads [24].

3. Novel implant strategies

One of the strategies to avoid or reduce GRCs, is the use of biodegradable scaffolds with biomechanical properties close to that of the host tissue yet with a structure that promotes tissue ingrowth. Electrospinning technology enables the production of ultrafine fibers, assembled as a non-woven matrix-like structure, which can physically mimic the structure of the natural extracellular matrix of most connective tissues (Fig. 5) [25].

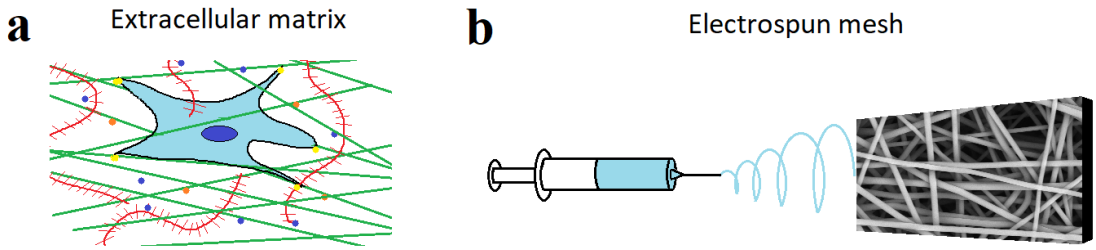

Fig. 5 Figurative depiction: **a**- natural extracellular matrix, **b**- electrospinning technology.

Such scaffolds have already been successfully used for tissue engineering [26]. We were involved in a European project, that aimed to explore this avenue. Bioactive Implantable Polymers based on Ureido-Pyrimidinone (BIP-UPy) is a project sponsored by the European Commission in its 7th framework programme (NMP3-LA-2012-310389). As part of its activities (2014-2017), the BIP-UPy consortium developed a pelvic floor implant, which has the potential that it can be complemented with certain bioactivity properties, to improve outcome or reduce GRCs. The polymers were obtained from SupraPolix BV (Eindhoven, The Netherlands) and spun by Coloplast (Humlebæk, Denmark). *In vitro* testing was performed by the Technical University of Lodz and University of Porto. KU Leuven was involved in the *in vivo* and *ex vivo* testing, which were done in several animal models, as will be described herein.

The self-complementary hydrogen bonding ureido-pyrimidinone (UPy) motif is widely used in the design of supramolecular polymers because of its high dimerization constant. Supramolecular polymers are characterized by the formation of arrays of directed, noncovalent interactions between the building blocks, using the self-assembling hydrogen bonding 2- ureido-[1H]-pyrimidin-4-one (UPy) [27]. Mechanical behavior and resorption rate are critical for the success of degradable implants. These properties can be modified by combining or changing ratios of the building blocks with existing degradable polymer blocks [28]. UPy-modified polymers have been used earlier as drug delivery vehicles, e.g. in a porcine myocardial infarction model [29] and in a modular approach as a bioactive elastomeric material for tissue engineering [30].

As a backbone, was used polycaprolactone (PCL). PCL is biocompatible and biodegradable, is easy to process and transform by electrospinning into filaments and fabrication of textile structures. PCL is compatible with a wide range of other polymers.

The Food and Drug Administration (FDA) approved PCL for use in humans [23-24]. It has already been used to guide regeneration of bone and vessels [25-26]. *Ex vivo* PCL has adequate biomechanical strength [31] and it induces a minimal foreign body response [32]. When UPy is bound to PCL, UPy impacts it's in vitro degradation. UPy-PCL degrades mainly via an oxidative pathway when compared to PCL alone. PCL is sensitive to enzymatic and hydrolytic degradation [33].

An alternative approach was used with *non-degradable* polyurethane (PU), which withstands *in vitro* repetitive strain better than heavier weight polypropylene (PP) (Gynecare^{TM}, Johnson & Johnson, weight: 96.6g/m^2 as in TVT) [34]. PUs have been extensively investigated in both hard and soft tissue engineering, in the form of injectable hydrogels or implantable devices (prefabricated scaffolds). In hard tissue engineering, PU-based constructs have been designed with the optimal flexibility and load bearing properties for orthopedic applications. Similarly, in soft tissue engineering, PU-based constructs with proper mechanical and structural properties have found wide application in the repair and regeneration of cardiac tissue, blood vessels, peripheral nerves and skin [35].

In later experiments, we used polycarbonate (PC) instead of PCL. PC is a degradable polyester, which has been successfully used in nerve and bone regeneration guidance [36]. It was modified by UPy-motifs for bioactivity.

4. Experimental mechanics

As a first step into the pipeline to clinical assessment [37] the material properties are obtained via mechanical testing. Mechanical testing may simulate the working performance, the behavior and the clinically relevant failure modes of implants. These should be the first steps before *in vivo* testing.

To characterize and enable the comparison of the wide range of implants and ancillary devices used in pelvic floor surgery, tensile testing is generally acknowledged, as the main method to study the behavior of the material [37]. Tensile properties are frequently included in material specifications to ensure quality. Finally, tensile properties are often used to predict the behavior of a material under more complex loading conditions.

Mesh stiffness describes the implant deformation in the elastic domain, where the deformed mesh recovers its original dimensions when the load is removed. These properties might be assessed using uniaxial tensile testing [34-37] (Fig. 6**a**).

Cyclic tests are performed to mimic the effects of repetitive loading, similar to expected *in vivo* loads. Mesh elastic and plastic deformations could be achieved using cyclic loading methods [37-36]. A temporary object shape change that returns to its original shape after the force is removed, is called *elastic deformation*. *Plastic deformations* are permanent changes in the object dimensions without fracture, resulting from the application of sustained stress beyond the elastic limit. The ball burst testing method has been used to characterize the multi-axial material properties [37] (Fig. 6**b**). This test simulates the *in vivo* loading conditions of mesh implants under multi-axial physiological loads [38-39]. Another setting is bi-axial biomechanical testing, which was not used in this thesis.

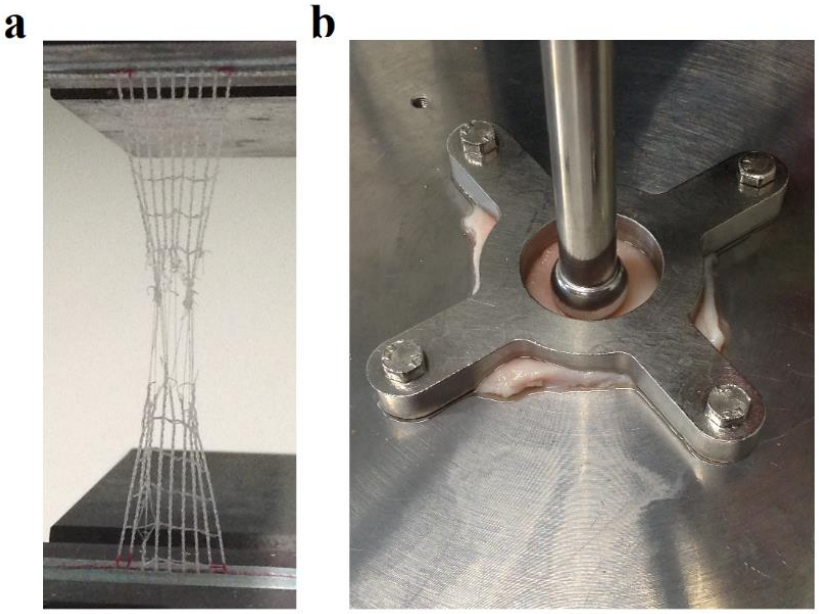

Fig. 6 Mechanical tests: **a-** uniaxial tensile test (mesh specimen), **b-** ball burst test (tissue specimen)

Experimental animal studies play an important role in a better understanding of the host response to implants and may help anticipate failure or local adverse effects. However, controlled *in vitro* degradation testing is used to complement animal trials, that study the host response to the material, design, and fabrication factors that affect *in vivo* implant ingrowth [38]. After implantation the mesh becomes part of the muscle-fascial complex and performs the tissues' mechanical functions [39]. However, the biodegradation processes could lead to premature loss of functional properties of the implant, or the surrounding tissues.

In vitro testing could be a first step towards the validation of new implants and solutions and seems to be a sensible approach to the latter, in the development cycle-animal experimentation. Proper material testing, both in dry conditions as well as after experimental implantation play an important role in that process. This may eventually reduce the number of animal experiments. *Ex vivo* testing of the explants and biomechanical assessment of pelvic floor structures and their functional role can improve the understanding of the pathogenesis of POP. It may also provide relevant information for surgical reconstructions. However, the properties of implants change after incorporation into the host. To evaluate these, animal models remain an essential part of the pipeline to the clinical usage [37] (Table 2).

It is important to examine the animal models that are most suited to evaluate the *ex vivo* testing. Anatomical features, such as size and structure, physiological loads and anatomical location in the animal model, should be as close as possible to what would be done in humans, either from an anatomical or biochemical viewpoint. However, it is difficult to mimic human physiological loads in animal models. Even so, the biochemical and wider responses to the implanted material can provide relevant information on the host response and mesh integration into the native tissue.

Table2. Anticipated time line of the current proposal for the introduction of novel devices into the market. Reproduced from Slack, Ostergard & Deprest [37].

Steps	Goals	Time line
Pre-marketing, nonclinical		
1. Preclinical file	Accurate description of product—toxicity studies for new polymers	0–6 months
2. Preclinical testing—animal	Host inflammatory response	0–12 months
3. Cadaveric studies	Anatomical documentation	6–12 months
Pre-marketing, clinical		
4. Clinical studies: phase II trial	Efficacy study Long-term safety	12–24 months Ongoing
Clinical studies: temporary registry	Surveillance study (n01,000)	30–42 months
"Yellow card" - MAUDE reporting? **Recommended: RCT**	Should prove whether product/procedure is advantageous/competitive	Should be conceived as early as possible

5. Animal models in pelvic floor surgery

The range of animal models used so far is wide, and has already been reviewed by several authors [42-44]. In this introduction, we briefly describe the animal models we used: rats, rabbits and sheep. Each model may have different contributions in terms of implant testing. Also, functional outcome can be measured in some species. When testing implants, outcomes typically documented are local complications (i.e. infection, exposure, contraction, fluid accumulation), active and passive biomechanical properties of the explant and evaluation of the host response. These outcome measures are believed to be relevant to the clinic. Rats are used for initial screening purposes. Rabbits are then used because of their dimensions and higher intra-abdominal pressure, factors that are biomechanically more representative. Finally, sheep allow the use of vaginal as well as abdominal surgery. The latter species can also be kept alive for longer periods.

Rodents (mice and rats) are inexpensive, easy to work with in large numbers, have low housing requirements and a low susceptibility to infections. *Rats* are used to study the biomechanical properties of candidate implants following integration into the host, when implants are used to simulate reconstructive surgical interventions. The *rat* abdominal wall model for implant testing was first used by Alponat et al. [40]. In that model, either a full-thickness abdominal wall defect is induced and primarily overlaid by mesh, acting therefore as a substitute of the abdominal wall (Fig. 7) [41].

In other words, the gap induced by removal of part of the abdominal wall is "bridged" by a tissue substitute or implant. This may be close to what is an incisional hernia in the clinic [42], or the use of a large mesh to support a prolapsed bladder, without focus on correcting the native tissues. Another reconstructive experimental procedure is the scenario where an incision is first primarily sutured and afterwards covered with mesh.

This is coined as “reinforcement” as well as “overlay”. For our translational experimental work herein, we will use the terms “gap bridging” and “reinforcement” hence to avoid the term “overlay” because it may cause confusion. Leuven group has experience with the above rat model [46] [48-49]. Herein, rats were used for initial evaluation of the novel implants tested in this thesis.

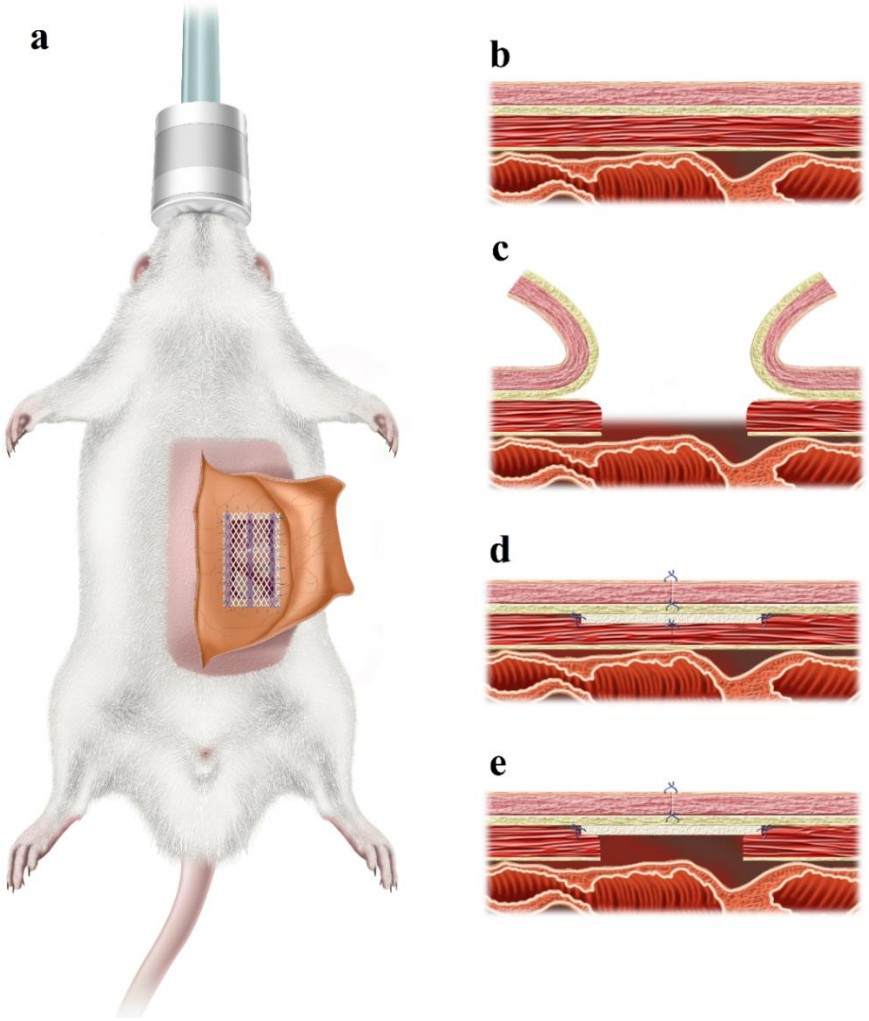

Fig. 7 Experimental setup for primary repair of full-thickness abdominal wall repair in a rat model. Cross-section of: **b**- intact anterior abdominal wall; **c**- full-thickness incision; **d**- primary repair of the defect and fixation of the implant; and **e**- overlaid mesh. Reproduced with permission from John Wiley and Sons. Drawing Dream Team, Leuven, Belgium.

Rabbits are medium sized animals with a longer life span, cheap and are easy to house. They are also used for mesh implantation, having an additional advantage that the abdominal wall is relatively large so that multiple implants can be tested simultaneously [43] (Fig. 8). Several studies, including studies from Leuven group, on abdominal wall repair models were done in New Zealand White rabbits and elegantly reviewed by Bellon et al. [44]. Given their lifespan, rabbits are also used to measure the host response on the longer term [45].

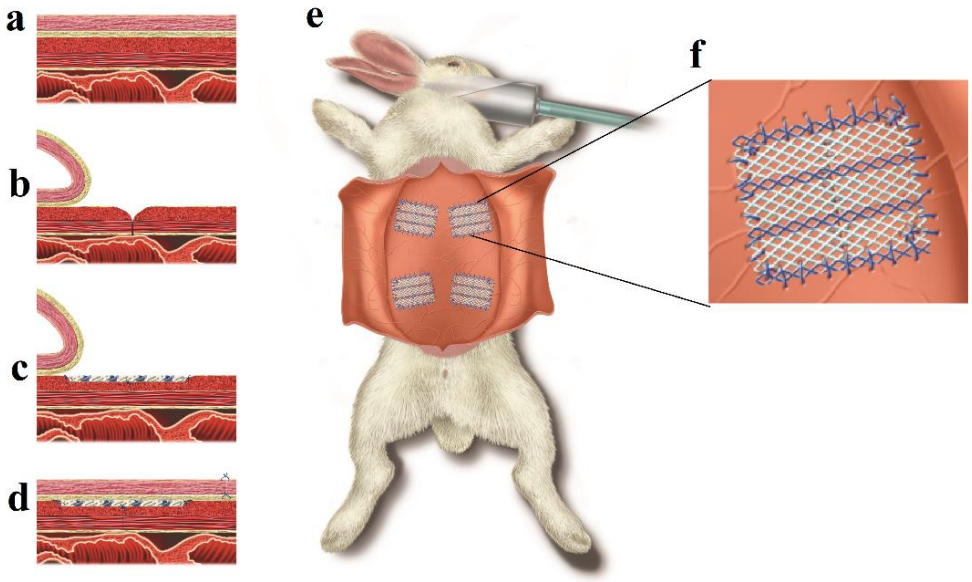

Fig. 8 Experimental setup for primary repair of full-thickness abdominal wall repair using four implants in one rabbit. Cross-section of: **a**- intact anterior abdominal wall; **b**- following preparation of skin flaps, creation of full-thickness incision; **c**- primary repair of the defect and fixation of the implant; and **d**- closure of the skin. **e**- magnification of the area in cross-section. Reproduced with permission from Elsevier. Drawing Dream Team Leuven, Belgium.

The *sheep* model is used in many research areas, such as coronary surgery [46], cardiovascular surgery [47], chronic pneumonia [48], orthopedics [49], pelvic organ prolapse [50], brain injuries [51], pregnancy and fetal growth [59-60]. The present research will focus on the sheep used as a model to study POP and mesh augmented prolapse repair. Sheep have a pelvic floor anatomy [52] and a fetal head-to-vaginal-birth-canal-ratio close to that of humans. Sheep have certain risk factors that are engaged in the process of POP, such as increased intra-abdominal pressure or parity [50]. Moreover, some sheep spontaneously develop utero-vaginal prolapse during pregnancy [53]. Sheep are large animals with high housing needs, they are expensive, quite vulnerable to infections and, as opposed to women, their pelvis is horizontal. There are no inbred animals and many laboratory techniques are not optimized for this species. Because of the comparable dimensions of sheep with humans, they have already been used in urogynaecology [54]. They can be used to train or study vaginal surgical techniques [55] hence also for testing the vaginal host response to implants (Fig. 9) [65-66].

De Tayrac [56] was the first to perform vaginal mesh implantation in the anterior and posterior vaginal wall. In that experiment, graft-related complications under the form of exposure, could be reproduced. Our group described its use to perform single incision mesh prolapse repairs [57]. In this model we were also able to reproduce exposures, their occurrence being different depending on the material and total mesh load used [68-69]. We have also used it to study geometric changes in the mesh using advanced imaging analysis techniques [58]. For this thesis, the sheep was used as a model for vaginal surgery [57], to test novel electrospun meshes and their effects on the biomechanical properties of, and the host response in the vagina.

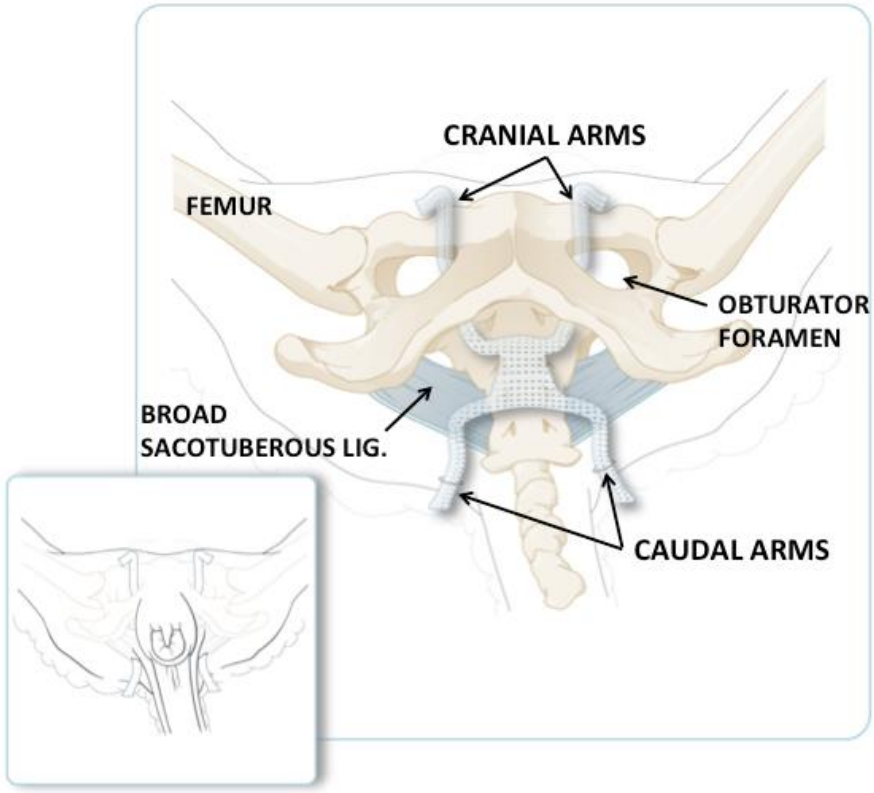

Fig. 9 Schematic illustration of the ovine pelvis with the cranial arms passing through the obturator foramen and caudal arms passing through the tail folds. The small panel illustrates the position of arms in the animal in recumbent position just before shortening the excessive amount of material. The main panel shows the same but with the skin muscles removed. Reproduced with permission from Wileys. Drawing Dream Team, Leuven, Belgium.

6. Computational mechanics

The use of simulation environments has become increasingly relevant due to the availability of experimental evidence. Simulation is an important tool for gaining deeper insights over many biomechanical problems [59]. Confined to the degree of assumptions and simplifications in the modelling of the material behavior, the predictions of these boundary-value problems can provide new insights for health issues. For example, through phenomenological material models one can investigate relevant biomedical problems such as PFD. Detailed anatomical description and mechanical loading conditions of the sheep pelvic cavity are not fully understood. This knowledge is relevant for transvaginal surgery planning and for experimental studies on PFD.

The complexity of pelvic floor dysfunction and some of its therapies, requires interdisciplinary research collaborations with technological fields such as engineering. Pelvic tissues are soft tissues comprising cells performing essential biochemical functions, while the elastin and collagen in the extracellular matrix (ECM), work as the load bearing constituents [60]. Collagen fibers, one of the main components of the extracellular matrix of soft pelvic tissues, are greatly responsible for the anisotropic mechanical behavior. Some researchers have found an intimate connection between the tissues' mechanics and histological structure [52], [61]. While collagen is largely

responsible for soft tissue tensile strength, elastin makes the tissue more compliant [62]. However, these findings must be linked with accurate material models. This connection is fundamental to understand the mechanical properties of pelvic tissues, especially in pathophysiological conditions.

The soft tissues of the human body have a highly nonlinear mechanical behavior and their passive properties can frequently be described by nonlinear hyperelastic or viscoelastic constitutive relations [62]. For realistic mechanical simulations it is important to rely on robust theoretical models. The nonlinear theory of elasticity in general, and the Holzapfel-Gasser-Ogden (HGO) model in particular, have been used to model fibrous soft tissues [63]. The HGO model is especially suited for tissues composed by two fiber families, such as arteries, pelvic floor tissues, etc. Previous research has shown that constitutive models in conjunction with Finite Element Analysis (FEA) can predict the biomechanical behavior of the implanted meshes and tissues [64]. The finite element method (FEM) is a very important development in numerical analysis. Over the years, FEM has spread to applications in many fields of engineering and science. FEA can help us understand the mechanical basis of PFD by pointing to areas experiencing critical levels of stress and strain [65].

SPECIFIC STUDY AIMS AND HYPOTESIS

As previously described, POP occurs when the muscles, ligaments and fascia (a network of supporting tissue) that hold these organs in their correct positions become structurally or functionally impaired. When operating on these structures, surgeons have turned to synthetic mesh-augmented repairs. However, mesh procedures have been associated with a high rate of complications. The use of mesh implants to correct prolapses requires knowledge of the mechanical properties of the mesh and of vaginal and surrounded tissues, so that the type of mesh can be chosen to match the actual resistance of the tissue as closely as possible. In that Odyssey towards better and more performing implants, we explored novel materials and new models.

The objectives of this project had the following aims:

1. To obtain the mechanical properties of novel electrospun, slowly degradable meshes for pelvic floor reconstruction *in vitro* (Chapter 2, Chapter 3) and *ex vivo*. (Chapter 4 and Supplement paper 1 and 2)
2. To study the mechanical behavior of ovine pelvic floor soft tissues (Chapter 5, Chapter 6). And to obtain adequate material model parameters (HGO model) for the *ex vivo* tensile tests (uniaxial, ball burst) simulations *in silico* environment (Chapter 7, Chapter 8 and Chapter 9).

To attain those objectives, the novel generation of electrospun implants, and subsequent explants from experimental surgeries on representative animal models (rats, rabbits and sheep), were characterized. Mesh implants were tested by uniaxial tensile testing and under *in vitro* simulated physiological conditions followed by cyclic loadings. To obtain the mechanical properties of the explants and native tissue samples (taken from the opposite side of the abdominal wall) were tested using uniaxial tensile testing (rats and rabbits) and ball burst testing (sheep).

Biomechanical and histological analysis were conducted, to document how vaginal wall and pelvic floor soft tissues changes during the pregnancy and recover one year after vaginal birth, using findings in virgin sheep as a reference point. The histological data was used to link tensile testing experiments with material-dependent parameters, to be used in further *in silico* simulations.

This research was conducted within a convention celebrated between:

KU Leuven, Faculty of Medicine, Department of Development and Regeneration at the Centre for Surgical Technologies, Belgium under the guidance of Prof. Dr. J. Deprest and his team, for the experimental studies with animal models.

and the

University of Porto, Faculty of Medicine, Hospital Sao Joao, under the guidance of Prof. A. A. Fernandes and his team, to evaluate the clinical significance of the research results (biomechanics, histological analysis, *in silico* studies).

References

[1] Hendrix SL, "Pelvic organ prolapse in the Women's Health Initiative: gravity and gravidity," *Am J Obstet Gynecol,* vol. 186, no. 6, pp. 1160-1166, 2002.

[2] Delancey JO, Kane Low L, Miller JM, Patel DA, Tumbarello JA, "Graphic integration of causal factors of pelvic floor disorders: an integrated life span model," *Am J Obstet Gynecol,* vol. 199, no. 6, pp. 1-5., 2008.

[3] Rahn D, Ruff M, Brown S, Tibbals H, Word A, "Biomechanical properties of the vaginal wall: effect of pregnancy, elastic fiber deficiency, and pelvic organ prolapse," *AJOG,* vol. 590, pp. e1-6, 2008.

[4] G Callewaert, M Albersen, K Janssen, MS Damaser, T Van Mieghem, CH van der Vaart, J Deprest, "The impact of vaginal delivery on pelvic floor function – delivery as a time point for secondary prevention," *BJOG,* vol. 123, no. 5, pp. 678-681, 2015.

[5] Patel DA, Xu X, Thomason AD, Ransom SB, Ivy JS, DeLancey JO, "Childbirth and pelvic floor dysfunction: an epidemiologic approach to the assessment of prevention opportunities at deivery," *Am J Obstet Gynecol,* vol. 195, pp. 23-28, 2006.

[6] MacLennan AH, Taylor AW, Wilson DH, Wilson D, "The prevalence of pelvic floor disorders and their relationship to gender, age, parity and mode of delivery," *BJOG,* vol. 172, no. 12, pp. 1460-1470, 2000 .

[7] Lukacz ES, Lawrence JM, Contreras R, Nager CW, Luber KM, " Parity, mode of delivery, and pelvic floor disorders," *Obstet Gynecol,* vol. 107, pp. 1253-1260, 2006.

[8] Bugge C, Adams EJ, Gopinath D, Reid F, "Pessaries (mechanical devices) for pelvic organ prolapse in women," *Cochrane Database,* pp. 3-5, 2013.

[9] Geynisman-Tan J, Kenton K, "Surgical Updates in the Treatment of Pelvic Organ Prolapse," *Rambam Maimonides Med J.,* vol. 8, no. 2, p. e0017, 2017.

[10] Wu JM, Matthews CA, Conover MM, Pate V, Jonsson Funk M, "Lifetime risk of stress urinary incontinence or pelvic organ prolapse surgery," *Obstet Gyneco,* vol. 123, no. 6, pp. 1201-1206, 2014.

[11] Løwenstein E1, Ottesen B, Gimbel H, "Incidence and lifetime risk of pelvic organ prolapse surgery in Denmark from 1977 to 2009," *Int Urogynecol J,* vol. 26, no. 1, pp. 49-55, 2015.

[12] Haylen BT, Freeman RM, Swift SE, Cosson M, Davila GW, Deprest J, Dwyer PL, Fatton B, Kocjancic E, Lee J, Maher C, Petri E, Rizk DE, Sand PK, Schaer GN, Webb R; Association, International Urogynecological; Society, International Continence; W, Joint IUGA/ICS, "An International Urogynecological Association (IUGA)/International Continence Society (ICS) joint terminology and classification of the complications related directly to the insertion of prostheses (meshes, implants, tapes) and grafts in female pelvic floor," *Neurourol Urodyn.,* vol. 30, no. 1, pp. 2-12, 2011.

[13] U.S. Food and Drug Administration, "Hernia Surgical Mesh Implants,"02 04 2018, Available: https://www.fda.gov/medicaldevices/productsandmedicalprocedures/implantsandprosthetics/herniasurgicalmesh/default.htm. [Accessed 26 07 2018].

[14] Food and Drug Administration, "Serious Complications Associated With Transvaginal Placement of Surgical Mesh in Repair of Pelvic Organ Prolapse and Stress Urinary Incontinence," Food and Drug Administration FDA, Public Health Notification, 2008.

[15] Agrawal A, Avill R, "Mesh migration following repair of inguinal hernia: a case report and review of literature," *Hernia,* vol. 10, pp. 79-82, 2006.

[16] Cobb WS, Kercher KW, Heniford BT, "The argument for lightweight polypropylene mesh in hernia repair," *Surg. Innov.*, pp. 63-69, 2005.

[17] Prabaharan M, Jayakumar R and Nair S, "Electrospun nanofibrous scaffolds-current status and prospects in drug delivery," *Advances in Polymer Science,* vol. 246, p. 241–262, 2011.

[18] Villarreal-Gómez LJ, Cornejo-Bravo JM, Vera-Graziano R, Grande D, "Electrospinning as a powerful technique for biomedical applications: a critically selected survey," *J Biomater Sci Polym,,* vol. 27, pp. 157-176, 2016.

[19] Sijbesma RP, Beijer FH, Brunsveld L, Folmer BJB, Hirschberg JK, Lange RFM, Lowe KJL, Meijer EW, "Reversible polymers formed from self- complementary monomers using quadruple hydrogen bonding," *Science,* vol. 278, pp. 1601-1604, 1997.

[20] Sontjens SHM, Renken RAER, van Gemert GML, Engels TAP, Bosman AW, Janssen HM, Govaert LE, Baaijens FPT, "Thermoplastic elastomers based on strong and well-defined hydrogen-bonding interactions," *Macromolecules,* vol. 41 , pp. 5703-5708, 2008.

[21] Bastings MM, Koudstaal S, Kieltyka RE, Nakano Y, Pape AC, Feyen DA, van Slochteren FJ, Doevendans PA, Sluijter JP, Meijer EW, Chamuleau SA, Dankers PY., "A fast pH-switchable and self-healing supramolecular hydrogel carrier for guided, local catheter injection in the infarcted myocardium.," *Adv Healthc Mater.* , vol. 3, no. 1, pp. 70-78, 2014.

[22] Dankers P, Harmsen MC, Brouwer LA, Van Luyn MJA, Meijer EW, "A modular and supramolecular approach to bioactive scaffolds for tissue engineering," *Nat. Mater.* , vol. 7, p. 568–574, 2005.

[23] Cipitria A, Skelton A, Dargaville T R, Dalton P D and Hutmacher D W, "Design, fabrication and characterization of PCL electrospun scaffolds—a review," *Journal of Materials Chemistry,* vol. 21, p. 9419–9453, 2011.

[24] Hutmacher DW, Schantz T, Zein I, Ng K W, Teoh S W and Tan K C, "Mechanical properties and cell cultural response of polycaprolactone scaffolds designed and fabricated via fused deposition modeling," *J Biomed Mater Res,* vol. 55, pp. 203-216, 2001.

[25] Lam CX, Savalani MM, Teoh SH, Hutmacher DW., "Dynamics of in vitro polymer degradation of polycaprolactone-based scaffolds: accelerated versus simulated physiological conditions.," *Biomed Mater,* vol. 3, no. 3, 2008.

[26] Mrówczyński W, Mugnai D, de Valence S3, Tille JC4, Khabiri E2, Cikirikcioglu M2, Möller M3, Walpoth BH5, "Porcine carotid artery replacement with biodegradable electrospun poly-e-caprolactone vascular prosthesis.," *J Vasc Surg,* vol. 59, no. 1, pp. 210-219, 2014.

[27] Chakroff J, Kayuha D, Henderson M, Johnson J , "Development and Characterization of Novel Electrospun Meshes for Hernia Repair.," *SOJ Mater Sci Eng,* vol. 3, no. 1, pp. 1-9, 2015.

[28] Palmer JA, Abberton KM, Mitchell GM, Morrison WA., "Macrophage Phenotype in Response to Implanted Synthetic Scaffolds: An Immunohistochemical Study in the Rat," *Cells Tissues Organs* , vol. 199, no. 2-3, pp. 169-183., 2014.

[29] Brugmans MCP, Söntjens SHM, Cox MAJ, Nandakumar A, Bosman AW, Mes T, Janssen HM, Bouten CVC, Baaijens FPT, Driessen-Mol A., "Hydrolytic and oxidative degradation of electrospun supramolecular biomaterials: In vitro degradation pathways," *Acta Biomater.,* vol. 27, pp. 21-31, 2015.

[30] Hillary CJ, Roman S, Bullock AJ, Green NH, Chapple C, MacNeil S, "Developing repair materials for stress urinary incontinence to withstand dynamic distension," *PLoS One,* 2016.

[31] Agarwal S, Wendorff J, Greiner A, "Use of electrospinning technique for biomedical applications," *Polymer,* vol. 49, no. 26, pp. 5603-5621, 2008.

[32] Wach RA, Adamus A, Kowalska-Ludwicka K, Grobelski B, Cala J, Rosiak JM, Pasieka Z, "In vivo evaluation of nerve guidance channels of PTMC/PLLA porous biomaterial," *Arch Med Sci.,* vol. 16, no. 11, pp. 210-219, 2015.

[33] Slack M, Ostergard D, Cervigni M, Deprest J, , "A standardized description of graft-containing meshes and recommended steps before the introduction of medical devices for prolapse surgery," *International Urogynecology Journal,* vol. 23, pp. 15-26, 2012.

[34] Afonso JS, Martins PALS, Girao MJB, Natal Jorge RM, Ferreira AJM, Mascarenhas T et al.,, " Mechanical properties of polypropylene mesh used in pelvic floor repair," *Int Urogynecol J,,* vol. 19, pp. 375-380, 2008.

[35] Dietz HP, Vancaillie P, Svehla M, Walsh W, Steensma AB, Vancaillie TG, " Mechanical properties of urogynecologic implanted materials," *Int Urogynecol J,,* vol. 14, pp. 239-243, 2003.

[36] Krause H, Bennett M, Forwood M, Goh J,, "Biomechanical properties of raw meshes used in pelvic floor reconstruction," *International Urogynecology Journal,,* vol. 19, p. 1677–1681, 2008.

[37] Jones KA, Feola A, Meyn L, Abramowitch SD, Maolli PA, , "Tensile properties of commonly used prolapse meshes," *International Urogynecology Journal,* vol. 20, pp. 847-853, 2009.

[38] Whitson BA, Cheng C, Christine O'keefe, "Multilaminate resorbable biomedical device under biaxial loading," *Journal of biomedical materials research,* 1998.

[39] Hympánová L, Rynkevic R, Román S, Mori da Cunha M, Mazza E, Zündel M, Urbánková I, Gallego M, Vangee J, Callewaert G, Chapplej C, Mac Neill S, Deprest J, "Assessment of Electrospun and Ultra-lightweight Polypropylene Meshes in the Sheep Model for Vaginal Surgery," *European Urology Focus,* 2018.

[40] Deprest J, Zheng F, Konstantinovic M, Spelzini F, Claerhout F, Steensma A, Ozog Y, De Ridder D., "The biology behind fascial defects and the use of implants in pelvic organ prolapse repair," *Int Urogynecol J Pelvic Floor Dysfunct ,* vol. 17, no. 1, pp. s16-s25, 2006.

[41] Bringman S, Conze J, Cuccurullo D, Deprest J, Junge K, Klosterhalfen B, Parra-Davila E, Ramshaw B, Schumpelick V. , "Hernia repair: the search for ideal meshes," *Hernia,* vol. 14, no. 1, p. 81–87, 2010.

[42] Abramowitch SD, Feola A, Jallah ., Moalli PA, "Tissue mechanics, animal models, and pelvic organ prolapse: a review.," *Eur. J. Obstet. Gynecol. Reprod. Biol. ,* pp. 146-158, 2009..

[43] Couri BM, Lenis AT, Borazjani A, Paraiso MFR, Damaser MS. , "Animal models of female pelvic organ prolapse: lessons learned.," *Expert review of obstetrics & gynecology. ,* vol. 7, no. 3, pp. 249-260, 2012.

[44] Andersen M, Winter L, "Animal models in biological and biomedical research - experimental and ethical concerns," *Anais da Academia Brasileira de Ciências,* Vols. On-line version ISSN 1678-2690, 2017.

[45] Alponat A, Lakshminarasappa SR, Yavuz N, Goh PM, "Prevention of adhesions by Seprafilm, an absorbable adhesion barrier: an incisional hernia model in rats.," *Am Surg.,* vol. 63, no. 9, pp. 818-9, 1997.

[46] Konstantinovic ML, Ozog Y, Spelzini F, Pottier C, De Ridder D, Deprest J, "Biomechanical Findings in Rats Undergoing Fascial," *Neurourol Urodyn.* , vol. 29, no. 3, pp. 488-93, 2010.

[47] Kingsnorth A, LeBlanc K, "Hernias: inguinal and incisional.," *Lancet,* vol. 362, no. 9395, p. 1561–1571, 2003.

[48] Zheng F, Lin Y, Verbeken E, et al., " Host response after reconstruction of abdominal wall defects with porcine dermal collagen in a rat model.," *Am J Obstet Gynecol,* vol. 191, p. 1961–1970., 2004.

[49] Ozog Y, Konstantinovic M, Zheng F, et al., "Porous acellular porcine dermal collagen implants to repair fascial defects in a rat model: biomechanical evaluation up to 180 days.," *Gynecol Obstet Invest,* vol. 68, p. 205–212, 2009.

[50] Ozog M. Konstantinovic E, de Ridder D, Edoardo M and Deprest J, "Shrinkage and biomechanical evaluation of lightweight synthetics in a rabbit model for primary fascial repair.," *Int. Urogynecol. J.,* vol. 22, p. 1099–1108, 2011.

[51] Bellón JM, Rodríguez M, Pérez-Köhler B, Pérez-López P, Pascual G, "The New Zealand White Rabbit as a Model for Preclinical Studies Addressing Tissue Repair at the Level of the Abdominal Wall," *Tissue Eng Part C Methods.,* vol. 23, no. 12, pp. 863-880, 2017.

[52] Claerhout F, Verbist G, Verbeken E, et al., "Fate of collagen-based implants used in pelvic floor surgery: A 2-year follow-up study in a rabbit model.," *Am J Obstet Gynecol* , vol. 198, pp. e1-94.e6., 2008.

[53] Drissi Boumzebra, Jan Otto Solem, Shaheen Nakeeb, Zohair Al Halees, "The Sheep as a Model for Coronary Artery Surgery Experiments on Beating Heart," *The Journal of Tehran University Heart Center* , vol. 1, no. 1, pp. 12-17, 2006.

[54] Katz MG, Kendle AP, Fargnoli AS, Mihalko KL, Bridges CR., "Sheep (Ovis Aries) as a Model for Cardiovascular Surgery and Management Before, During, and after Cardiopulmonary Bypass," *Journal of the American Association for Laboratory Animal Science,* vol. 54, no. 1, pp. 7-8, 2015.

[55] Gilmour JS, Jones GE, Rae AG., "Experimental studies of chronic pneumonia of sheep.," *Comp Immunol Microbiol Infect Dis.,* vol. 1, no. 2, pp. 285-293, 1979.

[56] Martini L, Fini M, Giavaresi G, Giardino R., "Sheep model in orthopedic research: a literature review.," *Comp Med,* vol. 51, no. 4, pp. 292-299, 2001.

[57] Couri BM, Lenis AT, Borazjani A, Paraiso MF, Damaser MS, "Animal models of female pelvic organ prolapse: lessons learned," *Expert Rev. Obstet Gynecol,* vol. 7, pp. 249-260, 2012.

[58] Stephen A. Back, Art Riddle, A. Roger Hohimer, "The Sheep as a Model of Brain Injury in the Premature Infant," *Animal Models of Neurodevelopmental Disorders* , vol. 104, pp. 107-128, 2015 .

[59] Vuguin PM, "Animal Models for Small for Gestational Age and Fetal Programing of Adult Disease.," *Hormone research,* vol. 68, no. 3, pp. 113-123, 2007.

[60] James S Barry , Russell V Anthony, "The Pregnant Sheep as a Model for Human Pregnancy," *Theriogenology.* , vol. 69, no. 1, p. 55–67, 2008.

[61] Urbankova I, Callewaert G, Blacher, Deprest D, Hympanova L, Feola , De Landsheere , Deprest J, "First delivery and ovariectomy affect biomechanical and structural properties of the vagina in the ovine model.," *Int Urogynecol J.,* 2018 .

[62] Shepherd PR, "Vaginal Prolapse in Ewes," *Vet Rec*, vol. 130, p. 564, 1992.

[63] Urbankova I, Vdoviakova K, Rynkevic R, Sindhwani N, Deprest D, Feola A, Herijgers P, Krofta L, Deprest J., "Comparative Anatomy of the Ovine and Female Pelvis," *Gynecol Obstet Invest.;82(6):*, vol. 82, no. 6, pp. 582-591, 2017.

[64] Kerbage Y, Giraudet G, Rubod C, et al., "Feasibility and benefits of the ewe as a model for vaginal surgery training.," *Int Urogynecol J*, pp. 1-5, 2017.

[65] Endo M, Urbankova I, Vlacil J, Sengupta S, Deprest T, Klosterhalfen B, Feola A, Deprest J. , "Cross-linked xenogenic collagen implantation in the sheep model for vaginal surgery. Gynecol Surg," p. 113–122, 2015.

CHAPTER 2

IN VITRO STUDY OF THE MECHANICAL PERFORMANCE OF HERNIA MESH UNDER CYCLIC LOADING

Rita Rynkevic[1], Pedro Martins[1], Francisco Pereira[1], Nilza Ramião[1], António A. Fernandes[1]

[1]INEGI, LAETA, Faculty of Engineering of the University of Porto, Porto, Portugal

Key words: In vitro degradation, cyclic loading, hernia mesh, synthetic polymers, mechanical behaviour

J Mater Sci: Mater Med (2017)28:176
DOI 10.1007/s10856-017-5984-6

CLINICAL APPLICATIONS OF BIOMATERIALS

Original Research

In vitro study of the mechanical performance of hernia mesh under cyclic loading

Rita Rynkevic[1] · Pedro Martins[1] · Francisco Pereira[1] · Nilza Ramião[1] · António A. Fernandes[1]

Published in Journal of Material Science: Materials in Medicine, vol. 28, 176. (2017)

ABSTRACT

The use of prostheses for hernia surgery, made from synthetic polymers may lead to development of postoperative complications. The reason for this can be the mismatch of the mechanical properties of meshes and the loads acting on them. The aim of this work was to investigate the behavior of 3 different hernia meshes under *in vitro* simulated physiological conditions followed by cyclic loadings.

Meshes, Ultrapro (poliglecaprone and polypropylene), Surgipro (polypropylene), Dynamesh (polyvinylidenefluoride) were selected. For *in vitro* degradation test, samples were kept in alkaline and acid mediums at 37 °C during 42 and 90 days and analyzed in terms of their weight loss and thickness changes. This was followed by cyclic loading in three increasing load stages.

The greatest weight loss and thickness reduction were suffered by Ultrapro mesh. The mesh showed pH independent characteristics. Surgipro mesh had pH independent behavior due to the degradation process, with slight weight loss and thickness reduction. The degradation mechanism of Dynamesh is highly dependent on the pH, with acid surrounding medium acting as a degradation catalyst. Mechanical hysteresis was observed in all three meshes. The larger deformations occurred in Surgipro (25%); necking phenomenon was also observed. The deformation of Dynamesh was 22%, the mesh unweaves under applied load and was unable to withstand the third period of cyclic loads. Ultrapro mesh exhibits the lowest level of deformation (10%).

Despite the different compositions and architectures of the meshes, all three underwent permanent plastic deformation, which will induce decreased mesh flexibility over time.

GRAPHICAL ABSTRACT

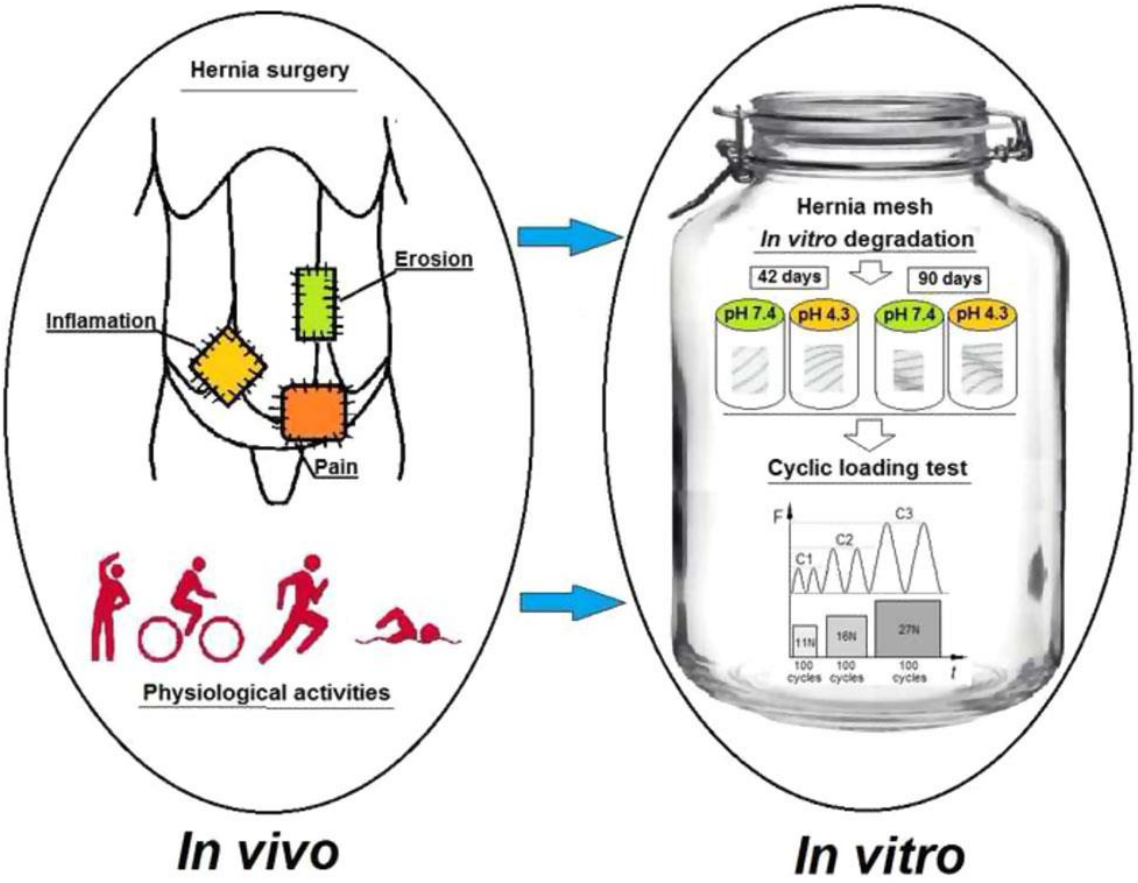

1. Introduction

In recent years, the number of laparotomy operations has been increasing all over the world [1]. The use of prostheses made from synthetic polymers reduced the number of relapses, but led to postoperative complications [2]. These complications are related to foreign body reaction, pathological fibrosis, mesh shrinkage, fistula, etc. [3- 5].

After implantation the mesh becomes part of the muscle-fascial complex. Besides covering the defect, it functions together with the muscles and fascia. Therefore, the complications arising after implantation may have a mechanical origin. Surgical mesh should have properties as compatible as possible to the biomechanics of abdominal wall. Complications can be linked with the mismatch of mesh mechanical properties and the acting loads [6]. Mesh should also be flexible and have shape-memory, i.e. return to its original shape after stretching in more than one direction [7].

Another important issue is material biodegradation. For products intended as replacement of organs and bodily functions, biodegradation process leads to the loss of functional properties of the implant. The working life of surgical meshes is associated with two periods: functional and passive. During the first period, the implant performs tissues functions. The second period is related to the biodegradation process, and its gradual substitution by native tissue (or ingrowth) during the recovery process. The rate of destruction of foreign material, should not exceed the rate of recovery (regeneration). If this condition is not met, recovery deceleration or premature loss of implant function will take place.

To mimic a biological environment, or the action of its components, mesh samples were placed for definite time periods in pH controlled liquid formulations. This was followed by cyclic loading in three increasing load stages. The aim of this investigation was to study the effect of in vitro degradation process and repetitive loadings, on the mechanical performance of the meshes used for hernia repair.

2. Material and methods

Meshes of different materials, Ultrapro mesh (poliglecaprone and polypropylene), Dynamesh (Polyvinylidenefluoride) and Surgipro (polypropylene), were selected for degradation process. Table 1 summarizes the main characteristics of the hernia meshes.

2.1 Sample preparation

Pattern and pore size have influence on the mechanisms of deformation of knitted meshes. Dynamesh and Ultrapro meshes were cut out into 50x10 mm strips along longitudinal axis, respecting the pore pattern. Surgipro mesh could withstand high loads, however the load cell of the testing machine has a limit of 50N, thus a smaller sample size 25x5 mm was selected. These sample dimensions were chosen in order to allow a constant length-to-width aspect ratio of 4, to minimize the nonlinear effects of clamping on the uniaxial mechanical properties. A total of 20 samples were obtained for each mesh (Table 1). *In vitro* degradation process and cyclic loading testing were performed according to the protocol specified below.

Table1. Main characteristics of the meshes, number of samples and sample dimensions used in present investigation. Scale bar (lower right): 5mm

Commercial name	**ULTRAPRO™ Partially Absorbable Lightweight Mesh [8]**	**DynaMesh ® -Endolap visible [9]**	**Surgipro™ Flat Sheet Mesh [10]**
Manufacturer	Ethicon	FEG Textiltechnik mbH	Covidien
Mesh geometry	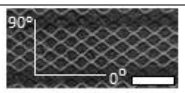	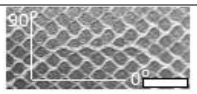	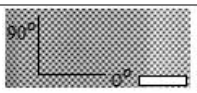
Application	Hernia	Hernia	Hernia
Product material and characteristics	Monocryl (*poliglecaprone*) and Prolene *(polypropylene)* Monofilament Partially absorbable Lightweight Knitted Macroporous	PVDF (*Polyvinylidenefluoride*) Monofilament Nonabsorbable Lightweight Warp-knitted structure Macroporous	PP *(Polypropylene)* Multifilament Nonabsorbable Standard Knitted Porous
Samples used for analysis			
Sample dimensions (mm)	50x10	50x10	25x5
Control samples	4	4	4
***In vitro* degradation 42 d.**	8	8	8
***In vitro* degradation 90 d.**	8	8	8
Uniaxial cyclic loading test	4 (control) + 16 (after degradation)	4 (control) + 16 (after degradation)	4 (control) + 16 (after degradation)

2.2 In vitro degradation analysis protocol and experimental set up

All stages of the work were conducted in accordance with ISO 10993 "Biological evaluation of medical devices" [11]. ISO 10993 is a method recommended by the standard, is an *in vitro* biodegradation test of material as a result of exposure to the biological environment.

To study the processes of dissolution and resorption *in vitro*, Phosphate Buffer Solution (PBS) [12] was used as a model of biological fluid [13]. One tablet was dissolved in 200 mL of distilled water, to obtain a solution with pH = 7.4. The biodegradation can occur under a wide range of pH, including acid mediums associated with inflammation [14]. Therefore, Potassium Hydrogen Phthalate (KHP) [15] was used to obtain the acid medium. One tablet was dissolved in 100 mL of distilled water to obtain a solution of pH=4.3.

The thickness and initial weight of each specimen, from each group, were measured before immersion into KHP and PBS mediums. Analytical balance with an inherent error of ± 0.001 g for each reading was used. Automatic pH-meter was used to control the acidity index in the tube. Samples were kept at 37°C (± 0.1ºC) during 42 and 90 days. After degradation process, the samples were washed in distilled water, dried at room temperature during 24 hours and weighed. The degradation of the material was evaluated via thickness change and weight loss. Dried samples were used for further evaluation of the mechanical properties, and their comparison before and after degradation.

2.3 Cyclic loading test protocol and experimental set up

Cyclic tests were performed in order to mimic the effects of repetitive loading, similar to expected *in vivo* loads. Loads were calculated using Laplace's Law assuming that 16 N/cm is required to withstand the maximum intra-abdominal pressure [16]. Moreover,

Cobb et al. found that the maximum tensile strength ranged from 11 to 27 N/cm during different physiological activities [17].

Using 11 N/cm, 16 N/cm and 27 N/cm, the equivalent forces acting on the mesh samples were estimated. A preload of 0.11 N was applied to remove the slack from the sample, using a constant elongation rate of 5 mm/min. The clamp-to-clamp distance was estimated using a digital imaging technique. After preloading, samples were loaded to the estimated forces and then unloaded back to 0.11 N. A constant elongation rate of 5 mm/min was used to load the specimen. Three levels of cyclic loading were set (C1, C2, C3), with 100 cycles applied at each level. After the 300 cycles, samples were stretched to failure. This number of cycles was selected in order to simulate and analyze the geometrical changes of a freshly implanted mesh under physiological loads during postoperative recovery. The equipment used in this study is a prototype developed at INEGI Biomechanics Laboratory. The testing machine, has four perpendicular aluminum alloy arms, connected to four actuators and two load cells (with a 50N capacity).

For knitted or woven meshes the definition of cross sectional area has limitations as the determination of the material thickness is user-dependent and the cross-sectional area does not define the amount of load-bearing filaments. Thus, for comparison purposes the percent elongation of the sample to the initial length of the sample was used.

2.4 Statistics

All statistical tests were made using a statistical software package (GraphPad Prism 5, USA). Quantitative data are represented as mean ± standard error of the mean (SEM). To determine the differences in elongation, weight loss and in thickness reduction, an unpaired Student's t-test was used (two-tailed, confidence level of 95%). The level of significance was set to $p<0.05$.

3. Results

During the degradation process Ultrapro mesh samples lost weight and thickness (Fig.1**b**); samples lost 38% ($p<0.001$) of their initial weight, in both KHP (acidic) and PBS (alkaline) mediums, after 42-days degradation and about 42% ($p<0.001$) after 90-days degradation. The mesh thickness decreased by 20% ($p<0.001$) after degradation in KHP medium and by 24% ($p<0.001$) in PBS. There was no significant difference between degradation in PBS and KHP mediums, neither between 42- and 90-day time points.

Fig.1**a** shows representative load-elongation curves of Ultrapro mesh behaviour under cyclic loading (C1-C3). The performance and comparison of samples at the considered time points (dry, after 42- and 90-days degradation in KHP and PBS mediums) are represented in Table 2.

After the first cycle (11 N/cm load) the permanent deformation of dry Ultrapro mesh samples was 10%. The permanent deformation after 42-day degradation was 8% and after 90-day degradation ~ 8.5 % for both mediums. After 100 cycles (of 11 N/cm) permanent deformation of dry mesh samples increased to 15%; after 42-day degradation permanent deformation increased to 12% and after 90-day degradation to 13%.

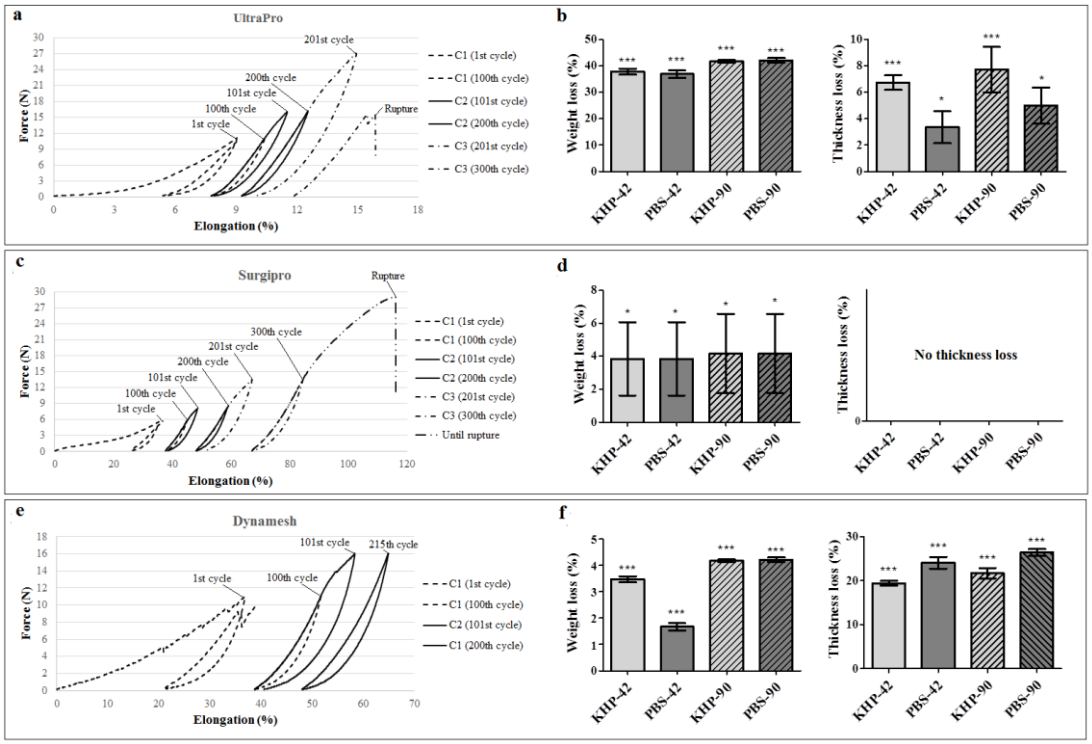

Fig. 1 Left side: mechanical behavior of Ultrapro (**a**), Surgipro (**c**) and Dynamesh (**e**) under cyclic loading (C1-C3), representative load–elongation curves. Right side: Vertical column bar graph, (mean with ± SEM) of Ultrapro (**b**), Surgipro (**d**) and Dynamesh (**f**) weight and thickness loss (%). Comparison performed using unpaired t-test, significant difference was set up when $p<0.001$ (***).

Table2. Elongation (mean (%) ± SEM) of Ultrapro samples, during cyclic loading test (C1-C3). Samples after degradation (KHP and PBS) at three time points (0d., 42d., and 90d.). Statistical intra-material comparisons of mesh, significant difference was set up when $p<0.05$ (**a**- difference between 0 and 42d./ 0 and 90d.; **b**- difference between KHP and PBS).

		Elongation (%)					
		C1 (11 N)		**C2 (16 N)**		**C3 (27 N)**	
Time points	**Samples**	1st cycle	100th cycle	101st cycle	200th cycle	201st cycle	215th -220th cycle
0d.	N=4	10.35 ± 0.27	14.86 ± 0.357	15.13 ± 0.387	17.78 ± 0.476	19.21± 0.749	29.16 ± 0.577
KHP-42d.	N=4	8.04 ± 0.159**a**	11.91 ± 0.159**a**	12.21±0.205**a**	14.50± 0.179**a**	15.44± 0.196**a**	27.89 ± 0.456
PBS-42d.	N=4	8.18 ± 0.123**a**	11.97 ± 0.086**a**	12.27±0.119**a**	14.60± 0.159**a**	15.64± 0.207**a**	28.00 ± 0.714
KHP-90d.	N=4	8.85 ± 0.235**a**	12.93 ± 0.291**a**	13.16±0.293**a**	15.57± 0.248**a**	16.69 ± 0.279**a**	19.38± 0.373**a**
PBS-90d.	N=4	8.56 ± 0.237**a**	12.60 ± 0.178**a**	12.87±0.217**a**	15.48± 0.459**a**	16.32 ± 0.191**a**	18.88± 0.623**a**

During the degradation Surgipro (PP) mesh samples lost 3.8 % of initial weight after 42-day degradation and 4.5% of the weight after 90-day degradation in both mediums (Fig.1**d**). Significant difference in weight loss among dry and degraded samples was found. There was no thickness variation after degradation. There was no significant difference in weight loss, after degradation in PBS and KHP mediums for both time point. Fig.1**c** shows representative load-elongation curves of Surgipro mesh during the cyclic loading test. The elongation (%) of dry and degraded samples and comparative results are presented in Table 3. After the first cycle (11N/cm), the permanent deformation of Surgipro mesh (dry and degraded) ranged between ≈ 23-26% (Table 3). For all samples, deformation increased by ≈ 10% after 100 cycles. In the beginning of the second period of cyclic loading (16 N/cm) deformation remained constant. In the end of the second period, permanent deformation of dry samples increased to 48% and of degraded samples

increased between 43-44%. Surgipro mesh withstood the third cyclic loading period (26 N/cm) deforming over 60 %. Sample rupture occurred at the load of 54 N/cm, stretching until 110%. No significant differences were found among all groups (Table 3).

Table3. Elongation (mean (%) with ± SEM) of Surgipro samples, during cyclic loading test (C1-C3), representing dry samples and samples after degradation (KHP and PBS) at three time points (0d., 42d., and 90d.). Statistical intra-material comparisons of mesh, significant difference was set up when $p<0.05$ (**a**- difference between 0 and 42d./ 0 and 90d.; **b**- difference between KHP and PBS)

		Elongation (%)					
		C1 (5.5 N)		**C2 (8 N)**		**C3 (13.5 N)**	
Time points	**Nr of samples**	1st cycle	100th cycle	101th cycle	200th cycle	201st cycle	300th cycle
0d.	N=4	25.83 ± 0.827	37.87 ± 1.402	38.61 ± 1.524	47.86 ± 2.376	50.32 ± 2.419	67.28 ± 2.454
KHP-42d.	N=4	23.09 ± 1.643	34.09 ± 2.317	35.03 ± 2.396	42.88 ± 2.948	45.23 ± 3.110	60.08 ± 4.419
PBS-42d.	N=4	25.00 ± 1.508	35.98 ± 2.016	36.68 ± 2.046	44.16 ± 2.735	46.49 ± 2.858	60.75 ± 3.443
KHP-90d.	N=4	23.84 ± 1.276	35.68 ± 1.570	36.20 ± 1.343	43.68 ± 7.834	46.87 ± 2.157	62.25 ± 3.557
PBS-90d.	N=4	25.35 ± 0.607	35.67 ± 1.118	36.34 ± 1.222	43.70 ± 1.871	47.27 ± 0.698	61.84 ± 0.446

Dynamesh samples lost weight and thickness during degradation (Fig.1**f**). After 42-day degradation samples lost 3.5% (in KHP) and 1.7% (in PBS). After 90-day degradation samples lost about 4% in both mediums. Significant difference in weight loss were found between dry and degraded samples (Fig.1**e**). The thickness decreased by 6.5% in KHP and 3.2% in PBS after 42-day degradation. After 90-day degradation in KHP thickness decreased by 8% and by 5% in PBS. Statistical analysis showed the thickness reduction was significant for all samples (Fig.1**f**). The weight and thickness loss were significantly different for PBS and KHP mediums (Fig.1**f**).

Table4. Elongation (mean (%) with ± SEM) of Dynamesh samples, during cyclic loading test (C1-C3), representing dry samples and samples after degradation (KHP and PBS) and three time points (0d., 42d., and 90d.). Statistical intra-material comparisons of mesh, significant difference was set up when $p<0.05$ (**a**- difference between 0 and 42d./ 0 and 90d.; **b**- difference between KHP and PBS)

		Elongation (%)			
		C1 (11 N)		**C2 (16 N)**	
Time points	**Nr of samples**	1st cycle	100th cycle	100th cycle	200th cycle
0d.	N=4	22.73 ± 0.883	39.78 ± 1.071	42.11 ± 1.384	55.24 ± 3.135
KHP-42d.	N=4	18.37 ± 1.268**a**	31.12 ± 2.020**a**	33.01 ± 2.140**a**	45.20 ± 4.026
PBS-42d.	N=4	19.24 ± 0.941	34.28 ± 2.294	35.52 ± 2.532	46.95 ± 4.703
KHP-90d.	N=4	20.23 ± 2.236	34.75 ± 2.409**a**	36.07 ± 2.786**a**	46.96 ± 2.727
PBS-90d.	N=4	21.75 ± 1.005	35.79 ± 0.921	36.97 ± 0.991	54.67 ± 8.665

Fig.1**e** presents the cyclic loading behaviour of Dynamesh. The elongation (%) of dry and degraded samples is shown in Table 4 and result comparison in Table 4. During the first cycle (11 N/cm load) dry Dynamesh samples deformed (permanently) by 22% (Table 4). After 42-day degradation, permanent deformations were 17% (KHP) and 19% (PBS). A significant difference was found between dry and KHP samples ($p<0.05$) (Table 4). There was no difference between 90-day degraded and dry samples.

After 100 cycles (11 N/cm load), permanent deformation of dry mesh increased to 40%. After 42-day degradation in KHP, permanent deformation increased to 31% and in PBS to 34%; after 90-day degradation deformation ranged between 34 - 35 % for both mediums. Significant differences were found between dry samples and samples after degradation in KHP, for both time points ($p<0.05$). In the beginning of the second period of cyclic loading (16 N/cm) deformation remains constant. In the end, permanent

deformation, of all samples, ranged between 45 - 55%. There was no significant difference between dry and degraded samples (Table 4). Dynamesh samples could not withstand applied loads over 22 N/cm. Therefore, the last cyclic period at 27 N/cm load, was not carried out.

4. Discussion

Research on the mechanical properties of available synthetic meshes demonstrated that no perfect product currently exists [7]. There is an ongoing search for the "ideal mesh", mainly through comparative investigations on mechanical properties among commercially manufactured prostheses [18-20]. However, different methods, materials and testing protocols were used. This situation makes the comparison of results difficult and sometimes conflicting. Modern histological and immunological tests expanded the understanding of the mechanisms of tissue response to the implant [21]. However, these techniques did not answer to the key questions regarding the production of an “ideal mesh”.

This work investigated the behavior of 3 different meshes under *in vitro* simulated physiological conditions and biomechanical loading. Samples were analyzed in terms of their weight loss, thickness changes and the variations of the mechanical properties after degradation in alkaline and acid mediums. Controlled *in vitro* degradation testing is typically used to complement animal trials to understand the material, design, and fabrication factors that affect *in vivo* implant ingrowth.

Material degradation can occur in a wide range of pH, as body pH balance differs from individual to individual. The inflammatory reaction of rapidly degradable biomaterials is more severe when compared to slowly degradable biomaterials [14]. The inflammatory response to an implanted prosthetic graft creates an unfavourable environment characterized by local acidic pH. The question then arises, “How does mesh mechanical properties change with pH?”. In this context, the pH-dependent degradation of the mesh assumes great importance, since these materials should be able to retain adequate strength under all possible physiologic and pathologic conditions. As expected, the greatest weight loss and thickness reduction were suffered by Ultrapro, a partially absorbable mesh made from poliglecaprone and polypropylene. The mesh showed pH independent characteristics as PBS and KHP mediums induced similar weight and thickness loss. Surgipro, a polypropylene mesh had pH independent behavior due to the degradation process, with slight weight loss and thickness reduction. The degradation mechanism of Dynamesh (polyvinylidenefluoride) is highly dependent on the pH, with acid surrounding medium acting as a degradation catalyst.

Despite their widespread acceptance, hernia mesh implants have been associated with many functional disturbances (e.g., restricted abdominal wall mobility) during long-term implantation [22], [23]. As well as, an immediate postoperative changes in pore dimensions of a textile implant were reported [24]. If implant undergoes immediate post-implantation deformation that could also cause GRCs. To simulate and analyze the geometrical changes of a freshly implanted textile mesh under physiological load conditions during postoperative recovery, three hundred cycles if increasing load were selected. To determine the physiological strain Junge et al. investigated the full thickness

of the abdominal wall of 14 fresh cadavers [25]. These authors found that longitudinal tensile strain ranged between 11% and 32% for an applied load of 16 N/cm. Literature review indicates that implants with macro porous structure have elongations ranging between 20-35% at 16 N/cm. Elongations of the small pore prostheses (heavy), ranged between 4-16% for the same load. This may result in limiting the mobility of the anterior abdominal wall [25].

The initial deformation of Surgipro was 25% and of Dynamesh was 22%. Ultrapro mesh exhibits the minimum elongation, 10%. Deformation grows 'faster' than load. After load removal, the sample did not recover, indicating the plastic deformation of the mesh. Mechanical hysteresis phenomenon was observed in the three meshes tested. During the stress relaxation tests, it was observed that the area of the hysteresis loop, increased inversely proportional to the relaxation rate, meaning an increase of dissipated energy. Surgipro was the most resistant mesh. It withstood the three periods of cyclic loads. However, necking phenomenon happened to the Surgipro. The edges of the Surgipro curled with applied load and did not return to their original positions after unloading. Dynamesh was unable to withstand the third period of cyclic loads. The mesh unweave under applied load and many of the individual threads broke.

Despite the different compositions and architectures of the meshes, all three underwent permanent plastic deformation, which will induce decreased mesh flexibility over time. A decreased flexibility of the hernia mesh is possibly related with reported complications, such as reduced abdominal wall mobility and long-termed pain and discomfort. In addition, degradation caused significant geometrical changes of the mesh. However, current experiment does not demonstrate that all these changes would develop in vivo. Tissue integration process might change the properties of a textile implant. In addition, this investigation has some shortcomings, such as material analyses under electron microscope, for a more detailed material research.

5. Conclusion

In vitro biodegradation and cyclic tests of mesh material renders an insight on potential *in vivo* mechanisms. Consequently, the results of *in vitro* studies should be considered with extreme caution, accounting for potential correlations with *in vivo* studies. Nevertheless, an *in vitro* first step towards the validation of new implants and solutions, seems a sensible approach to the -later in development cycle- animal experimentation.

Acknowledgment

This research has been supported in part by a grant of the EC in the FP7-framework (Bip-UPy; NMP3-LA-2012-310389). The authors gratefully acknowledge funding from: FCT, Portugal, under grants SFRH / BD / 96548 / 2013, SFRH / BPD / 111846 / 2015; UROSPHINX - Project 16842, COMPETE2020, through FEDER and FCT.

Conflict of interest statement

The authors do not have to disclose any financial or personal relationships with other people or organizations that could inappropriately influence (bias) their work.

References

[1] Kingsnorth A, LeBlanc K. “Hernias: inguinal and incisional.,” Lancet, vol. 362, nº 9395, p. 1561–1571, 2003.

[2] FDA, “Medical Devices: Hernia Surgical Mesh Implants,” U.S. Department of Health and Human Services, 07 04 2016 . [Online]. Available: http://www.fda.gov/MedicalDevices/ProductsandMedicalProcedures/ImplantsandProsthetics/HerniaSurgicalMesh/default.htm. [Acedido em 19 04 2016].

[3] Agrawal A, Avill R. “Mesh migration following repair of inguinal hernia: a case report and review of literature.,” Hernia, vol. 10, p. 79–82, 2006.

[4] Goswarmi R, Babor M, Ojo A. “ Mesh erosion into caecum following laparoscopic repair of inguinal hernia (TAPP): a case report and literature review,” J Laparoendosc Adv Surg Tech A, vol. 17, p. 669–672, 2007.

[5] Ozog Y, Konstantinovic M, Werbrouck E, De Ridder D, Edoardo M, Deprest J. “Shrinkage and biomechanical evaluation of lightweight synthetics in a rabbit model for primary fascial repair.,” Int. Urogynecol. J., vol. 22, p. 1099–1108, 2011

[6] Cobb WS, Kercher KW, Heniford BT. “The argument for lightweight polypropylene mesh in hernia repair.,” Surg. Innov., vol. 12, p. 63–69, 2005.

[7] Bringman S, Conze J, Cuccurullo D, Deprest J, Junge K, Klosterhalfen B, Parra-Davila E, Ramshaw B, Schumpelick V. “Hernia repair: the search for ideal meshes,” Hernia, vol. 14, nº 1, p. 81–87, 2010.

[8] Ethicon, “Ethicon,” Ethicon US, LLC, 2010 - 2016. [Online]. Available: http://www.ethicon.com/healthcare-professionals/products/hernia-repair-and-fixation/hernia-mesh-flat-mesh/ultrapro-partially-absorbable-lightweight-mesh. [Acedido em 22 03 2016].

[9] F. Textiltechnik, “Mesh Implants for Hernia Surgery,” © high standArt, Osnabrück, 2004 - 2016. [Online]. Available: http://en.dyna-mesh.com/aplprod/hernia/. [Acedido em 22 03 2016].

[10] Medtronic, “Covidien products,” Medtronic, 2015. [Online]. Available: http://products.covidien.com/pages.aspx?page=ProductDetail&id=13374&cat=Devices&cat2=Model. [Acedido em 22 03 2016].

[11] ISO 10993–2011, “Estimation of biological activity of medical products,” 2011.

[12] Sigma-Aldrich, “Phosphate buffered saline,” Sigma-Aldrich Co. LLC., [Online]. Available: http://www.sigmaaldrich.com/catalog/product/sigma/p4417?lang=pt&region=PT.

[13] ISO 13781–2011, “Resins and shaped elements poly-L-lactide for surgical implants. Degradation research in vitro.”

[14] Galgut P, Waite I, Smith R. “Tissue reaction to biodegradable and non-degradable membranes placed subcutaneously in rats, observed longitudinally over a period of 4 weeks,” J. Oral Rehabil, vol. 23, pp. 17-21, 1996.

[15] Sigma-Aldrich, “Buffer tablets pH 4.0,” Sigma-Aldrich Co. LLC., [Online]. Available: http://www.sigmaaldrich.com/catalog/product/riedel/36821?lang=pt&region=PT.

[16] Klinge U, Klosterhalfen B, Conze J, Limberg W, Obolenski B, Ottinger AP, Schumpelick V. “Modified mesh for hernia repair that is adapted to the physiology of the abdominal wall.,” Eur J Surg. , vol. 164, nº 12, pp. 951-960, 1998 .

[17] Cobb WS, Burns JM, Kercher KW, Matthews BD, James Norton H, Todd Heniford B. “Normal intraabdominal pressure in healthy adults,” J Surg Res. , vol. 129, nº 2, pp. 231-235, 2005.

[18] Cosson M, Debodinance P, Boukerrou M, Chauvet MP, Lobry P, Crépin G, Ego A. “Mechanical properties of synthetic implants used in the repair of prolapse and urinary incontinence in women: Which is the ideal material?,” Int. Urogynecol. J. vol. 14, p. 169–178., 2003

[19] Röhrnbauer B, Mazza E. “Uniaxial and biaxial mechanical characterization of a prosthetic mesh at different length scales.,” J. Mech. Behav. Biomed. Mater., Vols. %1 de %27-19, p. 29, 2014.

[20] Mazza E, Ehret A. “Mechanical biocompatibility of highly deformable biomedical materials.,” J. Mech. Behav. Biomed. Mater., vol. 48, p. 100–124, 2015.

[21] Konerding MA, Chantereau P, Delventhal V, Holste JL, Ackermann M. “Biomechanical and histological evaluation of abdominal wall compliance with intraperitoneal onlay mesh implants in rabbits: A comparison of six different state-of-the-art meshes.,” Med. Eng. Phys., vol. 34, p. 806–816, 2012.

[22] Müller M, Klinge U, Conze J, Schumpelick V. “Abdominal wall compliance after Marlex® mesh implantation for incisional hernia repair,” Hernia, vol. 2, nº 3, pp. 113-117, 1998.

[23] Welty G, Klinge U, Klosterhalfen B, Kasperk R, Schumpelick V. “Functional impairment and complaints following incisional hernia repair with different polypropylene meshes.,” Heria, vol. 5, nº 3, pp. 142-147, 2001.

[24] Sindhwani N, Liaquat Z, Urbankova I, Vande Velde G, Feola 2, Deprest J. “Immediate postoperative changes in synthetic meshes - In vivo measurements.,” J Mech Behav Biomed Mater, pp. 228-235, 2015.

[25] Junge K, Klinge U, Prescher A, Giboni P, Niewiera M, Schumpelick V. “Elasticity of the anterior abdominal wall and impact for reparation of incisional hernias using mesh implants,” Hernia, vol. 5, nº 3, pp. 113-118, 2001 Sep.

CHAPTER 3

IN VITRO SIMULATION OF *IN VIVO* DEGRADATION AND CYCLIC LOADING OF NOVEL DEGRADABLE ELECTROSPUN MESHES FOR PROLAPSE REPAIR

Rita Rynkevic[1, 2, 3], Pedro Martins[1], Antonio Fernandes[1], Jakob Vange[5], Monica Gallego[5], Radoslaw Wach[6], Tristan Mes[7], Anton Bosman[7], Jan Deprest[2, 3, 4]

[1] INEGI, LAETA, Faculdade de Engenharia da Universidade do Porto, Porto, Portugal.
[2] Centre for Surgical Technologies, Group Biomedical Sciences, KU Leuven, Leuven, Belgium
[3] Department of Development and Regeneration, Cluster Woman and Child, Group Biomedical Sciences, KU Leuven, Leuven, Belgium
[4] Pelvic Floor Unit, University Hospitals KU Leuven, Leuven, Belgium
[5] Coloplast A/S, Global R&D, Biomaterials, Humlebæk, Denmark
[6] Institute of Applied Radiation Chemistry, Chemistry Department, Lodz University of Technology, Lodz, Poland
[7] SupraPolix BV, Eindhoven, The Netherlands

Key words: Electrospun mesh; Ureido-Pyrimidinone; Polycaprolactone; Mechanical properties; Degradation

Submitted to Journal Polymer Testing (March, 2019)

ABSTRACT

Background and Objective: Synthetic durable textile meshes used in pelvic organ prolapse (POP) and incontinence surgery may lead to graft related complications (GRCs). Mechanisms involved in the genesis of GRCs include implant biocompatibility, biomechanical properties and the host response. Electrospinning allows production of micro-sized fibres, which can physically mimic the natural extracellular matrix of most connective tissues. When used for manufacturing implants it may reduce GRCs. Our aim was to measure the mechanical properties of novel prototype electrospun implants made of Ureido-Pyrimidinone-Polycaprolactone (UPy-PCL) and to simulate by hydration and repetitive loadings, *in vitro* the *in vivo* degradation of the implants and its impact on the mechanical performance. Electrospun mesh properties can be easily modified by controlling the diameter of the constituting fibres and by the ultimate thickness of the implant.

Material and Methods: Three types of UPy-PCL meshes, differing in their architecture were manufactured. For comparison, a reference nondegradable polypropylene knitted macroporous ultra-lightweight implant (Restorelle, Coloplast), clinically used for POP repair, was tested. First, the stability of UPy-meshes after sterilization by electron beam irradiation was confirmed. Then, implants were assessed by uniaxial tensile testing, considering longitudinal and transverse directions, and by water absorption testing. To mimic an *in vivo* biological environment, meshes were placed for predefined durations in pH-controlled baths, under cyclic loading in three increasing load stages.

Results and Conclusions: The electrospun meshes were more compliant and had higher maximum strains than the Restorelle mesh. UPy-PCL meshes are anisotropic, and a 10 % reduction in strength after water absorption was measured. UPy-PCL meshes did not display significant weight loss or thinning after *in vitro* degradation. They underwent plastic deformation and a significant difference in elongation was found after degradation in acid medium. Also, mechanical hysteresis was observed. During the degradation tests, Restorelle meshes did not lose weight or thickness. However, degradation affects its mechanical properties in both alkaline and acid testing conditions.

GRAPHICAL ABSTRACT

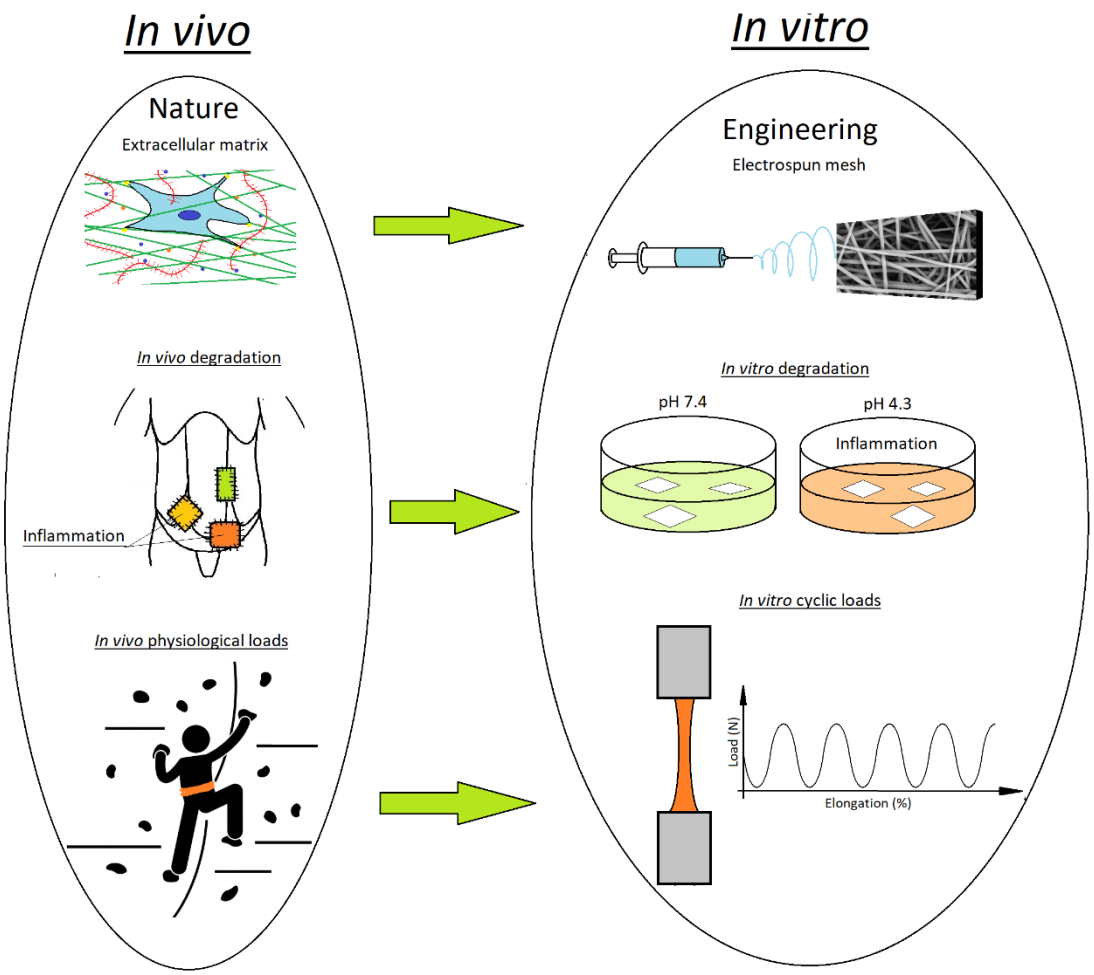

1. Introduction

Surgery is the mainstay of therapy for pelvic organ prolapse (POP). Meshes can be used to reinforce or substitute defective anatomical structures. However, their use may cause graft related complications (GRCs) [1]. Several causes may contribute to the occurrence of GRCs, such as surgical experience, patient factors and also material properties [2] [3]. In relation to the latter, insufficient biocompatibility and inappropriate biomechanical properties may lead to an adverse host response [4]. Most textile implants used today are based on the polymer polypropylene (PP) and are macroporous in nature. PP is non- resorbable hence it triggers a permanent host response. To decrease this, PP implants have been made increasingly lighter [5]. When GRC occur, they may persist until the material is exteriorised or removed. One of the more recent ones is Restorelle (Coloplast, Humlebaek, Denmark), an ultra-light textile with a stable geometric pattern. When tested in primates it seems to induce a favourable macrophage type 2 to type 1 ratio and anti-inflammatory cytokine profile [6], increased collagen and elastin synthesis, and reduced collagenase activity [7] than other light PP constructs. It also has less adverse effects on the perivaginal muscular layer [8] and smooth muscle contractility [9]. Despite that, the dry implant still has a stiffness above the average when compared with most other tested implants used for similar procedures [10].

A completely different approach may be to use non-textile biodegradable implants that are made in such a way that they mimic the biomechanical properties of the host tissue. Electrospinning technology enables the production of ultrafine fibres, assembled as a non-woven mesh-like structure, which can physically mimic the structure of the natural extracellular matrix of most connective tissues. Such scaffolds have been successfully used for tissue engineering [11]. Obviously, during the biodegradation process, the mechanical and functional properties of the implant change. Eventually, the graft may or may be not substituted by novel host tissue with appropriate functional properties. During the reconstructive remodelling process, the rate of degradation of the foreign material probably should be in balance with the rate of regeneration. In its absence, the repair may become unfunctional hence recurrence may occur.

Recently, new materials, including synthetic matrix supramolecular polymers, have been investigated (BIP-UPY, 2015) [12]. This is part of a project funded by the European Commission exploring a new concept of pelvic floor implant, biomechanically tailored to the native tissue properties, degradable, and with the potential to be bioactivated and act as a drug delivery vehicle [13]. Supramolecular polymers are characterized by the formation of arrays of directed, noncovalent interactions between the building blocks, using the self-assembling hydrogen bonding 2- ureido-[1H]-pyrimidin-4-one (UPy) [14]. Mechanical behavior and resorption rate are critical for the success of degradable implants. These properties can be modified by combining or changing ratios of the building blocks with existing degradable polymer blocks [15]. UPy-modified polymers have been used earlier as drug delivery vehicles, e.g. in a porcine myocardial infarction model [16] and in a modular approach as a bioactive elastomeric material for tissue engineering [17]. As a backbone, we used polycaprolactone (PCL). PCL is biocompatible and biodegradable, is easy to process and transform by electrospinning into filaments and

fabrication of textile structures. PCL is compatible with a wide range of other polymers. The Food and Drug Administration (FDA) approved PCL for use in humans [18] [19]. As a first step into the pipeline to clinical assessment [20], we tested the material characteristics of electrospun meshes and the effect of sterilization. Typically, the next step is to perform *in vivo* testing. In this paper, the results of an *in vitro* approach, simulating the degradation process and repetitive loadings, as would be present *in vivo* [21] are also reported.

2. Materials and methods

2.1 Mesh Production and Characterization

The polycaprolactone based supramolecular biomaterial comprising UPy polycaprolactone (UPy-PCL) was synthesized as previously described from a poly(ε-caprolactone) diol building block having a molecular weight of 2000 Da and diisocyanate modified 2-amino-4-hydroxy-5-(2-hydroxyethyl)-6-methylpyrimidine [22]. The resulting UPy-PCL is a thermoplastic elastomer with a glass transition at -58 °C and two melting points at 53 °C and 116 °C. The electrospun meshes studied in this work are prototypes purposely built with different fiber diameters. Supplement 1 displays the electrospinning conditions. Commercially available textile Restorelle (PP) mesh was used as a control, measuring 50×50 mm, and was supplied by the manufacturer (Coloplast) in sterile packs after sterilization by ethylene oxide. Table 1 displays generic information on both mesh types.

Table1. Mesh types used in the experiments. Testing method and principal directions of testing are marked. Scale bar (lower right): 5mm.

Implant	**UPy-PCL**	**Restorelle**
Image	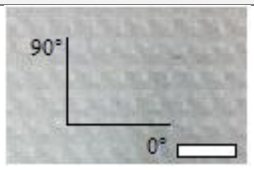	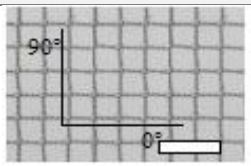
Material	Ureido-Pyrimidinone Variable fibre diameter, 2-3 micron	*Polypropylene* Monofilament 80 micron fibres
Degradability	Degradable	Non-degradable
Weave, description	Electrospinning	Knitting
Pore size	Microporous (c.a.10 μm)	1.8 mm; macroporous

Mesh thickness was measured (3 measurements per sample) using an electronic digital calliper. Table 2 provides detail on the number of PP and UPy-PCL meshes tested and characteristics in terms of fibre diameter and surface density. Further details on mesh preparation are in Supplement 2.

2.2 Effect of sterilization and mechanical testing protocol

To evaluate the mechanical effects of sterilization, a Zwick Z2 ripper with 100 N head and rubber-coated jaws were used. The grip-to-grip distance was 20 mm and the

crosshead speed was 10 mm/min. Maximum stress, strain and Young modulus (in the strain range of 0.02 − 0.06 mm/mm) were averaged from at least 5 specimens.

Further testing after sterilization was done on a 500-N tensiometer with a 200 N cell load (Zwick GmbH & Co. KG, Ulm, Germany). A preload of 0.1 N was applied to remove all slack from the mesh using a constant elongation of 10mm/min. This point was defined as elongation zero. A constant elongation rate of 10 mm/min was then used to load the specimen until failure. The data from the force-elongation curves were used for comparison. This is because the cross sectional area of the knitted meshes is difficult to estimate as the number of load-bearing filaments varies with the length, pore geometry and knitting pattern. Protocol details are provided in Supplement 2.

Table2. Characteristics of the meshes used in present investigation, test type, number of specimens and dimensions

Mesh characterisation						
Implant	**Serial nr.**	**Density (mg/cm^2)**	**Fibre diameter (µm)**	**Test type**	**Nr. of specimens**	**Specimen dimensions (mm)**
UPy-PCL	JV1178D-4	4.08	2.6	Uniaxial test	4	10×50
	JV1178D-7	4.17	2.6	Uniaxial test	4	10×50
UPy-PCL	JV1177C-2	3.98	2.3	Uniaxial test	4	10×50
	JV1177C-12	4.11	2.3	Uniaxial test	4	10×50
UPy-PCL	JV1173C-4	7.10	2.0	Uniaxial test	4	10×50
	JV1173C-6	7.55	2.0	Uniaxial test	4	10×50
UPy-PCL	JV1178D-5	4.11	2.6	Isotropy test	16	5×25
UPy-PCL	JV1178C-7	6.47	2.0	Absorption test	16	5×25
UPy-PCL	JV1177C	3.8-4.7	2.3	Sterilization	5	10×40
UPy-PCL	JV1178D-7	3.96	2.6	Degradation (0d) + cyclic test	4	5×25
				Degradation (42d) + cyclic test	8	5×25
				Degradation (90d) + cyclic test	8	5×25
UPy-PCL	JV1177C-7	4.17	2.3	Degradation (0d) + cyclic test	4	5×25
				Degradation (42d) + cyclic test	8	5×25
				Degradation (90d) + cyclic test	8	5×25
UPy-PCL	JV1173C-12	7.07	2.0	Degradation (0d) + cyclic test	4	5×25
				Degradation (42d) + cyclic test	8	5×25
				Degradation (90d) + cyclic test	8	5×25
Restorelle	5114043	8.5	80	Uniaxial test	4	10×50
				Isotropy test	8	10×50
				Absorption test	8	10×50
				Degradation (0d) + cyclic test	4	10×50
				Degradation (42d) + cyclic test	8	10×50
				Degradation (90d) + cyclic test	8	10×50

2.3 Simulated degradation and cyclic loading test protocols

This part of the work was conducted in accordance with the ISO 10993 "Biological evaluation of medical devices" standard [23]. To study processes of dissolution and resorption *in vitro*, Phosphate Buffer Saline (PBS; Sigma Aldrich) solution of pH 7.4, as a proxy of biological fluid [24], was used. To study biodegradation in an acid environment as in the presence of inflammation, a solution of Potassium Hydrogen Phthalate (KHP; Sigma Aldrich) with pH 4.3 was used. Details are provided in Supplement 3.

2.4 Statistical Methods

Statistics were done using GraphPad Prism 5 (GraphPad Software, Inc., La Jolla, CA, USA). Normality of the data was verified using the Kolmogorov-Smirnov test. Quantitative data are reported as mean ± standard error of the mean (SEM). For comparison between materials, disruption force and strain were analysed using one-way ANOVA analysis. The level of significance was set to $p<0.05$. Dunnett's post-test correction was used to determine whether the differences between multiple pairs were statistically significant. For intra-material comparisons, longitudinal versus transversal comparison, wet versus dry comparisons and to determine the difference in elongation, thickness and in weight loss after degradation and cyclic loading an unpaired Student´s t-test was used (confidence level of 95%). The level of significance was set to $p<0.05$.

3. Results

3.1 UPy-PCL mesh architecture

The architecture of UPy-PCL electrospun meshes are displayed in Figure 1. All meshes are composed of solid, uniform fibres. No signs of beads were observed, nor any indications of fibres fusion. Due to the 3-dimensional dispersed fibres, pore sizes and shape, the distances between the fibres are difficult to measure exactly (c.a. 10 µm). In this respect, UPy-PCL meshes behave like scaffolds.

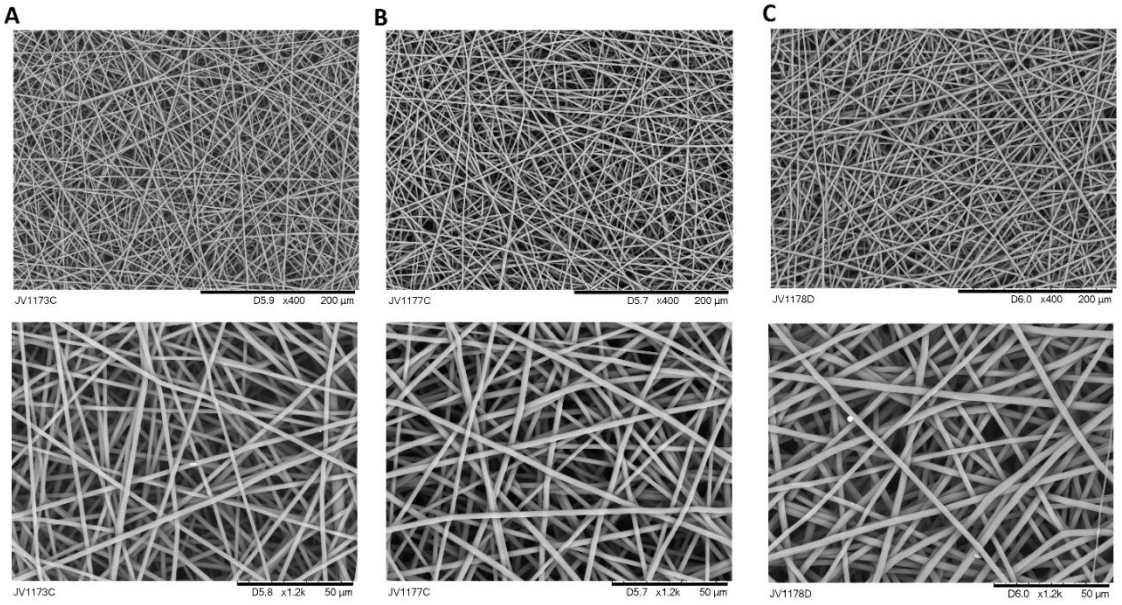

Fig. 1 Scanning electron microscope images of UPy-PCL mesh: A (JV1173C, 2.0 µm), B (JV1177C, 2.3 µm), C (JV1178D, 2.6 µm)

3.2 Impact of sterilization

The force-strain curves (Figure 2) resulting from uniaxial mechanical testing are characteristic for a non-woven mesh made of a semi-elastic polymer. The corresponding forces of the original and sterilized UPy-PCL samples are in the range of reversible deformation (Supplementary Table 1) [25]. The UPy-PCL provides sufficient ultimate

stress and elasticity (Young modulus) to the mesh, and sets itself apart from meshes made from neat PCL that show a yield point with extensive deformation, as reported earlier [22]. Moreover, comparing the force-strain profiles and the numeric values of both meshes reveals that there is no significant change after sterilization, and the differences in numerical values are within the statistical error.

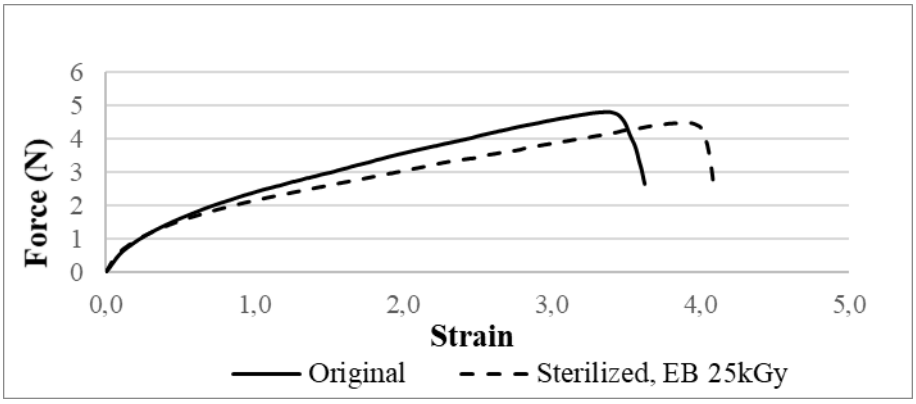

Fig. 2 Example force-strain profiles of UPy-PCL mesh, original and after sterilization by EB.

3.3 Mechanical properties

Extensive examination of various types of sterile UPy-PCL resulted in data regarding the maximum load and strain that are compared in Figure 3. All UPy-PCL meshes have similar mechanical characteristics, which are significantly different from those of Restorelle. Overall, Restorelle mesh is much stiffer and quite resistant to fracture. In contrast, the UPy-PCL meshes are very compliant. The failure load for Restorelle XL was c.a. 17 N (elongation 60 %) and for UPy-PCL meshes it was in the range of 4-6 N (elongation 250-300 %) (Figure 3b). Significant differences in tensile properties were observed between different UPy-PCL meshes corresponding with different fibre diameters and the area density, as depicted in Supplementary Table 2.

The mechanical properties in the failure region showed that UPy-PCL mesh with a 2.3 μm fibre diameter had smaller load bearing capabilities (4.22 ± 0.07 N) than other UPy-PCL meshes. Meshes with fibre diameter 2.0 μm and density of 7.55 g/cm$_2$ sustained higher maximum loads (6.87 ± 0.14 N; $p<0.001$). For the same fibre diameter, mesh density influenced mesh strain at failure since the denser meshes were less extensible (Supplementary Table 2).

Tensile properties of the Restorelle (PP) mesh were isotropic (Figure 4), whereas slight anisotropic behaviour was observed for UPy-PCL (JV1178D; Figure 4). The transverse direction of UPy-PCL was more compliant and showing a lower failure load (2.25 ± 0.03 N), while the longitudinal direction was more resistant to deformation (2.66 ± 0.05 N) (Supplementary Table 3).

Figure 5 displays the tensile data on UPy-PCL (JV1178D) and Restorelle mesh before and after water absorption. Saturation with water slightly changed the properties of electrospun mesh, by increasing its elongation by 15%, while it lowered resistance to loads by 10% ($p<0.05$, Supplementary Table 3). The mechanical behaviour of Restorelle

(PP) mesh after water absorption was not different as compared to without water absorption (Figure 5).

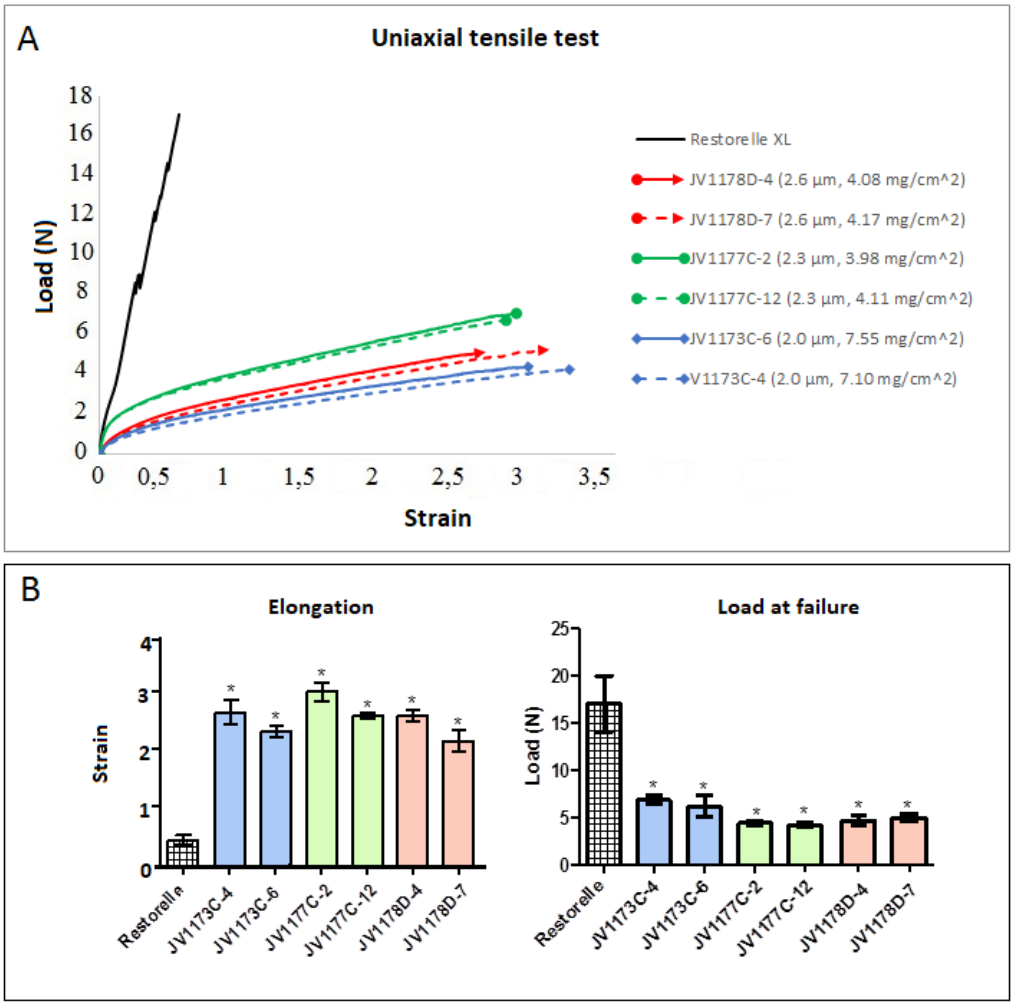

Fig. 3 **a**- Tensile properties of the Restorelle and UPy-PCL meshes by mean force–strain curves. **b**- Vertical column bar graphs mean with ± SEM of uniaxial properties. Electrospun mesh have significantly different properties from Restorelle $p<0.05$ (∗).

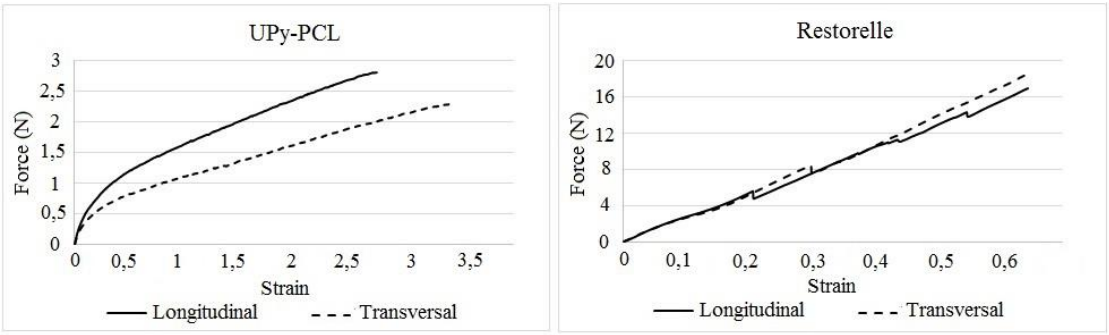

Fig. 4 Tensile properties of UPy-PCL (JV1178D) and Restorelle, mean force-strain curves in longitudinal and transverse directions.

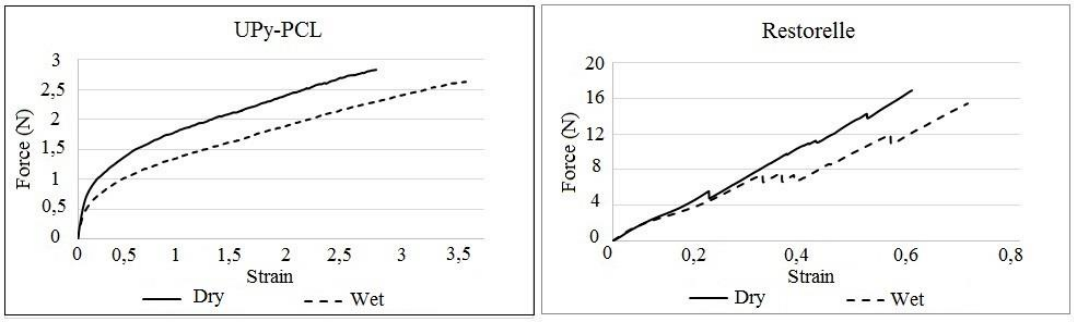

Fig. 5 Tensile properties of UPy-PCL (JV1178D) and Restorelle meshes in dry and wet conditions; mean force–strain curves (both in longitudinal direction).

3.4 Simulated degradation and cyclical loading

The results of the degradation and cyclic loading tests of the electrospun UPy-PCL meshes were very different depending on the fiber diameters. Detailed results can be found in Figure 6 and Supplementary Tables 4-6. When looking at the weight changes there were no significant changes during the *in vitro* degradation testing, whatever the fiber diameter used in UPy-PCL meshes.

Weight changes were up to -7.5%, the actual values depending on the incubation medium and the time point. Overall, the mesh thickness significantly reduced during simulated degradation. For example, the 2.0 μm meshes thinned by around 20-25% (42 days) to 35-40% (90 days) depending on the medium used ($p<0.05$; Figure 6a). The same pattern was observed in the 2.3 and 2.6 μm meshes, i.e. a progressive reduction in thickness of a similar magnitude (e.g. for 2.3 μm it was 12- 15% at 42 d, and 30-33% at 90 d; $p<0.01$). When exposed to stepwise progressive cyclical loading all UPy-PCL underwent plastic deformation (Figure 6). The only mesh type resisting repetitive forces to some extent was the one with fiber diameter 2.0μm. The mechanical properties deteriorated significantly when the meshes were exposed to an acid medium for 90 days (Supplementary Table 4). The other ones were very fragile: they were deforming drastically under low load.

Conversely, the thickness of Restorelle (PP) remained unchanged (-1 to 2%; Figure 7), irrespective of the conditions. There was neither weight loss during simulated degradation. The force-elongation curves were however significantly different for dry and degraded samples (Supplementary Table 6). In both settings, Restorelle undergoes permanent plastic deformation. After the first cycle at 3 N/cm load, the permanent deformation of Restorelle dry mesh was 6%; it was less following degradation in KHP (acid medium) or PBS (neutral medium) (4%; $p<0.01$). The deformation increased at each stepwise increase in force (to 4 and 5 N/mm) following the same pattern, i.e. more in dry than in wetted meshes. PP mesh did not disrupt in the third period of cyclic loads (5 N/cm), yet deformed by ≥ 60% (dry) and ≥ 40% (90d of degradation).

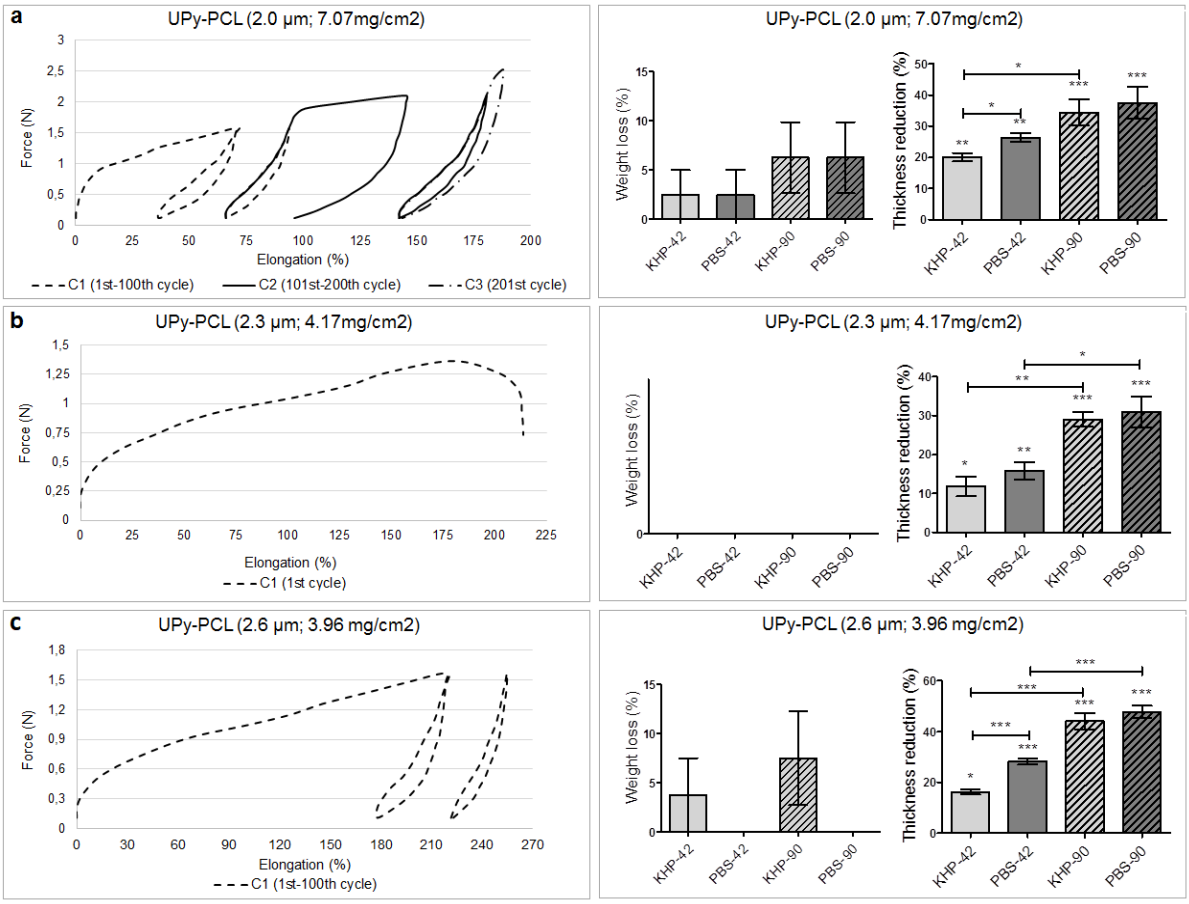

Fig. 6 **a, b, c** - UPy-PCL (2.0 µm), UPy-PCL (2.3 µm) and UPy-PCL (2.6 µm) electrospun mesh properties under cyclic loading (C1-C3), representative load–elongation curves- left; vertical column bar graph, (mean ± SEM) of the mesh weight and thickness loss- right.

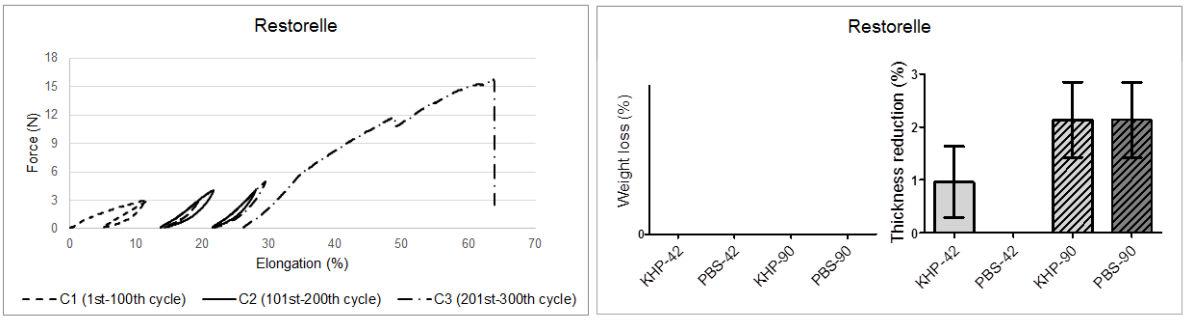

Fig. 7 Restorelle mesh properties under cyclic loading (C1-C3), representative load–elongation curve- left; vertical column bar graph, (mean ± SEM) of the mesh weight and thickness loss- right.

4. Discussion

Herein we performed a series of *in vitro* experiments with novel electrospun degradable implants to assess their mechanical performance in comparison to an often clinically used lightweight textile PP mesh. The dry characteristics of UPy-PCL were not affected by electron beam irradiation for sterilization. First, the electrospun UPy-PCL meshes are significantly less stiff than PP. This property has also been described for other electrospun materials, based on other polymers [4]. It is believed that this a beneficial

feature, because it matches better with the properties of native host tissues. Second, the UP-PCL implants were anisotropic, in contrast to the reference mesh. The clinical relevance of anisotropy of mesh is however at present unknown [26], nevertheless it is anticipated that this may be advantageous for certain locations in the body. Given the predominant loading state *in vivo* is biaxial; anisotropy might be a useful feature [26, 27]. Testing the dry characteristics of the mesh does not fully simulate what happens *in vivo.* We therefore investigated the biomechanical properties also in wet conditions. Whereas the compliance of PP did not change, that of UPy-PCL increased, irrespective of the fibre diameters used in the spinning. Water absorption alters the interactions (friction) between individual fibers of the implants. To reproduce *in vivo* loading conditions, the implants were exposed to cyclical loading. This would mimic the mechanical impact of physiological cyclic loads such as regular movement, breathing, and exceptional activities of for instance coughing, running, jumping, etc. [28, 29]. All UPy-PCL implants showed hysteresis in the first cycle that were greater than what was measured in Restorelle. When the loads were increased, plastic deformation was greater for both materials. The same was observed after 90 days of simulated degradation, though the differences were less clear. These tests mimic the ability of shape memory or for the mesh to return to its original shape after stretching [30, 31]. Plastic deformation occurring after implantation has been named as a cause of GRCs [32, 33].

We also simulated degradation, both in acid as well as more neutral media. The former was to mimic the conditions locally present, by the inflammatory response. Inflammation creates an unfavorable environment characterized by a local acid pH [34]. Over time, UPy-PCL meshes did not demonstrate significant weight loss. It is known that pristine PCL is degraded by hydrolysis (a process that can be catalyzed by acid), whereas it's modified form UPy-PCL is rather degraded by oxidation [35]. We therefore assume that this simulated environment did not oxidize the implant.

The implants however were thinning progressively. Since the mass loss was minor, it is believed that the mesh geometry did change after degradation, with collapse and denser packing of fibres. It appears that none of the two processes happened to the PP.

This experiment has several strengths, such as simulation of hydration, degradation and the use of repetitive physiological loads. Such testing apparently discloses different information than dry characterization. However, the current experiment does not necessarily predict that all these changes would indeed develop *in vivo*. The material will be remodelled by the host; hence the ingrowing tissue may lead to different properties of the mesh. We will further investigate the fate of these meshes in animal models and draw parallels to these findings whenever possible. There are other shortcomings, such as the lack of physical characterisation of the mesh geometry, e.g. by analysis under the electron microscope, or the actual performance under biaxial testing.

5. Conclusion

In vitro mechanical performance testing of novel UPy-PCL electrospun implants showed that they are more compliant than a reference lightweight textile polypropylene. Both materials undergo permanent plastic deformation, however the electrospun does more so. Simulated degradation induces significant geometrical and mechanical property

changes under cyclical load. A future experiment should document changes *in vivo*, because then other factors such as tissue ingrowth will modify that process. However, controlled *in vitro* extensive degradation testing preceding the implantation may complement animal trials to understand the material, the design, and the manufacturing factors that would affect *in vivo* implant ingrowth. This may eventually reduce the number of animal experiments.

Acknowledgement

This research has been supported in part by a grant of the EC in the FP7-framework (Bip-Upy; NMP3-LA-2012-310389). The EC does not bear any responsibility for any statement made in this paper. Some authors have been supported by the Fundação para a Ciência e a Tecnologia I.P. (FCT, Portugal) under the grants SFRH/BD/96548/2013 and SFRH/BPD/111846/2015. We also gratefully acknowledge the funding of Project UROSPHINX - Project 16842, co-financed by Programa Operacional Competitividade e Internacionalização (COMPETE2020), through Fundo Europeu de Desenvolvimento Regional (FEDER) and by National Funds through FCT – Fundação para a Ciência e Tecnologia. JDP was a clinical researcher financed by the Fonds Wetenschappelijk Onderzoek Vlaanderen.

Conflict of interest statement

The authors do not have to disclose any financial or personal relationships with other people or organizations that could inappropriately influence (bias) their work.

References

[1] Maher C, Feiner B, Baessler K, Christmann-Schmid C, Haya N, Marjoribanks J. „Transvaginal mesh or grafts compared with native tissue repair for vaginal prolapse," Cochrane, 2016.

[2] Abed H, Rahn DD, Lowenstein L, Balk EM, Clemons JL, Rogers RG, „Incidence and management of graft erosion, wound granulation, and dyspareunia following vaginal prolapse repair with graft materials: a systematic review," Int Urogynecol J, vol. 22, nr. 7, pp. 789-798, 2011.

[3] Manodoro S, Endo M, Uvin P, Albersen M, Engels A, Schmidt B, De Ridder D, Feola A, Deprest J. „Graft-related complications and biaxial tensiometry following experimental vaginal implantation of flat mesh of variable dimensions," BJOG, pp. 120-124, 2013.

[4] Roman S, Mangir N, Bissoli J, MacNeil S. „Biodegradable scaffolds designed to mimic fascia-like properties for the treatment of pelvic organ prolapse and stress urinary incontinence," Journal of Biomaterials Applications, vol. 30, nr. 10, pp. 1-11, February 2016.

[5] Cobb WS, Kercher KW, Heniford BT, „The argument for lightweight polypropylene mesh in hernia repair," Surg. Innov. pp. 63-69, 2005.

[6] Brown AS, Yang C, Fung KY, Bachem A, Bourges D, Bedoui S, Hartland EL, Van Driel IR, „Cooperation between Monocyte-Derived Cells and Lymphoid Cells in the Acute Response to a Bacterial Lung Pathogen," PLOS, nr. http://dx.doi.org/10.1371/journal.ppat.1005691, June 14, 2016.

[7] Liang R, Zong W, Palcsey S, Abramowitch S, Moalli PA, „Impact of prolapse meshes on the metabolism of vaginal extracellular matrix in rhesus macaque," American Journal of Obstetrics and Gynecology, vol. 212, nr. 2, p. 174.e1–174.e7, February 2015.

[8] Liang R, Abramowitch S, Knight K, Palcsey S, Nolfi A, Feola A, et al., „Vaginal degeneration following implantation of synthetic mesh with increased stiffness.," BJOG, vol. 120, nr. 2, pp. 233-43, 2013.

[9] Feola A, Abramowitch S, Jallah Z, Stein S, Barone W, Palcsey S, Moalli PA, „Deterioration in biomechanical properties of the vagina following implantation of a high-stiffness prolapse mesh," BJOG, vol. 120, p. 224–232, 2013.

[10] Maurer MM, Röhrnbauer B, Feola A, Deprest J, Mazza E, „Prosthetic Meshes for Repair of Hernia and Pelvic Organ Prolapse: Comparison of Biomechanical Properties," Materials, vol. 8, pp. 2794-2808, 2015.

[11] Villarreal-Gómez LJ, Cornejo-Bravo JM, Vera-Graziano R, Grande D, „Electrospinning as a powerful technique for biomedical applications: a critically selected survey," J Biomater Sci Polym, vol. 27, nr. 2, pp. 157-176, 2016.

[12] SF Programme, „Bioactive Implantable Polymers based on Ureido-Pyrimidinone," Seventh Framework Programme, [Online]. Available: http://www.bipupy.eu/. [Geopend 25 05 2018].

[13] Brunsveld L, Folmer BJ, Meijer EW, Sijbesma RP, „Supramolecular polymers," Chem. Rev., vol. 12, p. 4071–4098, 2001.

[14] Sijbesma RP, Beijer FH, Brunsveld L, Folmer BJB, Hirschberg JK, Lange RFM, Lowe JKL, Meijer EW, „Reversible polymers formed from self- complementary monomers using quadruple hydrogen bonding," Science, vol. 278, pp. 1601-1604, 1997.

[15] Sontjens SHM, Renken RAER, van Gemert GML, Engels TAP, Bosman AW, Janssen HM, Govaert LE, Baaijens FPT, „Thermoplastic elastomers based on strong and well-defined hydrogen-bonding interactions," Macromolecules, vol. 41, pp. 5703-5708, 2008.

[16] Bastings MM, Koudstaal S, Kieltyka RE, Nakano Y, Pape AC, Feyen DA, van Slochteren FJ, Doevendans PA, Sluijter JP, Meijer EW, Chamuleau SA, Dankers PY. „A fast pH-switchable and self-healing supramolecular hydrogel carrier for guided, local catheter injection in the infarcted myocardium". Adv Healthc Mater., vol. 3, nr. 1, pp. 70-78, 2014.

[17] Dankers PYW, Harmsen MC, Brouwer LA, Van Luyn MJA, Meijer EW, „A modular and supramolecular approach to bioactive scaffolds for tissue engineering," Nature Materials, vol. 4, p. 568–574, 2005.

[18] Cipitria A, Skelton A, Dargaville TR, Dalton PD, Hutmacher DW, „Design, fabrication and characterization of PCL electrospun scaffolds—a review," Journal of Materials Chemistry, vol. 21, p. 9419–9453, 2011.

[19] Hutmacher DW, Schantz T, Zein I, Ng KW, Teoh SW and Tan KC, „Mechanical properties and cell cultural response of polycaprolactone scaffolds designed and fabricated via fused deposition modeling," J Biomed Mater Res, vol. 55, pp. 203-216, 2001.

[20] Slack M, Ostergard D, Cervigni M, Deprest J, „A standardized description of graft-containing meshes and recommended steps before the introduction of medical devices for prolapse surgery," International Urogynecology Journal, vol. 23, p. 15–26., 2012.

[21] Rynkevic R, Martins P, Pereira F, Ramião N, Fernandes AA, „In vitro study of the mechanical performance of hernia mesh under cyclic loading.," J Mater Sci Mater Med., vol. 28, nr. 11, p. 176, 2017 .

[22] Janssen HM, Van Gemert G, Meijer E, Bosman A, „Preparation of supramolecular polymer containing quadruple hydrogen bonding units in the polymer backbone," Patent - US7838621, 2005.

[23] ISO 10993–2011, „Estimation of biological activity of medical products," 2011.

[24] ISO 13781–2011, „Resins and shaped elements poly-L-lactide for surgical implants. Degradation research in vitro.".

[25] Chantereau P, Brieu M, Kammal M, Farthmann J, Gabriel B, Cosson M, „Mechanical properties of pelvic soft tissue of young women and impact of aging," International Urogynecology Journal, vol. 25, nr. 11, p. 1547–1553 , 2014.

[26] Ozog Y, Konstantinovic ML, Werbrouck E, Ridder DD, Mazza E, Deprest J, „Shrinkage and biomechanical evaluation of light weight synthetics in a rabbit model for primary fascial repair," International Urogynecology Journal, vol. 22, p. 1099–1108, 2011.

[27] Saberski ER, Orenstein SB, Novitsky YW, „ Anisotropic evaluation of synthetic surgical meshes.," Hernia, vol. 15, nr. 1, pp. 42-52, 2011 Feb.

[28] Patterson S, Ho YC, Wang WC, „The Effect of Cyclic Loading on the Mechanical Performance of Surgical Mesh," ICEM, Vol. 6, 2010 .

[29] Tomaszewska A, „Mechanical behaviour of knit synthetic mesh used in hernia surgery," Acta Bioeng Biomech, vol. 18, nr. 1, pp. 77-86, 2016.

[30] Bringman S, Conze J, Cuccurullo D, Deprest J, Junge K, Klosterhalf B, Parra-Davila E, Ramshaw B, Schumpelick V, „Hernia repair: the search for ideal meshes," Hernia, vol. 14, nr. 1, pp. 81-87, 2010.

[31] Junge K, Klinge U, Prescher A, Giboni P, Niewiera M, Schumpelick V, „Elasticity of the anterior abdominal wall and impact for reparation of incisional hernias using mesh implants," Hernia, vol. 5, nr. 3, pp. 113-118, 2001.

[32] Baessler K, Maher CF, „Mesh augmentation during pelvicfloor reconstructive surgery: risk and benefits," Curr Opin Obstet Gynecol, vol. 18, p. 560–566, 2006.

[33] Abed H, Rahn DD, Lowenstein L, Balk EM, Clemons JL, Rogers RG; Systematic Review Group of the Society of Gynecologic Surgeons. „Incidence and management of graft erosion, wound granulation, and dyspareunia following vaginal prolapse repair with graft materials: a systematic review," Int Urogynecol J, vol. 22, nr. 7, pp. 789-798, 2011.

[34] Galgut P, Waite I, Smith R, „Tissue reaction to biodegradable and non-degradable membranes placed subcutaneously in rats, observed longitudinally over a period of 4 weeks," J. Oral Rehabil, vol. 23, pp. 17-21, 1996.

[35] Brugmans MCP, Söntjens SHM, Cox MAJ, Nandakumar A, Bosman AW, Mes T, Janssen HM, Bouten CVC, Baaijens FPT, Driessen-Mol A., „Hydrolytic and oxidative degradation of electrospun supramolecular biomaterials: In vitro degradation pathways," Acta Biomater., vol. 27, pp. 21-31, 2015.

Supplement 1:

All three batches were made by electro-spinning. The UPy-PCL polymer was dissolved in 15-17 wt% in a chloroform based organic solvent mixture (chloroform, methanol, acetonitrile, acetic acid). Electrospinning is done with the following parameters: Voltage (nozzle): -18.5 kV; Voltage(drum): +5 kV; Nozzle-drum distance: 22 cm; Drum speed: 3 s-1; Flow polymer solution: 5 ml/h; Dimension of drum: 25 cm diameter x 50 cm length. The polymer solution is pumped from a syringe-pump, and the syringe is heated to 40°C. The mesh is spun to the desired area density. After the spinning process, the mesh is stored in a vacuum oven overnight at 45°C/<1 mBar. Fiber size distribution is measured with Scanning Electron Microscopy (SEM), Hitachi TM3000. The mesh is cut to the sizes described in table 2 and weighed to determine the exact area density. They are then packaged with a molecular sieve desiccant pack in an atmosphere of nitrogen and sterilized by electron beam irradiation with a standard sterilization dose of 25 kGy.

Supplement 2:

For the primary characterisation electrospun and PP implants were cut into 50×10 mm strips along the longitudinal axis. This size was chosen in order to allow a clamp-to-clamp distance of 40 mm for a constant length-to-width aspect ratio of four, to minimize the nonlinear effects of clamping on the uniaxial biomechanical properties. A total of four specimens were obtained for each mesh and separately tested.

To characterize isotropy, measurements were performed in two perpendicular directions. UPy- PCL (JV1178D-5) mesh was divided along the longitudinal and transverse axis into sixteen 25×5 mm strips (eight strips in longitudinal direction, eight strips in transverse direction). As pattern and pore size influence the mechanisms of deformation of knitted meshes [36], Restorelle mesh was divided along its longitudinal axis into eight 50×10 mm strips (four strips in longitudinal direction and four transverse). For water absorption tests, UPy-PCL implants (JV1178C-7) were divided along their longitudinal axis into sixteen 25×5 mm strips. Restorelle mesh was divided along its longitudinal axis into eight 50×10 mm strips. Half of the strips were first soaked in normal saline (0.9% NaCl) at room temperature (20° C) for 24 hours prior to tensiometry.

For the degradation test, UPy-PCL meshes were divided along the longitudinal axis into 25x5 mm strips. A total of twenty specimens were obtained for each mesh type and divided for further testing as in Table 2. Restorelle mesh was divided along its longitudinal axis into twenty 50×10 mm strips, to include a minimum of 3 complete pores.

Supplement 3:

The thickness and initial weight of each specimen were measured before degradation. Specimens were kept at 37 ° C during 42 and 90 days. After degradation, the specimens were washed in distilled water, dried at room temperature during 24 hours and weighed. The material degradation was evaluated via the thickness change and weight loss. Dried specimens were used for further evaluation of the mechanical properties.

Cyclic tests were performed to mimic the effects of repetitive in vivo loads. UPy-PCL mesh failure load, under uniaxial tensile test of a 0.5 cm wide mesh sample, ranged from 3 to 6N/cm. Restorelle samples were loaded to 3N, 4N and 5N, respectively. As dimensions differ, 1.5N, 2N and 2.5N loads were applied for UPy-PCL mesh, the equivalent testing forces for linear force distributions of 3N/cm, 4N/cm and 5N/cm.

A preload of 0.11N was applied to remove the slack from the sample, using a constant elongation rate of 5 mm/min. The clamp-to-clamp distance was estimated using a digital imaging technique. After preloading, samples were loaded to the estimated forces and then unloaded back to 0.11N. A constant elongation rate of 5 mm/min was used. Three cyclic loading levels were set (C1, C2, C3), with 100 cycles at each level. After 300 cycles, samples were stretched to failure. The elongation (%) to the initial length of the sample was calculated.

The equipment used in this study is a prototype developed at INEGI Biomechanics Laboratory. The testing machine has four perpendicular alloy aluminium arms, connected to four actuators and two load cells (with a 50N capacity).

Supplemental tables

Table1. Mechanical test parameters UPy-PCL mesh (JV1177C), original and after sterilization by EB at 25 kGy.

UPy-PCL mesh	Young Modulus	σ	E
	MPa	MPa	[%]
Original	18.8 ± 1.0	14.6 ± 0.5	354 ± 21.5
EB sterilized	21.4 ± 1.6	12.9 ± 0.9	365 ± 38.9

Table2. Tensile properties of UPy-PCL mesh (mean with ± SEM) and statistical intra material comparisons using unpaired t-test, significant difference noted when p<0.05 (*), p<0.001 (***).

Mechanical properties of UPy-PCL meshes							
Mesh serial number	Nr	**JV1178D-4**	**JV1178D-7**	**JV1177C-2**	**JV1177C-12**	**JV1173C-4**	**JV1173C-6**
Density and fibre diameter		(4.08 mg/cm^2, 2.6 µm)	(4.17 mg/cm^2, 2.6 µm)	(3.98 mg/cm^2, 2.3 µm)	(4.11 mg/cm^2, 2.3 µm)	(7.10 mg/cm^2, 2.0 µm)	(7.55 mg/cm^2, 2.0 µm)
Force (N)	n = 4	4.72± 0.16	5.03± 0.11	4.47± 0.07	4.22± 0.07	6.88± 0.14	6.26± 0.33
Strain	n = 4	2.79 ± 0.12	3.38 ± 0.09	3.30 ± 0.07	3.45 ± 0.07	2.86 ± 0.08	3.07 ± 0.02
Intra material comparison							
		By fibre diameter (µm)			**By mesh density (mg/cm^2)**		
Mesh serial number	**Nr**	**JV1178D vs JV1177C**	**JV1178D vs JV1173C**	**JV1177C vs JV1173C**	**JV1178D-4 vs JV1178D-7**	**JV1177C-2 vs JV1177C-12**	**JV1173C-4 vs JV1173C-6**
Value		2.6 vs 2.3	2.6 vs 2.0	2.3 vs 2.0	4.08 vs 4.17	3.98 vs 4.11	7.10 vs 7.55
Force (N)	n=8	0,0017(**)	<0.0001(***)	<0.0001(***)	0,1710	0,0561	0,1617
Strain	n=8	0,0028(**)	0,3783	0,0081(**)	0,0032(**)	0,0044(**)	0,0101(*)

Table3. Tensile properties of the mesh (mean ± SEM) and statistical intra material comparisons using unpaired t-test, significance level was set to p<0.05 (*), p<0.001 (***).

Mechanical properties of meshes (isotropy testing)							
Restorelle	Nr. of the specimens	Force (N)	Strain	**UPy-PCL**	Nr. of the specimens	Force (N)	Strain
Longitudinal	n=4	17.08 ± 0.93	0.64 ± 0.02	Longitudinal	n=8	2.66 ± 0.05	3.06 ± 0.05
Transversal	n=4	17.71 ± 0.62	0.62 ± 0.03	Transversal	n=8	2.250 ± 0.03	3.55 ± 0.07
p value		0.5915	0.5503	P value		0.0001 (***)	0,0011 (**)
Mechanical properties of meshes (water saturation test)							
Restorelle	Nr. of the specimens	Force (N)	Strain	**UPy-PCL**	Nr. of the specimens	Force (N)	Strain
Dry	n=4	17.08 ± 0.93	0.63 ± 0.03	Dry	n=8	3.11 ± 0.08	3.25 ± 0.08
Wet	n=4	15.75 ± 1.07	0.67 ± 0.02	Wet	n=8	2.76 ± 0.09	3.77 ± 0.05
p value		0.1636	0.1357	P value		0,0160 (*)	0,0006 (***)

Table4. Elongation (mean (%) with ± SEM) of UPy-PCL (2.0 µm) electrospun mesh, during cyclic loading test (C1-C2), representing dry specimens and specimens after degradation (KHP and PBS) and three time points (0d, 42d., and 90d.). Significant difference among dry and degraded specimens was noted for p<0.05 (*), p<0.01 (**), p<0.001 (***)

Elongation (%)					
		C1 (3 N/cm)		**C2 (4 N/cm)**	
Time points	Nr of specimens	**1st cycle**	**100th cycle**	**101st cycle**	**200th cycle**
0d.	N=4	33.08 ± 2.18	61.71 ± 2.19	88.51 ± 4.73	133.71 ± 4.34
KHP-42d.	N=4	29.55 ± 1.67	53.78 ± 2.75	96.03 ± 2.97	NA
PBS-42d.	N=4	32.23 ± 2.72	56.79 ± 2.25	91.53 ± 4.58	141.20 ± 14.04
KHP-90d.	N=4	7.55 ± 1.46***	NA	NA	NA
PBS-90d.	N=4	25.45 ± 2.11	47.50 ± 3.58**	83.91 ± 3.79	NA

Table5. Elongation (mean (%) with ± SEM) of UPy-PCL (2.3 µm) and UPy-PCL (2.6 µm) electrospun meshes, during cyclic loading test (C1), representing dry specimens and specimens after degradation (KHP and PBS) and three time points (0d., 42d., and 90d.). Significant differences among dry and degraded specimens were set for p<0.05 (*), p<0.01 (**), p<0.001 (***)

Elongation (%)					
		UPy-PCL (2.3 µm)		**UPy-PCL (2.6 µm)**	
		C1 (3 N/cm)		**C1 (3 N/cm)**	
Time points	Nr of specimens	**1st cycle**	**100th cycle**	**1st cycle**	**100th cycle**
0d.	N=4	198.3 ± 8.34	NA	177.3 ± 19.83	229.5 ± 8.087
KHP-42d.	N=4	93.59 ± 10.35**	NA	121.2 ± 14.63	NA
PBS-42d.	N=4	190.7 ± 6.36	NA	230.5 ± 22.62	NA
KHP-90d.	N=4	11.35 ± 5.66***	NA	9.010 ± 1.786**	NA
PBS-90d.	N=4	174.2 ± 7.71	NA	203.5 ± 16.54	NA

Table6. Elongation (mean (%) with ± SEM) of Restorelle mesh, during cyclic loading test (C1-C3), representing dry specimens and specimens after degradation (KHP and PBS) and three time points (0d., 42d., and 90d.). Significant difference among dry and degraded specimens was set up when p<0.05 (*), p<0.01 (**), p<0.001 (***)

Elongation (%)							
		C1 (3 N/cm)		**C2 (4 N/cm)**		**C3 (5 N/cm)**	
Time points	Nr of specimens	**1st cycle**	**100th cycle**	**101th cycle**	**200th cycle**	**201st cycle**	**300th cycle**
0d.	N=4	5.93 ± 0.39	15.33 ± 0.66	15.99 ± 0.61	22.56 ± 1.39	22.78 ± 1.366	63.93 ± 2.16
KHP-42d.	N=4	4.08 ± 0.14***	10.13 ± 0.26***	10.44 ± 0.27***	15.38 ± 0.37**	16.73 ± 1.32*	54.67 ± 1.72*
PBS-42d.	N=4	4.24 ± 0.21**	10.15 ± 0.41***	10.39 ± 0.43***	16.65 ± 0.31**	16.85 ± 0.32**	50.28 ± 1.66**
KHP-90d.	N=4	3.55 ± 0.29**	9.46 ± 0.46***	9.96 ± 0.65***	15.14 ± 1.16**	15.52 ± 1.16**	39.19± 1.52 ***
PBS-90d.	N=4	4.33 ± 0.26*	10.73 ± 0.62**	11.03 ± 0.63**	17.78 ± 1.17*	17.96 ± 1.14*	41.40 ± 1.54***

CHAPTER 4

ASSESSMENT OF ELECTROSPUN AND ULTRA-LIGHT-WEIGHT POLYPROPYLENE MESHES IN THE SHEEP MODEL FOR VAGINAL SURGERY

Lucie Hympánová MD [a,b,c], Rita Rynkevic MSc [a,b,f], Sabiniano Román PhD [g], Marina G. M. C. Mori da Cunha PhD [a,b], Prof. Edoardo Mazza [h,i], Manuel Zündel PhD [h], Iva Urbánková MD [a,b,c], Monica R. Gallego PhD [e], Jakob Vange MSc [e], Geertje Callewaert MD [a,b,d], Prof. Christopher Chapple [j], Prof. Sheila MacNeil [g], Prof. Jan Deprest [a,b,d]

[a] Centre for Surgical Technologies, Group Biomedical Sciences, KU Leuven, Leuven, Belgium
[b] Department of Development and Regeneration, Woman and Child, Group Biomedical Sciences, KU Leuven, Leuven, Belgium
[c] Institute for the Care of the Mother and Child, Third Faculty of Medicine, Charles University, Prague, Czech Republic
[d] Pelvic Floor Unit, University Hospitals KU Leuven, Leuven, Belgium
[e] Coloplast A/S, Global R&D, Biomaterials, Humlebæk, Denmark
[f] INEGI, Faculdade de Engenharia da Universidade do Porto, Universidade do Porto, Porto, Portugal
[g] Department of Materials and Science Engineering, Kroto Research Institute, University of Sheffield, Sheffield, United Kingdom
[h] Institute of Mechanical Systems, ETH Zurich, Zurich, Switzerland
[i] EMPA, Swiss Federal Laboratories for Materials Science and Technology, Dübendorf, Switzerland
[j] The Royal Hallamshire Hospital, Sheffield, United Kingdom

Key words: Biocompatibility; Biomaterials; Biomechanics; Pelvic organ prolapse; Vaginal surgery

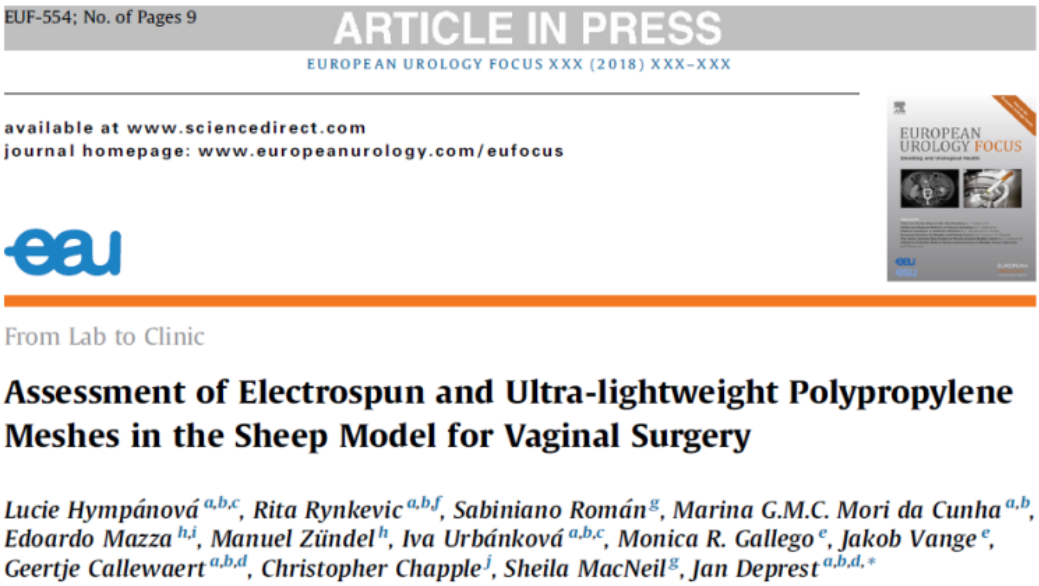

EUF-554; No. of Pages 9
ARTICLE IN PRESS
EUROPEAN UROLOGY FOCUS XXX (2018) XXX–XXX
available at www.sciencedirect.com
journal homepage: www.europeanurology.com/eufocus
EUROPEAN UROLOGY FOCUS
From Lab to Clinic

Assessment of Electrospun and Ultra-lightweight Polypropylene Meshes in the Sheep Model for Vaginal Surgery

Lucie Hympánová [a,b,c], Rita Rynkevic [a,b,f], Sabiniano Román [g], Marina G.M.C. Mori da Cunha [a,b], Edoardo Mazza [h,i], Manuel Zündel [h], Iva Urbánková [a,b,c], Monica R. Gallego [e], Jakob Vange [e], Geertje Callewaert [a,b,d], Christopher Chapple [j], Sheila MacNeil [g], Jan Deprest [a,b,d,]*

In press in the Journal European Urology Focus (2018)

ABSTRACT

Background: There is an urgent need to develop better materials to provide anatomical support to the pelvic floor without compromising function.

Objective: Our aim was to assess outcomes after simulated vaginal prolapse repair in a sheep model, using three different materials: (1) ultra-light-weight polypropylene (PP) non-degradable textile (Restorelle) mesh, (2) electrospun biodegradable ureidopyrimidinone-polycarbonate (UPy-PC) and (3) electrospun non-degradable polyurethane (PU) mesh, by comparison to simulated native tissue repair (NTR). These implants may reduce implant-related complications and avoid vaginal function loss.

Design: A controlled trial in 48 ewes which underwent NTR or mesh repair with either PP, UPy-PC or PU meshes (n=12/group). Explants were examined 60 and 180 days (6/group each) postimplantation.

Intervention: Posterior rectovaginal dissection, NTR or repair with mesh.

Outcome Measurements and Statistical Analysis: Implant-related complications, vaginal contractility, compliance and host response were assessed. Power calculation and ANOVA testing were used to enable comparison between the four groups.

Results: There were no visible implant–related complications. None of the implants compromised vaginal wall contractility and passive biomechanical properties were similar to those after NTR. Shrinkage over the surgery area was around 35% for NTR and all mesh augmented repairs. All materials were integrated well with similar connective tissue composition, vascularization and innervation. The inflammatory response to all were mild with electrospun implants inducing both more macrophages yet with relatively more type 2 macrophages present at an early stage than the PP mesh

Conclusions: Three very different materials were all well tolerated in the sheep vagina. Biomechanical findings were similar for all mesh augmented and native tissue repairs. Constructs induced slightly different mid-term inflammatory profiles.

Patient Summary: Product innovation is needed to reduce implant-related complications. We tested two novel electrospun and an ultra-light-weight textile PP implant in a physiologically relevant model for vaginal surgery. All gave encouraging outcomes.

Acknowledgement

We thank Rosita Kinnart and Ivan Laermans (Centre for Surgical Technologies, KU Leuven), Catherine Luyten and Petra Stevens (Department of Development and Regeneration, G-PURE laboratory, KU Leuven) for technical support. We thank Tristan Mes and Anton Bosman (SupraPolix BV, Eindhoven, The Netherlands) for kindly providing the UPy-PC material, Radoslaw Wach and Alicja Olejnik (TUL, Lodz, Poland) for material sterilization and Patricia Dankers (TU Eindhoven, Eindhoven, The Netherlands).

Disclosures

This work has been in part supported by the European Commission in its 7th framework program (BiP-UPy; NMP3-LA-2012-310389), including the stipend of LH, MC. The research program of JD has received funding from Johnson & Johnson, Blasingame, Burch, Garrard and Ashley (Atlanta, GA), Clayton Utz (Sydney, Australia). Agreements are handled via the KU Leuven transfer office LRD. MZ and EM were supported by the Swiss National Science Foundation under Grant SNF 155918. RR, SR, IU, MG, GC, SM and CHCH report no conflict of interest.

Take home message

Three very different materials (two electrospun, degradable ureidopyrimidinone-polycarbonate, non-degradable polyurethane and ultra-light-weight polypropylene) were all well tolerated in the sheep vagina and did as well as native tissue repair. While the biomechanical properties were similar, the inflammatory profiles were slightly different.

1. Introduction

In women, the prevalence of pelvic organ prolapse (POP) is 5-10% [1]. The overall life-time risk for POP surgery is 20% [2]. Surgical techniques seek to provide support to the pelvic organs without compromising function. Initially polypropylene (PP) meshes, as used in hernia repair, were used for vaginal insertion as well, but were found to induce implant-related complications (IRC) of around 10% [3]. The severity and the difficulty of treating IRC have led to several manufacturers withdrawing their meshes from the market. Current techniques in pelvic reconstruction surgery are being re-examined and stakeholders agree that there is an urgent need to develop and critically assess materials to improve long-term cure rates without increasing the risk of complications [4,5].

The materials used most commonly consist of knitted durable PP. Over time heavy-weight materials have been replaced by more open, lighter meshes, as the latter experimentally induce a milder host response, potentially reducing the risk of complications [6]. There are at least three hypotheses for why current implants cause adverse effects in woman: physical mismatching between the mechanical properties of the material and that of the host tissue, i.e. the PP implants cope badly with sustained deformation [7]; the response to the bulk PP material stimulates a chronic foreign body reaction which is ever ongoing; and the combination of the two, the use of the material known to provoke sustained inflammation in a specific site in the body for which it is not appropriately designed.

An alternative to knitted constructs is to use non-textile electrospun materials with an extracellular matrixlike structure [8]. Electrospun materials facilitate cell adherence, infiltration and natural extracellular matrix production [9,10]. We spun polycarbonate (PC) modified by ureidopyrimidinone (UPy) motifs. UPy-PC is a thermoplastic elastomer with PC soft blocks and hard blocks composed of interacting and phase separated hydrogen bonding units based on the 2-ureido-[1H]-pyrimidin-4-one (UPy) motif [11]. PC are degradable polyesters, which have been succesfully used in nerve and bone regeneration guidance [12,13]. UPy-modified polymers have been designed to be used as drug delivery vehicles, e.g. in a porcine myocardial infarction model [14] and in a modular approach as a bioactive elastomeric material for tissue engineering [15]. We earlier showed that reconstruction of the abdominal wall with meshes spun from supramolecular polyesters modified with UPy conserve biomechanical properties of native tissue [16]. An alternative approach is to use a non-degradable polyurethane (PU), which we have shown withstands in vitro repetitive strain better than heavier weight PP (GynecareTM, Johnson & Johnson, weight: 96.6g/m2) [7]. Also, PU was well integrated in the rabbit abdominal wall inducing a predominantly macrophage type 2 (M2) response when compared to commercially available heavy weight GynecareTM PP which induces a sustained inflammation predominated by macrophages type 1 (M1) [17].

The vaginal environment differs biomechanically and generates a different inflammatory response compared to other body locations [18]. Neither the degradable UPy-PC nor the non-degradable PU electrospun implants have been tested in an animal model for vaginal surgery. Therefore, we aimed to use the sheep to evaluate these two materials and wanted to compare outcomes to a simulated native tissue repair (NTR) and implantation with a novel generation lighter-weighted PP, that has better biomechanical

properties and yields a more favorable inflammatory response than other PP constructs [19–21]. Neither have been tested in the sheep model for vaginal surgery before. We assessed the functional repair including tissue morphology, contractility and passive biomechanical properties of the vagina and the host cellular response.

2. Materials and methods

2.1 Implants

Three types of implants were used: (1) ultra-light-weight textile PP Restorelle (Coloplast, Humlebaek, Denmark) (fiber diameter 80µm, pore size 1.6-2.0mm) [16]; (2) electrospun UPy-PC and (3) electrospun PU [17]. The electrospinning process of the single layer UPy-PC [16] and trilayer PU mesh, which had a design of random-aligned-random orientated fibers are described in supplement 1. The microstructure of both electrospun meshes was confirmed by electron microscopy (data not shown; supplementary figure 1), with a thickness of around 300µm, fibre diameter of 1-2µm and pore sizes of 10-20µm. Vaginal implants measured 35x35mm.

2.2 Animals, surgical procedure, and study design

Anesthesia and surgical procedures are detailed in supplement 2. Prior to surgery 48 multiparous Lakens sheep were randomly divided into four groups: three for mesh implantation; a fourth underwent primary NTR by a single surgeon (LH). Based on a power calculation for the primary outcome variable (passive biomechanics; supplement 3), 6 animals per group were required. Ewes underwent posterior vaginal wall surgery as previously described [22]. Following hydro-dissection, the rectovaginal septum was dissected to create space for the implant. Meshes were fixed with interrupted non-degradable 3/0 polypropylene sutures (Prolene®, Ethicon, Zaventem, Belgium) in the corners and halfway along each side (figure 1a, b).

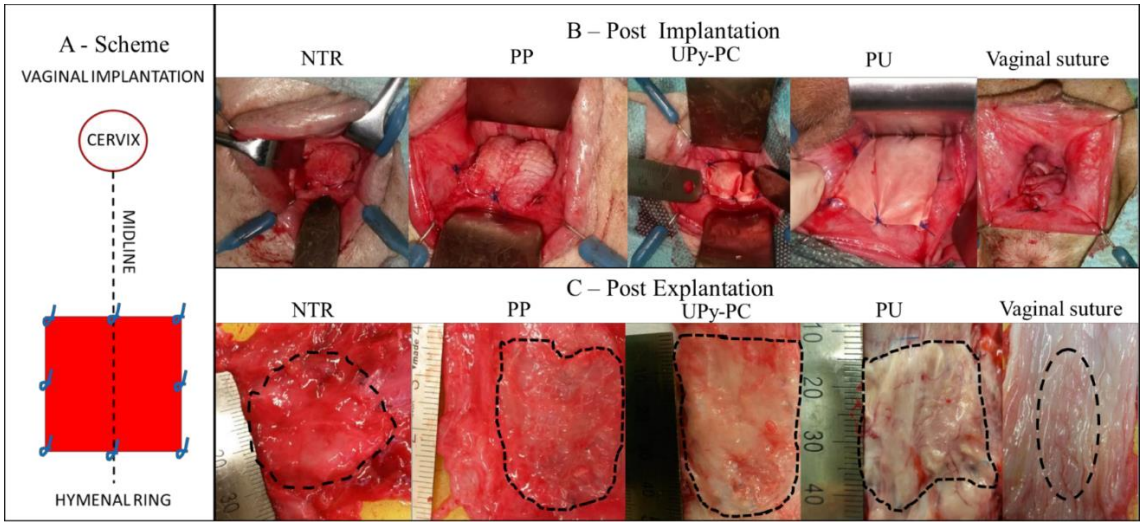

Fig. 1 Schematic drawing of posterior vaginal wall mesh implantation 3cm from the hymenal ring, fixed with permanent polypropylene stitches. B. The visual appearance of native tissue repair prior to plication in the first figure, implanted meshes after fixation prior to vaginal closure in next three. The last figure is the vaginal wall after closure. C. The appearance of materials on the vaginal wall

post-explantation identified by the presence of non-degradable sutures. The last figure shows the healed vaginal closure.

NTR consisted of rectovaginal dissection, plication of the fascial structure over the rectum with three degradable 3/0 polyglactine 910 (Vicryl®, Ethicon) sutures and the borders of the operative field were marked with non-degradable PP sutures similar to the mesh groups. The vaginal wall was closed with a running 3/0 polyglactin 910 (Vicryl) suture. A vaginal tampon was inserted for 24 hours. Ewes were examined for postoperative complications and euthanized at 60 or 180 days after surgery.

2.3 Harvesting of implants

Ewes were premedicated and euthanized by intravenous pentobarbital (20mL/50kg Release®, Ecuphar, Oostkamp, Belgium). Further details are in supplement 4. During the gross anatomical examination, we looked for IRC (defined as in humans; i.e. prominence, separation, exposure) [23]. Exposure of a PP suture are reported separately. We looked also for fluid collection, infection, and synechiae (figure 1c, supplementary figure 3). The length and width of the implant area marked by the PP sutures were measured (supplementary figure 4) to calculate the shrinkage [16]. In the NTR group, similar measurements were made as a proxy for "shrinkage" of the dissection and suturing area. The vagina and perivaginal tissues were resected 'en bloc', the explant prepared and cut into three pieces for active (3x7mm) and passive biomechanical measurements (30mm diameter) and histology (5x5mm). The strip for active biomechanics was immediately tested. The sample for passive biomechanics was kept in 0.9% NaCl saline solution at room temperature until testing (< 5 hours after sacrifice). The histology specimen was fixed in 10% formalin solution

2.4 Active biomechanical testing

Vertical organ baths were filled with 37°C Krebs solution and bubbled with carbon dioxide and oxygen (supplement 5). Specimens were measured, weighed, hung in the system (figure 2a), twice pre-tensioned to 0.5mN and allowed to equilibrate for 60 min. Then specimens were subjected to contractile stimulation by increasing concentrations of KCl (10, 20, 40, 50, 80, 120mM). Contractile forces were recorded using custom-made software. Measurements were analyzed using Origin software (OriginLab Corporation; Northampton, US). All values were normalized to sample weight, transducer calibration and gravitation constant. Maximum contraction force at 80mM KCl was compared.

2.5 Passive biomechanical testing

Pre-implantation 'dry' materials were subjected to a uniaxial test in dry and wet conditions according to a standardized protocol [16,24]. Explant tensiometry was done using ball burst testing (figure 2a) with an 11.5mm plunger on a Zwick tensiometer (200N cell load) and TestExpert software (Zwick GmbH & Co. KG, Ulm, Germany) as described previously [25,26]. The thickness of the explants was measured, they were clamped with the epithelium facing up, the plunger was centered over the explant and preloaded to 0.1N. The plunger speed was 10mm/min. The test was aborted either when the specimen ruptured or the load force reached 200N. The force (N) - displacement (mm)

curves (figure 2b) were used to define the stiffness (i.e. $\Delta F/\Delta x$). To avoid uncertainties due to sample clamping and reference position, the structural stiffness was measured as the tangent of the force-displacement curve at a predefined force of 30N.

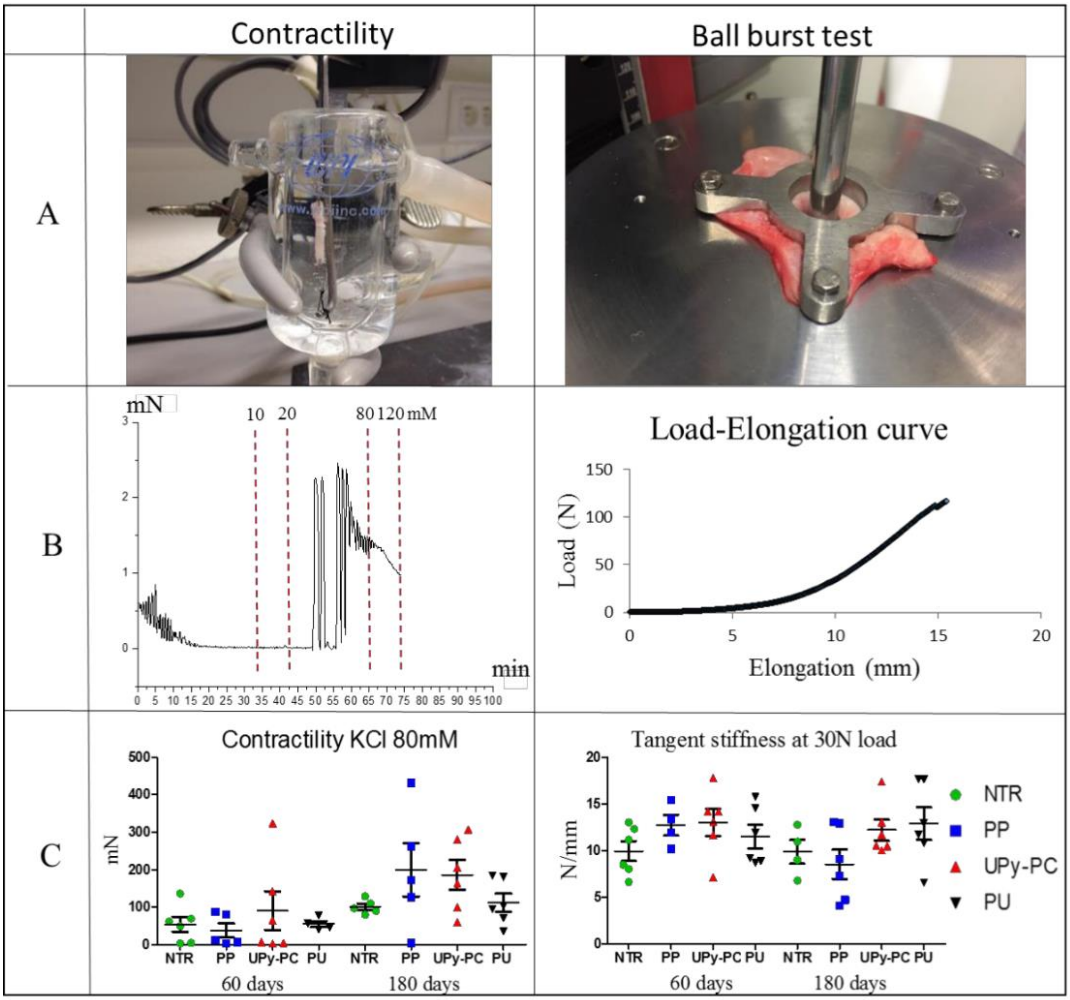

Fig. 2 Examination of mechanical properties and propensity of tissue to contract. A. The appearance of apparatus used to examine tissue contractility and to assess mechanical strength and stiffness of tissue using a ball burst apparatus. B. Representative contractility (force-time) and ball burst (load-elongation) curves. C. Results of vaginal contractility and stiffness with comparable results for all groups at both time points.

2.6 Morphological study

Haematoxylin and Eosin (H&E) and Gouldner's Trichrome staining were performed to quantify the foreign body giant cells (FBGC), polymorphonuclear cells (PMN), blood vessels and connective tissue [16,17,27]. Immunohistochemistry was performed to detect neovascularization (CD34), neuronal network (PGP 9.5), myofibroblast and smooth muscle (α-SMA), leukocytes (CD45), M1 (HLA-DR) and M2 (CD163) macrophages (supplement 6). Semi-quantitative readings were done by three researchers blinded to the treatment groups [17]. The M2/M1 ratio was calculated. The impact of implants on the

thickness of the lamina muscularis was assessed by measuring its thickness on α- SMA stain.

2.7 Statistics and ethics

Statistical analysis was performed with GraphPad Prism 7.0 (GraphPad Software, Inc; La Jolla, USA). Data normality was tested by the Kolmogorov-Smirnov test. Two-way ANOVA was used for normally distributed data and multiple comparisons between individual groups using a Tukey's test. The Kruskal-Wallis followed by the Dunn's post hoc test was used for data that was not normally distributed. Data are reported as mean ± SD or median and SE as appropriate. The significance level was defined as $p < 0.05$. This experiment was approved by the Ethics Committee on Animal Experimentation of the Faculty of Medicine, KU Leuven.

3. Results

3.1 Biomechanical characteristics of meshes prior to implantation

The stiffness of all materials was significantly reduced in wet conditions compared to dry (supplementary figure 2). The UPy-PC electrospun meshes had the lowest stiffness in these conditions. PP implants lost 25-30% of their stiffness within ten cycles of loading, in contrast to the two electrospun materials which showed relatively little change in response to cyclic deformation.

3.2 Gross anatomy

We did not observe any IRC. All implants looked well incorporated into the deeper vaginal tissues. There were two exposed PP sutures (n=1 NTR, n=1 UPy-PC) and 7 ewes developed limited vaginal synechiae along the mid-vaginal suture line that were not dividable by blunt dissection (n=2 NTR, n=3 PP, n=2 UPy-PC; supplementary figure 3). Macroscopically, UPy-PC appeared partially degraded in half of the ewes at 60 days and in 90% by 180 days. PU and PP appeared to be still intact. Shrinkage of vaginal implants was comparable between mesh groups and to that of the NTR at both time points (overall average 35.6±9.3%; data in supplementary table 2).

3.3 Mechanical properties

The highest contraction force was seen at 80mM KCl (figure 2b) hence this concentration was used for comparative purposes. All the vaginal tissues contracted to a similar extent and this was not significantly different to that of vaginal tissue from the NTRs (figure 2c). Ball burst testing also showed comparable mechanical properties which did not differ significantly from that in NTRs (figure 2c).

3.4 Cellular responses to implants

The infiltrate in the NTR explants showed very few inflammatory cells, and virtually no FBGC (Figure 3). In the other specimens, the implants could be recognized as being under the lamina propria and muscularis. There were no differences in the cellular infiltrate around the materials at day 60 and at 180 days, apart from the fact that in the UPy-PC group the material was progressively degraded. At 60 days, the UPy-PC mesh material was clearly recognizable over the entire length of the specimen. By 180 days

there was no recognizable material for two explants, in two it was visible in some areas, and in another two it was present over the entire explant. There was an abundance of inflammatory cells around the surface of all meshes (Figure 4). In PP implants, inflammatory cells were around the filaments, with looser connective tissue and vessels in between. In electrospun implants, the inflammatory infiltrate was denser filling the gaps between the more densely packed fibers. At 60 days, there were significantly more FBGC in UPy-PC than in PU implants (Figure 5a), yet not at the later time point.

The macrophage infiltrates (both M1 and M2) were most vigorous for the two electrospun meshes (UPy-PC and PU) as seen both at 60 and 180 days (Figure 6g). However, the extent of macrophage infiltration ratio of M2:M1 was very close to 1 for all groups by 180 days without any significant differences between them. The amount of connective tissue, thickness of the lamina muscularis and neovascularization were similar for all groups. Immunoreactivity for α-SMA tended to be lower in NTR samples, the difference being significant only when compared to UPy-PC at 60 days and to PU at 180 days. The neuronal stain showed small nerves close to the implants or dissection area (NTR) but the density of nerves was comparable for all groups.

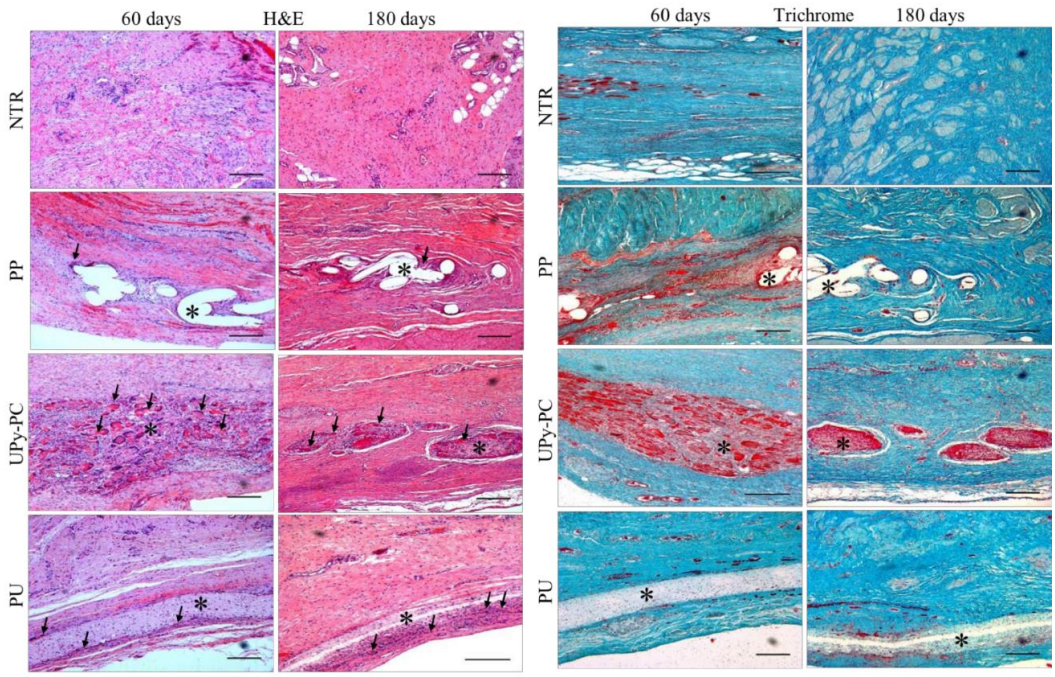

Fig. 3 Representative figures of H&E and Gouldner's Trichrome staining of native tissue repair (NTR), polypropylene (PP), UPy-PC and polyurethane (PU) explants at the location of mesh (100x magnification) with vaginal epithelium facing up. Mesh structures are represented by asterisks and foreign body giant cells by black arrows. With Gouldner's Trichrome the connective tissue is stained blue and cells are stained red.

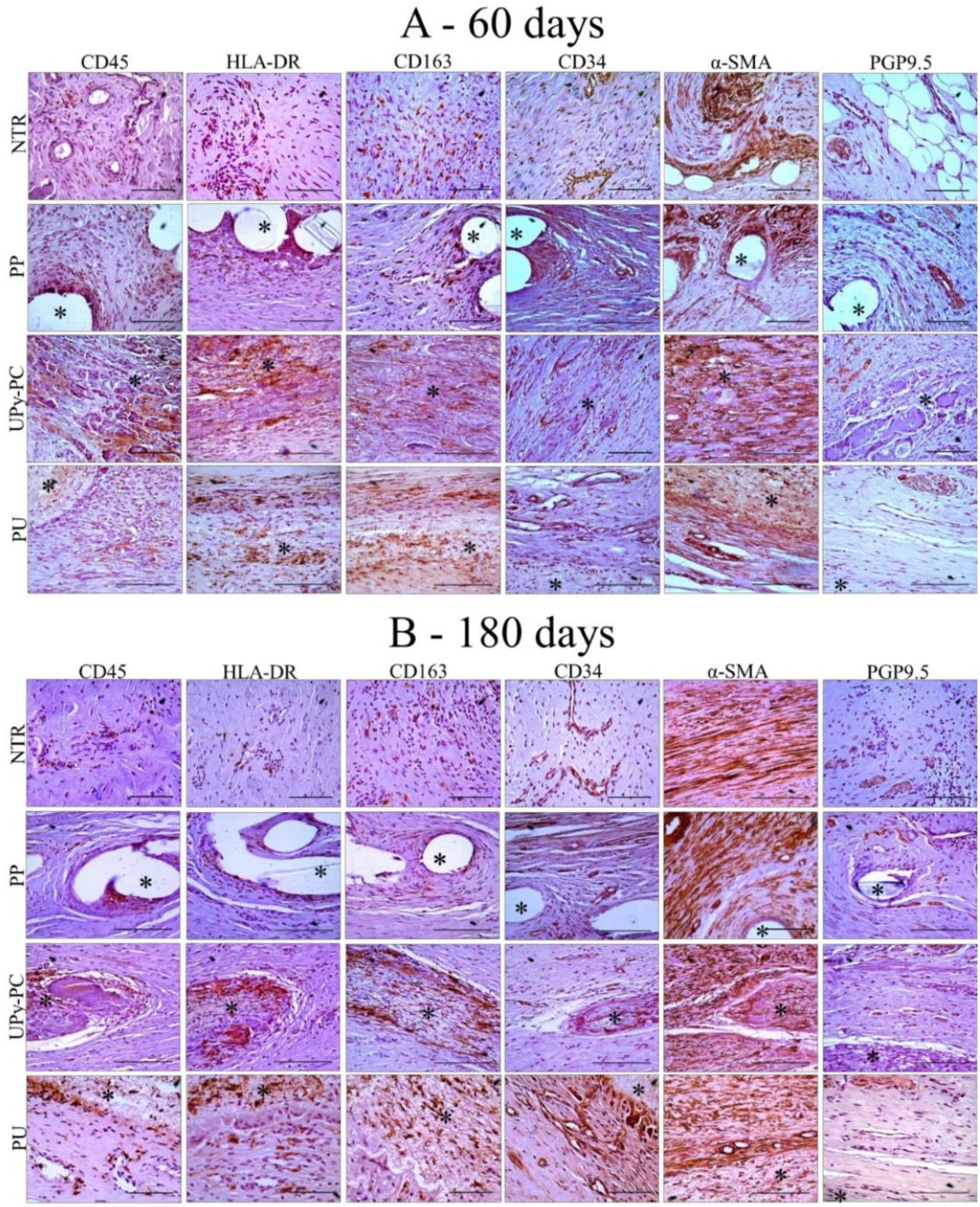

Fig. 4 Identification of cellular infiltrate into the explanted vagina (for NTR) and materials implanted into vagina of sheep at 60 (A) and 180 (B) days . Mesh structures are represented by asterisks. Results shown are immunostaining for leukocytes (CD 45), macrophage type 1 (HLA-DR), macrophage type 2 (CD163), endothelial cells of the blood vessels (CD 34), myofibroblast and smooth muscle cells (α-SMA) and neurons (PGP 9.5).

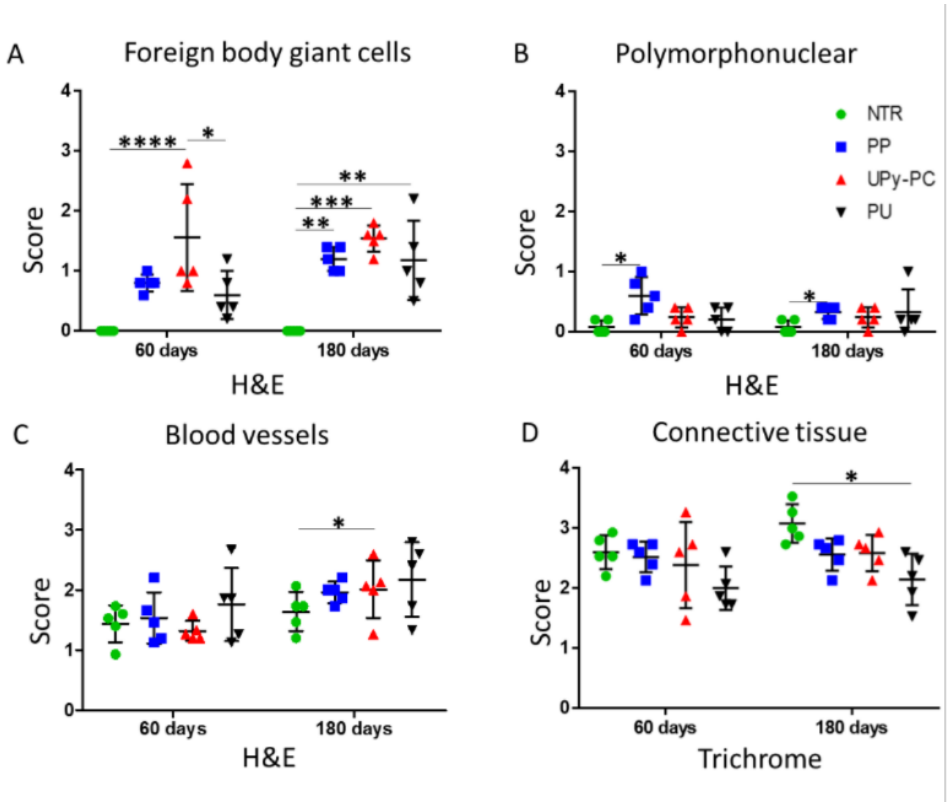

Fig. 5 Response of the host tissue to implanted materials based on H&E and Gouldner's Trichrome staining. The figure shows individual observations in sheep at 60 and 180 days. A. Foreign body giant cells. B. Polymorphonuclear cells. C. Blood vessel counts. D. Connective tissue. Values differing significantly from the control are indicated with asterisks. * p<0.05, ** p<0.01, *** p<0.001, **** p<0.0001

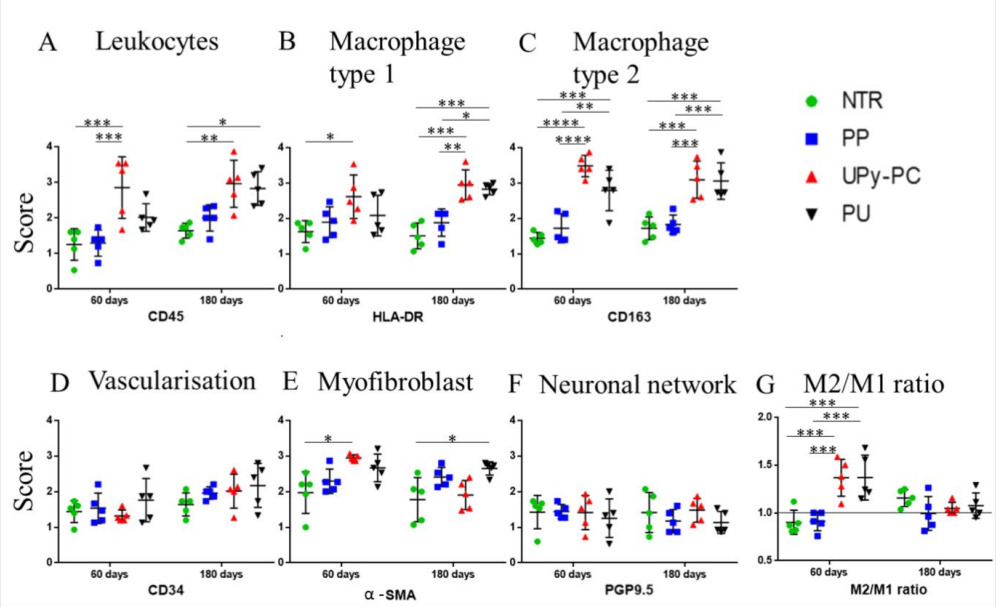

Fig. 6 Analysis of extent of cellular infiltration into vaginal explants. Results show analyses of individual sheep at 60 and 180 days. Graphs summarizing score results from immunohistochemistry. A. Leukocytes B. Macrophage type 1 C. Macrophage type 2 D. Vascularisation E. Myofibroblasts F. Neuronal network. G. Shows the ratio of M2 to M1 macrophages. * p<0.05, ** p<0.01, *** p<0.001, **** p<0.0001

4. Discussion

This is the first study in which three candidate vaginal mesh materials are compared for their effect on the vagina using a large animal model relevant to human vaginal prolapse surgery. In earlier sheep experiments we demonstrated that vaginally inserted heavy weight (58 g/m²) PP implants can induce IRC [25-27]. In contrast the current experiments confirm that a 18 g/m² PP implant produced less contraction and no erosion and was comparable to the two electrospun materials studied.

As heavier PP implants have been shown to adversely affect connective tissue deposition and smooth muscle conservation in both primates and sheep [26,28] we expected an inflammatory response dominated by M1 macrophages as previously observed for heavy weight PP [17] for the PP material we used in the study. However, the type of immune response was very similar for all three materials with an M2/M1 ratio close to 1 for all at 180 days. Similarly the appearance of the new tissue formed was similar, in terms of vascularization, myofibroblasts and neuronal network for all three. The only slight difference seen was in the extent of the inflammatory response seen to the electrospun materials compared to the textile material, which could be explained by the higher surface area of the electrospun materials.

The biomaterial design and concept for these three meshes follows three very different strategies to provide support to the pelvic floor. The Restorelle PP is a textile implant, tough very light, yet it still has a higher initial stiffness and undergoes more deformation when tested under cyclic loading prior to implantation, compared to the two electrospun materials which present more viscoelastic properties. We found Restorelle explants having biomechanical properties comparable to NTR and the two electrospun material explants. In addition, smooth muscle cells play a key role in vaginal contractility, and their function was also unaffected by the implants.

The degradable electrospun material was designed to replace failing tissue temporarily but induce a constructive remodeling process while being replaced by new native tissue. UPy-PC mesh showed a rapid degradation compared to previous absorbable materials which failed when used to treat POP [29]. Additionally the UPy-motifs on it are designed to permit the future addition of bioactive properties to this polymer which remains to be investigated. At the time of writing this approach is not yet that developed that it can be taken to the clinic.

In contrast, non-degradable electrospun PU is designed to act as a permanent implant which mimics the elastic properties of native fascia for a better compliance. The biomechanical and morphological properties of the explant are designed to be close to that of native tissue.

We acknowledge limitations in this study. This animal model does not allow an in-depth study of the immune response, as our sheep are not inbred animals and more detailed molecular tools are currently lacking. The study duration was six months, and exposure may theoretically surface later [3]. The simulated NTR does not truly mimic the operation in women as the ewes did not have a site-specific defect as women with rectocele would have – yet it is as close as we can get today to the human condition of

POP. Also, we did not include in this study a heavy weight PP mesh as we have done in an earlier study where it caused erosion in 3/10 sheep [26].

On the other hand, the field of developing materials for use in the pelvic floor badly needs the inclusion of animal studies in which materials can be demonstrated to fail. This was lacking during the period in which PP meshes developed to be used in pelvic floor surgery and were used in clinical medicine without any relevant animal testing. This is the first study done in this animal model for these materials and more analyses are needed to determine their long-term performance. The reasons why current materials are failing and giving clinical complications are not fully understood. The most obvious hypothesis is that there is a mismatch between the rigid and non-elastic mechanical properties of the heavy weight PP mesh and the pelvic floor native tissues which leads to fibrosis and contraction.

Additionally the chemical characterization of the materials post implantation needs to be better understood. Some think that PP show micro-cracking at the surface of the filaments and that substances released could stimulate a bad inflammatory response [30].

In view of this we suggest that future testing needs to consider both accelerated ageing tests and accelerated fatigue tests to reproduce the hydrolytic and oxidative environment of the pelvic floor as well as more extensive animal testing prior to introducing new materials clinically.

5. Conclusions

We draw two conclusions from this study: (1) Mechanical properties of explants comparable to that of NTR can be achieved with very different implant materials (both a degradable and non-degradable electrospun implant as well as with a textile light weight PP like Restorelle); (2) the vagina tolerates all three materials without any evidence of adverse effects on vaginal mechanical properties and equally the host inflammatory and other cellular responses to these materials were all acceptable. While there are concerns with the degradation ratio of the UPy-PC material we suggest that both PU and Restorelle are potential candidates to take for further investigation.

References

[1] Milsom, I., Gyhagen, M., The epidemiology, natural history and prevention of pelvic floor disorders, Glob. Libr. Women's Med.,. (2014). doi:DOI 10.3843/GLOWM.10481.

[2] Abdel-fattah, M., Familusi, A., Fielding, S., Ford, J., Bhattacharya, S., Primary and repeat surgical treatment for female pelvic organ prolapse and incontinence in parous women in the UK: a register linkage study, BMJ Open. 1 (2011) e000206–e000206. doi:10.1136/bmjopen-2011-000206.

[3] Abed, H., Rahn, D.D., Lowenstein, L., Balk, E.M., Clemons, J.L., Rogers, R.G., Incidence and management of graft erosion , wound granulation , and dyspareunia following vaginal prolapse repair with graft materials : a systematic review, Int Urogynecol J. 22 (2011) 789. DOI 10.1007/s00192-011-1384-5.

[4] SCENIHR, Opinion on The safety of surgical meshes used in urogynecological surgery, 2015. doi:10.2772/63702.

[5] Slack, M., Ostergard, D., Cervigni, M., Deprest, J., A standardized description of graft-containing meshes and recommended steps before the introduction of medical devices for prolapse surgery, Int. Urogynecol. J. 23 (2012). doi:10.1007/s00192-012-1678-2.

[6] Kelly, M., Macdougall, K., Olabisi, O., McGuire, N., In vivo response to polypropylene following implantation in animal models: a review of biocompatibility, Int. Urogynecol. J. (2016). doi:10.1007/s00192-016-3029-1.

[7] Hillary, C.J., Roman, S., Bullock, A.J., Green, N.H., Chapple, C.R., MacNeil, S., Developing repair materials for stress urinary incontinence to withstand dynamic distension, PLoS One. 11 (2016) e0149971. doi:10.1371/journal.pone.0149971.

[8] Liu, H., Ding, X., Zhou, G., Li, P., Wei, X., Fan, Y., Electrospining of nanofibers for tissue engineering applications, J. Nanomater. (2013). doi:10.1155/2013/495708.

[9] Cipitria, A., Skelton, A., Dargaville, T.R., Daltonac, P.D., Hutmacher, D.W., Design, fabrication and characterization of PCL electrospun scaffolds—a review, J. Mater. Chem. 21 (2011) 9419. doi:10.1039/c0jm04502k.

[10] Vashaghian, M., Zandieh, B., Roovers, J.P., Smit, T.H., Electrospun matrices for pelvic floor repair: effect of fiber diameter on mechanical properties and cell behavior, Tissue Eng. Part A. 22 (2016). doi:10.1089/ten.TEA.2016.0194.

[11] Dankers, P.Y.W., van Leeuwen, E.N.M., van Gemert, G.M.L., Spiering, A.J.H., Harmsen, M.C., Brouwer, L.A., Janssen, H.M., Bosman, A.W., van Luyn, M.J.A., Meijer, E.W., Chemical and biological properties of supramolecular polymer systems based on oligocaprolactones, Biomaterials. 27 (2006) 5490–5501. doi:10.1016/j.biomaterials.2006.07.011.

[12] Wach, R.A., Adamus, A., Kowalska-Ludwicka, K., Grobelski, B., Cala, J., Rosiak, J.M., Pasieka, Z., In vivo evaluation of nerve guidance channels of PTMC/PLLA porous biomaterial, Arch. Med. Sci. (2012). doi:10.5114/aoms.2013.34732.

[13] Asikainen, A.J., Noponen, J., Mesimäki, K., Laitinen, O., Peltola, J., Pelto, M., Kellomäki, M., Ashammakhi, N., Lindqvist, C., Suuronen, R., Tyrosine derived polycarbonate membrane is useful for guided bone regeneration in rabbit mandibular defects, J. Mater. Sci. Mater. Med. 16 (2005) 753–758. doi:10.1007/s10856-005-2613-6.

[14] Bastings, M.M.C., Koudstaal, S., Kieltyka, R.E., Nakano, Y., Pape, A.C.H., Feyen, D.A.M., Van Slochteren, F.J., Doevendans, P.A., Sluijter, J.P.G., Meijer, E.W., Chamuleau, S.A.J., Dankers, P.Y.W., A fast pH-switchable and self-healing supramolecular hydrogel carrier for guided, local catheter injection in the infarcted myocardium, 3 (2014) 70–78. doi:10.1002/adhm.201300076.

[15] Dankers, P.Y.W., Harmsen, M.C., Brouwer, L. a, Van Luyn, M.J. a, Meijer, E.W., A modular and supramolecular approach to bioactive scaffolds for tissue engineering, Nat. Mater. 4 (2005) 568–574. doi:10.1038/nmat1418.

[16] Hympanova, L., Mori da Cunha, M.G.M.C., Rynkevic, R., Zündel, M., Gallego, M.R., Vange, J., Callewaert, G., Urbankova, I., Van der Aa, F., Mazza, E., Deprest, J., Physiologic musculofascial

compliance following reinforcement with electrospun polycaprolactone-ureidopyrimidinone mesh in a rat model, J. Mech. Behav. Biomed. Mater. 74 (2017) 349–357. doi:https://doi.org/10.1016/j.jmbbm.2017.06.032.

[17] Roman, S., Urbánková, I., Callewaert, G., Lesage, F., Hillary, C., Osman, N.I., Chapple, C.R., Deprest, J., MacNeil, S., Evaluating alternative materials for the treatment of stress urinary incontinence and pelvic organ prolapse: a comparison of the in vivo response to meshes implanted in rabbits, J. Urol. 196 (2016) 261–269. doi:http://dx.doi.org/10.1016/j.juro.2016.02.067.

[18] Abramov, Y., Golden, B., Sullivan, M., Botros, S.M., Miller, J.-J.R., Alshahrour, A., Goldberg, R.P., Sand, P.K., Histologic characterization of vaginal vs. abdominal surgical wound healing in a rabbit model, Wound Repair Regen. 15 (2007) 80.

[19] Brown, B.N., Mani, D., Nolfi, A.L., Liang, R., Abramowitch, S.D., Moalli, P.A., Characterization of the host inflammatory response following implantation of prolapse mesh in rhesus macaque, Am. J. Obstet. Gynecol. 213 (2015) 668.e1-668.e10. doi:10.1016/j.ajog.2015.08.002.

[20] Liang, R., Zong, W., Palcsey, S., Abramowitch, S., Impact of prolapse meshes on the metabolism of vaginal extracellular matrix in rhesus macaque, Am. J. Obstet. Gynecol. 212 (2015) 174.e1-174.e7. doi:10.1016/j.ajog.2014.08.008.

[21] Barone, W.R., Moalli, P.A., Abramowitch, S.D., Textile properties of synthetic prolapse mesh in response to uniaxial loading., Am. J. Obstet. Gynecol. (2016) 1–9. doi:10.1016/j.ajog.2016.03.023

[22] Urbankova, I., Callewaert, G., Sindhwani, N., Turri, A., Hympanova, L., Feola, A., Deprest, J., Transvaginal mesh insertion in the ovine model, J. Vis. Exp. (2017). doi:10.3791/55706.

[23] Haylen, B.T., Freeman, R.M., Swift, S.E., Cosson, M., Davila, G.W., Deprest, J., Dwyer, P.L., Fatton, B., Kocjancic, E., Lee, J., Maher, C., Petri, E., Rizk, D.E., Sand, P.K., Schaer, G.N., Webb, R.J., An International Urogynecological Association (IUGA) / International Continence Society (ICS) joint terminology and classification of the complications related directly to the insertion of prostheses (meshes, implants, tapes) & grafts in female pelvic flo, Int. Urogynecol. J. Pelvic Floor Dysfunct. 22 (2011) 3–15. doi:10.1007/s00192-010-1324-9.

[24] Maurer, M.M., Röhrnbauer, B., Feola, A., Deprest, J., Mazza, E., Mechanical biocompatibility of prosthetic meshes: A comprehensive protocol for mechanical characterization, J. Mech. Behav. Biomed. Mater. 40 (2014) 42–58. doi:10.1016/j.jmbbm.2014.08.005.

[25] Manodoro, S., Endo, M., Uvin, P., Albersen, M., Vláčil, J., Engels, A., Schmidt, B., De Ridder, D., Feola, A., Deprest, J., Graft-related complications and biaxial tensiometry following experimental vaginal implantation of flat mesh of variable dimensions, BJOG. 120 (2013) 244–250. doi:10.1111/1471-0528.12081.

[26] Feola, A., Endo, M., Urbankova, I., Vlacil, J., Deprest, T., Bettin, S., Klosterhalfen, B., Deprest, J., Host reaction to vaginally inserted collagen containing polypropylene implants in sheep, Am J Obs. Gynecol. (2015). doi:10.1016/j.ajog.2014.11.008.

[27] Badylak, S., Kokini, K., Tullius, B., Simmons-Byrd, A., Morff, R., Morphologic study of small intestinal submucosa as a body wall repair device., J. Surg. Res. 103 (2002) 190. doi:doi:10.1006/jsre.2001.6349.

[28] Liang, R., Abramowitch, S., Knight, K., Palcsey, S., Nolfi, A., Feola, A., Susan Stein, Moalli, P. a., Vaginal degeneration following implantation of synthetic mesh with increased stiffness, BJOG. 120 (2013) 233.

[29] Fitzgerald, J.F., Kumar, A.S., Biologic versus Synthetic Mesh Reinforcement : What are the Pros and Cons ?, Clin Colon Rectal Surg. (2014) 140–148.

[30] Wood, A.J., Cozad, M.J., Grant, D.A., Ostdiek, A.M., Bachman, S.L., Grant, S.A., Materials characterization and histological analysis of explanted polypropylene , PTFE , and PET hernia meshes from an individual patient, J Mater Sci Mater Med. (2013) 1113–1122. doi:10.1007/s10856-013-4872-y.

Supplementary material 1: Spinning details

Polyurethane Z3A1 was purchased from Biomer technologies (Cheshire, UK) and was dissolved in 70:30 DMF:THF at 10% (wt/v). Polyurethane tri-layer scaffolds were created by loading solutions of PU Z3 into 5ml syringes fitted with blunt-tipped 21G needles, placed into a syringe pump (GenieTMPlus, Kent Scientific, USA). Tri-layers consist of random-aligned-random orientations. Random fibres were produced by delivering polymer solutions at a rate of 40µl/min per syringe with an accelerating voltage of 20kV DC from a high voltage supply (Genvolt, UK) and collected on an aluminium foil covered earthed mandrel (8 cm diameter, 16 cm length) rotating at 300rpm, with a needle to collector distance of 20cm at 21oC and ~30% humidity. Aligned fibers were produced using a voltage of 23kV, a mandrel rotation speed of 600rpm and a needle to collector distance of 5cm. Interwoven random-aligned-random fiber morphologies (supplementary figure 1 a, b) were produced using two separate syringe pumps. Each layer was produced using 20ml of polymer, using a 5ml overlap between separate layers (one syringe pump delivering random fibers, while the other pump delivered aligned fibers). The production of this trilayer electrospun scaffold is covered by a patent filed by the University of Sheffield No P226373GB.

Ureidopyrimidinone-polycarbonate (UPy-PC) polymer was obtained from SupraPolix, Eindhoven, The Netherlands. Electrospinning was performed by Coloplast, Humlebaek, Denmark. The spinning method employed a coaxial nozzle with the inner needle (17G) used to pump the polymer (13%wt) and outer (19G) for pure solvent (chloroform, methanol, acetonitrile, acetic acid. Fibers were spun using voltage – 18.2 (kV) on the nozzle and +5(kV) on the drum, which was rotating (3 s-1), size 20x50cm. The needle collector distance was 22cm. The final mesh was a single layer composed of randomly oriented fibres.

Supplementary material 2: Surgical procedure

All animals underwent simultaneous vaginal and abdominal wall native tissue repair or reconstruction with the implant under sterile conditions. Premedication (30min.) and antibiotic prophylaxis (10min.) was administered prior to induction of anesthesia with mixed 1ml/50 kg xylazine HCl (Xyl-M®; VMD; Arendonk; Belgium) and 0.5ml/50 kg tramadolhydrochloride (Tramadol EG®; Eurogenerics; Bruxelles; Belgium) IM injection followed by one dose of natriumcefazoline 2g IV (Cefazoline Sandoz®; Sandoz; Vilvoorde; Belgium). Anesthesia was induced with 0.075 mL/kg ketamine HCl 100 mg/mL (Ketamine 1000®, Ceva Sante Animale, Belgium) IV injection, following intubation and maintained with 2.5 % Isoflurane (Iso-Vet®; Piramal Healthcare; Morpeth; UK) in 5 L/min oxygen. Sheep were placed in the dorsal decubitus position with pelvic limbs secured in hip flexion to allow vaginal implantation. Urinary bladders and rectums were emptied, surgical areas were sheared. Vagina and perineum were disinfected with Polyvidone Iodium 7.5% (Braunol®, B. Braun Medical, Belgium) and covered by a sterile drape.

Retractor and hooks (Lone star® retractor system; Trumbull, USA) were placed to make wide access to the vestibulum vaginae. The posterior vaginal wall was grasped with Allis forceps 3 cm cranially from the hymen. Aqua-dissection with 10 ml Hartman solution was performed in the posterior vaginal wall 2cm cranially to the hymeneal ring, then a longitudinal 3cm incision was made at that place. Hooks were used to open incisions. The rectovaginal septum was bluntly (finger and gauze) and sharply (scissors) dissected to create a suitable space for implant between the vaginal epithelium and rectal serosa. The dry mesh was measured with a micrometer before vaginal implantation. Implants were fixed with interrupted 3/0 polypropylene sutures (Prolene®, Ethicon, Zaventem, Belgium) firstly in the corners and then halfway along its borders. In the case of native tissue repair the procedure was carried out in the same way including the PP fixation sutures but without any implant. In this group, posterior plication was performed afterwards with three 3/0 polyglactine 910 (Vicryl®, Ethicon) sutures. The vaginal wall was closed with a running 3/0 polyglactine 910 suture.

Postoperative analgesia contained meloxicam (Metacam®, Boehringer Ingelheim, Rhein, Duitsland) (0.5 mg/kg), Buprenorphine 0.3 mg/mL and Chlorocresol 1.35 mg/mL (Vetergesic, Ecuphar, Belgium) 1 mL/day IM injection up to the third day after surgery. Animals were clinically observed for one week. Surgical sites were regularly examined to note early postoperative complications. Sheep were euthanized at 60 or 180 days after surgery.

Supplementary material 3: Animals used and ethics

Animals were treated in accordance with current national guidelines on animal welfare. The sample size was calculated using a two-sided t-test. Based on biomechanical results (comfort zone stiffness) from a previous experiment, where UPyPC mesh was used for reconstruction of the abdominal wall in rabbits. We calculated the number of explants required (n=6 group; 90% power). Sheep were seven years old having had each more than four vaginal deliveries and weighing 51.5 ± 5.7 kg. None of the ewes had obvious prolapse, however formal staging of the prolapse was not performed.1 Animals were housed one week after surgery at the animal facility and then at the farm with unrestricted access to the food, water, chew and with free access to open space.

Supplementary material 4: Obduction

Premedication prior euthanasia was performed by intramuscular administration of 1 ml/50 kg xylazine. Exposure was defined as a state of vaginal mesh visualized through separated vaginal epithelium.2 Length and width of the mesh was measured 3 times (Supplementary figure 4) to calculate contraction (mean length*mean width) vaginal mesh explants were measured immediately after explantation. Length and width were measured three-times.

Supplementary material 5: Contractility

Transducers (ISOMETTRAND 220V.5-5.0GR, Harvard Apparatus, Holliston, United States) calibration was performed prior testing. The Krebs solution had the following composition (mM): NaCl 119, KCl 4.6, CaCl2 1.5, MgCl2 1.2, NaHCO3 15, NaH2PO4 1.2, glucose 5.5, pyruvate 2.2). KCl solution (1M) was used to add exact µl to the bath each time to reach required concentration (mM). During measuring, Krebs was continuously bubbled with a mixture of 95% O2 and 5% CO2 to keep the pH at 7.4. The specimens were weighed after testing.

Supplementary material 6: Histology

Staining was performed on 6 µm section. Gouldner's Trichrome staining (Merck Millipore) was performed following manufacture's protocol to stain extracellular connective tissue. For immunohistochemistry (IHC) staining, sections were processed with a mouse and rabbit specific HRP/DAB (ABC) Detection IHC Kit (Abcam) and six different monoclonal antibodies (supplementary table 1). Antibodies were diluted in 1% bovine albumin serum (BSA) (Sigma-Aldrich).

Hematoxylin and Eosin stains were performed to quantify the presence of foreign body giant cells (FBGC), polymorphonuclear (PMN) and vessels. Five randomly chosen non- overlapping fields per slide (5 samples per group) were scored at a magnification of ×400 and averaged (n=5). Fields were randomly selected at the interface between the implant and surrounding tissue. An ordinal scale was used similar to that described by Badylak 3, where scores are made as follows: none of the cells/vessels per high-power field (score 0), 1–5 (score 1), 6–10 (score 2) and >10 (score 3).

Trichrome stains extracellular connective tissue (mainly unspecified collagen) blue. Five non-overlapping images 400x magnification were obtained and semi-quantitatively evaluated for percentage of area occupied by collagen at interface mesh-surrounding tissue.

Semi-quantitative assessment of the extent of immunostaining was performed on a blinded observer basis using a qualitative grading scale; absent=0, mild presence=1, large presence=2, abundance=3, great abundance=4. Five representative images from samples at each time point were assessed by three blinded researchers (n=5). Example photographs (Supplementary figure 5) depicting 1, 2, 3 and 4 were provided for reference and the median value from these scores was used. The M2/M1 ratio was also calculated for each group using the values from the blind scoring of the immunostaining (n=5). For calculation of macrophages M2/M1 ratio were used to determined scores. On apha-SMA images, smooth muscle and vessels were excluded from evaluation.

All histologic measurements were done by 3 researchers blinded to the treatment groups, though absolute blinding is not possible given the materials were recognizible in the specimens.

Supplementary tables

Supplementary table 1. Table contains used antibodies, their concentrations and companies of their origin: Abcam (Cambridge, UK), DAKO (Glostrup, Denmark), AbD Serotec (Kidlington, UK).

Antibody	Concentration	Company
rabbit anti-CD34	1:2000	Abcam
mouse anti-smooth muscle actin (SMA)	1:200	DAKO
mouse anti-PGP9.5	1:1000	Abcam
mouse anti-CD45	1:200	AbD Serotec
mouse anti-HLA-DR	1:100	Abcam
mouse anti-CD163	1:200	AbD Serotec

Supplementary table 2. Shrinkage of the implanted area with implants (PP, PU, UPy-PC) or without (NTR) measured within polypropylene sutures.

	60d				**180d**			
Shrinkage %	NTR	PP	UPy-PC	PU	NTR	PP	UPy-PC	PU
	34.9±11.3	29.6±7.8	22.8±14.1	42.4±8.7	32.6±6.6	46.7±14.2	27.4±16.1	48.4±6.1

Supplementary figures

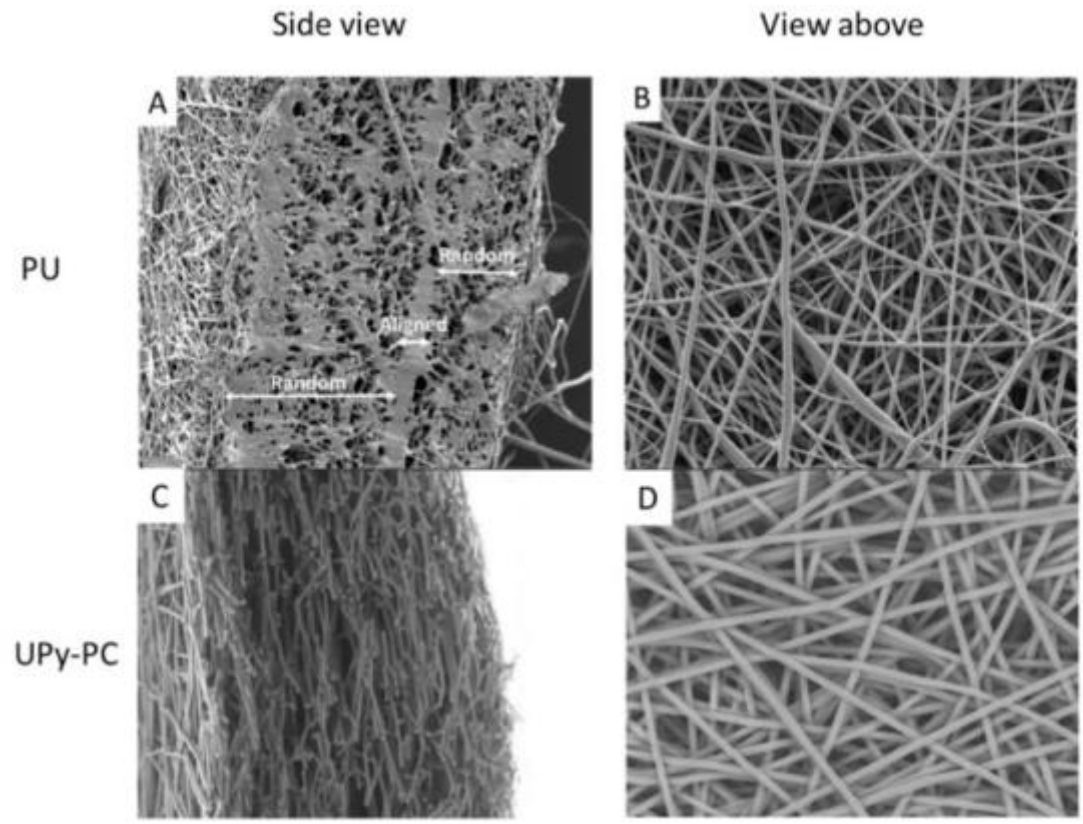

Supplementary figure 1. Electron microscopy images of polyurethane (A,B) and UPy-PC (C,D) scaffold. Figure A. 1000x magnification demonstrates the tri-layered structure and figure B. at 5000x magnification shows the detail of fiber random orientation. Figure C. 500x magnification, random fibers orientation D.1200x.

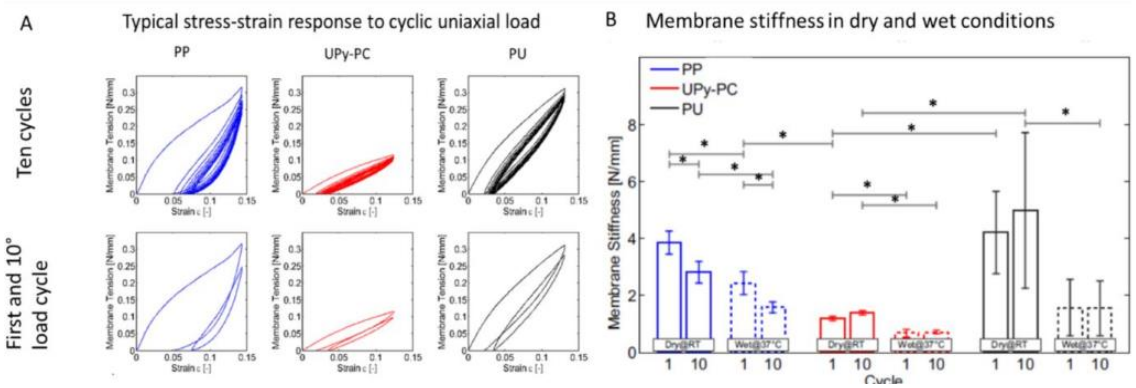

Supplementary figure 2. Figure A displays typical stress-strain response of materials to uniaxial load within cyclic loading. Figure B displays membrane stiffness of materials in dry and wet conditions after one and 10 cycles of uniaxial load. Significant difference $p>0.05$ is marked with asterisk.

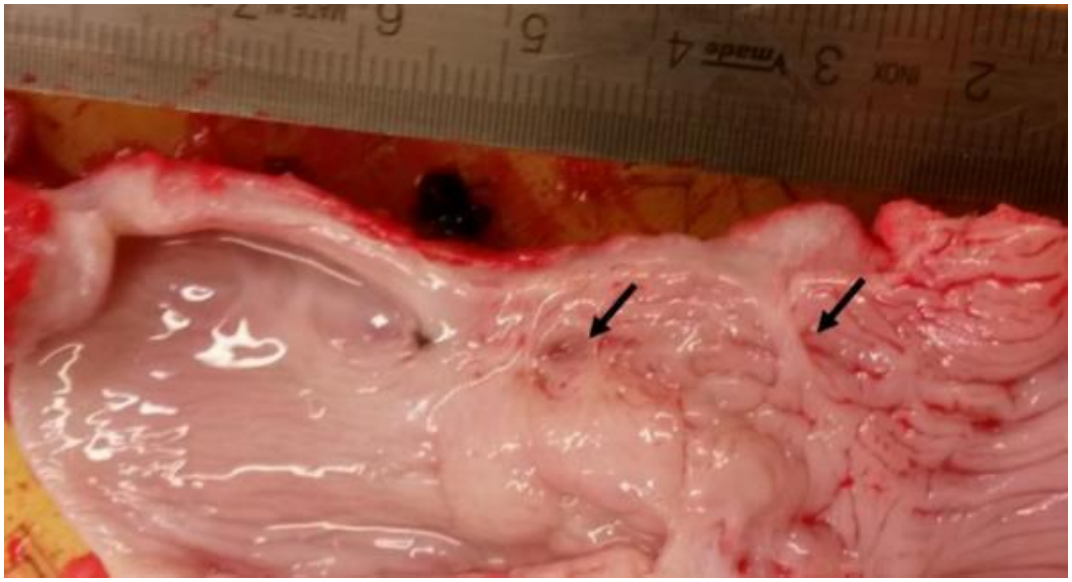

Supplementary figure 3. Figure of one of the cases of synechiae, mild vaginal adhesions to sutured area marked with arrows.

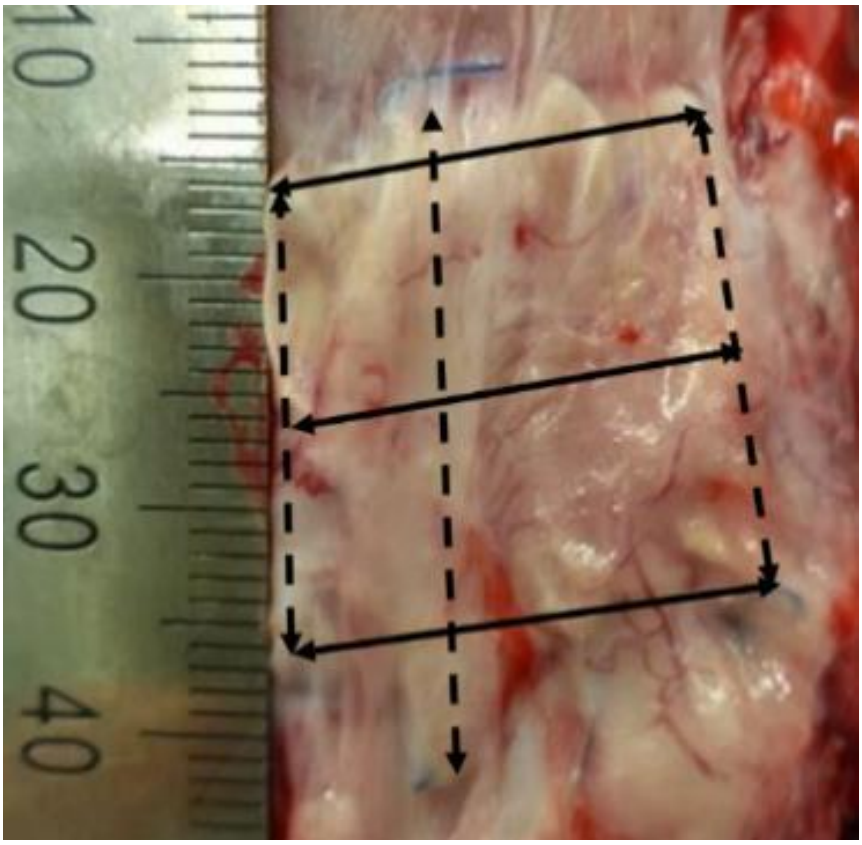

Supplementary figure 4. Mesh width and length were measured three times each, permanent sutures were used as markers. Location of measurements are marked by arrows.

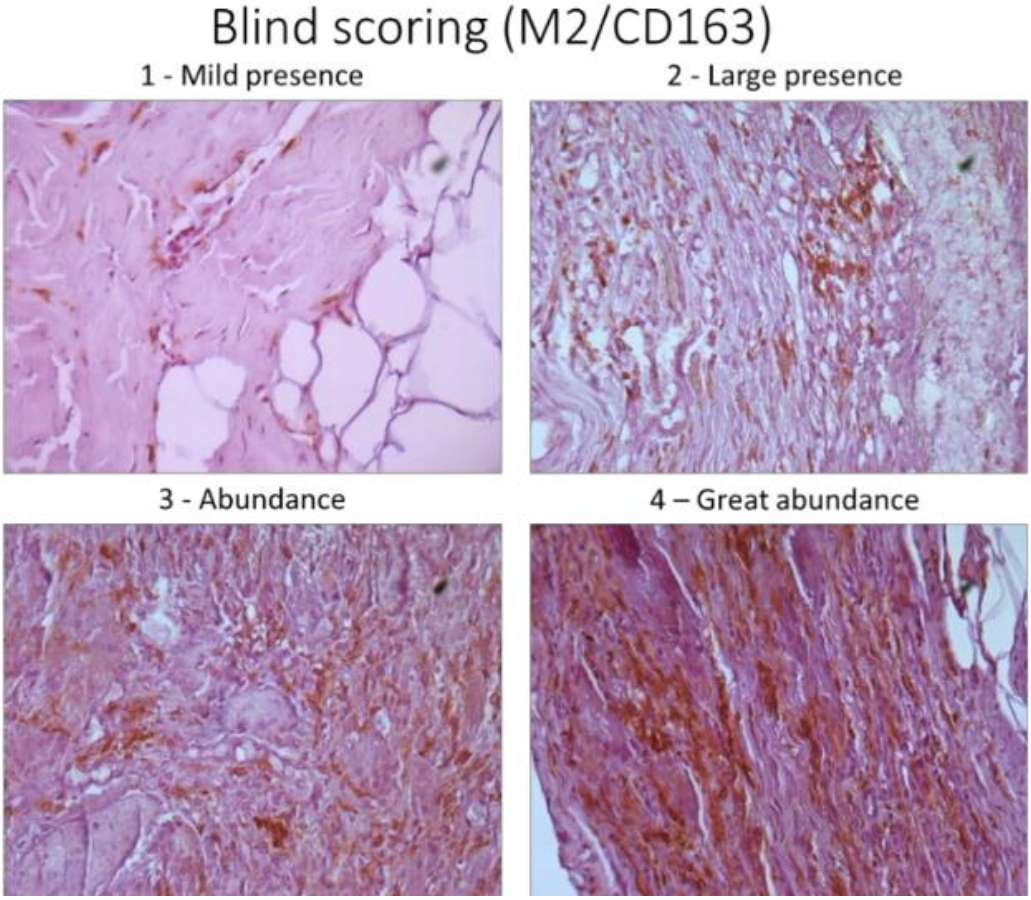

Supplementary figure 5. An example of representative figures used for scoring (1-4).

CHAPTER 5

BIOMECHANICAL AND MORPHOLOGICAL PROPERTIES OF THE MULTIPAROUS OVINE VAGINA AND EFFECT OF SUBSEQUENT PREGNANCY

Rita Rynkevic[1, 2, 3, 4], Pedro Martins[1, 2], Lucie Hympanova [3, 4], Henrique Almeida [5], Antonio A. Fernandes [1], Jan Deprest [3, 4]

[1]University of Porto, Faculty of Engineering, Portugal,
[2]INEGI, University of Porto, Faculty of Engineering, Portugal,
[3]KU Leuven, Department Development and Regeneration, Biomedical Sciences, Leuven, Belgium.
[4]Centre for Surgical Technologies, Group Biomedical Sciences,
[5]University of Porto, Faculty of Medicine, Department of Experimental Biology, Portugal

Key words: vaginal tissue, biomechanical properties, tissue morphology, animal model, pregnancy

Contents lists available at ScienceDirect

Journal of Biomechanics

journal homepage: www.elsevier.com/locate/jbiomech
www.JBiomech.com

Biomechanical and morphological properties of the multiparous ovine vagina and effect of subsequent pregnancy

Rita Rynkevic [a,b,c,d], Pedro Martins [a,b,*], Lucie Hympanova [c,d], Henrique Almeida [e], Antonio A. Fernandes [a,b], Jan Deprest [c,d]

[a] University of Porto, Faculty of Engineering, Portugal
[b] INEGI, University of Porto, Faculty of Engineering, Portugal
[c] KU Leuven, Department Development and Regeneration, Biomedical Sciences, Leuven, Belgium
[d] Centre for Surgical Technologies, Group Biomedical Sciences, Belgium
[e] University of Porto, Faculty of Medicine, Department of Experimental Biology, Portugal

Published in Journal of Biomechanics 57, 94-102 (2017)

ABSTRACT

Background and Objective: Pelvic floor soft tissues undergo changes during the pregnancy. However, the degree and nature of this process is not completely characterized. This study investigates the effect of subsequent pregnancy on biomechanical and structural properties of ovine vagina.

Material and Methods: Vaginal wall from virgin, pregnant (in their third pregnancy) and parous (one year after third vaginal delivery) Swifter sheep (n=5 each) was harvested. Samples for biomechanics and histology were cut in longitudinal axis (proximal and distal regions). Outcome measurements describing Young's modulus, ultimate stress and elongation were obtained from stress-strain curves. For histology, samples were stained with Miller's Elastica staining. Collagen, elastin and muscle cells and myofibroblasts contents were estimated, using image-processing techniques. Statistical analyses were performed in order to determine significant differences among experimental groups. Significant regional differences were identified.

Results: The proximal vagina was stiffer than distal, irrespective the reproductive status. During the pregnancy proximal vagina become more compliant than in parous (+47.45%) or virgin sheep (+64.35%). This coincided with lower collagen (-15 to -21%), higher elastin (+30 to +60%), and more smooth muscle cells (+17 to +37%). Vaginal tissue from parous ewes was weaker than of virgins, coinciding with lower collagen (-10%), higher elastin (+50%), more smooth muscle cells (+20%).

Discussion and conclusions: It could be proposed that after pregnancy biomechanical properties of vagina do not recover to those of virgins. Since elastin has a significant influence on the compliance of soft tissues and collagen is the main "actor" regarding strength, histological analysis performed in this study justifies the mechanical behaviour observed.

1. Introduction

Pelvic floor soft tissues undergo changes during pregnancy, labour and delivery, and may be affected by age and hormonal status [1-3].

During the physiological processes, such as pregnancy and parturition, the vaginal wall and pelvic floor organs undergo adaptation. After delivery, these structures should return to a prepregnant-like state. Epidemiologic studies suggest that many women fail to recover completely from this event; indeed, vaginal distention trauma appears to play an important role as a cause of pelvic organ prolapse (POP) [4, 5]. Prolapse of internal genital organs, is a condition in which the pelvic organs (bladder, cervix, vaginal and rectal wall) form a hernia into the vaginal lumen.

A detailed biomechanical assessment of vaginal tissue structures can improve the understanding of how subsequent pregnancies may affect the tissue properties and composition. Several studies have been conducted that evaluate the biomechanical properties of human vaginal tissues [6-12], yet access to fresh samples is limited, due to restrictions on the dimensions of specimens, due to ethical concerns. Animal models, such as mice, rabbits, dogs (domestic mammals) or non-human primates are used instead to evaluate biomechanical properties of relevant tissues [13-18]. To define changes in vaginal distensibility induced by pregnancy and vaginal delivery, some studies were already carried out on rats [19, 20]. In the work reported a sheep animal model will be used since its pelvic floor tissue anatomy is structurally similar (dimensions and organization) to that of humans [21, 22]. Moreover PFD (Pelvic Floor Disorders) risk factors such as increased intraabdominal pressure, parity or obesity, are comparable to that in humans [22, 23]. Sheep may also spontaneously develop utero-vaginal prolapse during pregnancy [24, 25]. Some studies on sheep vaginal tissue properties have been conducted already. One study compared ovine and human posterior vaginal tissue in terms of histological composition [26]. In another, ovine proximal vaginal tissue biochemical composition and biomechanical properties at different reproductive stages were determined [27, 28]. Several papers/reports have been published on vaginal tissue composition and mechanical properties, however they used different methods, different animal models, different testing and sample collections protocols, which makes the comparison of results difficult and sometimes conflicting.

The objective of this study was to identify pregnancy-induced changes and effect of vaginal deliveries on the biomechanical and morphological properties of vaginal wall. The virgin sheep was used as baseline model for this study. To investigate the link between biomechanical tissue properties and tissue morphology, all the layers of the vaginal tissue were carefully analysed and evaluated. It was conducted a detailed morphological comparison between proximal and distal regions of sheep vaginal wall. Thickness and contents (collagen, elastin and smooth muscle) of each region were investigated using image analysis.

2. Methods

2.1 Animals

Ewes were either young post-menarchal virgins (n=5; avg. weight = 45 kg), near term (n=5; 140 days; term = 145 d; avg. weight = 65 kg) after two prior vaginal deliveries, further referred to as gravida-3, and at least one year after three vaginal deliveries (n=5; avg. weight = 60 kg), referred to as para-3. Virgin sheep were nine-months-old, while the gravida-3 and para-3 sheep were 3 and 4 years old, respectively. Swifter sheep typically have two to three lambs per litter; which was also the case in the present study. Ewes were obtained from the Zoötechnical Institute of the Katholieke Universiteit (KU) Leuven. Animals were treated according to an experimental protocol approved by the Ethics Committee for Animal Experimentation of the Faculty of Medicine of KU Leuven. They were euthanized by intravenous injection of 10 mL of a mixture of embutramide 200 mg, mebezonium 50 mg and tetracaine hydrochloride 5 mg (T61; Hoechst Marion Roussel, Brussels, Belgium). Animals were placed in the dorsal recumbent position and pelvic floor organs were completely excised.

2.2 Sample preparation

The tissue was divided into samples for biomechanical testing and for histological analyses according to a standardized topographic protocol (Fig. 1a). Standardized samples for biomechanics were punched using a dog bone shape cutting form (2mm x 25mm) along the longitudinal axis (Fig. 1b). Testing was done within two hours after prelevation; prior to measurements tissues were kept in a wet saline soaked gauze at room temperature (~20ºC).

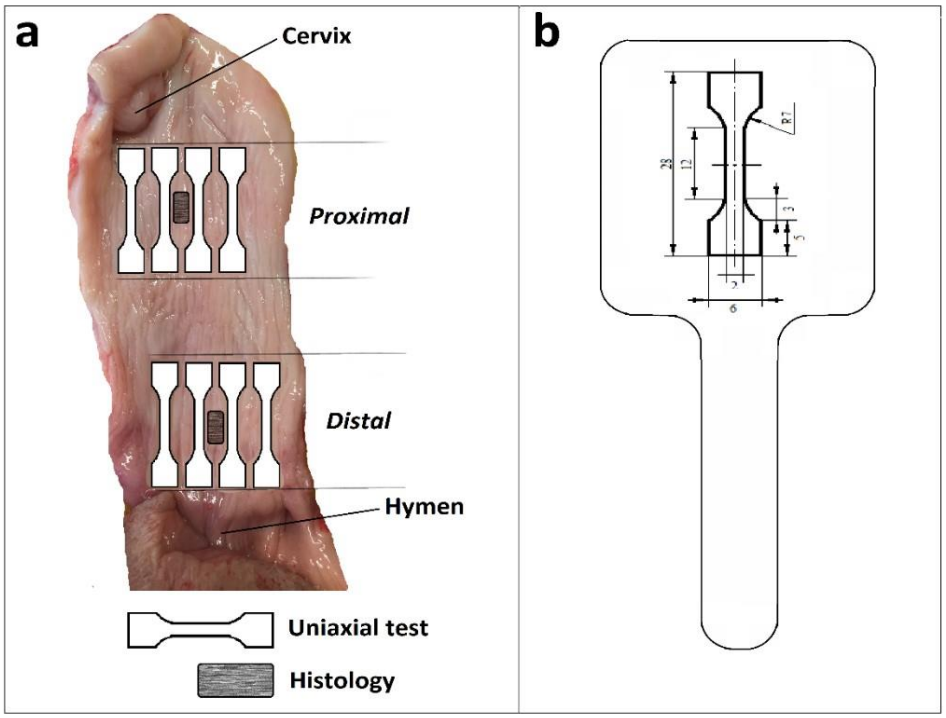

Fig. 1. a-Schematic division of the tissue into samples: dog bone shape samples for biomechanical testing and for histology, b- dog bone shape sample cutting form blade (with dimensions) mounted in a transparent acrylic frame

2.3 Uniaxial tensile testing protocol

Uniaxial testing was performed using a Zwick tensiometer with a 200 N load cell (Zwick GmbH & Co. KG, Ulm, Germany). The orientation of the set up was vertical. One clamp was attached to the base of the testing device, the other was attached to the crosshead of the device via a load cell. By using a specific algorithm, the load cell transforms resistance variations into force values.

Tissue specimens were fixed using small grips which in turn are inserted into the pneumatic clamps. The purposely built small grips allowed to reduce the stress concentration effect on the tissues and avoid slippage [8]. The tensile test was carried out by applying longitudinal axial load. Samples were pre-loaded till 0.1 N to remove slack from the tissue using a constant elongation of 5 mm/min, and then the clamp-to-clamp distance was measured. This point was defined as elongation zero. The width and thickness were measured using callipers, with an accuracy of 0.05 mm. Measurements were taken at three locations along the sample length and averaged in order to assess the sample geometric homogeneity. The average cross-sectional area value was used to calculate the stress, which is defined as the force divided by the initial (prior to testing) cross sectional area.

A constant elongation rate of 10 mm/min was used to load the specimen to failure, along the longitudinal axis. Each test was ended automatically when the load fell below 60% of the maximum load. The load and elongation were recorded throughout the testing period. The strain was calculated by dividing the elongation by the clamp-to-clamp length. The corresponding stress-strain curve was computed.

2.4 Histochemical assay

Specimens were fixed in 4% paraformaldehyde (PFA) for 24 hours, washed in PBS and stored in ethanol. Then they were oriented, embedded in paraffin and cut into 6-µm slices, for assessment of the full thickness of the vaginal wall. Slices were stained with Miller's Elastica staining. The thickness of the epithelium, lamina propria, muscularis and adventitia layers was measured. Then, the amount of collagen, elastin and smooth muscle was estimated for each layer.

2.5 Morphometric analysis

Only full thickness images, i.e. showing a complete set of histological components, were analysed. Images were captured at 10× magnification using a Zeiss microscope (Zeiss Axioplan 400, Oberkochen, Germany) with attached digital camera, along the axis perpendicular to the epithelium. We used Matlab (Release 2015®, The MathWorks, Inc) to stitch individual images into one full thickness image [28] (Fig. 3). Images were processed using ImageJ (open platform for scientific image analysis) and a Colour Deconvolution plugin. Applying a threshold algorithm, RGB images were binarized. The total content of collagen (%), elastin (%), and smooth muscle (%) were determined from thresholded images, relative to the total sample area [29].

2.6 Statistics

Statistical analysis was performed to compare mechanical properties and structural composition of the proximal and distal vagina among experimental groups. Based on the

averaged results over all samples of an individual, the mean value per individual was used for analysis. Results of gravida-3 were compared to virgin animals. Results of para-3 were also compared to gravida-3, and were indicated to virgin sheep, making this study a cross-sectional experiment. All statistical tests were conducted using the statistical software package GraphPad Prism 5, USA. Quantitative data are represented as mean ± standard error of the mean (±SEM). Paired student´s t-test was used (with confidence level of 95%) for the within group-comparisons (between proximal and distal region). A statistically significant difference was reported if $p<0.05$. Kolmogorov-Smirnov tests showed the data follows a normal distribution, a requirement for ANOVA. One-way ANOVA and post hoc test (Tukey's correction) were carried out for the intergroup comparisons. The level of significance was set to $p<0.05$.

3. Results

3.1 Mechanical properties

Fig. 2a displays the reconstructed (mean) stress-strain curves for the three groups, both for the distal and proximal vagina. Outcome measurements describing the mechanical properties of the native tissue were obtained from the stress-strain curve (Fig. 2a). The Young's modulus in the comfort zone was defined as the modulus over an interval of 10-20 % of total elongation (point A). The Young's modulus within the stress zone was defined as the modulus over an interval of 70-80 % of total elongation (point B). The point where these linear segments intersect was defined as the inflection point indicating also the length of the comfort zone (point D). Ultimate stress (point C) and strain at ultimate stress (point E) were measured. The distance between point D and point E represents the length of the stress zone. The comfort zone of the curve is usually considered to be within the physiological range of deformation, whereas the stress zone is in the range of supra-physiological stress (Fig. 2) [30].

Overall, the average computed stress-strain curves demonstrate a hyperelastic behaviour of vaginal tissue, irrespective of the groups or location of measurement. There were regional differences between samples taken near the hymen (distal) and samples taken near the cervix (proximal), irrespective of the reproductive status studied (Fig. 1b). In all cases the proximal vagina was stiffer than the distal, both in the comfort and stress zone. Though not a longitudinal experiment, comparison between groups represents the effect of pregnancy and delivery. Fig. 2b displays the results for four representative points on the computed curves.

The biomechanical changes with higher clinical relevance occur in the proximal vagina in the physiological load range (comfort zone). Gravida-3 animals have higher compliance, 63.9% ($p<0.01$), than virgin sheep. One year after third delivery proximal vagina is 48.9% ($p< 0.05$) less compliant than in the third pregnancy. However, it is still 29.4% ($p<0.05$) more compliant than in virgin ewes.

In the distal vagina, the same behaviour is observed are less steep. There is a non-significant increase in compliance during third pregnancy, a significant decrease thereafter (32.1 %; $p<0.01$), which falls within the range of virgin values. The stress zone

compliance followed a more pronounced change both by third pregnancy and one year after delivery. The ultimate stress and strain are represented in Fig. 2b.

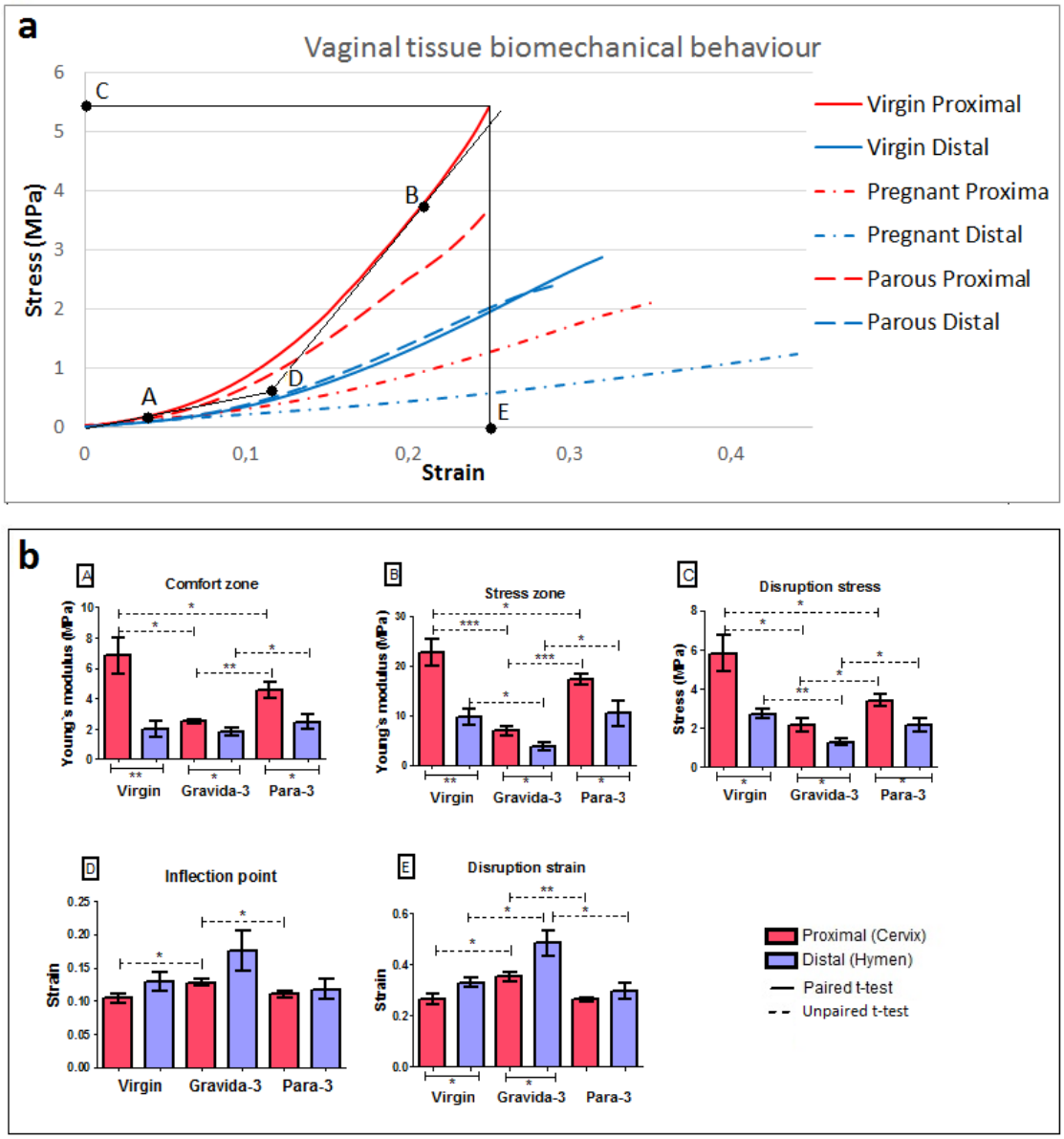

Fig. 2. **a**- Mechanical behaviour of the distal and proximal vaginal tissue of virgin, parous and pregnant sheep. Stress-strain curves represent averaged value of 5 virgins, parous and pregnant samples both for the distal and proximal vagina. Relevant points (A, B, C, D, E) characterize the curves. **b**- Vertical column bar graph, mean with (SEM), representing proximal vagina (red bars) and distal vagina (blue bars). Significant differences between groups are displayed above the bars; differences within groups are indicated under the bars. Significant difference noted when $p<0.05$ (*). $p<0.01$ (**). $p<0.001$ (***).

3.2 Histology of vaginal layers

Full thickness high quality histologic images of both vaginal wall regions are provided in Fig. 3. On all analysed images, it was possible to discriminate four distinct layers: the stratified squamous epithelium, the lamina propria, containing a multidirectional network of collagen and elastin fibres, a muscularis of smooth muscles cells, and below, loose connective adventitia (Fig. 3) [31].

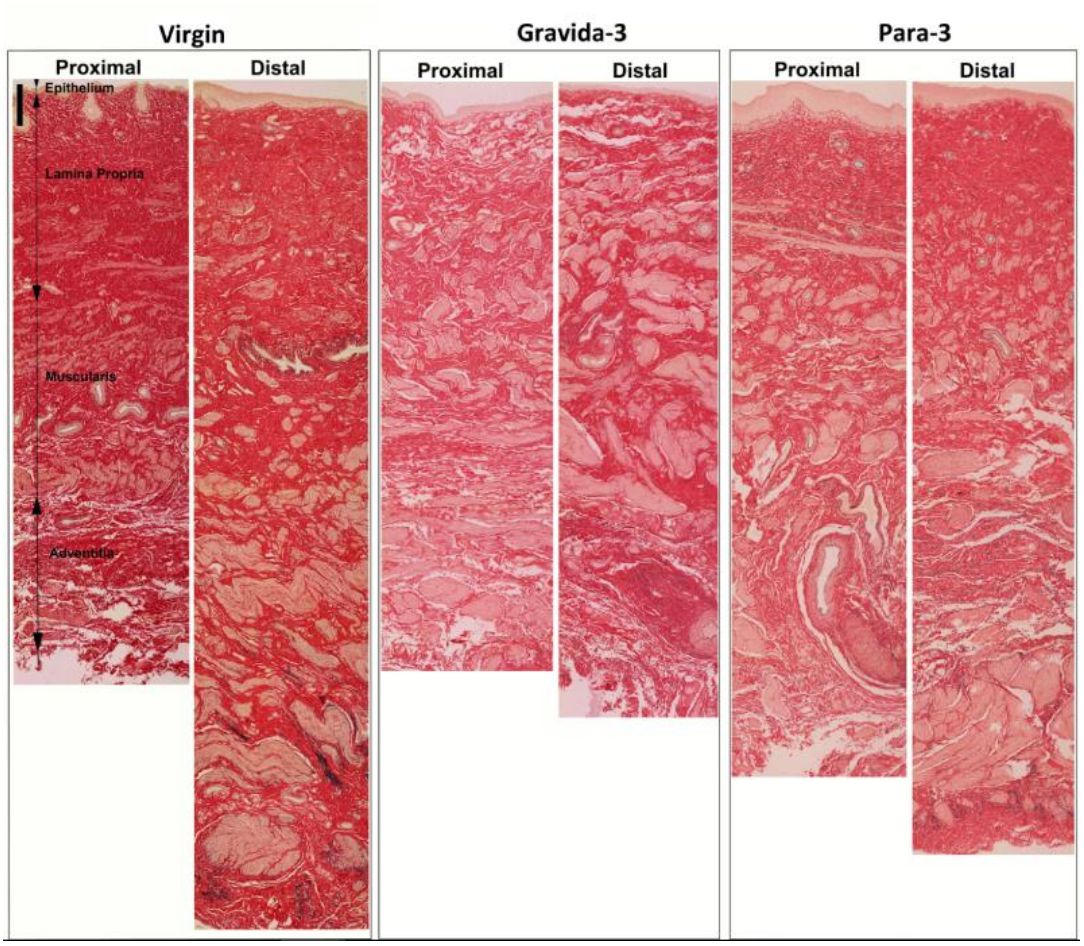

Fig. 3. Histological structure of the proximal and distal ovine vaginal wall using Miller's Elastica staining of virgin, parous and pregnant sheep. Scale bar (upper left) for sections - 200 µm.

Fig. 4 displays the quantitative assessment of collagen, elastin, smooth muscle cells and myofibroblasts throughout the entire thickness of the vagina. The proximal vaginal thickness be less than that of the distal, except during pregnancy. Thinner vaginal walls coincided with a higher collagen, yet lower elastin content and less smooth muscle cells.

In pregnancy, regional differences were not present, except for elastin, which was lower in the proximal vagina. When comparing life cycle stages, the proximal vagina of pregnant sheep had a decrease in collagen, an increase in elastin and smooth muscle cell count. Changes induced by pregnancy were similar in proximal and distal vagina. Changes for para-3 animals followed the same trends, but were not significantly different except for smooth muscle cells.

3.3 Morphological analysis

Fig. 5 compiles the (semi-) quantitative morphological analysis of vaginal wall layers. In virgins, epithelial thickness was smaller in the proximal vagina than distal vagina (47.8%, $p<0.001$). There were no regional differences in parous and pregnant sheep. Comparing different groups, proximal vaginal epithelium was thicker in pregnant sheep than in virgins (39.7%, $p<0.01$), and thinner than in parous (-41.9%, $p<0.001$). Conversely, the distal vaginal epithelium of pregnant ewes was thinner than that of virgins (-26.8%) and parous (-51.4%, $p<0.001$) ewes.

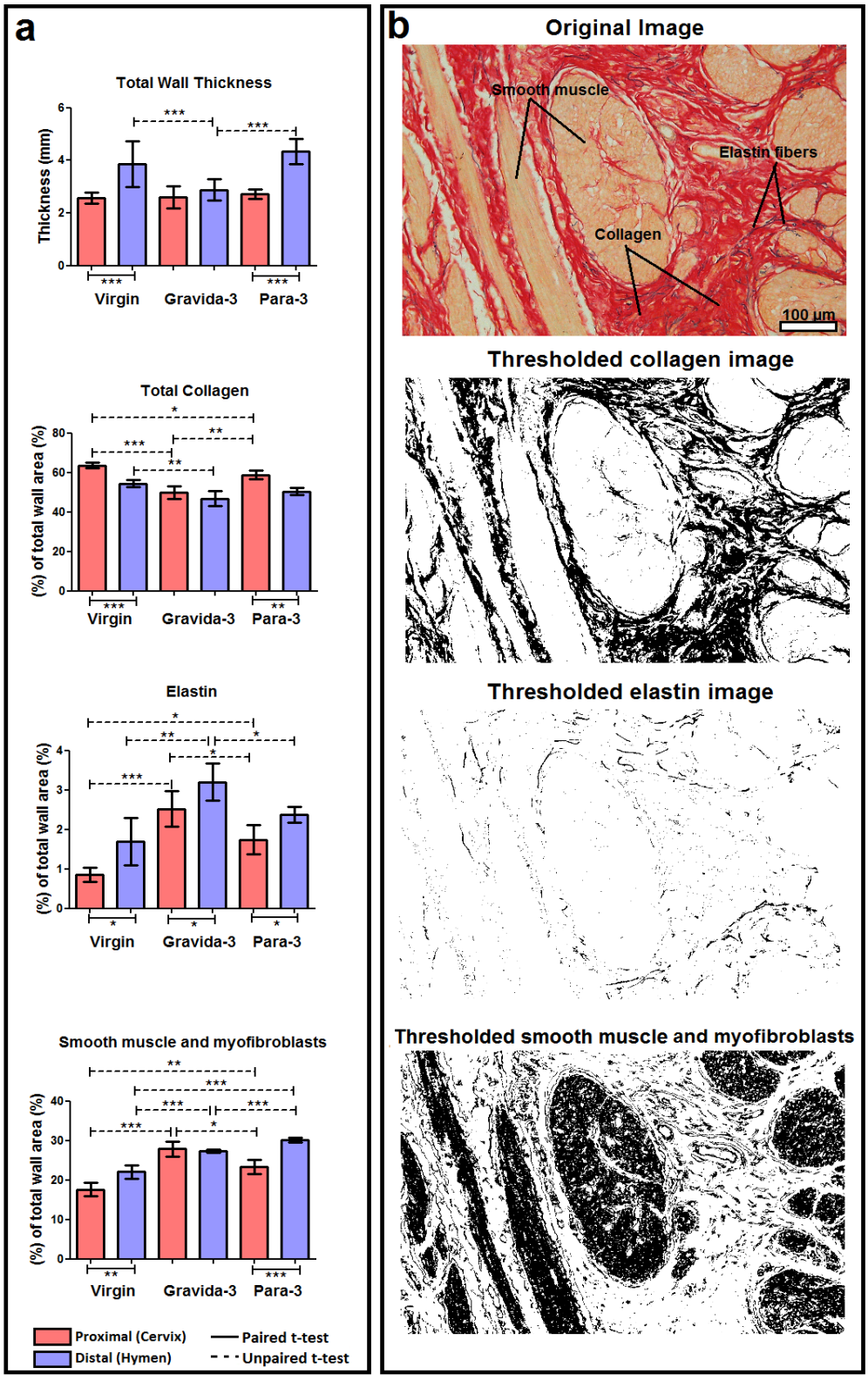

Fig. 4. **a** - Vertical column bar graphs (mean with ± SEM) representing vaginal wall thickness (mm), total collagen (%), elastin (%) and smooth muscle and myofibroblasts content. Proximal vagina (red bars), distal vagina (blue bars). Significant differences between groups are displayed above the bars; differences within groups are indicated under the bars. Significant difference noted when $p<0.05$ (*). $p<0.01$ (**). $p<0.001$ (***). **b** – Histological image of vaginal tissue, stained with Miller's Elastica (collagen- red, elastin fibres- jet black, smooth muscle cells- yellow); scale bar (lower right). Thresholded images used to determine collagen, elastin and smooth muscle content

The lamina propria in the proximal region was thinner than in the distal region, in virgins (-32.0%, $p<0.05$) and pregnant sheep (19.6%, $p<0.05$). Intergroup comparison demonstrated that the proximal lamina propria of pregnant sheep was thinner than of virgins (-26.6%) and parous ewes (-16.5%). Conversely, the distal lamina propria was thicker in virgin sheep than in pregnant (-37.8%, $p<0.01$) and parous (42.1%, $p<0.001$) ewes. The total collagen content in the proximal region was significantly higher than in distal region, irrespective of the group. The collagen content of the proximal lamina propria of virgin's animals was higher than that of parous (11.8%, $p<0.01$) and pregnant (32.8%, $p<0.001$) ewes. The collagen content in the distal region followed the same trends. An opposite observation was made for elastin content. In the proximal region, there were significantly less elastin fibres than in the distal region, irrespective of the group studied. Pregnant sheep had a higher amount of elastin fibres than virgin (90.0%, $p<0.001$) and parous (39.5%, $p<0.05$) in the proximal vagina. The elastin content in the distal region followed the same pattern as in proximal.

The muscularis was the thickest constituting layer. The proximal muscularis was thicker than distal in virgin (39.8%, $p<0.01$) and parous (40.5%, $p<0.001$) sheep, except in pregnant ewes. Group differences included a thinner proximal muscularis in virgin sheep than in pregnant (18.3%) and parous (28.11%, $p<0.01$) ewes.

The distal muscularis was thinner in pregnant sheep compared to that of virgins (19.4%) and parous (42.8%, $p<0.001$) sheep. The total collagen content in the muscularis of the proximal region was higher than of distal region, in parous (21.5%, $p<0.01$) and pregnant ewes (21.1%, $p<0.05$). The muscularis of pregnant ewes contained less collagen in the proximal (15.9%, $p<0.05$) as well as distal (26.1%, $p<0.01$) vagina, than parous. For virgin sheep, there was no significant regional difference. The proximal muscularis had a significantly lower elastin fibre count than the distal region, irrespective of the group studied. The proximal vagina of pregnant sheep had higher amount of elastin fibres than of virgins (59.1%, $p<0.001$) and para-3 ewes (43.7%, $p<0.05$). The proximal lamina propria of virgins had the lowest content of elastin fibres. The elastin content in the distal region followed the same trends.

The proximal adventitia was thinner than the distal in virgins (19.1%, $p<0.01$) and parous (56.4%, $p<0.001$) sheep. The proximal region of virgin sheep had a higher total amount of collagen than that of pregnant ewes (35.6%, $p<0.05$). Conversely, elastin was always lower in proximal region irrespective of the group studied. The elastin content in the distal region followed the same trends. Consistently with observations in the other layers, a higher elastin fibre content was found in the pregnant sheep.

4. Discussion

This research has shown that along the studied reproductive statuses, vaginal tissue undergoes profound histologic and mechanical changes, particularly during pregnancy. During pregnancy, the distal vagina becomes as thin as proximal, i.e., vaginal wall thickness becomes homogenous. Vaginal tissue from pregnant sheep becomes very extensible.

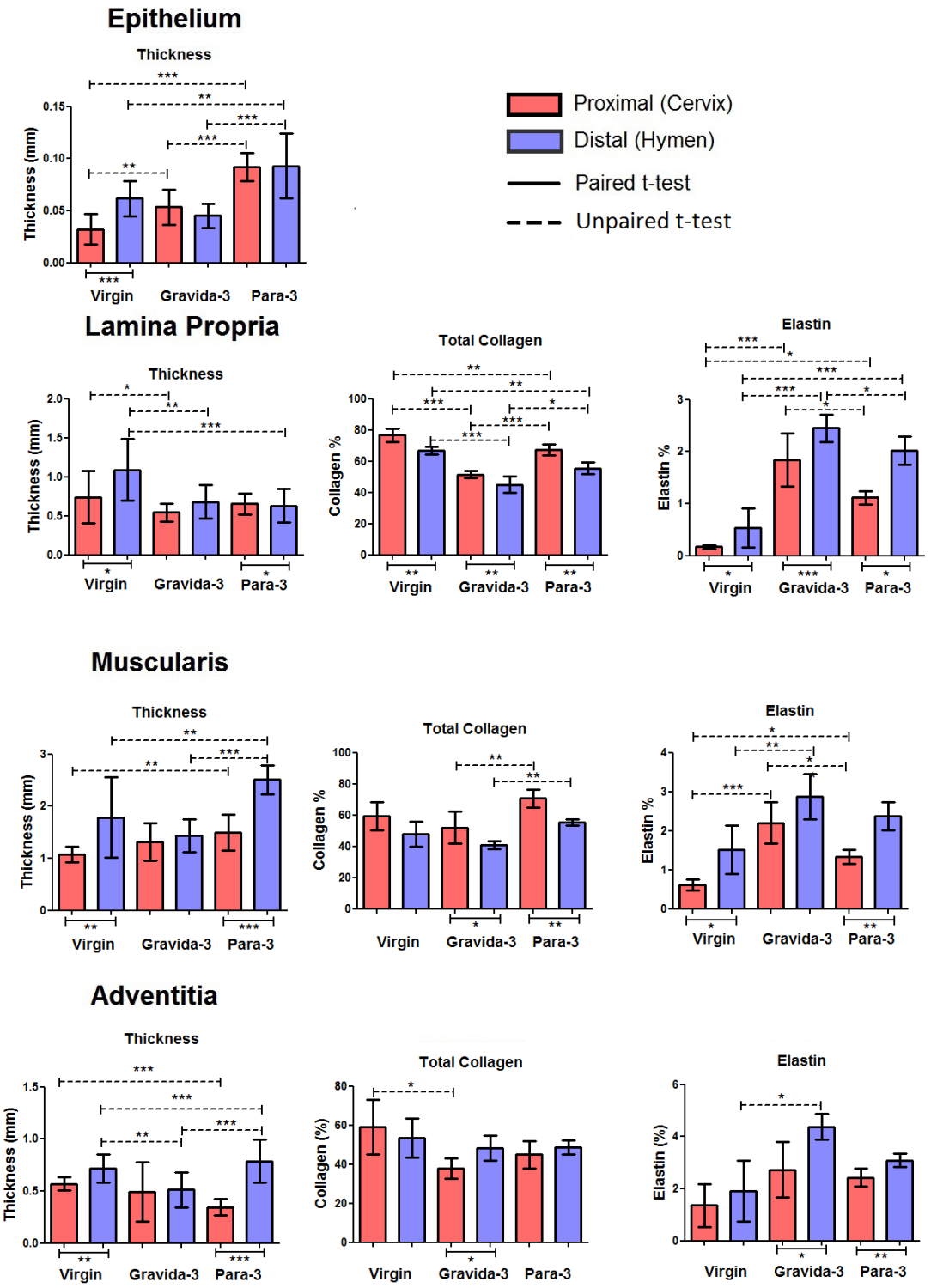

Fig. 5. Morphological analysis of different vaginal wall layers. Vertical column bar graph, mean with ±SEM of wall thickness (mm), total collagen (%) and elastin (%) content of virgin, parous and pregnant sheep. Proximal vagina (red bars), distal vagina (blue bars). Significant differences between groups are displayed above the bars; differences within groups are indicated under the bars. Significant difference noted when $p<0.05$ (*). $p<0.01$ (**). $p<0.001$ (***).

This is associated with significantly low total collagen and high elastin content. In contrast, virgin sheep had the highest total collagen, which was associated with a high ultimate stress. On the other hand, it contained less elastin fibres, which could explain the higher resistance to stretching (Figure 4). After third delivery, the vagina was stiffer than during pregnancy, but not to the level of stiffness observed in virgins. This mechanical behavior is coherent with the collagen and elastin levels discussed above. If these observations were longitudinal, it could be proposed that the biomechanical properties of the vaginal tissue after pregnancy would not recover to those of virgins. These results agree with studies in rats, where the stiffness and strength of vaginal tissues decreased during pregnancy [32]. It was found that they do not recover to the original levels [33].

There were significant regional differences in the ovine vagina. The proximal vagina was stiffer than distal. This is in line with other studies reporting that proximal vagina of post-menopausal sheep is stiffer than distal [26]. However, our research shows that this trend is supported both nulliparous, pregnant and parous sheep, regardless of reproductive status. The quantity and quality of collagen and elastin in connective tissue and organs play a leading role in the biomechanical processes occurring in these tissues.

Biochemical analyses are "gold standard" techniques used for precise total collagen and elastin content measurements [21]. These techniques have been compared with histomorphometric image analysis. Some studies, using image analysis techniques for histology have been published [34]. It was concluded that morphometric analysis proved to be adequate and can be used as a simple, rapid and low-cost technology for evaluating total collagen [35].

This research used image analysis techniques, which allowed a detailed analysis of tissue structure. It was observed that proximal vagina has a higher amount of collagen and a lower amount of elastin than distal vagina. A higher total collagen and lower elastin count coincided with a higher ultimate stress and Young’s modulus. A recent review concluded that the vagina predominantly comprises collagen type I, which is largely responsible for its tensile strength [21, 36].

The morphological analysis showed that during the pregnancy, epithelial thickness becomes homogeneous. One year after delivery, it becomes thicker. In a virgin sheep, the epithelial layer is thin, especially in proximal region. Below the epithelial layer is the lamina propria. Among all investigated layers, lamina propria contains the highest amount of total collagen, and lowest amount of elastin fibres. The lamina propria of proximal vagina is thinner. It contains more collagen and less elastin than distal vagina, among all studied groups. Muscularis is one of the thickest layers of the vaginal wall; it contains less collagen and more elastin fibers, than lamina propria. The muscularis layer of proximal vagina, for all groups, is thinner and contains more collagen and less elastin than distal vagina. Finally, adventitia covers the vagina and attaches it to the surrounding pelvic organs. The adventitia contains less total collagen than other layers, but it has more elastin fibers. The adventitia layer in proximal vagina is thinner and contains less elastin, than distal. (Figure 5).

The current work can be complemented through the active biomechanical properties and estrogen and hormone level measurements. Moreover, the number of groups was

limited, i.e. one delivery/pregnancy group would be ideal to complete a longitudinal study.

Since there are no standards for soft tissue testing, several techniques available in literature were applied [10, 18]. In the present work, some new techniques and tools were adopted. The testing of fresh vaginal specimens is not common; frozen tissue samples are commonly used in other studies [26]. The punch tools for cutting small samples and the additional small grips (which avoid significant damage to the samples and reduce slippage), are an innovation introduced by the present work. The maximum number of specimens was taken (n=3-6) from one sample (animal); these were averaged allowing more accurate results. Two linear regions were investigated, by taking Young's modulus in comfort and stress zone. Comfort zone is considered to be within the physiological range of deformation, whereas the stress zone is in the range of supra-physiological stress. The combined knowledge of the two moduli gives a more detailed understanding of the changes occurring in vaginal tissues during pregnancy and how they recover after delivery. High-resolution histological images were obtained using image processing techniques, making it easier to analyse the full thickness tissues' structure.

5. Conclusions

A detailed comparative analysis of the biomechanical properties, histological and morphometric parameters, for proximal and distal vaginal wall and the effect of repeated pregnancies vaginal deliveries was studied. Morphometric analysis for each vaginal wall layer of the sheep model (squamous epithelium, lamina propria, muscularis and adventitia) was done in a clear and detailed way. Base line observations in young virgin animals were made. Remarkable changes were observed during the third pregnancy which were visible one year after third delivery. It was interesting (although expected) to observe a link between histology and tissue biomechanics. Since elastin has a significant influence on the compliance of soft tissues and collagen is the main "actor" regarding strength, the histological analysis performed in this study justifies the mechanical behaviour observed.

Conflict of interest statement

The authors do not have to disclose any financial or personal relationships with other people or organizations that could inappropriately influence (bias) their work.

Acknowledgment

This research has been supported in part by a grant of the EC in the FP7-framework (Bip-Upy; NMP3-LA-2012-310389). The authors gratefully acknowledge funding from: FCT, Portugal, under grants SFRH / BD / 96548 / 2013, SFRH / BPD / 111846 / 2015; UROSPHINX - Project 16842, COMPETE2020, through FEDER and FCT. JD was a clinical researcher supported by FWO Vlaanderen.

References

[1] Lukacz ES, Lawrence JM, Contreras R, Nager CW, Luber KM, "Parity, mode of delivery, and pelvic floor disorders," *Obstet Gynecol,* vol. 107, pp. 1253-1260, 2006.

[2] Ashton-Miller JA, Delancey JO, "Functional anatomy of the female pelvic floor," *Ann N Y Acad Sci,* vol. 1101, p. 266–296, 2007.

[3] Bump RC, Mattiasson A, Bo K, et al., "The standartization of terminology of female pelvic organ prolapse and pelvic floor dysfunction," *Am J Obstet Gynecol,* pp. 175:10-7, 1996.

[4] Patel DA, Xu X, Thomason AD, Ransom SB, Ivy JS, DeLancey JO. "Childbirth and pelvic floor dysfunction: an epidemiologic approach to the assessment of prevention opportunities at delivery". Am. J. Obstet. Gynecol. 195, 23–28, 2006.

[5] Hendrix SL, et al., " Pelvic organ prolapse in the Women's Health Initiative: gravity and gravidity," *Am J Obstet Gynecol,* vol. 186(6), pp. 1160-1166, 2002.

[6] Goh JT, "Biomechanical properties of prolapsed vaginal tissue in pre- and postmenopausal women," *Int Urogynecol J Pelvic Floor Dysfunct ,* vol. 13, nº discussion 79, pp. 76-79, 2002.

[7] Lei L, Song Y, Chen R, "Biomechanical properties of prolapsed vaginal tissue in pre- and postmenopausal women," *Int Urogynecol J Pelvic Floor Dysfunct,* vol. 18, p. 603–607, 2007.

[8] Rubod C, Boukerrou M, Brieu M, Jean- Charles C, Dubois P, Cosson M, "Biomechanical properties of vaginal tissue: preliminary results," *Int Urogynecol J Pelvic Floor Dysfunct,* vol. 19, p. 811–816, 2008.

[9] Pena E, Calvo B, Martinez MA, et al., " Experimental study and constitutive modeling of the viscoelastic mechanical properties of the human prolapsed vaginal tissue," *Biomech Model Mechanobiol,* vol. 9, p. 35–44, 2010.

[10] Martins P, Lopes Silva-Filho A, Rodrigues Maciel da Fonseca AM, Santos A, Santos L, Mascarenhas T, Natal Jorge RM, Ferreira AJ, "Biomechanical properties of vaginal tissue in women with pelvic organ prolapse," *Gynecol Obstet Invest,* vol. 75(2), pp. 85-92, 2013.

[11] Chantereau P, Brieu M, Kammal M, Farthmann J, Gabriel B, Cosson M, "Mechanical properties of pelvic soft tissue of young women and impact of aging," *Int Urogynecol J,* vol. Nov;25(11), pp. 1547-1553, 2014 .

[12] Goh JT, "Biomechanical and biochemical assessments for pelvic organ prolapse," *Curr Opin Obstet Gynecol ,* vol. 15, p. 391–394, 2003.

[13] Rahn DD, Acevedo JF, Roshanravan S, Keller PW, Davis EC, Marmorstein LY, et al. , "Failure of Pelvic Organ Support in Mice Deficient In Fibulin-3," *Am J Pathol.,* vol. 174, p. 206–215., 2009.

[14] Miesner MD, Anderson DE, "Management of Uterine and Vaginal Prolapse in the Bovine," *Vet Clin North Am Food Anim Pract.,* vol. 24, p. 409–419, 2008.

[15] Otto L, Slayden DO, Clark A, "The rhesus macaque as an animal model for pelvic organ prolapse," *Am J Obstet Gynecol,* vol. 186, p. 416–421, 2002.

[16] Mattson J, Kuehl TJ, Yandell PM, Pierce LM, Coates KW, "Evaluation of the aged female baboon as a model of pelvic organ prolapse and pelvic reconstructive surgery," *Am J Obstet Gynecol,* vol. 192, p. 1395–1398, 2005.

[17] Ulrich D, Edwards SL, Su K, White JF, Ramshaw JA, Jenkin G, Deprest J, Rosamilia A, Werkmeister JA, Gargett CE, "Influence of reproductive status on tissue composition and biomechanical properties of ovine vagina. 7;9(4):e," vol. 9(4), 2014 Apr.

[18] Rubod C, Boukerrou M, Brieu M, Dubois P, Cosson M, "Biomechanical properties of vaginal tissue. Part 1: new experimental protocol," *J Urol.,* vol. 178(1), pp. 320-325, 2007.

[19] Feola A, Moalli P, Alperin M, Duerr R, Gandley RE, Abramowitch S, "Impact of pregnancy and vaginal delivery on the passive and active mechanics of the rat vagina," *Ann Biomed Eng.,* vol. 39, p. 549–558, 2011.

[20] Tokar S, Feola A, Moalli PA, Abramowitch S, "Characterizing the Biaxial Mechanical Properties of Vaginal Maternal Adaptations During Pregnancy," em *ASME 2010 Summer Bioengineering Conference,*, Naples, Florida, USA, 2010.

[21] Ulrich D, Edwards SL, Letouzey, Su K, White JF, Rosamilia A, Gargett CE Werkmeister JA, "Regional variation in tissue composition and biomechanical properties of postmenopausal ovine and human vagina," vol. 9(8), 2014 Aug 22.

[22] Abramowitch SD, Feola A, Jallah Z, Moalli PA, "Tissue mechanics, animal models, and pelvic organ prolapse: a review," *Eur J Obstet Gynecol Reprod Biol.,* pp. 146-158, 2009.

[23] Patnaik SS, Weed B, Borazjani A, Bertucci R, Begonia M, Wang B, Williams L, Liao J, "Biomechanical Characterization of Sheep Vaginal Wall Tissue: A Potential Application in Human Pelvic Floor Disorders," em *ASME,* 2012.

[24] Shepherd PR, "Vaginal Prolapse in Ewes," *Vet Rec,* vol. 130, pp. 564-564, 1992.

[25] Couri BM, Lenis AT, Borazjani A, Paraiso MF, Damaser MS, "Animal models of female pelvic organ prolapse: lessons learned," *Expert Rev. Obstet Gynecol,* vol. 7, pp. 249-260, 2012.

[26] Ulrich D, Edwards SL, Su K, White JF, Ramshaw JA, Jenkin G, Deprest J, Rosamilia A, Werkmeister JA, Gargett CE, 2014. Influence of reproductive status on tissue composition and biomechanical properties of ovine vagina. Publ. Lib. Sci. 9.

[27] Rynkevic R, Martins P, Joyeux L, Engels A, Almeida H, Fernandes AA, Deprest J, "Microstructural Vaginal Tissue Transformations In Virgin, Pregnant And Postpartum Ewes" *Neurourology and Urodynamics,* vol. 35, nº 3, pp. 150-152, 2016.

[28] Vedaldi A, Fulkerson B, "VLFeat: An Open and Portable Library," 2008. Available: http://www.vlfeat.org. [Acessed on 07 03 2018].

[29] De Landsheere L, Munaut C, Nusgens B, Maillard C, Rubod C, Nisolle M, Cosson M, Foidart JM, "Histology of the vaginal wall in women with pelvic organ prolapse: a literature review.," *Int Urogynecol J.,* vol. 24, nº 12, pp. 2011-20, 2013.

[30] Ozog Y, Konstantinovic M, Werbrouck E, De Ridder D, Mazza E, Deprest J., "Persistence of polypropylene mesh anisotropy after implantation: an experimental study," BJOG, vol. 118, nº 10, pp. 1180-5, 2011.

[31] Junqueira LC, Mescher AL, 2009. Junqueira's Basic Histology, 12th. McGraw-Hill Medical, New York. Chapter 22.

[32] Alperin M, Feola A, Duerr R, Moalli P, Abramowitch S, " Pregnancy- and delivery-induced biomechanical changes in rat vagina persist postpartum," *Int Urogynecol J.,* vol. 21, nº 9, pp. 1164-74, 2010 Sep

[33] Drewes PG, Yanagisawa H, Starcher B, Hornstra I, Csiszar K, Marinis SI, et al., "Pelvic organ prolapse in fibulin-5 knockout mice: pregnancy-induced changes in elastic fiber homeostasis in mouse vagina," Am J Pathol. American Society for Investigative Pathology, vol. 170, pp. 578-589, 2007.

[34] De Landsheere L, Brieu M, Blacher S, Munaut C, Nusgens B, Rubod C, Noel A, Foidart JM, Nisolle M, Cosson M, "Elastin density: Link between histological and biomechanical properties of vaginal tissue in women with pelvic organ prolapse?," Int Urogynecol J, vol. 27, nº 4, pp. 629-635, 2016.

[35] Caetano GF, Fronza M, Leite MN, Gomes A, Frade MA, "Comparison of collagen content in skin wounds evaluated by biochemical assay and by computer-aided histomorphometric analysis," Pharm Biol, vol. 14, pp. 1-5, 2016.

[36] Ramshaw JA, Peng YY, Glattauer V, Werkmeister JA , "Collagens as biomaterials.," *J Mater Sci Mater Med 20 ,* vol. Suppl 1, p. S3–58, 2009.

CHAPTER 6

THE EFFECT OF CONSECUTIVE PREGNANCIES ON THE OVINE PELVIC SOFT TISSUES: LINK BETWEEN BIOMECHANICAL AND HISTOLOGICAL COMPONENTS

Rita Rynkevic[1, 2, 3], Pedro Martins[1, 2], Diogo Andre[1, 2], Marco Parente[1, 2], Teresa Mascarenhas[4], Henrique Almeida[5], Antonio A. Fernandes[1, 2]

[1] University of Porto, Faculty of Engineering, Portugal,
[2] INEGI, University of Porto, Faculty of Engineering, Portugal,
[3] KU Leuven, Department Development and Regeneration, Biomedical Sciences, Leuven, Belgium.
[4] Faculty of Medicine, University of Porto, Alameda Prof. Hernâni Monteiro, Portugal
[5] University of Porto, Faculty of Medicine, Department of Experimental Biology, Portugal

Key words: pelvic floor, soft tissues, animal model, biomechanical properties, histological components, pregnancy

Annals of Anatomy 222 (2019) 166–172

Contents lists available at ScienceDirect

Annals of Anatomy

journal homepage: www.elsevier.com/locate/aanat

RESEARCH ARTICLE

The effect of consecutive pregnancies on the ovine pelvic soft tissues: Link between biomechanical and histological components

Rita Rynkevic[a,b,c,d], Pedro Martins[a,b,*], Antonio Andre[b], Marco Parente[a,b], Teresa Mascarenhas[e], Henrique Almeida[f], Antonio A. Fernandes[a,b]

Published in Journal Annals of Anatomy, vol. 222, 166-172 (2019)

ABSTRACT

Background: Pelvic organ prolapse, various types of incontinence (urinary incontinence, defecatory dysfunction), chronic cystourethritis, and sexual dysfunctions remain the most common disorders in urogynecology. Currently, it is believed that the nature and number of births plays a major role in their development. Moreover, after these events, pelvic floor tissues may not recover to their original statuses. The close anatomical relationship among the vaginal wall, bladder and rectum often contribute to the emergence of anatomical-functional failure of adjacent organs and systems.

Basic procedures: The aim of this study was to investigate the effect of consecutive pregnancies on pelvic floor soft tissues, conducting biomechanical and histological analysis. Fifteen Swifter ewes: virgins, parous and pregnant were used. Samples, for uniaxial tension tests and histological analysis, were cut out from fresh tissue. A description of the mechanical properties of native tissue was obtained from the stress-strain curve. Histological samples were stained with Miller's Elastica staining and analyzed using ImageJ software. Collagen, elastin, and smooth muscle contents (%) were analyzed along the full wall thickness of the selected organs. The links between mechanical properties of the soft tissues and histological parameters were analyzed.

Main Findings: Mechanically, vaginal wall tissue and cervix of pregnant sheep were more compliant. In contrast, bladder and rectum became stiffer and had the highest total collagen content. Parous sheep rectum and bladder were stiffer, compared to virgin sheep.

Principal Conclusions: Tensile strength appears to be linked to total collagen content. Elastin and smooth muscle show a direct influence on tissue compliance.

1. Introduction

The dysfunction of the pelvic floor is understood as a complex of disorders. It affects the ligamentous apparatus and pelvic floor muscles that hold the pelvic organs in a normal position and provide urine and feces containment (Kenton and Mueller, 2006).

Pelvic organ prolapse, various types of incontinence (urinary incontinence, defecatory dysfunction), chronic cystourethritis, sexual dysfunctions remain the most common disorders in urogynecology. Function failure of the pelvic floor muscles and organs has several reasons: age, heredity, childbirth traumatism, birth of a large fetus, severe physical exertion associated with increased intra-abdominal pressure, between others. Currently, it is believed that the nature and number of births plays a major role in this process. This occurs mainly due to damage of the perineal muscles and pelvic diaphragm during childbirth (MacLennan et al., 2000; Karasick and Spettell, 1997). Some authors consider that caesarean section has a protective role for the pelvic floor (Larsson et al., 2009; Lukacz et al., 2006), which seems in contradiction with cases of prolapse in nulliparous women as reported by Buchsbaum et al., 2006. Moreover, there is no significant difference in the incidence of prolapse in women after vaginal delivery "per vias naturalis" and women that underwent caesarean section (Larsson et al., 2009).

Regarding the elastin and collagen contributions for tissue's load bearing, evidence shows that collagen fibers play a dominant role (Urbankova et al. 2018). Collagen is largely responsible for soft tissue tensile strength, while elastin makes the tissue more compliant (Fung, 1993). The factors such as collagen dispersion and orientation, undulation and orientation, type I:III ratio may contribute to the changes occurring during the pregnancy (Urlich et al., 2014). De Landsheere et al. (2013) found less collagen in pregnant vaginal tissue and no significant difference in collagen type III between pregnant, virgin and parous. While collagen type I is largely responsible for tissue' tensile strength (Jackson et al., 2002). Elastin fibers may play an important role in pelvic floor mechanics, however, alone they are unable to change the mechanical properties of the pelvic floor (Rahn et al., 2008).

The close anatomical relationship between the vaginal wall, bladder and rectum often contribute to the emergence of anatomical-functional failure of adjacent organs and systems. The levator ani muscle stabilizes the abdominal and pelvic organs. Urethra and the rectum are mechanically closed by the levator ani muscle; it relaxes at the beginning of urination and defecation.

The aim of this study was to investigate the impact of subsequent pregnancies on pelvic floor soft tissues, through the analysis of the relationship between biomechanical parameters and histological components. This research can contribute to improve the understanding of pelvic floor soft tissues transformation before delivery, both in terms of biomechanics and histology. The study also includes a follow-up of the recovery of pelvic floor soft tissues one year after vaginal parturition, using virgin sheep as baseline model.

Since studies on fresh human pelvic soft tissues are limited, due to shortage of material and ethical concerns, the sheep model was used in these studies. Despite being a quadruped, the pelvic floor tissues and anatomy of sheep are comparable (relatively) in size and structure to humans (Abramowitch et al., 2009). Moreover, the risk factors such

as increased intraabdominal pressure, parity or obesity are similar (Abramowitch et al., 2009; Sourav et al., 2012; Couri et al., 2012; Shepherd, 1992). It is possible to perform vaginal surgery with/without graft insertion (Urbankova et al., 2017). Furthermore, there are some studies regarding the comparative analysis of the ovine and female pelvic floor anatomy (Urbankova et al., 2017).

2. Methods

2.1 Animal model

Three groups of Swifter ewes (virgin, pregnant and parous) were selected: virgins (n=5; mean weight = 45 kg), pregnant (n=5; term = 145 days; mean weight = 65 kg) after two prior vaginal deliveries and parous (n=5; mean weight = 60 kg) at least one year after three vaginal deliveries, were used. Virgin sheep were nine-month-old, while pregnant were three years old and parous four years old. Ewes used in this study were obtained from the Zoötechnical Institute of the KU Leuven. Animals were maintained and treated according to an experimental protocol approved by the Ethics Committee for Animal Experimentation of the KU Leuven Faculty of Medicine. All the animal procedures undertaken as part of the work described in this paper were carried out in accordance with the European regulations for animal use and care (European Directive 2010/63/EU and National Decree-Law 113/2013). Ewes were euthanized by intravenous injection of 10 mL of a mixture of embutramide 200 mg, mebezonium 50 mg and tetracaine hydrochloride 5 mg (T61; Hoechst Marion Roussel, Brussels, Belgium).

2.2 Sample preparation

For this study vaginal wall (distal part), rectum (distal part), bladder, cervix, uterus, levator ani muscle (LAM) and external anal sphincter (EAS) were collected. The distal part of vaginal wall and rectum were selected, since it is prone to tears induced by vaginal delivery.

Excised tissues were divided into samples for biomechanical testing and for histological analyses. The storage time of the soft tissues (until testing) did not exceed 4 hours.

For the biomechanical testing vaginal tissue specimens were cut along the longitudinal axis using a dog bone shape punch (2mm x 30mm). Samples from rectum, bladder, uterus and cervix were cut in the longitudinal axis using a rectangular shape cutting form (10mm x 50mm). External anal sphincter and levator ani muscles were carefully separated from surrounding tissues. Each tissue was then tested as a single sample to preserve its integrity. Prior to measurements tissues were kept in wet (saline soaked) gauze at room temperature (~ 20 º C). Each specimen was tested as soon as it was prepared to reduce unnecessary over-exposure to the environment.

For histological analysis vaginal wall, rectum, bladder and uterus (the uterus only from virgin and parous sheep) were fixed in 4% paraformaldehyde during 24 hours. Then, specimens were washed in PBS and stored in ethanol. 6-µm tissue slices were stained with Miller's Elastica staining.

2.3 Uniaxial tensile testing

Tensile tests were performed using Zwick tensiometer (Zwick GmbH & Co. KG, Ulm, Germany). Samples were pre-loaded untill 0.1 N using a constant elongation of 5 mm/min. Specimens' width and thickness were taken at three locations along the sample length and averaged, to calculate the stress. After the pre-load specimens were loaded using a constant elongation rate of 10 mm/min until failure. The strain of the analyzed specimens was calculated by dividing the elongation ($\Delta L=L\_1-L\_0$) by the clamp-to-clamp length (L_0). The Young's modulus (MPa) was calculated from the stress-strain curve in-the comfort zone, limited to the physiological range (10-20%) of deformation and at the stress zone, in the range of supraphysiological stress (70-80%) (Ozog et al., 2011). The point where these linear segments intersect was defined as the inflection point.

2.4 Histological image processing analysis

Images, showing a complete set of histological components, were analyzed. Separate images were captured at 10× magnification, using Zeiss microscope (Zeiss Axioplan 400, Oberkochen, Germany). Then using a Matlab (Release 2015®, The MathWorks, Inc.) stitching script based on the algorithms available from VLFeat library (Vedaldi and Fulkerson, 2008), individual images were connected into one full thickness image. After stitching, all images were processed using ImageJ (open platform for scientific image analysis) and the Color Deconvolution plugin. Applying a threshold algorithm, RGB images were converted to binary images (Rynkevic et al., 2017). The contents (%) of total collagen, elastin, and smooth muscle were determined from processes images, relative to the total area (%) of the sample.

High-resolution histological images were obtained using image processing techniques, making it easier to analyze the full thickness of the tissues' microstructure (Caetano et al., 2016).

2.5 Statistical analyses

All statistical analyses were conducted using a statistical software package (GraphPad Prism 5, USA). Statistical analyses were performed to investigate possible significant differences in mechanical properties and structural composition among experimental groups. Quantitative data are represented as mean ± standard error of the mean (SEM). Kolmogorov-Smirnov tests showed the data follows a normal distribution, a requirement for ANOVA. One-way ANOVA and post hoc test (Tukey's correction) were carried out for the intergroup comparisons. The level of significance was set to $p<0.05$.

3. Results

For the virgin sheep, the biomechanical properties of the vaginal wall, cervix, uterus, bladder, rectum, and muscles (external anal sphincter and levator ani muscle) differed significantly (Fig. 1). Vaginal wall was stiffer and less extensible than rectal tissue and bladder. Cervix and uterus were less stiff than vagina, but stiffer than bladder and rectal

tissue. The muscles could withstand significant deformation compared to the vaginal wall, cervix and uterus, however, much less than rectum and bladder.

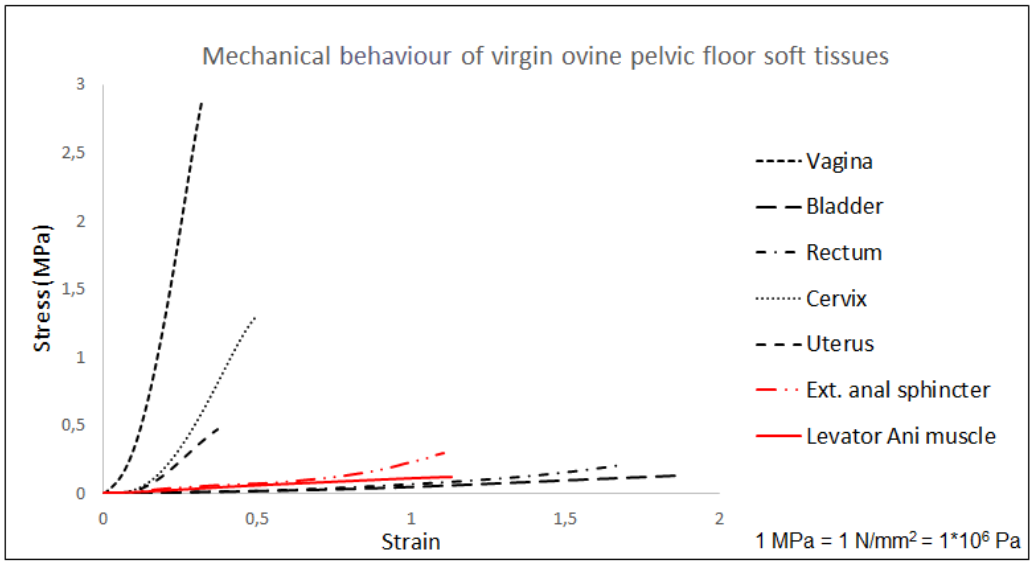

Fig. 1. Mechanical behaviour of virgin sheep pelvic floor soft tissues

Full thickness high quality histologic images of sheep vaginal wall, uterus, bladder and rectal wall are provided in Figure 2. To understand the impact of pregnancy and multiple deliveries on pelvic floor soft tissues, each organ was considered separately (Fig. 3). Table 1 summarises mechanical behaviour and quantitative morphological analysis of distal part of vaginal wall. Pregnant sheep vaginal tissue was more compliant, than of virgin sheep (39.8%; $p<0.05$). (Table 1). One year after third delivery vagina of parous sheep was less compliant than in the third pregnancy (40.7 %; $p<0.05$).

The results of the morphological analysis showed that thickness of vaginal wall changed during the pregnancy (Table 1). Vaginal wall was thinner in pregnant sheep than in virgins (25.5%; $p<0.05$) and then in parous (33.6%; $p<0.05$). The vaginal wall of parous sheep became thicker than of virgin (10.9%) ewes. The total collagen content in vaginal wall was significantly higher in virgin sheep than in pregnant (14.1%; $p<0.05$) or parous (7.3%; $p<0.05$). An opposite observation was made for elastin content. Pregnant sheep had a higher amount of elastin fibres than virgin (47.2%; $p<0.05$) and parous (25.9%, $p<0.05$). Smooth muscle cells and myofibroblasts content were higher in parous sheep than in pregnant (10.6 %; $p<0.05$) and virgin (26.74%; $p<0.05$). During the pregnancy, smooth muscle cells content increased, compared to virgin levels (19.45%; $p<0.05$).

Table 2 represents mechanical behaviour of cervical tissue. Biomechanical characteristics of the tissue showed that pregnancy affects the mechanical properties of the cervix. It became more compliant than in virgin (35.9%, $p<0.05$) and in parous sheep (31.7%; $p<0.05$).

Mechanical behavior and morphological parameters of virgin and parous sheep uterus are represented in Table 3. Uniaxial tests showed significant difference in mechanical behavior between virgin and parous sheep uterus. Young's moduli in comfort and stress

zone differed significantly (70.9%; $p<0.05$), (55.4%; $p<0.05$). Elongation increased as well (34.9%; $p<0.05$). Morphological analysis showed, that parous sheep uterus became thicker (39,6%; $p<0.05$), it contained less total collagen (30.05%; $p<0.05$) and more elastin fibers (17.3%; $p<0.05$) than of virgin sheep.

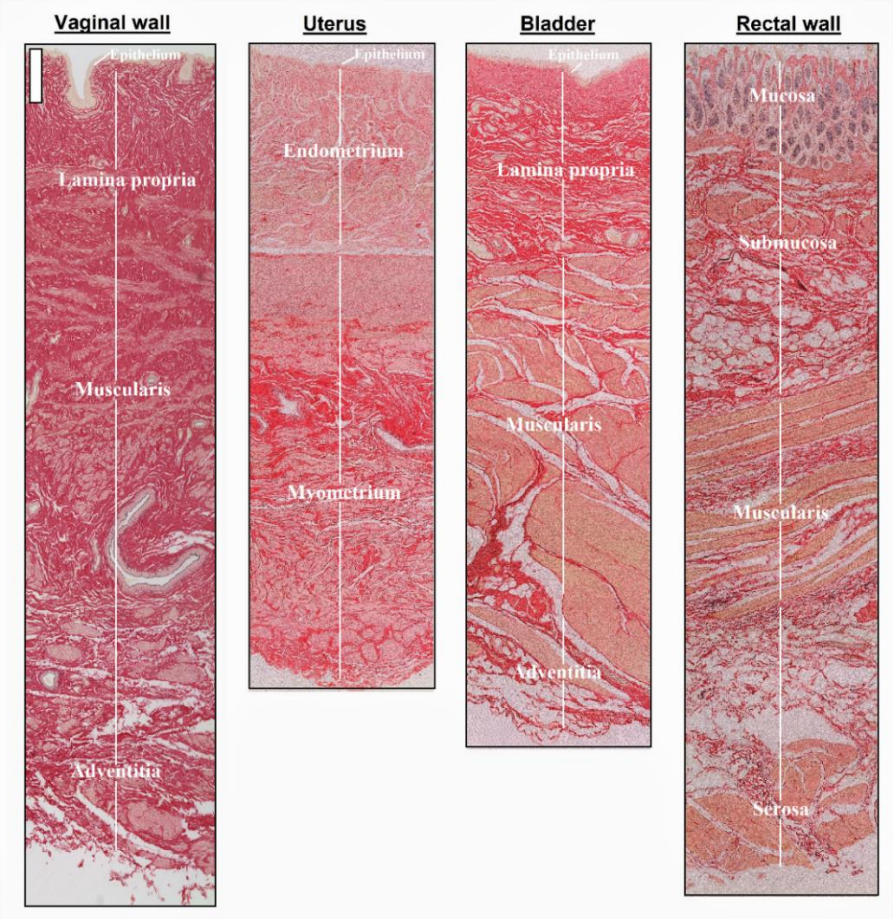

Fig. 2. Histological image of the ovine vaginal wall, uterus, bladder and rectal wall using Miller's Elastica staining. Scale bar (upper left) for sections - 200 µm.

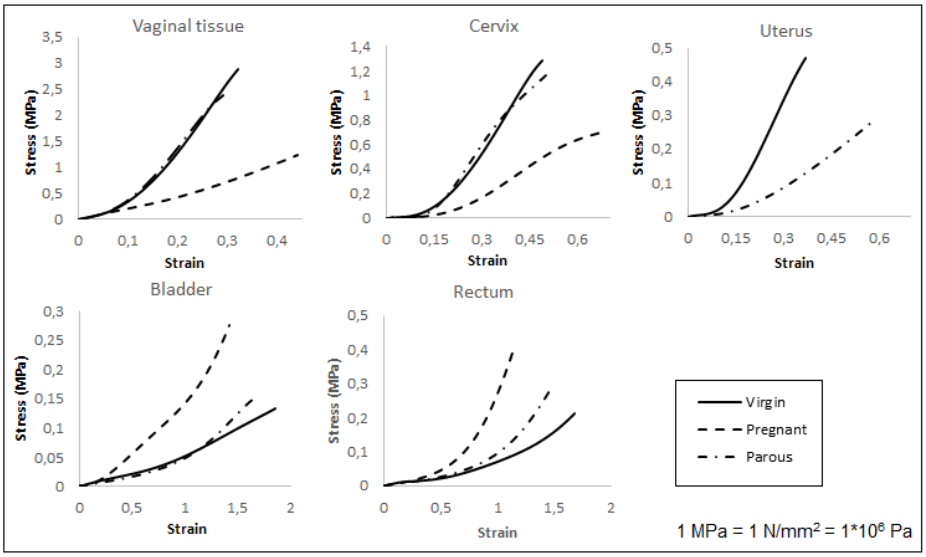

Fig. 3. Representative Stress - Strain curves showing mechanical behaviour of the pelvic floor soft tissues of virgin (n=5), parous (n=5) and pregnant (n=5) sheep.

Table1. Mechanical characteristics and morphological analysis of ovine vaginal wall. Data is presented as mean (± SEM), significant differences among the groups were set to p <0.05: **a**- virgin vs pregnant, **b**- pregnant vs parous, **c**-parous vs virgin

Biomechanical properties of ovine distal vagina						
Tissue	Nr	Young's modulus at comfort zone (MPa)	Young's modulus at stress zone (MPa)	Inflection point	Strain at Ultimate stress	Ultimate Stress (MPa)
Virgin	N=5	2.000 ± 0.529	9.738 ± 1.697 **a**	0.1294 ± 0.014	0.3277 ± 0.017 **a**	2.704 ± 0.239 **a**
Pregnant	N=5	1.759 ± 0.27 **b**	3.879 ± 0.748 **b**	0.1758 ± 0.031	0.4822 ± 0.049 **b**	1.253 ± 0.177 **b**
Parous	N=5	2.629 ± 0.528	10.58 ± 2.575	0.1181 ± 0.014	0.2958 ± 0.030	2.111 ± 0.342
Morphological analysis of ovine distal vagina						
Tissue	Nr	Collagen (%)	Elastin (%)	Smooth muscle (%)	Thickness (mm)	
Virgin	N=5	54.42 ± 0.8644 **a**	1.693 ± 0.3009 **a**	22.07 ± 0.8352 **a**	3.864 ± 0.2541 **a**	
Pregnant	N=5	46.86 ± 1.6513 **b**	3.201 ± 0.2112 **b**	27.40 ± 0.1955 **b**	2.880 ± 0.1039 **b**	
Parous	N=5	50.45 ± 0.8979 **c**	2.370 ± 0.0999	30.13 ± 0.2940 **c**	4.340 ± 0.1374	

Table2. Mechanical characteristics of ovine cervix. Data is presented as mean (± SEM), significant differences among the groups were set to p <0.05: **a**- virgin vs pregnant, **b**- pregnant vs parous, **c**-parous vs virgin

Biomechanical properties of ovine cervix						
Tissue	Nr	Young's modulus at comfort zone (MPa)	Young's modulus at stress zone (MPa)	Inflection point	Strain at Ultimate stress	Ultimate Stress (MPa)
Virgin	N=5	0.2764 ± 0.037	2.031 ± 0.331 **a**	0.2477 ± 0.017 **a**	0.5000 ± 0.017 **a**	1.248 ± 0.116 **a**
Pregnant	N=5	0.2425 ± 0.029	1.727 ± 0.285 **b**	0.1808 ± 0.012	0.7098 ± 0.048 **b**	0.807 ± 0.059 **b**
Parous	N=5	0.2620 ± 0.036	2.699 ± 0.331	0.1867 ± 0.008 **c**	0.4644 ± 0.029	1.172 ± 0.104

Table3. Mechanical characteristics of ovine uterus. Data is presented as mean (± SEM), significant differences among the groups were set to p <0.05: **a**- virgin vs pregnant, **b**- pregnant vs parous, **c**-parous vs virgin

Biomechanical properties of ovine uterus						
Tissue	Nr	Young's modulus at comfort zone (MPa)	Young's modulus at stress zone (MPa)	Inflection point	Strain at Ultimate stress	Ultimate Stress (MPa)
Virgin	N=5	0.3785 ± 0.026 **a**	1.704 ± 0.129 **a**	0.1591 ± 0.011 **a**	0.366 ± 0.015 **a**	0.441 ± 0.027 **a**
Pregnant	N/A	N/A	N/A	N/A	N/A	N/A
Parous	N=5	0.1048 ± 0.012	0.7603 ± 0.096	0.2936 ± 0.029	0.563 ± 0.054	0.287 ± 0.038
Morphological analysis of ovine uterus						
Tissue	Nr	Collagen (%)	Elastin (%)	Smooth muscle (%)	Thickness (mm)	
Virgin	N=5	35.83 ± 2.601 **a**	4.664 ± 0.2881 **a**	55.97 ± 0.8007	1.780 ± 0.06680 **a**	
Pregnant	N/A	N/A	N/A	N/A	N/A	
Parous	N=5	25.42 ± 1.556	5.634 ± 0.2780	56.63 ± 0.8171	2.951 ± 0.05119	

Pregnant sheep bladder became more rigid. Young's moduli in comfort and stress zones were higher compared to virgin (74.6%; p<0.05) and parous sheep (74.9%; p<0.05) (Table 4). The pregnant sheep bladder became less extensible than virgin's (21.2%; p<0.05) and parous sheep (20.5%; p<0.05). Bladder became significantly thinner during the pregnancy (20.2%; p<0.05). Pregnant sheep bladder conteined more total collagen (34.6%; p<0.05; 13.6%; p<0.05), less elastin (37.6%; p<0.05; 21.6%; p<0.05) and less smooth muscle cells (31.3%; p<0.05; 24.1%; p<0.05) than virgin and parous sheep.

Table4. Mechanical characteristics and morphological analysis of ovine bladder. Data is presented as mean (± SEM), significant differences among the groups were set to p <0.05: **a**- virgin vs pregnant, **b**- pregnant vs parous, **c**-parous vs virgin

Biomechanical properties of ovine bladder						
Tissue	Nr	Young's modulus at comfort zone (MPa)	Young's modulus at stress zone (MPa)	Inflection point	Strain at Ultimate stress	Ultimate Stress (MPa)
Virgin	N=5	0.0345 ± 0.007 **a**	0.2185 ± 0.027 **a**	0.5753 ± 0.069	1.783 ± 0.117 **a**	0.1523± 0.011 **a**
Pregnant	N=5	0.1341 ± 0.012 **b**	0.4272 ± 0.030 **b**	0.6148 ± 0.066	1.403 ± 0.055 **b**	0.3140± 0.024 **b**
Parous	N=5	0.0336 ± 0.002	0.1378 ± 0.012	0.6806 ± 0.051	1.727 ± 0.096	0.2047 ± 0.026
Morphological analysis of ovine bladder						
Tissue	Nr	Collagen (%)	Elastin (%)	Smooth muscle (%)	Thickness (mm)	
Virgin	N=5	34.20 ± 0.8313 **a**	6.090 ± 0.6831 **a**	53.81 ± 1.250 **a**	2.922 ± 0.1855 **a**	
Pregnant	N=5	52.31 ± 1.8271 **b**	3.798 ± 0.5333 **b**	36.94 ± 1.479 **b**	2.337 ± 0.1105	
Parous	N=5	45.20 ± 0.5299 **c**	4.843 ± 0.2618	48.69 ± 1.794 **c**	2.560 ± 0.0754	

However, the total collagen content of parous sheep was higher (24.3%; p<0.05), the elastin fiber content (20.4%) and smooth mucle cell content were lower (10.1% p<0.05) than of virgin sheep.

Significant differences in mechanical properties of the rectum of virgin, pregnant and parous sheep were found (Table 5). Young's moduli of comfort and stress zones were higher in pregnant sheep, compared to virgin (61.9%, p<0.05; 44.1%, p<0.05) and to parous sheep (46.8%, p<0.05; 19.9%, p<0.05), respectively. Parous sheep rectum became stiffer than of virgin (30.5%, p<0.05). However, during the pregnancy rectum became less elastic than of virgin (23.8%, p<0.05) and parous (22.4%, p<0.05).

Table5. Mechanical characteristics and morphological analysis of ovine rectum. Data is presented as mean (± SEM), significant differences among the groups were set to p <0.05: **a**- virgin vs pregnant, **b**- pregnant vs parous, **c**-parous vs virgin

Biomechanical properties of ovine rectum						
Tissue	Nr	Young's modulus at comfort zone (MPa)	Young's modulus at stress zone (MPa)	Inflection point	Strain at Ultimate stress	Ultimate Stress (MPa)
Virgin	N=5	0.0406 ± 0.0047 **a**	0.2037 ± 0.0190 **a**	0.940 ± 0.055 **a**	1.497 ± 0.126 **a**	0.250 ± 0.027 **a**
Pregnant	N=5	0.1052 ± 0.0071 **b**	0.3642 ± 0.0332 **b**	0.656 ± 0.062 **b**	1.144 ± 0.094 **b**	0.404 ± 0.029 **b**
Parous	N=5	0.0559 ± 0.006	0.2920 ± 0.0224 **c**	0.840 ± 0.039	1.474 ± 0.062	0.283 ± 0.014 **c**
Morphological analysis of ovine rectum						
Tissue	Nr	Collagen (%)	Elastin (%)	Smooth muscle (%)	Thickness (mm)	
Virgin	N=5	29.71 ± 0.878 **a**	12. 36 ± 1.1081 **a**	57.34 ± 0.6928 **a**	2.304 ± 0.1359	
Pregnant	N=5	39.39 ± 2.016 **b**	7.790 ± 0.8203 **b**	50.93 ± 1.233	2.357 ± 0.1207	
Parous	N=5	35.16 ± 1.505 **c**	9.754 ± 0.3816	53.44 ± 3.217	2.165 ± 0.1156	

There were no significant differences in rectal wall thickness. Pregnant sheep rectum conteined more total collagen (24.6%; p<0.05) than virgin and parous (10.7%; p<0.05) sheep. It contained less elastin fibers than virgin (36.9%, p<0.05) and parous (20.1%, p<0.05) sheep and less smoth muscle cells. Parous sheep total collagen content was higher (15.5%; p<0.05), elastin fiber content was lower (18.7%) than in virgin. Smooth muscle cell content was significantly higher in virgin sheep compared to pregnant (11.2%, p<0.05) and parous (6.8%).

The EAS, surrounds the margin of the anus and helps to control and delay defecation through its contraction. Computed stress-strain curve parameters demonstrate a hyperelastic behaviour of EAS (Figure 4). There was significant difference in the Young´s

modulus at comfort zone between virgin and pregnant sheep ($p<0.05$). Pregnant sheep muscle was more compliant (Table 6). However, Young`s modulus at stress zone and ultimate stress of parous sheep was significantly higher than of virgin ($p<0.05$) and pregnant ($p<0.05$).

During the pregnancy, muscle becomes more compliant (Figure 4). LAM of parous sheep become significantly stiffer compared to virgin ($p<0.05$) and pregnant sheep ($p<0.05$) (Table 6).

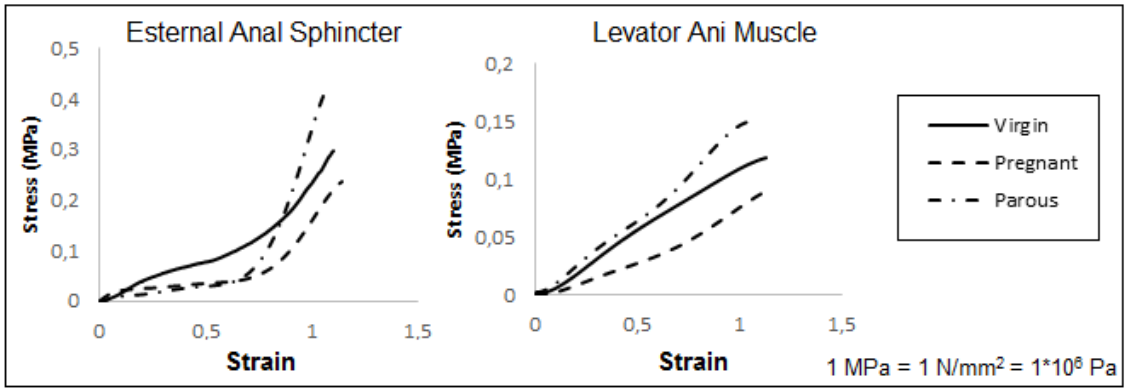

Fig. 4. Representative Stress - Strain curves showing mechanical behaviour of the pelvic floor muscles (EAS and LAM) of virgin (n=5), parous (n=5) and pregnant (n=5) sheep.

Table6. Mechanical characteristics of ovine external anal sphincter and levator ani muscle. Data is presented as mean (± SEM), significant differences among the groups were set to $p<0.05$, **a**-virgin vs pregnant, **b**- pregnant vs parous, **c**-parous vs virgin

Biomechanical properties of ovine external anal sphincter						
Tissue	Nr	Young's modulus at comfort zone (MPa)	Young's modulus at stress zone (MPa)	Inflection point	Strain at Ultimate stress	Ultimate Stress (MPa)
Virgin	N=5	0.1629 ± 0.021 **a**	0.3768 ± 0.051 **a**	0.8073 ± 0.081	1.204 ± 0.138	0.2990 ± 0.039
Pregnant	N=5	0.1069 ± 0.013	0.3456 ± 0.072 **b**	0.6852 ± 0.092	1.289 ± 0.113	0.2664 ± 0.019 **b**
Parous	N=5	0.1122 ± 0.015	0.5424 ± 0.079 **c**	0.5877 ± 0.033 **c**	1.311 ± 0.117	0.4073 ± 0.026 **c**
Biomechanical properties of ovine levator ani muscle						
Tissue	Nr	Young's modulus at comfort zone (MPa)	Young's modulus at stress zone (MPa)	Inflection point	Strain at Ultimate stress	Ultimate Stress (MPa)
Virgin	N=5	0.1477 ± 0.011 **a**	0.1120 ± 0.007 **a**	0.5486 ± 0.043	1.125 ± 0.043	0.1215 ± 0.013 **a**
Pregnant	N=5	0.07670 ± 0.01 **b**	0.07841 ± 0.00 **b**	0.4878 ± 0.051	1.037 ± 0.097	0.0917 ± 0.009 **b**
Parous	N=5	0.1413 ± 0.012	0.1486 ± 0.017 **c**	0.4673 ± 0.041	1.186 ± 0.111	0.1847 ± 0.023 **c**

4. Discussion

This investigation combines histological analysis of the sheep pelvic floor soft tissue with biomechanical studies. This was achieved by comparing groups of individuals at different life stages, before, during and after pregnancy. The impact of subsequent pregnancies and vaginal deliveries on pelvic floor soft tissues was considered. Comparison between groups showed the effect of pregnancy on vaginal tissues. Image analysis techniques were used for histology analysis.

This research has shown that along the studied reproductive statuses, pelvic floor soft tissue undergoes profound histological and mechanical changes, particularly during pregnancy. Vaginal wall tissue and cervix became very compliant. This was associated with significant decrease in total collagen and a significant increase in elastin and smooth muscle cell content. These results agree with studies in rats, where strength of vaginal tissues decreased during pregnancy (Alperin et al., 2010). External anal sphincter and levator ani muscle also showed compliant behavior. In contrast, bladder and rectum had the highest increase in total collagen, which was associated with a high ultimate stress (Ramshaw et al., 2009). In a sheep the bladder is located inferior to the uterus. During pregnancy the uterus takes up significantly more space and severely limits the expansion of the urinary bladder.

This study has shown that soft tissues from the pelvic floor of parous sheep do not fully recover one year after vaginal deliveries. Parous sheep uterus became compliant and did not return to virgins' level, in agreement with studies by Drewes et al. (2007). Histological analysis confirmed the biomechanical findings. One year after vaginal delivery uterus became more compliant than of virgin sheep. Parous sheep uterus contained less collagen (total) and more elastin fibers and smooth muscle cells. Parous sheep rectum and bladder had higher ultimate stress, compared to virgin sheep. Total collagen content was higher in parous sheep, as expected. There were significant differences between levator ani muscle and external anal sphincter of virgin and parous sheep; they became less compliant one year after vaginal deliveries.

The elastic fibers and smooth muscle cells in the rectum and urinary bladder walls contribute to their distensibility and elasticity. This allows them to stretch and return to their original size and form several times a day (Boron et al., 2016).

For both parous and pregnant sheep, the elastin fibres and smooth muscle cell contents of rectum and bladder were significantly decreased. These changes reduced their flexibility and capacity. As a result, this could be related with frequent urination or urinary incontinence, involuntary defecation and haemorrhoids or pelvic organ prolapse. Previous studies on animal models confirm these observations, demonstrating the importance of elastic fibres for maintaining structural and functional integrity of the female pelvic floor (Ferrell, et al., 2009, Liu et al., 2006; Liu et al., 2004).

The current work has some limitations. There was a lack of uterus samples from the pregnant sheep due to birth via c-section. There was no histological analysis of the external anal sphincter, levator ani and cervix due to considerations regarding the integrity of the analyzed specimens. Another limitation of the present work is the lack of an interobserver variability analysis, since the image thresholding required to estimate the relative quantities of tissue components, was semi-automatic. However, other studies comparing this image analysis technique with immunohistochemistry concluded that the former can be used as a simple, rapid, low-cost technology for evaluating histologic features (Caetano et al., 2016).

Basic science may improve clinical outcomes of pelvic floor disorders through advances on the understanding of disease mechanisms, and an improved knowledge about normal physiology.

A database of histology and biomechanical information combined with life history data, with adequate data mining resources may pave the way to produce patient customized prosthetics, with mechanical properties tailored to individual requirements.

5. Conclusions

A comparative biomechanical and histological analysis of pelvic floor soft tissues was carried out. It was observed that pelvic floor soft tissues (vagina, bladder, and rectum) undergo profound histologic and mechanical changes, particularly during pregnancy and do not recover to original levels one year after delivery. A link between the mechanical properties of the vaginal walls, bladder and rectum and their histological components – elastin, total collagen, and smooth muscle was observed. In particular tensile strength appears to be linked to total collagen fraction and elastin and smooth muscle fraction with tissue compliance.

Conflict of interest statement

The authors do not have to disclose any financial or personal relationships with other people or organizations that could inappropriately influence (bias) their work.

Acknowledgment

This research has been supported by Fundação para a Ciência e a Tecnologia I.P. (FCT, Portugal) under the grand SFRH/BD/96548/2013, SFRH/BPD/111846/2015; UROSPHINX - Project 16842, COMPETE2020, through FEDER and FCT; and in part by a grant of the EC in the FP7-framework (Bip-Upy; NMP3-LA-2012-310389).

References

Abramowitch, S.D., Feola, A., Jallah, Z., Moalli, P.A., 2009. Tissue mechanics, animal models, and pelvic organ prolapse: Eur. J. Obstet. Gynecol. Reprod. Biol. 144, 146–158.

Alperin, M., Feola, A., Duerr, R., Moalli, P., Abramowitch, S., 2010. Pregnancy- and delivery-induced biomechanical changes in rat vagina persist postpartum. Int. Urogynecol J. 21, 1164-1174.

Boron, W.F. Boulpaep, E.L., 2016. Medical Physiology. 3: Elsevier Health Sciences.

Buchsbaum, G.M., Duecy, E.E., Kerr, L.A., Huang, L.S., Perevich, M., Guzick, D.S., 2006. Pelvic organ prolapse in nulliparous women and their parous sisters. Obstet. Gynecol. 108, 1388-1393.

Caetano, G.F., Fronza, M., Leite, M.N., Gomes, A., Frade, M.A., 2016. Comparison of collagen content in skin wounds evaluated by biochemical assay and by computer-aided histomorphometric analysis. Pharm. Biol. 14, 1-5.

Couri, B.M., Lenis, A.T., Borazjani, A., Paraiso, M.F, Damaser, M.S., 2012. Animal models of female pelvic organ prolapse: lessons learned. Expert Rev. Obstet. Gynecol. 7, 249-260.

De Landsheere, L., Munaut, C., Nusgens, B., Maillard, C., Rubod, C., Nisolle, M., Cosson, M., Foidart, J.M., 2013. Histology of the vaginal wall in women with pelvic organ prolapse: a literature review. International Urogynecology Journal 24, 2011-2020.

Drewes, P.G., Yanagisawa, H., Starcher, B., Hornstra, I., Csiszar, K., Marinis, S.I., 2017. Pelvic organ prolapse in fibulin-5 knockout mice: pregnancy-induced changes in elastic fiber homeostasis in mouse vagina. Am J Pathol. American Society for Investigative Pathology. 170, 578-589.

Ferrell, G., Lu, M., Stoddard, P., Sammel, M.D., Romero, R., Strauss, J.F., Matthews, C.A., 2009. A single nucleotide polymorphism in the promoter of the LOXL1 gene and its relationship to pelvic organ prolapse and preterm premature rupture of membranes. Reprod. Sci. 16, 438–446.

Fung, Y.C., 1993. Biomechanics: Mechanical Properties of Living Tissues. New York: Springer.

Jackson, S., James, M,, Abrams, P., 2002. The effect of oestradiol on vaginal collagen metabolism in postmenopausal women with genuine stress incontinence. BJOG.109, 339-44.

Karasick, S., Spettell, C.M., 1997. The role of parity and hysterectomy on the development of pelvic floor abnormalities revealed by defecography. AJR Am J Roentgenol. 169, 1555-1558.

Kenton, K., Mueller, E.R., 2006 The global burden of female pelvic floor disorders. BJU Int. 98, 6–7.

Larsson, C., Källen, K., Andolf, E., 2009. Cesarean section and risk of pelvic organ prolapse: a nested case-control study. Am. J. Obstet. Gynecol. 200, 243.

Liu, X., Zhao Y., Pawlyk, B., Damaser, M., Li, T., 2006 Failure of elastic fiber homeostasis leads to pelvic floor disorders. Am. J. Pathol. 168, 519–528.

Liu, X., Zhao, Y., Gao, J., Pawlyk, B., Starcher, B., Spencer, J.A., Yanagisawa, H., Zuo, J., Li, T., 2004. Elastic fiber homeostasis requires lysyl oxidase-like 1 protein. Nat. Genet. 36, 178–182.

Lukacz, E.S., Lawrence, J.M., Contreras, R., Nager, C.W., Luber, K.M., 2006. Parity, mode of delivery, and pelvic floor disorders. Obstet. Gynecol. 107, 1253-1260.

MacLennan, A.H., Taylor, A.W., Wilson, D.H., Wilson, D., 2000. The prevalence of pelvic floor disorders and their relationship to gender, age, parity and mode of delivery. BJOG. 172, 1460-1470.

Ozog, Y., Konstantinovic, M., Werbrouck, E., De Ridder, D., Mazza, E., Deprest, J., 2011. Persistence of polypropylene mesh anisotropy after implantation: an experimental study. BJOG. 118, 1180-1185.

Patnaik, S., Weed, B., Borazjani, A., Bertucci, R., Begonia, M., Wang, B., Williams, L., Liao, J., 2012. Biomechanical characterization of sheep vaginal wall tissue: a potential application in human pelvic floor disorders. ASME. 1193-1193.

Rahn, D.D., Ruff, M.D., Brown, S.A., Tibbals, H.F., Word, R.A., 2008. Biomechanical properties of the vaginal wall: effect of pregnancy, elastic fiber deficiency, and pelvic organ prolapse. Am J Obstet Gynecol. 198, e1-6.

Ramshaw, J.A., Peng, Y.Y., Glattauer, V., Werkmeister, J.A., 2009. Collagens as biomaterials. J. Mater. Sci. Mater. Med. 1, S3–58.

Rynkevic, R., Martins, P., Hympanova, L., Almeida, H., Fernandes, A.A., Deprest, J., 2017. Biomechanical and morphological properties of the multiparous ovine vagina and effect of subsequent pregnancy. J. Biomechancs 24, 94-102.

Shepherd, P.R., 1992 Vaginal prolapse in ewes. Vet. Rec. 130, 564-564.

Urbankova, I., Callewaert, G., Sindhwani, N., Turri, A., Hympanova, L., Feola, A., Deprest, J., 2017a. Transvaginal mesh insertion in the ovine model. J Vis Exp. 27, 125.

Urbankova, I., Vdoviakova, K., Rynkevic, R., Sindhwani, N., Deprest, D., Feola, A., Herijgers, P., Krofta, L., Deprest, J., 2017b. Comparative anatomy of the ovine and female pelvis. Gynecol Obstet Invest.

Urbankova, I., Callewaert, G., Blacher, D., Deprest, D., Hympanova, L., Feola, A., De Landsheere, L., Deprest, J., 2018. First delivery and ovariectomy affect biomechanical and structural properties of the vagina in the ovine model. International Urogynecology Journal

Ulrich, D., Edwards, S.L., Su, K., White, J.F., Ramshaw, J.A., Jenkin, G., Deprest, J., Rosamilia, A., Werkmeister, J.A., Gargett, C.E., 2014. Influence of reproductive status on tissue composition and biomechanical properties of ovine vagina. PLOS, 9.

Vedaldi, A., Fulkerson B., 2008. VLFeat: an open and portable library [Online], 03 07, 2016. http://www.vlfeat.org.

CHAPTER 7

LINKING HYPERELASTIC THEORETICAL MODELS AND EXPERIMENTAL DATA OF VAGINAL TISSUE THROUGH HISTOLOGICAL DATA

Rita Rynkevic [a,b,c,d], João Ferreira [a,b], Pedro Martins [a,b,*], Marco Parente [a,b], Antonio A. Fernandes [a,b]

[a] University of Porto, Faculty of Engineering, Portugal
[b] INEGI, University of Porto, Faculty of Engineering, Portugal
[c] KU Leuven, Department Development and Regeneration, Biomedical Sciences, Leuven, Belgium
[d] Centre for Surgical Technologies, Group Biomedical Sciences, Belgium
*Corresponding author at: INEGI, Campus da FEUP, Rua Dr. Roberto Frias, 400, 4200-465 Porto, Portugal

Key words: vaginal tissue, biomechanical properties, histology, genetic algorithm, hyperelastic model

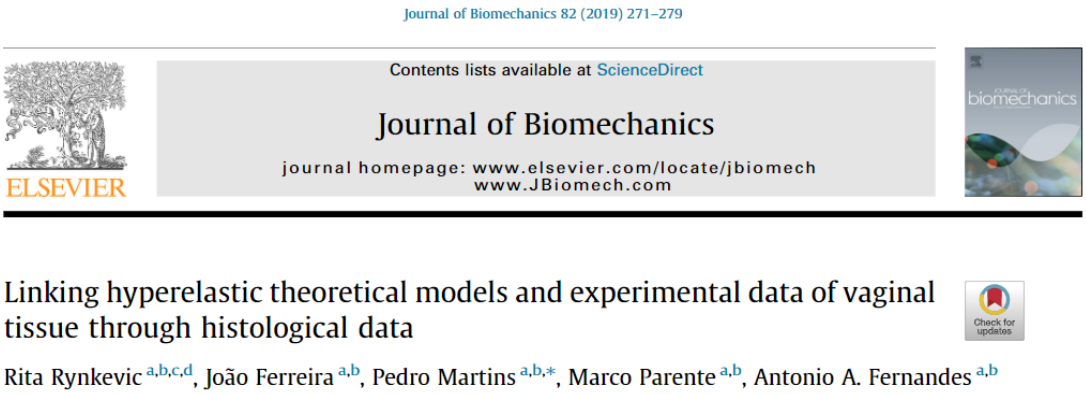

Published in Journal of Biomechanics, vol. 82, 271-279, (2019)

ABSTRACT

Mechanical characterization of living tissues and computer-based simulations related to medical issues, has become increasingly important to improve diagnostic processes and treatments evaluation. This work proposes a link between the mechanical testing and the material model predictions through histological data of vaginal tissue. Histological data was used to link tensile testing experiments with material-dependent parameters; the approach was adequate to capture the nonlinear response of ovine vaginal tissue over a large strain range.

The experimental data obtained on a previous study, has two main components: tensile testing and histological analysis of the ovine vaginal tissue. Uniaxial tensile test data and histological data were collected from three sheep groups: virgins, pregnant and parous. The distal part of vaginal wall was selected since it is prone to tears induced by vaginal delivery.

The HGO (Holzapfel-Gasser-Ogden) model parameters were fitted using a stochastic approach, namely the Simple Genetic Algorithm (SGA). The SGA was able to fit the experimental data successfully ($R2 > 0.986$). The dimensionless coefficient ξ, was highly correlated with histological data. The ratio was seen to increase linearly with increasing collagen content.

Coefficient ξ brings a new way of interpreting and understanding experimental data; it connects the nonlinear mechanical behaviour (tensile test) with tissue's morphology (histology). It can be used as an 'inverse' (approximate) method to estimate the mechanical properties without direct experimental measurements, through basic histology.

In this context, the proposed methodology appears very promising in estimating the response of the tissue via histological information.

1. Introduction

The use of simulation environments has become increasingly relevant in the exploitation of experimental evidence, to gain deeper insights over many biomechanical problems (Delingette, 1998). Confined to the degree of assumptions and simplifications in the modelling of the material behaviour, the predictions of these boundary-value problems can provide new insights for health issues. For example, through phenomenological material models one can explore relevant biomedical problems such as pelvic floor dysfunctions (PFD). The pathophysiological nature for PFD is not yet clear. However, it is known to be related to abnormal stretching combined with defective synthesis of the pelvic tissues' constituents (Fenner and Hsu, 2010). Pelvic tissues are soft tissues comprising cells performing essential biochemical functions, while the elastin and collagen in the extracellular matrix (ECM) work as the load bearing constituents (Holzapfel, 2000a, 2000b, 2000c).

Collagen fibres, one of the main components of the extracellular matrix of soft pelvic tissues, are greatly responsible for the anisotropic mechanical behaviour. The mechanics of pelvic floor soft tissues is strongly influenced by the concentration and structural arrangement of the constituents, dictated by the topographical location and respective function in the pelvic floor cavity (Couri et al., 2012)

Pelvic floor soft tissues undergo mechanical and histological changes during their adaptation to pregnancy. Some researchers have found an intimate connection between the tissues' mechanics and histological structure (Urbankova et al., 2018; Ulrich et al., 2014). While collagen is largely responsible for soft tissue tensile strength, elastin makes the tissue more compliant (Fung, 1993). However, these findings still have to be linked with accurate material models. For instance, some first attempts to relate histological data with material properties for vaginal tissue can be found in (De Landsheere et al., 2016; Ulrich et al. 2014). This connection is fundamental to understand the mechanical properties of pelvic tissues, especially in pathophysiological conditions.

The goal of this work is to present the study of the main stages involved in the mechanical characterization of biological soft tissues. Starting from theoretical hyperelastic concepts, the material-dependent parameters are estimated using Genetic Algorithms (GAs). GAs were applied to experimental data for curve fitting and, ultimately to predict the tissues' mechanical behaviour through numerical simulation.
This work presents a strategy to correlate tensile testing experiments, with a given material model, adequate to capture the nonlinear response over a large strain range. The data from longitudinal samples were fit using a simple GA. The fitted material parameters demonstrated a relation with the tissues' microstructure, i.e. collagen and elastin densities. Moreover, the resultant material parameters reflect the particularities of the physiological state associated with pregnancy.

The available (limited) histological information was seen to have a relation with the Holzapfel-Gasser-Ogden model parameters. The adopted approach enables the prediction of tissue mechanics without experimental data, but rather relying on histological and histochemical information.

2. Methods

2.1 Animal model

Experimental stress-stretch curves and histological images from the distal vaginal wall of Swifter sheep, were obtained by Rynkevic et al. (2017). The distal part of vaginal wall was selected since it is prone to tears induced by vaginal delivery. The experimental data was collected from three sheep groups: virgins (n = 5; avg. weight = 45 kg, 9 months old), pregnant (n = 5; term = 145 days; avg. weight = 65 kg, 3 years old) and parous (n = 5; avg. weight = 60 kg, 4 years old). Pregnant sheep had two prior vaginal deliveries and the third was a C-section. Parous sheep were included one year after the third vaginal delivery. Animals were treated according to a protocol approved by the Ethics Committee for Animal Experimentation of the Faculty of Medicine of KU Leuven.

2.2 Experimental Data and Histological Analysis

Uniaxial tensile testing was performed using a vertical Zwick tensiometer (Zwick GmbH & Co, KG, Ulm, Germany). Dog bone shaped samples (2 mm 25 mm) were pre-loaded until 0.1 N (at elongation of 5 mm/min) to remove slack from the tissue. A constant elongation rate of 10 mm/min was used to load the specimen to failure, along the longitudinal axis.

For histological analysis, 6-mm slices were stained with Miller's elastic staining and were captured using a Zeiss microscope (Zeiss Axioplan 400, Oberkochen, Germany) at 10 magnification. An image-stitching algorithm using Matlab (Release 2015, The MathWorks, Inc) was applied to combine multiple micrographs from the same stain. The resulting high-resolution images were processed using ImageJ (open platform for scientific image analysis) and a Colour Deconvolution plugin (Caetano et al., 2016). The total content (%) of collagen, elastin, and smooth muscle were quantita tively determined from thresholded images, relative to the total area (%) of the stain, using image processing techniques (De Landsheere et al., 2016).

2.3 Hyperelastic Materials

Phenomenological approaches to model the mechanical behaviour of soft tissues, describe the material by means of a strainenergy function (SEF or stored-energy) per unit volume (Holzapfel, 2000a, 2000b, 2000c), wherein the inherent complex microstructure is assumed as a homogeneous continuum. The tensile testing data shows nonlinear responses, while the histological data shows the tissue is comprised of collagen and elastin fibres embedded in a matrix of smooth muscle cells (SMCs) and other constituents. As observed by Urbankova et al. (2017), the histological images of the studied ovine vaginal specimens revealed 4 tissue layers. A stratified squamous epithelium, a lamina propria containing a multidirectional network of collagen and elastin fibres, a muscularis containing smooth muscle cells arranged in circular and longitudinal directions (e_1 and e_2 directions in Fig. 1a), and an adventitia which merges with the adventitia of bladder and rectum.

Based on the histological data, the material parameters were reduced to a minimal set, rich enough to allow the comprehension of tissue mechanics in terms of its structure. Therefore, given its mechanical response, the vaginal tissue can be modelled as a fibre reinforced hyperelastic material.

Fig. 1a shows the distribution of smooth muscle (light rose) at a through-thickness cut of the sample. Lamina propria shows the highest level of collagen (in red) among the three layers (as corroborated by Rynkevic et al. (2017)). In lamina propria, smooth muscle (light rose) is surrounded by collagen. The samples were stretched along $\boldsymbol{e}_1$-direction, the (observed) preferential direction of collagen fibers in lamina propria (Fig. 1a). Such direction was a reference to mount the specimens in the testing apparatus. In the uniaxial tensile testing conditions, the fibres of all layers tend to align in the stretching direction ($\boldsymbol{e}_1$) (Calvo et al., 2009). Therefore, a transversely isotropic model (one family of fibres) approximates the material response under the tensile testing conditions.

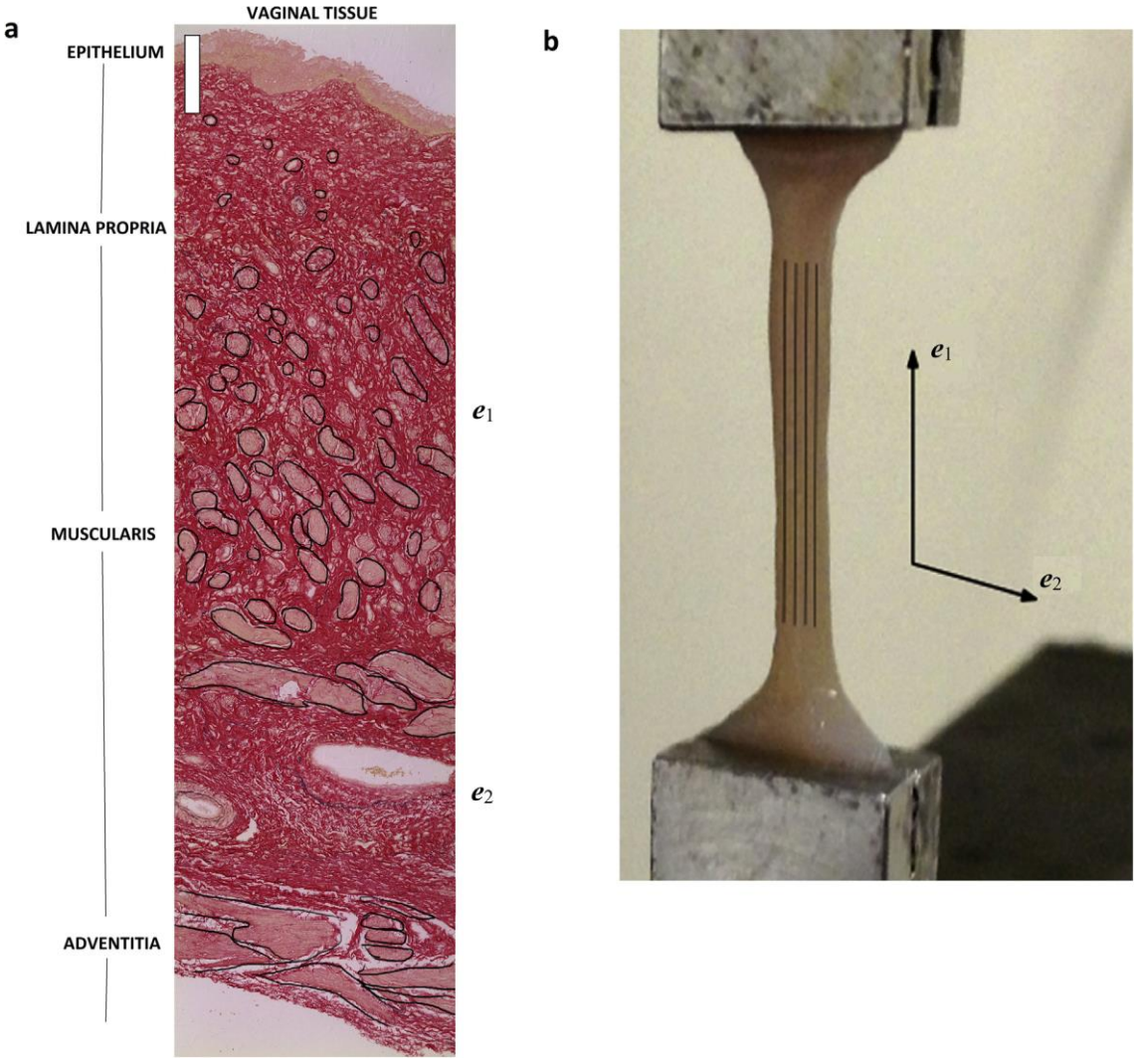

Fig. 1 a – Histological image of the ovine vaginal tissue (distal part), stained with Miller's Elastica. Staining results: total collagen (red), elastin fibres (jet-black). Scale bar (upper left) for sections – 200 mm. e1 and e2 directions correspond to the circular and longitudinal directions of smooth muscle (e1 direction is normal to the cut section). b – Tensile testing of the dog bone shaped specimen (ovine vaginal tissue) with main fibre orientation. (For interpretation of the references to colour in this figure legend, the reader is referred to the web version of this article).

The deformation gradient $\mathbf{F}$ estimates the 3-dimensional deformation of vaginal tissue, understood as a soft elastic continuum. The right Cauchy–Green tensor $\mathbf{C} = \mathbf{F}^{\mathrm{T}}\mathbf{F}$ measures rotation independent deformation. Moreover, the tensile test results had no evidence of significant volume changes, thus allowing an isochoric approach. The sample is submitted to uniaxial deformation, considered homogeneous, with stretch λ in the mean fibre direction $\mathbf{M}$, taken as the $\boldsymbol{e}_1$-direction (see Fig. 1b).

Therefore, the matrix (or ground substance) contains the fibres and deforms according to the deformation gradient $[\mathbf{F}] = \mathrm{diag}\left[\lambda, \lambda^{-\frac{1}{2}}, \lambda^{-\frac{1}{2}}\right]$ and $\mathbf{M} = [1,0,0]^{\mathrm{T}}$, so that the deformed fibre direction, , $\mathbf{m} = [\mathbf{F}]\mathbf{M}$ gives $\mathbf{m} = [\lambda, 0,0]^{\mathrm{T}}$.
The first invariant is $I_1 = \mathrm{tr}\mathbf{C}$ while the fourth invariant is denoted by $I_4 = \mathbf{M} \cdot (\mathbf{CM})$, which for the deformation state imposed in the samples are reduced to $I_1 = \lambda^2 - 2\lambda^{-1}$ and $I_4 = \lambda^2$.

Under these assumptions and according to the available histological information, the simpler version of the HGO model (Holzapfel et al., 2000) seems adequate to describe the mechanical behaviour of the samples. The strain-energy is postulated as:

$$\boldsymbol{\Psi} = \underbrace{\frac{\mu}{2}(I_1 - 3)}_{\text{matrix}} + \underbrace{\frac{k_1}{2k_2}\left(e^{k_2(I_4-1)^2} - 1\right)}_{collagen\ fibers} \tag{1}$$

where μ, k_1, and k_2 are the constant parameters that define the mechanical response (Abaqus 6.11). While the shear modulus (μ) is related to the matrix content; k_1 and k_2 reflect the fibers contribution. For convenience, we define the dimensionless ratio:

$$\xi = \frac{k_1}{2k_2\mu} \tag{2}$$

as a suitable regulator for the matrix and fibre contributions. It represents the contribution to elastic energy of collagen fibres relative to the matrix content.

The resultant parameters are consistent with the requirements for use in finite element methods, in complex initial boundaryvalue problems (Drucker, 1959). They are suited to characterize the pelvic floor tissues undergoing large deformations. The Cauchy stresses σ are obtained push-forwarding the second Piola- Kirchhoff stresses $\mathbf{S} = \mathbf{F}^{-1}\frac{\partial \Psi}{\partial \mathbf{F}}$, i.e., $\boldsymbol{\sigma} = \mathbf{FSF}^{\mathrm{T}}$.

2.4 Data Fitting

The material model presented contains 3 parameters (μ, $k_1$and k_2) that must be adjusted to obtain a reliable characterization of the tissue. Therefore, these 3 parameters were treated as functional coefficients that minimize the error metric, taken to be the sum of the squares of the residuals. For a given set of m experimental points, the error metric is:

$$s = \sum_m \left(\frac{\sigma_{exp} - \sigma}{\sigma_{exp}}\right)^2 \tag{3}$$

where residual states for the difference between the observed stresses σ_{exp} and the Cauchy stress provided by the material model σ. By treating such residuals in their dimensionless form, the fitting process became independent on the stress levels observed in the experiments. Thus, the objective function can be expressed as:

$$\underset{\{\mu, k_1, k_2\} \in R^+}{\arg\min} \quad \sum_m \left(\frac{\sigma_{exp}-\sigma}{\sigma_{exp}}\right)^2 \tag{4}$$

We ensure material stability (Drucker stability condition) by searching over positive domains (Drucker, 1959) rather than adding restrictions to the optimisation problem. The fast convergence of traditional gradient-based optimizers has the drawback of requiring objective function derivatives (Khalil et al., 2006), which can become a huge challenge when nonlinearities are present. Gradient-free optimizers such as Genetic Algorithms are a stochastic alternative to select the best parameters guaranteeing local optima solutions. Moreover, due to their metaheuristic nature, they can handle complex and irregular solution spaces, as the ones studied in this work.

Therefore, a simple tournament selection operator, uniform crossover and creep and jump mutations, were employed (Maletta and Pagnotta, 2004). This scheme was used to generate a population of individuals (candidate solutions) under Darwinian principles (David and Goldberg, 1989), and genetic variability controls. That is, if better individuals are not generated, elitism is ensured by keeping the best-fitted individual from the last generation and only generations having less than 10% of similar individuals allow the algorithm to move on. Each candidate solution is evaluated trough the fitness function f, defined as:

$$f = \frac{1}{1+s} \tag{5}$$

Table 1 summarizes the implementation of the fitting procedure, and Fig. 2 describes the required pipeline to obtain the material parameters from the data sets. All routines were implemented in Fortran 90.

Table1. Control Parameters and Strategies for the implementation of the Simple Genetic Algorithm.

Number of Parameters	3
Population size	40
Selection	Tournament (semifinal)
Crossover	Uniform
Crossover probability	0.6
Mutation probability	0.02
Maximum equal individuals	4
Elite individuals	1
Stopping Criterion	51 generations

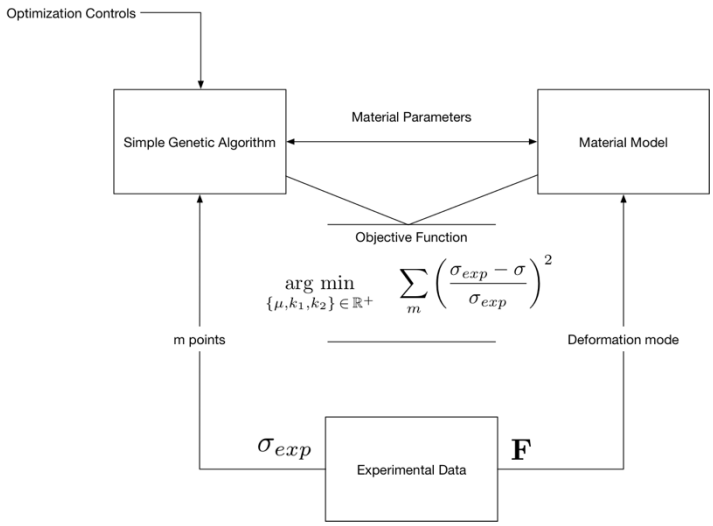

Fig. 2 Graphical representation of the fitting procedure. Each experimental data set contains m points of stretch-stress obtained during tensile testing. The material parameters generated by the simple genetic algorithm are evaluated by the material model through Cauchy stresses response and tested according to the fitness function based on the sum of residuals.

2.5 Statistical analysis

Statistical analysis was performed to compare mechanical properties and material model parameters of the distal vagina among experimental groups. The fitted values per individual was used for analysis. Quantitative data are represented as mean ± standard error of the mean (±SEM). A statistically significant difference was reported if $p < 0.05$. Kolmogorov-Smirnov tests showed the data follows a normal distribution. One-way ANOVA and post hoc test (Tukey's correction) were carried out for the intergroup comparisons. The level of significance was set to $p < 0.05$.

3. Results

3.1 Individual analysis

The tensile testing results of the vaginal tissue from the virgin group evidences consistent results (Fig. 3). Sheep 5 shows a more compliant mechanical behaviour, consistent with observed collagen and elastin densities (53.21% and 1.86%), Table 2. The reasons behind such disparate mechanical are unknown as the life and hormonal status of the Sheep 5 are the same of the others from virgin group. Nevertheless, Sheep 5 results were not excluded from the study. The results displaying higher stresses were associated with higher total collagen contents (Fig. 3, Table 2) for all animals, while an increase in elastin content was associated with higher stretches.

The HGO model parameters were fitted using a stochastic approach, namely the SGA. In the HGO model, parameter μ is linked with the energy required to deform the tissue matrix. For highly fibered tissues i.e. vaginal tissues, μ gives a significant contribution for lower stretches (comfort zone (Rynkevic et al., 2017)). However, its influence at higher stretches is diminished. Parameters k_1 and k_2 regulate the deformation energy

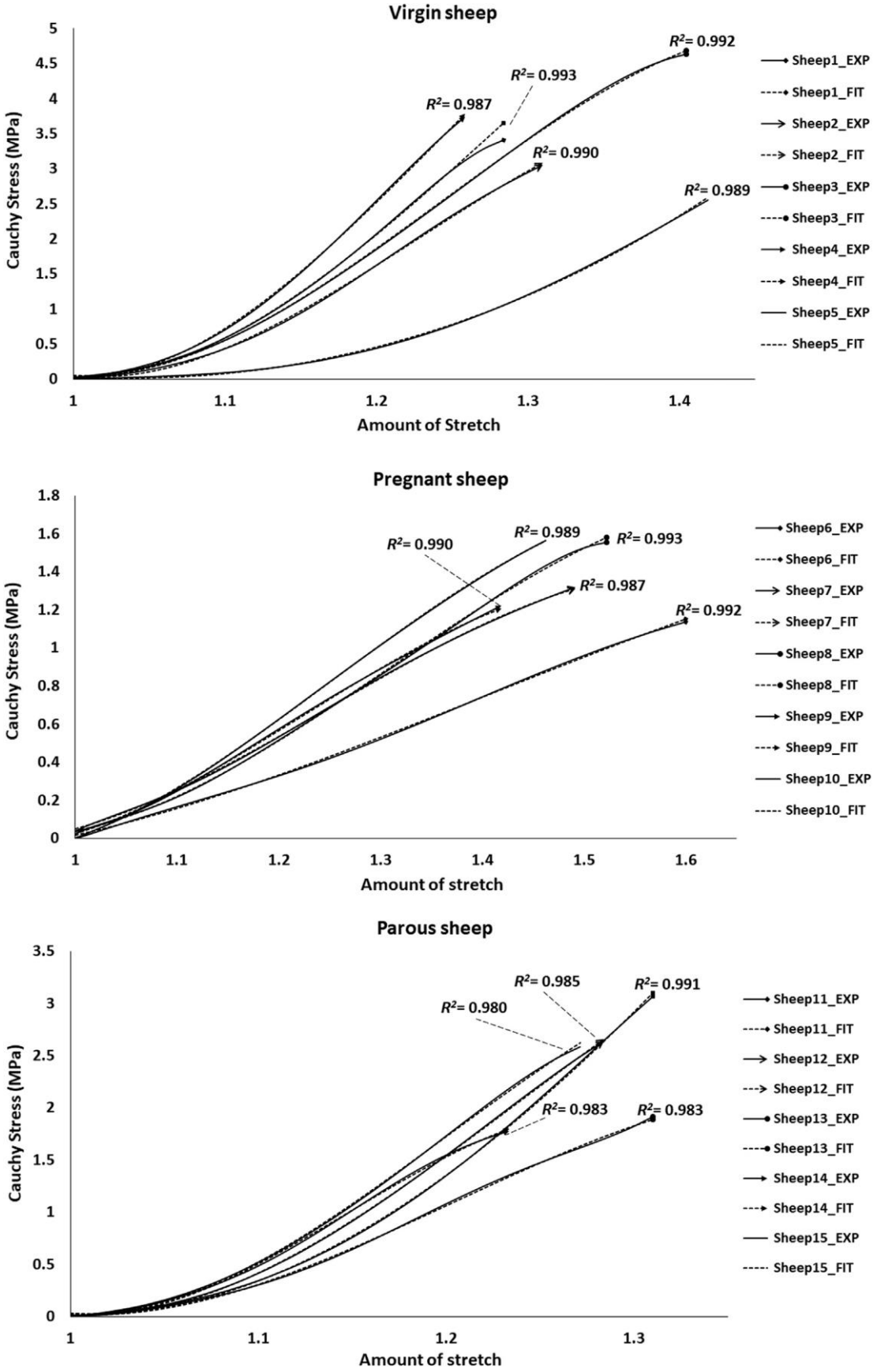

Fig. 3 Mechanical behaviour (experimental and fitting curves) of the vaginal tissue of the virgin, pregnant and parous ewes. Experimental data (solid). fitting data (dashed) and coefficient of determination (R^2).

associated with fibers. They have a significant (stress) contribution for higher stretches (stress zone (Rynkevic et al., 2017)), due to the exponential part of the HGO strain-energy function (Eq. (1)).

In general, the SGA was able to capture the mechanical behavior of the vaginal tissue (Fig. 3). The 3-dimensional admissible solutions' hyperspace {μ, k1, k2} was compatible with numerically stable simulation environment. The SGA was able to fit the experimental data successfully (R2 > 0.986), Fig. 3.

The primer histological differences found between groups were detailed in (Rynkevic et al., 2017). Table 2 contains histological data (collagen and elastin relative densities) and HGO model parameters (Eq. (1)). Paired t-test ($p < 0.05$) was performed. There is a significant difference in virgin and the other groups. There is also a significant difference between virgin and pregnant for the model parameters: μ, k_1 and k_2. During pregnancy the vaginal tissue becomes more compliant, with a decrease in total collagen and an increase in elastin content. In contrast, virgin sheep had the stiffest vaginal tissue, with highest total collagen and lowest elastin fibre contents. The dimensionless coefficient ξ, is highly correlated (R^2) with histological data (Fig. 4). The ratio was seen to increase linearly with increasing collagen content. ξ coefficient connects the nonlinear mechanical behaviour (tensile test) with tissue's morphology (histology).

Table2. Histological component densities and fitting parameters of the virgin, pregnant, and parous ewes. Averaged data is presented as mean (± SEM), significant differences among the groups were set to $p < 0.05$. a – virgin vs pregnant, b – pregnant vs parous, c – virgin vs parous.

	Collagen (%)	**Elastin (%)**	**Smooth muscle cells (%)**	***k₁* (MPa)**	***k₂***	**Shear modulus μ (MPa)**	***ξ=k₁/(2k₂*μ)***
Virgin (N=5)							
Sheep 1	58.78	0.656	22.22	1.829	0.781	0.286	4.101
Sheep 2	55.01	0.678	21.55	1.452	0.419	0.492	3.517
Sheep 3	60.60	1.922	24.10	1.400	0.129	1.550	3.501
Sheep 4	58.87	0.517	22.42	2.100	1.065	0.518	1.905
Sheep 5	53.21	1.861	20.08	0.435	0.774	0.195	1.440
Mean ± SEM	57.29 ± 1.37 a	1.693 ± 0.301 a	22.07 ± 0.84 a	1.443 ± 0.632 a	0.634 ± 0.363 a	0.608 ± 0.544 a	2.893 ± 1.152 ac
Pregnant (N=5)							
Sheep 6	43.97	3.85	27.94	0.011	0.197	0.827	0.0350
Sheep 7	46.89	3.55	27.39	0.015	0.066	1.291	0.0856
Sheep 8	46.66	2.77	27.12	0.046	0.207	1.239	0.0894
Sheep 9	46.92	2.96	27.15	0.014	0.056	1.394	0.0885
Sheep 10	49.76	2.87	27.10	0.037	0.091	1.521	0.1346
Mean ± SEM	46.86 ± 1.65 b	3.20 ± 0.21 b	27.40 ± 0.20 b	0.025 ± 0.016 a	0.124 ± 0.073 a	1.254 ± 0.262 a	0.087 ± 0.035 ac
Parous (N=5)							
Sheep 11	53.81	2.59	31.05	1.113	0.919	0.428	1.4133
Sheep 12	50.13	2.45	30.08	1.210	0.726	0.768	1.0845
Sheep 13	48.24	2.53	30.93	0.726	0.581	0.675	0.9261
Sheep 14	49.23	2.01	29.12	1.205	0.890	0.635	1.0647
Sheep 15	50.84	2.27	29.48	1.346	0.697	0.820	1.1777
Mean ± SEM	50.45 ± 0.90 c	2.370 ± 0.10	30.13 ± 0.29 c	1.120 ± 0.235 a	0.763 ± 0.141 a	0.665 ± 0.151 a	1.133 ± 0.181 ac

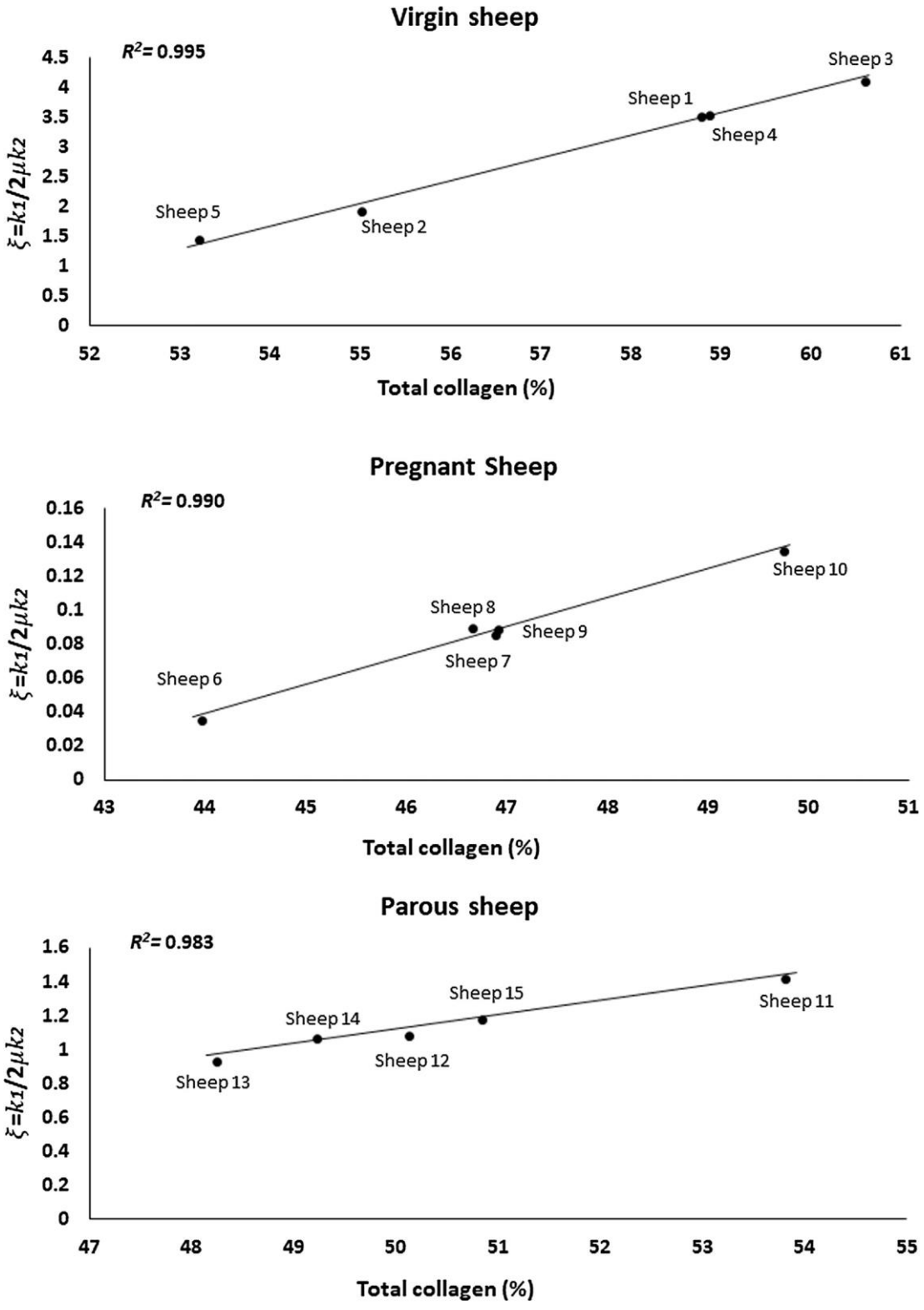

Fig. 4 ξ vs total collagen (%) relationship for virgin, pregnant and parous ewes

3.2 Group analysis

Fig. 5 shows the typical mechanical behaviour of each sheep group considered, virgin, parous and pregnant. During pregnancy, vaginal tissue becomes highly extensible, when compared to the baseline virgin sheep. This situation is associated with an increase on elastin content (by 1.51%) and a decreased total collagen fraction (by 7.58%), Table 3. There is recovery of the vaginal tissues to levels near their pre-pregnancy state. The curve for parous sheep has the same mechanical behaviour as virgin however, ultimate stress and strain are lower. This mechanical behaviour agrees with histology, as collagen and elastin fractions return levels close to the virgin group.

As described in individual analysis (3.1) the fittings were accurate (high R^2 for all groups) and able to capture the mechanical behaviour of the vaginal tissue in different reproductive statuses, Fig. 5.

As observed for the individual sheep (3.1), n is proportional to the total collagen content (Table 3, Fig. 6). Overall the relations found for individuals (3.1), regarding the link between tissue's morphology and mechanical properties are valid for the group analysis; higher ξ values are linearly associated (R^2 = 0.982) with higher total collagen contents.

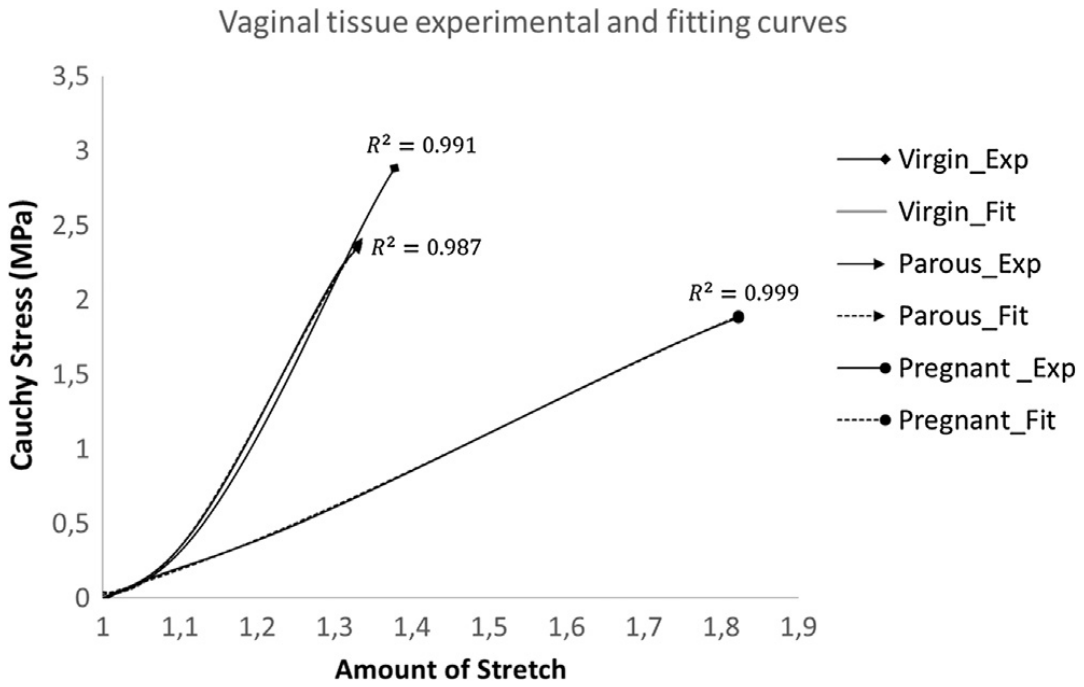

Fig. 5 Mechanical behaviour (experimental and fitting curves) of the vaginal tissue of the virgin, pregnant and parous sheep groups. Experimental data (solid), fitting data (dashed) and coefficient of determination (R^2)

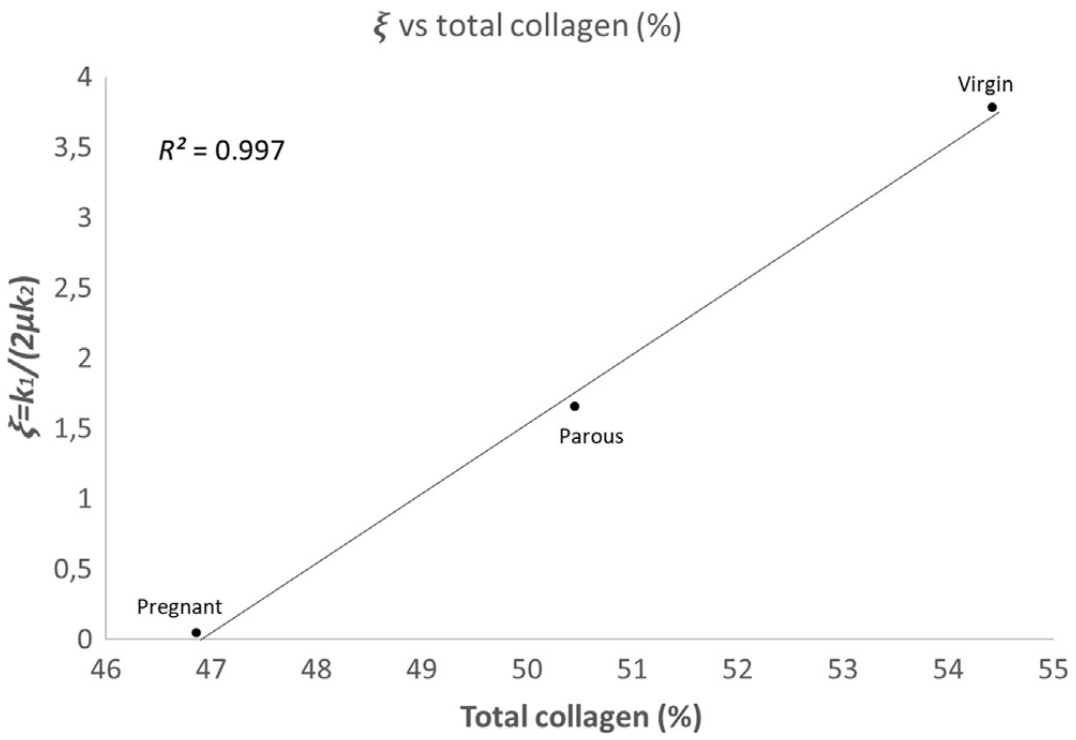

Fig. 6 ξ vs total collagen (%) relationship for virgin, pregnant and parous sheep groups.

Table3. Collagen, elastin and fitting parameters of virgin, pregnant and parous sheep.

	Total collagen (%)	**Elastin (%)**	**k_1 (MPa)**	**k_2**	**Shear modulus μ (MPa)**	**$\xi=k_1/(2k_2*\mu)$**
Virgin	54.42	1.693	0.948	0.193	0.647	3.788
Pregnant	46.86	3.201	0.007	0.065	0.995	0.050
Parous	50.45	2.370	0.871	0.290	0.905	1.658

4. Discussion

The computational simulation of the mechanical behavior of biological systems, is highly dependent on representative constitutive models (Bonet and Wood, 1997). Such models are theoretical abstractions which are assumed to capture the overall behavior of the studied materials under a given set of boundary conditions i.e., under uniaxial or biaxial tension. In the context of the present work, the HGO model parameters are akin to the mechanical properties for 'simpler' constitutive models (ex. Hooke's law). However, due to the hyperelastic mechanical behavior, commonly observed in fibered soft tissues, an intuitive understanding and interpretation of the parameter fittings (from optimization) in relation to the experimental data, is difficult.

The experimental work has two main components, tensile testing, and histological analysis. During a previous investigation (Rynkevic et al., 2017) it was observed a link between the mechanical behavior and tissue's morphology, obtained via histology. There was a consistent relation between local stiffness (Young's moduli in physiological – comfort zone and supra-physiological domains – stress zone) and histological components (elastin, total collagen, and smooth muscle).

For realistic mechanical simulations it is important to rely on robust theoretical models. The nonlinear theory of elasticity in general (Holzapfel, 2000a, 2000b, 2000c), and the HGO model in particular, have been used to model fibrous soft tissues. HGO model is especially suited for tissues composed by two fiber families, such as arteries, pelvic floor tissues, etc.

We present for the first time a relation between HGO coefficients { μ, k_1, k_2}, obtained via SGA, $\xi = k_1/(2k_2{*}\mu)$. Through ξ, it was found an agreement between HGO model predictions and experimental data, robust over different kinds of reproductive statuses. To establish correlations for all the 3 groups under analysis, it was found necessary to include all parameters of the model via ξ. Other hypotheses involving less parameters were unsuccessfully investigated. The HM (Histologically-Motivated) coefficient, ξ, establishes a link between tissue's microstructure and the theoretical model results. It was found a consistent correlation between total collagen content and HM coefficient. This correlation is observed at the individual (Fig. 4) and group levels (Fig. 6). Moreover, the same relation was seen in significantly different physiological conditions (virgin, pregnant, etc.).

HM coefficient (ξ) brings a new way of interpreting and understanding experimental data. It can be used as an 'inverse' (approximate method) to estimate the mechanical properties without direct experimental measurements, through basic histology. The converse is possible, using correlations shown in Figs. 4 and 6.

The vaginal tissue undergoes significant remodeling and alterations during pregnancy (Ulrich et al., 2014) Factors such as collagen dispersion, orientation, I:III ratio, crosslinks, and undulation may potentially contribute to these parameters. While immature crosslinks and undulation facilitate tissue compliance (Jackson et al., 2002), collagen type I is largely responsible for tissue' tensile strength. (De Landsheere et al., 2013) found less collagen in pregnant vaginal tissue and no significant difference in collagen type III between pregnant, virgin and parous. To investigate the influence of reproductive status on the material (vaginal tissue) behavior, further research should focus on the use more detailed histological and histochemical data to build relevant material models.

Although biochemical analyses provide precise total collagen and elastin content measurements (Ulrich et al., 2014), morphometric analyses like the one used in this work proved to be an adequate compromise for microstructure evaluation (Caetano et al., 2016; De Landsheere et al., 2016). Using this simple, rapid and a low-cost technology for tissue microstructure evaluation, Rynkevic et al. (2017), Urbankova et al. (2018), and Alperin et al. (2010) found mechanical and histological data agreeing with the results from biochemical analysis (Ulrich et al., (2014)).

In the research it was observed that vaginal tissue from pregnant sheep becomes very extensible, associated with significantly low total collagen and high elastin content. In contrast, virgin sheep had the highest total collagen, which was associated with a high ultimate stress. On the other hand, it contained less elastin fibres, which could explain the higher resistance to stretching (Urbankova et al., 2018). After third delivery, the vagina was stiffer than during pregnancy, but not to the level of stiffness observed in virgins. This mechanical behavior is coherent with the collagen and elastin levels discussed above. These results agree with studies in rats, where the stiffness and strength of vaginal tissues

decreased during pregnancy (Alperin et al., 2010). The proximal vagina had a higher amount of collagen than distal vagina. A higher total collagen coincided with a higher ultimate stress and Young's modulus.

The HM coefficient may play a significant role on the accurate *in silico* simulation of biological tissues and structures. It enables the estimation of critical mechanical properties hard to obtain through experimentation, or unavailable, as often occurs for the human model. Therefore, given that hyperelasticity theory has been used, nonlinear simulations based on this data, are within reach.

Depending on the tissue and boundary conditions under analysis, one may require the use of more sophisticated models. These may include damage mechanisms (Linka et al., 2018; Balzani et al., 2012), tissue rupture (Gültekin et al., 2018), among others. Since they require information of the protein contents, fluid fractions and fibers orientations, the choice of the histological technique may be relevant (Linka et al., 2017; Nebelung et al., 2017). Further research should address statistical analysis and a combination of tissues and loading conditions in the definition of a histologically-motivated coefficient.

The significance of HM coefficient should be understood within scope of uniaxial loading conditions. The correlation between ξ and total collagen content, may not hold in different loading conditions such as the biaxial or triaxial loading.

The non-dimensional HM coefficient (ξ) was introduced for the first time. ξ establishes a direct link between biology and mechanics by connecting the total collagen content (tissue's microstructure) to the HGO model parameters (nonlinear mechanical behavior). Histological data was seen play the fundamental role of bridging experimental findings and theoretical models.

In this context, the proposed methodology appears very promising in estimating the response of the tissue via histological information.

Acknowledgements

This research has been supported by Fundação para a Ciência e a Tecnologia I.P. (FCT, Portugal) under grants SFRH/BD/96548/2013, IF/00159/2014, SFRH/BD/107860/2015, SFRH/BPD/111846/2015; UROSPHINX - Project 16842, COMPETE2020, through FEDER and FCT; and in part by a grant of the EC in the FP7-framework (Bip-Upy; NMP3-LA-2012-310389).

References

Abaqus 6.11. Abaqus Documentation , Dassault Systèmes, Providence, RI, USA.

Alperin, M., Feola, A., Duerr, R., Moalli, P., Abramowitch, S., 2010. Pregnancy- and delivery-induced biomechanical changes in rat vagina persist postpartum. Int. Urogynecol. J. 21 (9), 1164–1174.

Balzani, D., Brinkhues, S., Holzapfel, G.A., 2012. Constitutive framework for the modeling of damage in collagenous soft tissues with application to arterial walls. Comput. Methods Appl. Mech. Eng. 213, 139–151.

Bonet, J., Wood, R.D., 1997. Nonlinear Continuum Mechanics for Finite Element Analysis. Cambridge University Press, Cambridge.

Caetano, G.F., Fronza, M., Leite, M.N., Gomes, A., Frade, M.A., 2016. Comparison of collagen content in skin wounds evaluated by biochemical assay and by computer-aided histomorphometric analysis. Pharmaceut. Biol. 14, 1–5.

Calvo, B., Peña, E., Martins, P., Mascarenhas, T., Doblaré, M., Natal Jorge, R.M., Ferreira, A., 2009. On modelling damage process in vaginal tissue. J. Biomech. 42, 642–651.

Couri, B.M., Lenis, A.T., Borazjani, A., Paraiso, M.F.R., Damaser, M.S., 2012. Animal models of female pelvic organ prolapse: lessons learned. Expert Rev. Obstet. Gynecol. 7, 249–260.

David, E., Goldberg, D.E., 1989. Genetic algorithms in search, optimization, and machine learning. Addison-Wesley Longman Publishing Co., Inc.

De Landsheere, L., Brieu, M., Blacher, S., Munaut, C., Nusgens, B., Rubod, C., Noel, A., Foidart, J.M., Nisolle, M., Cosson, M., 2016. Elastin density: Link between histological and biomechanical properties of vaginal tissue in women with pelvic organ prolapse? IInt. Urogynecol. J. 27, 629–635.

De Landsheere, L., Munaut, C., Nusgens, B., Maillard, C., Rubod, C., Nisolle, M., Cosson, M., Foidart, J.M., 2013. Histology of the vaginal wall in women with pelvic organ prolapse: a literature review. Int. Urogynecol. J. 24, 2011–2020.

Delingette, H., 1998. Towards realistic soft tissue modeling in medical simulation. Proc. IEEE, Inst. Electr. Electron. Eng. 86, 512–523.

Drucker, D.C., 1959. A definition of a stable inelastic material. ASME J. Appl. Mech. 26, 101 195.

Fenner, D.E., Hsu, Y., 2010. Pathophysiology of the pelvic floor: Basic physiology, effects of ageing, and menopausal changes. Pelvic Floor Disorders, 25–32.

Fung, Y.C., 1993. Biomechanics: Mechanical Properties of Living Tissues. Springer, New York.

Gültekin, O., Dal, H., Holzapfel, G.A., 2018. Numerical aspects of anisotropic failure in soft biological tissues favor energy-based criteria: A rate-dependent anisotropic crack phase-field model. Comput. Methods Appl. Mech. Eng. 331, 23–25.

Holzapfel, D.A., 2000a. Nonlinear Solid Mechanics. John Wiley and Sons, Chichester.

Holzapfel, G.A., Gasser, T.C., Ogden, R.W., 2000. A new constitutive framework for arterial wall mechanics and a comparative study of material models. J. Elasticity 61, 1–48.

Holzapfel, G.A., 2000b. Biomechanics of Soft Tissue. Biomech preprint series, Graz, Austria.

Holzapfel, G.A., 2000c. Nonlinear Solid Mechanics: A Continuum Approach for Engineering. John Wiley and Sons Ltd, Chichester, United Kingdom.

Jackson, S., James, M., Abrams, P., 2002. The effect of oestradiol on vaginal collagen metabolism in postmenopausal women with genuine stress incontinence. BJOG 109 (3), 339–344.

Khalil, A.S., Bouma, B.E., Kaazempur Mofrad, M.R., 2006. A combined FEM/genetic algorithm for vascular soft tissue elasticity estimation. Cardiovasc. Eng. 6, 93– 102.

Linka, K., Hillgärtner, M., Itskov, M., 2018. Fatigue of soft fibrous tissues: Multi-scale mechanics and constitutive modeling. Acta Biomaterialia 72, 398–410.

Linka, K., Itskov, M., Truhn, D., Nebelung, S., Thüring, J., 2017. T2 MR imaging vs. computational modeling of human articular cartilage tissue functionality. J. Mech. Behav. Biomed. Mater. 74, 477–487.

Maletta, C., Pagnotta, L., 2004. On the determination of mechanical properties of composite laminates using genetic algorithms. Int. J. Mech. Mater. Des. 1, 199–211.

Nebelung, S., Sondern, B., Oehrl, S., Tingart, M., Rath, B., Pufe, T., Raith, S., Fischer, H., Kuhl, C., Jahr, H., Truhn, D., 2017. Functional mr imaging mapping of human articular cartilage response to loading. Radiol. J. 282, 464–474.

Rynkevic, R., Martins, P., Hympanova, L., Almeida, H., Fernandes, A.A., Deprest, J., 2017. Biomechanical and morphological properties of the multiparous ovine vagina and effect of subsequent pregnancy. J. Biomech. 57, 94–102.

Ulrich, D., Edwards, S.L., Su, K., White, J.F., Ramshaw, J.A., Jenkin, G., Deprest, J., Rosamilia, A., Werkmeister, J.A., Gargett, C.E., 2014. Influence of reproductive status on tissue composition and biomechanical properties of ovine vagina. PLOS, 9.

Urbankova, I., Vdoviakova, K., Rynkevic, R., Sindhwani, N., Deprest, D., Feola, A., Herijgers, P., Krofta, L., Deprest, J., 2017. Comparative Anatomy of the Ovine and Female Pelvis. Gynecol Obstet Invest.

Urbankova, I., Callewaert, G., Blacher, D., Deprest, D., Hympanova, L., Feola, A., De Landsheere, L., Deprest, J., 2018. First delivery and ovariectomy affect biomechanical and structural properties of the vagina in the ovine model. Int. Urogynecol. J.

CHAPTER 8

HISTOLOGICALLY-DRIVEN SIMULATIONS OF VAGINAL TISSUE: APPLICATION TO BALL BURST TESTING

João Ferreira [a,b] , Rita Rynkevic [a,b,c,d], Pedro Martins [a,b,*], Marco Parente [a,b], Nele Famaey [f] , Jan Deprest [c,d,e] , Antonio A. Fernandes [a,b]

[a] University of Porto, Faculty of Engineering, Portugal
[b] INEGI, University of Porto, Faculty of Engineering, Portugal
[c] KU Leuven, Department Development and Regeneration, Biomedical Sciences, Leuven, Belgium
[d] Centre for Surgical Technologies, Group Biomedical Sciences, Belgium
[e] Pelvic Floor Unit, University Hospitals KU Leuven, Leuven, Belgium
[f] Biomechanics Section Department of Mechanical Engineering, KU Leuven, Leuven, Belgium
*Corresponding author at: INEGI, Campus da FEUP, Rua Dr. Roberto Frias, 400, 4200-465 Porto, Portugal

Key words: vaginal tissue, biomechanical properties, histology, genetic algorithm, hyperelastic model

Article in preparation

ABSTRACT

Due to the nature of soft tissues, an intuitive understanding and interpretation of the parameter fittings in relation to the experimental data, is difficult. We herein introduce a histologically-motivated (HM) coefficient that establishes a link between the tissue microstructure and metarial model through histological data. We use it in the prediction of the mechanical properties of vaginal tissue that is subjected to multiaxial loading conditions. The material parameters were based on a HM coefficient obtained from tensile testing and histological data of comparable tissues.

Uniaxial tensile test data and histological data were collected from three groups of sheep at different time points in their life cycle, including virgins, pregnant and parous ewes. From this data, a correlation between material parameters and histological data was obtained. Spherical indentation (ball burst) tests were then performed in specimens with similar tissue structure. The histological data of these samples was used in conjunction with the correlations already established for the uniaxial samples data, to define the material parameters of the ball burst samples.

Mechanical properties of the ball burst specimens were predicted through basic histology and using FEM simulations, without direct mechanical measurements. The predicted force and displacement values of the FEM simulation displayed a good correlation with the experimental (ball burst) testing results. No fitting of the ball burst results was performed.

In this way, the use of uniaxial tests coupled with useful histological information offers a promising approach to predicting macroscopic material behavior under multiaxial loading conditions in biomechanics.

1. Introduction

Pelvic organ prolapse (POP) is defined as the abnormal descent of pelvic organs through the vagina [1]. It may involve the anterior or posterior vaginal wall, as well as the uterus or, when the uterus is absent, the apex of the vagina. Vaginal wall properties are influenced by different life events. During reproductive life, pregnancy and vaginal delivery are the first major inciting factors [2-3]. The second major inciting factor is age associated with menopause, which induces a continuous decline in pelvic floor function [3]. Additional interfering factors may boost the development of pelvic floor dysfunction (PFD), among which, obesity seems the most relevant one [4].

Surgery is the mainstay of therapy for POP and urinary incontinence (UI) [4-6], and for some procedures implants are used. Despite good anatomical outcomes, one of the main limitations is the occurrence of graft related complications (GRCs) [7]. Many obstacles make research on GRCs difficult. One of the most important is the limited access to human tissues for experimentation, and if available, they may be too small to permit comprehensive testing. Therefore, animal models are an essential part of medical research. They provide an opportunity to study physiological and pathophysiological processes in a complex living organism. Animal models are often used for experimental testing of implants for POP treatment [8]. They provide the possibility for assessing the host response to implantation, the occurrence of local complications (i.e. exposure, infection, contraction, fluid accumulation) and later explantation to determine active and passive biomechanical tissue properties [9]. Among different animals used for experimental testing, sheep have a pelvic floor anatomy and fetal head-birth canal-ratio close to that of humans [10]. Several studies were conducted using ewes to test novel implant materials [8], [11] and to evaluate the potential of vaginal surgical techniques [12], [13].

There is a growing interest, in the study of the mechanical behavior of pelvic floor soft tissues. So-called hyperelastic material models are used in finite element model simulations that may help to answer questions about the tissue behavior [14], damage processes [15] and pelvic floor dynamics [16]. A Histologically-Motivated (HM) coefficient derived in a previous study [17], based on the HGO (Holzapfel-Gasser-Ogden) model parameters [18], was fitted using a stochastic approach, namely the Simple Genetic Algorithm (SGA). The HM coefficient links the nonlinear mechanical behavior with histological parameters of the tissue. It might be used as an ‘inverse’ approximation method to estimate the mechanical properties without direct experimental measurements, based on the evaluation of the tissue total collagen obtained from histology of biopsied samples. This is an important generic step forward, that can have applications in the pathophysiology of several diseases (like hernia, POP or UI) and its surgical repair by means of implants.

In this study we aimed to characterize the multiaxial behavior of the sheep vaginal tissue using a HM coefficient based on uniaxial data and histological parameters obtained in previous studies [17], [19].

2. Methods

2.1 Animal model

Swifter ewes at different lifecycle stages were used, either virgins (mean. weight = 45 kg; range 11-12 months), pregnant (term = 145 days; mean weight = 65 kg; range 2-3 years) after two prior vaginal deliveries and multiparous (mean weight = 60 kg; range 4-5 years) one year after three vaginal deliveries. Each group included 5 sheep and the testing methods used included uniaxial tensile test or ball-burst test. Ewes were obtained from the Zootechnical Institute of KU Leuven, and the protocol was approved by the Ethics Committee for Animal Experimentation of KU Leuven's Faculty of Medicine. All animals were treated in accordance with current national guidelines on animal welfare. Ewes were euthanized by an intravenous injection of 10 mL of a mixture of embutramide 200 mg, mebezonium 50 mg and tetracaine hydrochloride 5 mg (T61; Hoechst Marion Roussel, Brussels, Belgium).

2.2 Preparation of vaginal tissue specimens and testing protocol

Considering that the mechanical properties are region-specific, the region of interest was fixed to one specific area of the vagina, i.e. the distal part undergoing relevant changes in pregnancy and after labor and delivery [20] as also occurs in women [21]. Details on the obduction and prelevation of the samples are provided in a previous work [19].

Uniaxial tensile and ball burst tests were obtained from previously done studies [22] [20]. Both uniaxial and ball burst tests were performed using a vertical Zwick tensiometer (Zwick GmbH & Co, KG, Ulm, Germany) with a setup represented in Figure 1. During uniaxial tensile tests, dog bone shaped samples (2 mm x 25 mm) were pre-loaded until 0.1 N at an elongation rate of 5 mm/min. A constant elongation rate of 10 mm/min was then used to load the specimens along the longitudinal axis until failure.

Ball burst testing was performed using a ring clamp of 20.0 ± 0.2 mm diameter. A polished steel ball of 11.50 ± 0.02 mm in diameter was pressed against the specimen (30 mm x 30 mm) through the opening of the clamping mechanism. Samples were pre-loaded until 0.1 N at an elongation rate of 5 mm/min and a constant ball displacement rate of 10 mm/min was provided by the test machine. Outcome measurements of force (N) and ball displacement (mm) were recorded.

2.3 Finite element modelling

Finite element simulations of the spherical indentation of free-standing vaginal tissues were performed in Abaqus 6.12 [23]. Since the region of interest is at the interaction between ball and sample, the vaginal tissue samples were represented as layered disks using C3D8H elements. The sample was clamped between two rigid rings with a force around 30 N to mimic the weight of the upper disk and the clamping force of the screws. Zero friction was assumed between the sample and contact surfaces of the steel ball as the samples were hydrated.

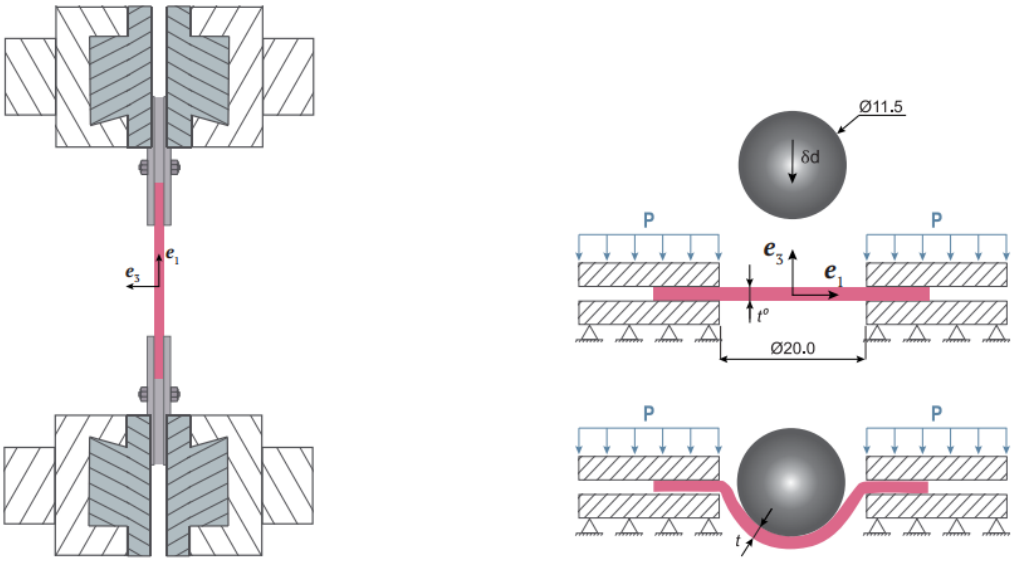

(a) Tensile test. (b) Ball burst test.

Fig. 1 Experimental set up. (a) Tensile test. The sample is stretched along $\boldsymbol{e}_1$ direction, the (observed) preferential direction of collagen fibers in the lamina propria. (b) Ball burst test. Spherical ball moves along $\boldsymbol{e}_3$-direction to deform transversely the sample.

According to the histological analysis, a single family of collagen fibers seems to be an adequate representation of the microstructure of the layer of interest. Therefore, each layer of the distal vaginal tissue was modelled as a fiber-reinforced hyperelastic material according to the Holzapfel- Gasser-Ogden (HGO) strain energy function [18], as follows:

$$\boldsymbol{\Psi} = \underbrace{\frac{\mu}{2}(I_1 - 3)}_{\text{matrix}} + \underbrace{\frac{k_1}{2k_2}\left(e^{k_2(I_4-1)^2} - 1\right)}_{collagen\ fibers} \tag{1}$$

The parameters μ, k_1, and k_2 define the mechanical response. While the shear modulus μ is related to the matrix content; k_1 and k_2 reflect the fiber contribution. The first invariant is $\boldsymbol{I}_1$ = tr $\mathbf{C}$ while the fourth invariant is denoted by $\boldsymbol{I}_4 = \mathbf{a}_0 \cdot (\mathbf{C}\mathbf{a}_0)$, where $\mathbf{C} = \mathbf{F}^{\mathrm{T}}\mathbf{F}$ is the right Cauchy–Green tensor and $\mathbf{a}_0$ the preferential fiber direction in the initial configuration. The deformation gradient $\mathbf{F}$ describes the 3-dimensional deformation of vaginal tissue. The material coefficients of each layer were estimated from a HM coefficient obtained from uniaxial tests, and from histological data of samples taken from similar tissues (same model, same life event stage and same anatomic region) [19].

For convenience, the HM coefficient is defined as the dimensionless ratio:

$$\xi = \frac{k_1}{2k_2\mu} \tag{2}$$

as a suitable regulator for the matrix and fiber contributions. It represents the contribution to the elastic energy of collagen fibers relative to the matrix content. The Cauchy stress tensor $(\boldsymbol{\sigma})$ is obtained by applying a push-forward operation to [24] the second Piola-Kirchhoff tensor ($\mathbf{S}$), $\boldsymbol{\sigma} = \mathbf{F}\mathbf{S}\mathbf{F}^{\mathrm{T}}$, whereby, $\mathbf{S} = \mathbf{F}^{-1}\frac{\partial \Psi}{\partial \mathbf{F}}$,.

The tissues were, in general, thick enough (10% to 20% of the section diameter) to accommodate bending-stress concentrations. Bending stiffness can be significant for

thick tissue specimens indented from a planar state and exhibiting a nonlinear stress response. Therefore, stress cannot be obtained directly in a ball burst test because of bending and finite thickness effects.

2.4 Statistics

Statistical analysis was performed to compare mechanical parameters and structural composition of the distal vagina between the tested groups. The statistical software package GraphPad Prism 5, (San Diego, CA - USA) was used. Kolmogorov-Smirnov tests showed the data follows a normal distribution. Quantitative data are represented as mean ± standard error of the mean (±SEM). Paired student´s t-test was used with a confidence level of 95% for the within group-comparisons. A statistically significant difference was reported if $p<0.05$.

3. Results

3.1 Experimental Data and Histological Analysis

The mechanical behavior of the ovine vaginal wall analyzed from samples tested with uniaxial and ball burst tests, was compared (Table 1). The vaginal wall of pregnant sheep was more compliant than that of virgins ($p<0.05$) or parous ($p<0.05$) ewes in both tests. Virgin sheep vaginal wall was the stiffest tissue.

Table1. Mechanical characteristics of the distal vaginal wall of sheep during uniaxial and ball burst testing. Data is presented as mean (± SEM) and significance levels for comparison between groups: **a**- virgin vs pregnant, **b**- pregnant vs parous, **c**-parous vs virgin; the level of significance was set to $p<0.05$.

Mechanical properties of ovine distal vagina					
		Ball burst test		Uniaxial test	
Tissue	Nr	Stiffness N/mm	Elongation (mm)	Stress N/mm^2	Strain
Virgin	N=5	10.88 ± 2.07 **a**	7.99 ± 0.36 **a**	2.70 ± 0.24 **a**	0.33± 0.02 **a**
Pregnant	N=5	4.74 ± 0.26 **b**	18.45 ± 0.73 **b**	1.25 ± 0.18 **b**	0.48 ± 0.05 **b**
Parous	N=5	9.30 ± 0.73	10.99 ± 0.72 **c**	2.11 ± 0.34	0.30 ± 0.03

Figure 2 shows the distribution of smooth muscle cells (light rose) and collagen (red) on a full thickness histologic section. Thickness, total collagen and smooth muscle cells contents (%) of the sheep distal vagina were measured (Table 2). The distal vagina of pregnant sheep was significantly thinner compared to that of virgin and parous sheep and contained less collagen fibers. Total collagen content in the distal vagina of virgin sheep was significantly higher and smooth muscle cell content was significantly lower than in pregnant and parous. Smooth muscle cell content was higher in parous sheep than in pregnant and virgin. During pregnancy, smooth muscle cell content increased as compared to levels in virgin sheep.

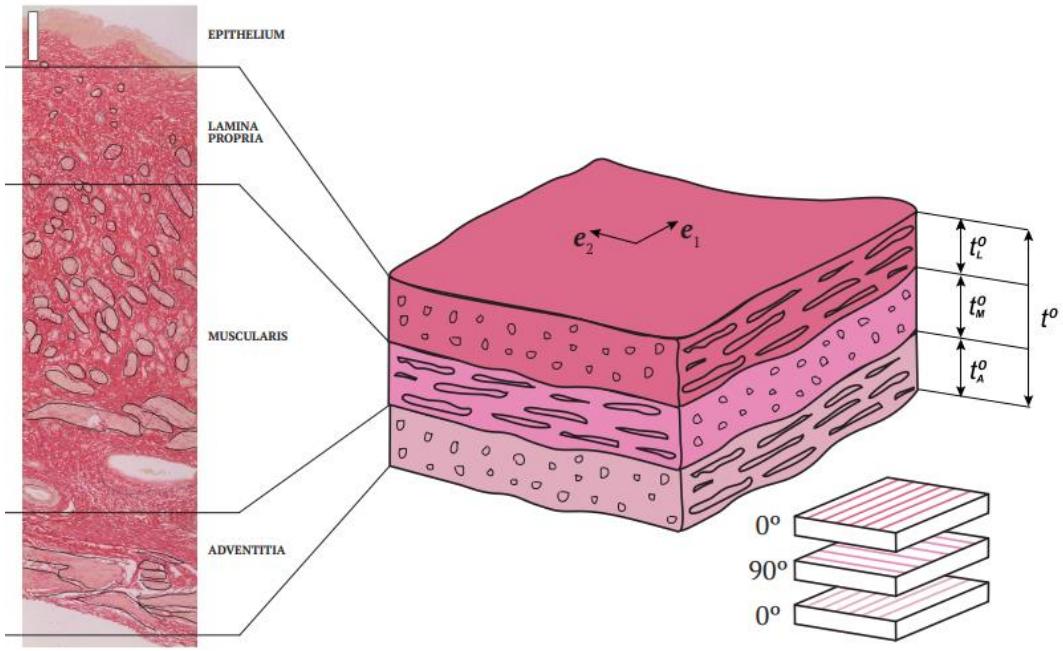

Fig. 2 Histological image of the ovine vaginal wall (distal part) stained with Miller's Elastica. Scale bar (upper left) for sections - 200 µm. smooth muscle cells are outlined in black. The. $\boldsymbol{e}_1$-direction is normal to the cut section. Samples in the simulation of ball burst test were considered composed by three layers: *Lamina propria* (L), *Muscularis* (M), *Adventitia* (A), t^o- thickness.

Table2. Morphological analysis of the distal vaginal wall of the sheep used for uniaxial testing, with the following comparisons: **a**- virgin vs pregnant, **b**- pregnant vs parous, **c**-parous vs virgin. The level of significance was set to $p < 0.05$.

Morphological analysis of ovine distal vagina				
Tissue	Nr	Thickness (mm)	Collagen (%)	Smooth muscle (%)
Virgin	N=5	3.86 ± 0.25 **a**	54.42 ± 0.86 **a**	22.07 ± 0.84 **a**
Pregnant	N=5	2.88 ± 0.11 **b**	46.86 ± 1.65 **b**	27.40 ± 0.20 **b**
Parous	N=5	4.34 ± 0.14	50.45 ± 0.90 **c**	30.13 ± 0.29 **c**

Vaginal wall layers (epithelium, lamina propria, muscularis and adventitia) were discriminated and their parameters are displayed in Table 3. Data from the epithelial layer were not considered because this layer lacks collagen fibers. The lamina propria has the highest level of collagen except in pregnant sheep. The lamina propria smooth muscle cells were surrounded by collagen fibers and were oriented in the $\boldsymbol{e}_1$ direction, while in the muscularis layer in the $\boldsymbol{e}_2$ direction. (Figure 2). The thickest layer was the muscularis, and it contained less collagen than the other layers, except in parous sheep.

Table3. Thickness and total collagen (%) content of the distal vaginal wall layers in sheep where uniaxial testing was performed, with comparisons between **a**- virgin vs pregnant, **b**- pregnant vs parous, **c**-parous vs virgin. The level of significance was set to $p < 0.05$.

Morphological analysis of ovine distal vagina				
Tissue		Virgin	Pregnant	Parous
Lamina propria	Thickness (mm)	1.09 ± 0.11 **a**	0.69 ± 0.06	0.63 ± 0.06 **c**
	Total collagen (%)	66.67 ± 1.27 **a**	44.96 ± 2.37 **b**	55.56 ± 1.95 **c**
Muscularis	Thickness (mm)	1.78 ± 0.22	1.44 ± 0.08 **b**	2.51 ± 0.08 **c**
	Total collagen (%)	47.89 ± 4.06	40.93 ± 1.12	55.41 ± 1.05 **b**
Adventitia	Thickness (mm)	0.72 ± 0.04 **a**	0.52 ± 0.04 **b**	0.79 ± 0.06
	Total collagen (%)	53.28 ± 4.99	48.41 ± 2.87	48.81 1.79

3.2 Linking the uniaxial data and the histology of the ball burst samples

Thicknesses of the ball burst specimens were manually measured as an average of 3 measurements along the cross-section of the specimen. The results are summarized in Figure 3(a). The linking is presented under the assumption that the relative thicknesses of each layer in the ball burst test specimens were the same as in tensile test specimens' thicknesses. Similar cross sections of tensile specimens and ball burst test specimens were assumed. Therefore, to define the thickness of each layer, the measured total thickness was distributed according to the measured layers' thickness fraction of the tensile test specimens (Fig. 3(b)).

From the tensile tests' stress-true strain curves, supported by the histological images, it is clear that the tissue microstructure is highly related to the status of the ewe during her reproductive life (virgin, pregnant, or parous). Such patterns from tensile tests curves remained crisp then in the ball burst punch-displacement curves (see experimental data provided in Fig.6). Therefore, the response curves show shape similarities either in uniaxial tensile or ball burst tests. These observations led to the following considerations: (i) as k_2 influences the curvature in the mechanical response, it was assumed constant within a group; (ii) μ was also kept the same for all layers within the same group due to its connection to the extracellular matrix (ECM) properties; (iii) k_1 was calculated using the HM coefficient ξ; (iv) ξ_l, or the HM coefficient of a given layer, for the ball burst specimens was calculated by interpolation using the collagen content of the layer and the global coefficient, ξ for the tensile test specimens. These considerations are summarized in Table 1.

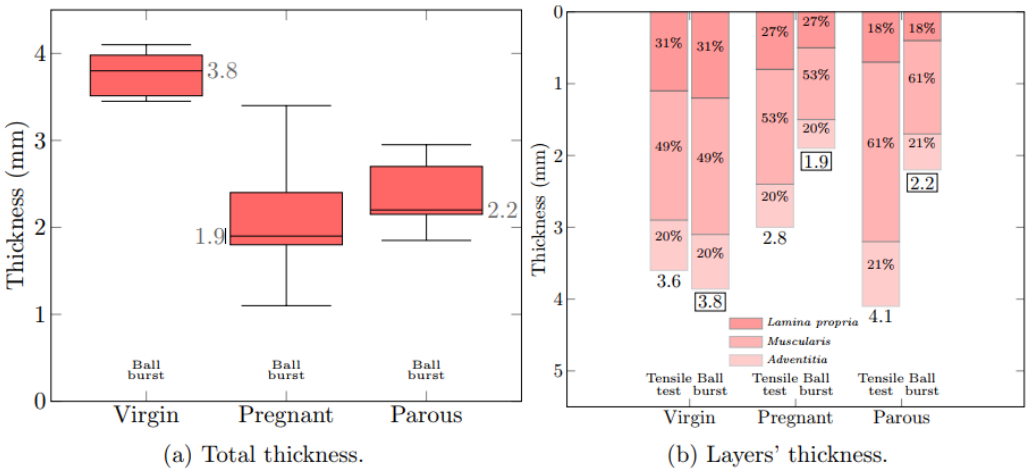

Fig. 3 Ball burst specimens. (a) Total thickness directly measured. (b) Calculation of the hickness of the layers while splitting the total thickness according to the relative thickness of each layer of the tensile specimens.

Table4. Material parameters of each layer of the ball burst test specimens calculated taking the material parameters of the tensile specimens as the reference. Vertical axis in logarithmic scale. k_2 assumed invariable within the same group. μ kept the same for all layers within the same group. ξ of each layer of the ball burst specimens calculated by interpolation using the collagen content of the layer and the ξ value of the tensile test specimens. k_1 calculated using the histologically-motivated coefficient ξ.

Tensile Test										
			Virgin			Pregnant			Parous	
Name	Symbol	Lamina	Muscularis	Adventitia	Lamina	Muscularis	Adventitia	Lamina	Muscularis	Adventitia
Collagen (%)			54.42			46.86			50.45	
Thickness	t^0		3.6			2.8			4.1	
Layer Thickness	t_i^0	1.1	1.8	0.7	0.8	1.6	0.6	0.7	2.5	0.9
Fraction	t^0/t_i^0	0.31	0.49	0.2	0.27	0.53	0.2	0.18	0.61	0.21
HM ratio	$\xi = k_1/(2k_2\mu)$ (-)		3.79			0.050			1.66	
Initial Shear Modulus	μ (MPa)		0.65			0.99			0.91	
Fibre parameter	k_1 (MPa)		0.95			0.0065			0.87	
Fibre parameter	k_2 (-)		0.19			0.065			0.29	
Ball Burst Test										
			Virgin			Pregnant			Parous	
		Lamina	Muscularis	Adventitia	Lamina	Muscularis	Adventitia	Lamina	Muscularis	Adventitia
Collagen (%)		66.49	48.92	54.99	44.5	43.85	51.62	55	60.72	53.67
Thickness	t^0		3.8			1.9			2.2	
Layer Thickness	t_i^0	1.2	1.9	0.8	0.5	1.0	0.4	0.4	1.3	0.47
HM ratio	$\xi = k_1/(2k_2\mu)$ (-)	4.63	3.40	3.83	0.048	0.048	0.055	1.81	1.99	1.76
Initial Shear Modulus	μ (MPa)		0.65			0.99			0.90	
Fibre parameter	$k_1 = \xi(2k_2\mu)$ (MPa)	0.36	0.42	0.19	0.0017	0.0032	0.0014	0.17	0.64	0.193
Fibre parameter	k_2 (-)		0.19			0.065			0.29	

3.3 Finite element Modelling

The uniaxial tensile test provides valuable information about the directional mechanical properties of the vaginal tissue, while the ball burst test provides multiaxial mechanical properties of the whole tissue structure. Ball burst testing applies an orthogonal load to the central portion of the tissue specimen whilst the uniaxial test applies in-plane load or deformation to the specimen (Figure 1). Therefore, ball burst tests give an indirect measurement of the material strength where anisotropy is blurred due to the geometric constraints to which the specimens are subjected. Here, we intend to demonstrate that the histologically-driven parameters are capable to capture the overall material behavior of the tested specimens. The dominant fiber direction of lamina propria, muscularis and adventitia were derived from the spatial distribution of smooth muscle. Simulations were performed by approximating the specimens to a stacked tissue with fibers oriented as [0,90,0]. Each layer behaves as a transversely isotropic hyperelastic material [25]; three parameters μ, k_1 and k_2 (along with the mean fiber direction a_0), model the mechanics of each layer. Such assumption does not account for the inherent discontinuities between the materials' constituents and treat each layer of the specimen as a continuum.

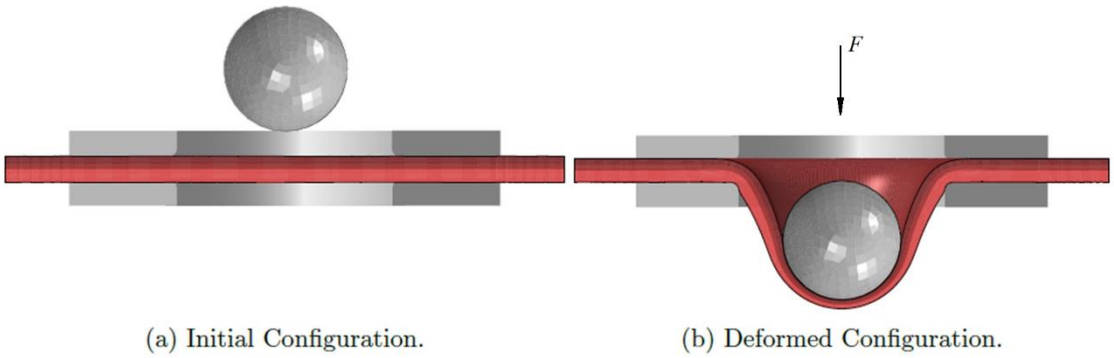

Fig. 4 Geometrical model used in the simulations. Samples considered as three-layered disks, each behaving according to the HGO model. Refined mesh (431520 hexahedral linear and hybrid elements (C3D8H)) ensuring convergence and no locking issues. (a) Clamped sample in the initial configuration. (b) The rigid sphere contacts the sample without friction imposing transversal displacements to the sample. Sample in the deformed configuration.

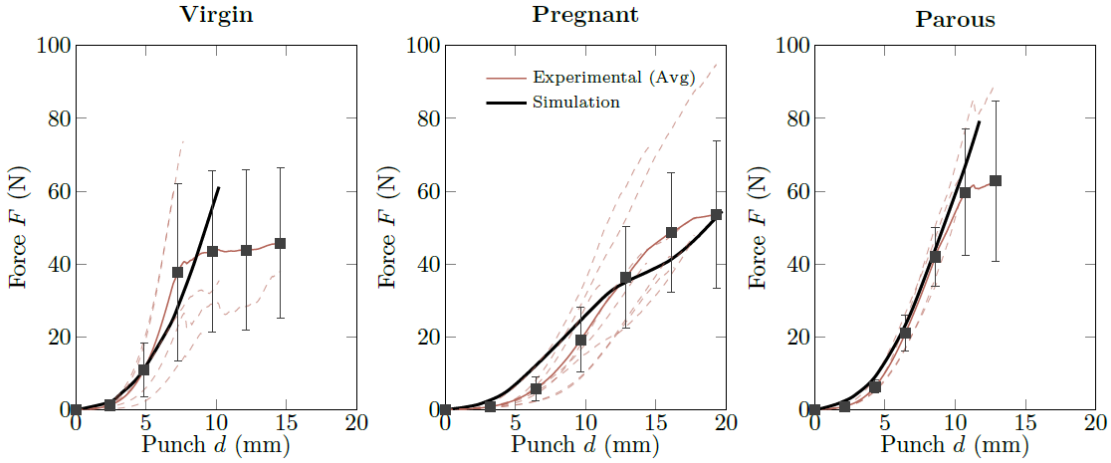

Fig. 5 Force-Punch displacement (d) curves of the vaginal tissue during ball burst testing. Predicted response within the variability range of the experiments. Averaged data linearly interpolated from the data points and extrapolated to the nearest grid points when applicable. Material parameters based solely on a HM coefficient. No curve fitting performed.

4. Discussion

Biaxial and multiaxial testing of the vaginal tissue might be relevant, since vaginal tissue is known to be anisotropic [26]. These tests might provide more detailed information about the tissue mechanical behavior. However limited material dimensions often force the researches to use uniaxial testing.

The ball burst test results, presented in this study, showed that force-punch curves of the vaginal tissue were able to distinguish different phases during the ovine reproductive life. The same observations were noted during uniaxial tensile testing. The microstructure and mechanical properties of the vaginal wall undergo changes during pregnancy. A previous study has showed the possible link between tissues histology and mechanical behavior [19]. Therefore, the present work uses the microstructural information to

describe the mechanical response of distal vaginal specimens under ball burst testing conditions. By relying solely on the tissue thickness, total collagen content and on the HM coefficient of similar specimens subjected to uniaxial tensile conditions, the mechanical response of the ball burst specimens was characterized.

The tensile test samples were stretched along the $\boldsymbol{e}_1$-direction, the (observed) preferential direction of collagen fibers in the lamina propria. Of all three layers, the lamina propria has the highest level of collagen, except for the pregnant sheep group. Since in uniaxial tensile testing conditions the fibers of all layers tend to align in the stretching direction [27], a transversely isotropic model (one family of fibers) was used to define the sample response under the tensile testing conditions. On the other hand, a layered tissue was taken into account for modelling the tissue behavior on ball burst testing conditions. It was assumed that cross sections were similar for the tensile specimens and the ball burst specimens. The mean thickness (excluding the outliers) was used in the simulations.

Predictions on the mechanical behavior of biological systems are highly dependent on representative constitutive models. The Holzapfel-Gasser-Ogden (HGO) model seems adequate for many soft biological tissues [18] [17], which is the case for all tested vaginal tissues [28]. We have calculated the HM coefficient extrapolating from its correlation with the collagen content of tensile specimens from a previous work [17]. Simple arguments to obtain the material parameters were then employed. Three parameters μ, k_1 and k_2, along with the mean fiber direction a_0, modeled the mechanics of each layer. From continuum mechanics assumptions, it means that each layer is a continuum media and there is a discontinuity in the stress distribution between two adjacent layers. It was assumed that reproductive status induces changes to the crosslinking and content of the total collagen fibers. Such considerations resulted in taking the same extra-cellular matrix (ECM) for all three layers and, therefore, the same μ parameter. Parameter k_1 obtained from the tensile fitting was weighted according to the layer's thickness ratio. Since the slope of the response curves of the ball burst tests is comparable to the uniaxial tests, k_2 was kept constant for all three layers.

Boundary conditions consider possible relative sliding between clamping disks and tissue, with no friction. This condition was important in the early stages of the punching. Some tearing of the samples was observed during the experimental tests. Since no damage of the tissue was considered, all the simulated force-punch curves tend to be above the experimental ones.

The link between histological information and tissue mechanical response, made through HM coefficient, was validated in a simulation environment. The predicted force and stress resultants of the numerical simulation display a good correlation with the ball burst testing results. Mechanical behavior of the ball burst samples was correlated with the histological and mechanical properties of the tensile test samples. No curve fitting was performed for the ball burst results. The use of mechanical behavior of the distal vagina during the uniaxial tests coupled with histological parameters, gives an opportunity to predict the tissue behavior under multiaxial loading conditions.

Conclusions

The proposed methodology may be viewed as a new application of uniaxial data, for the extrapolation of in silico tissue mechanical behavior. It may work for other tissues since the arbitrariness in the postulation of an HM coefficient turns out to be transversal to the nature of the tissues. Other approaches may be applied as long as the chosen material model is coherent with the tissue' microstructure and with the available histological data.

Based upon uniaxial testing and relevant histological information, the method seems capable to predict the overall response (mechanical behavior) of vaginal tissue subjected to a complex deformation mode.

Acknowledgements

This research has been supported by Fundação para a Ciência e a Tecnologia I.P. (FCT, Portugal) under grants SFRH/BD/96548/2013, IF/00159/2014, SFRH/BD/107860/2015, SFRH/BPD/111846/2015; UROSPHINX - Project 16842, COMPETE2020, through FEDER and FCT; and in part by a grant of the EC in the FP7-framework (Bip-Upy; NMP3-LA-2012-310389) and by the POP-ART Duomed chair

References

[1] Haylen BT, de Ridder D, Freeman RM, et al., "An international urogynecological association (IUGA)/international continence society (ICS) joint report on the terminology for female pelvic floor dysfunction," *Neurourol Urodyn,* vol. 29, 2009.

[2] Callewaert, G., Albersen, M., Janssen, K., Damaser, M.S., Van Mieghem, T., Van Der Vaart, C.H., Deprest, J., , "The impact of vaginal delivery on pelvic floor function – delivery as a time point for secondary prevention," *BJOG.*, p. 678–681, 2016.

[3] DeLancey, J.O.L., Low, L.K., Miller, J.M., Patel, D.A., Tumbarello, J.A., , "Graphic integration of causal factors of pelvic floor disorders: an integrated life span model," *Am. J. Obstet. Gynecol.*, vol. 610, pp. 1-5, 2008.

[4] Myers DL, Sung VW, Richter HE, Creasman J, Subak LL., "Prolapse symptoms in overweight and obese women before and after weight loss.," *Female Pelvic Med Reconstr Surg.*, vol. 18, no. 1, pp. 55-9., 2012.

[5] Ford, A.A., Rogerson, L., Cody, J.D., Ogah, J., , "Mid-urethral sling operations for stress urinary incontinence in women (Review),," *Cochrane Database Syst. Rev.*, p. 1–287., 2015.

[6] Vashaghian, M., Ruiz-Zapata, A.M., Kerkhof, M.H., Zandieh-Doulabi, B., Werner, A., Roovers, J.P., Smit, T.H., , "Toward a New Generation of Pelvic Floor Implants With Electrospun Nanofibrous Matrices: A Feasibility Study,," *Neurourol. Urodyn.*, vol. 36, p. 565–573, 2017.

[7] D.M. Furlong, D.M. Elser, M.M. Moen, "Complications Related to Graft or Mesh Augmentation in Vaginal Reconstructive Surgery," *JMIG*, vol. 16, no. 6, p. 148, 2009.

[8] Urbankova, I., Callewaert, G., Sindhwani, N., Turri, A., Hympanova, L., Feola, A., Deprest, J.,, "Transvaginal mesh insertion in the ovine model," *J. Vis. Exp.*, 2017.

[9] Hympánová L, Rynkevic R, Román S, Mori da Cunha MGMC, Mazza E, Zündel M, Urbánková I, Gallego MR, Vange J, Callewaert G, Chapple C, MacNeil S, Deprest J., "Assessment of Electrospun and Ultra-lightweight Polypropylene Meshes in the Sheep Model for Vaginal Surgery.," *Eur Urol Focus.*, pp. S2405-4569, 2018.

[10] Urbankova, I., Vdoviakova, K., Rynkevic, R., Sindhwani, N., Deprest, D., Feola, A., Herijgers, P., Krofta, L., Deprest, J., , "Comparative anatomy of the ovine and female pelvis,," *Gynecol Obs. Invest*, pp. 1-10, 2017.

[11] Endo, M., Urbankova, I., Vlacil, J., Sengupta, S., Deprest, T., Klosterhalfen, B., Feola, A., Deprest, J., , "Crosslinked xenogenic collagen implantation in the sheep model for vaginal surgery,," *Gynecol. Surg.*, p. 113–122., 2015.

[12] Kerbage, Y., Giraudet, G., Rubod, C., Garabedian, C., Rivaux, G., Cosson, M., " Feasibility and benefits of the ewe as a model for vaginal surgery training," *Int. Urogynecol. J.*, vol. 28, p. 1573–1577, 2017.

[13] Mansoor, A., Curinier, S., Campagne-Loiseau, S., Platteeuw, L., Jacquetin, B., Rabischong, B.,, " Development of an ovine model for training in vaginal surgery for pelvic organ prolapse," *Int. Urogynecol. J.* , vol. 28, p. 1595– 1597, 2017.

[14] Silva E, Parente M, Brandão S, Mascarenhas T, Natal Jorge R, "Characterizing the Biomechanical Properties of the Pubovisceralis Muscle Using a Genetic Algorithm and the Finite Element Method.," *J Biomech Eng.*, vol. 141, no. 1, 2019.

[15] Oliveira DA, Parente MP, Calvo B, Mascarenhas T, Natal Jorge RM, "Numerical simulation of the damage evolution in the pelvic floor muscles during childbirth.," *J Biomech.* , vol. 49, no. 4, pp. 594-601, 2016.

[16] Vila Pouca MCP, Ferreira JPS, Oliveira DA, Parente MPL, Mascarenhas T, Natal Jorge RM, "On the effect of labour durations using an anisotropic visco-hyperelastic-damage approach to simulate vaginal deliveries.," *J Mech Behav Biomed Mater.* , vol. 88, no. 8, pp. 20-126., 2018.

[17] Rynkevic R, Ferreira J, Martins P, Parente M, Fernandes A.A, "Linking hyperelastic theoretical models and experimental data of vaginal tissue through histological data," *Journal of Biomechanics,* vol. 82, no. 3, pp. 271-279, 2019.

[18] Holzapfel GA, Gasser TC, Ogden RW. , "A new constitutive framework for arterial wall mechanics and a comparative study of material models.," *Journal of Elasticity.,* vol. 61, pp. 1-48, 2000.

[19] R. Rynkevic, P. Martins, L. Hympanova, H. Almeida, A. A. Fernandes, and J. Deprest,, "Biomechanical and morphological properties of the multiparous ovine vagina and e↵ect of subsequent pregnancy,," *Journal of Biomechanics,* vol. 57, pp. 94-102, 2017.

[20] Urbankova I, Callewaert G, Blacher, Deprest D, Hympanova L, Feola , De Landsheere , Deprest J,, " First delivery and ovariectomy affect biomechanical and structural properties of the vagina in the ovine model.," *Int Urogynecol J,* 2018.

[21] Kattan SA, "Maternal urological injuries associated with vaginal deliveries: change of pattern.," *Int Urol Nephrol.* , vol. 29, no. 2, pp. 155-61, 1997.

[22] Rynkevic R, Martins P, Hympanova L, Almeida H, Fernandes AA, Deprest J., " Biomechanical and morphological properties of the multiparous ovine vagina and effect of subsequent pregnancy," *J Biomech.,* vol. 57, pp. 94-102, 2017.

[23] D. Systemes, "ABAQUS v6.12 Documentation". Providence, RI, USA 2012.

[24] Holzapfel G.A., Nonlinear Solid Mechanics: A Continuum Approach for Engineering, Chichester, United Kingdom: John Wiley and Sons Ltd, 2000.

[25] E. Pena, B. Calvo, M. A. Martinez, P. Martins, T. Mascarenhas, R. M. N. Jorge, A. Ferreira, and M. Doblare,, "Experimental study and constitutive modeling of the viscoelastic mechanical properties of the human prolapsed vaginal tissue," *Biomechanics and Modeling in Mechanobiology,* vol. 9, no. 1, pp. 35-44, 2010.

[26] Stacy Tokar, Andrew Feola, Pamela A. Moalli and Steven Abramowitch, "Characterizing the Biaxial Mechanical Properties of Vaginal Maternal Adaptations During Pregnancy," in *ASME 2010 Summer Bioengineering Conference*, Naples, Florida, USA,, 2010.

[27] B. Calvo, E. Pena, P. Martins, T. Mascarenhas, M. Doblare, R. M. Natal Jorge, and A. Ferreira,, "On modelling damage process in vaginal tissue," *Journal of Biomechanics,* vol. 42, no. 5, p. 642–651, 2009.

[28] Rubod C, Boukerrou M, Brieu M, Dubois P, Cosson M., "Biomechanical properties of vaginal tissue. Part 1: new experimental protocol.," *J Urol.* , vol. 178, pp. 320-325, 2007.

CHAPTER 9

CREATION OF AN OVINE PELVIC FLOOR THREE-DIMENSIONAL MODEL USING MAGNETIC RESONANCE

Rita Rynkevic[1,2,3], Pedro Martins[1], Pavelas Trusevičius [4], Nele Famaey [5], António A. Fernandes[1], Jan Deprest[2,3,6]

[1]INEGI, LAETA, Faculty of Engineering of the University of Porto, Porto, Portugal
[2]Centre for Surgical Technologies, Group Biomedical Sciences, KU Leuven, Leuven, Belgium
[3]Department of Development and Regeneration, Woman and Child, Group Biomedical Sciences, KU Leuven, Leuven, Belgium
[4]Buivydiškės Veterinary Clinic, Vilnius, Lithuania
[5] Biomechanics Section Department of Mechanical Engineering, KU Leuven, Leuven, Belgium
[6]Pelvic Floor Unit, University Hospitals KU Leuven, Leuven, Belgium

Key words: pelvic floor, 3D model, animal model, magnetic resonance

Short communication submitted to Journal Research in Veterinary Science (March, 2019)

ABSTRACT

Background: Different animal models are used for experimental studies. For studies on the pathophysiology and therapy of pelvic organ prolapse (POP), rodents, rabbits, sheep and non-human primates, are the most popular. There is increasing concern about the sacrifice of so many animals for scientific purposes, therefore new methods are being developed to reduce the need for animal testing. *In silico* models are a novel approach to the problem, including for POP studies.

Methods: Swifter sheep was used as a model to study POP, since the pelvic floor tissues and anatomy are comparable in size and structure to humans. Magnetic Resonance (MR) imaging data of the pelvic region from nulliparous sheep was then used to create *in silico* 3D geometrical models of the ovine pelvic floor organs, structures and soft tissues.

Results: The proposed 3D geometrical model of the ovine pelvic floor, was able to capture the relevant features of the ovine anatomy. The model is prepared to be used as an auxiliary learning tool and reference material for pre-clinical studies, with potential application in other areas such as biomedical engineering, material science, tissue engineering, veterinary medicine, etc.

Conclusions: The fusion of known experimental data with *in silico* 3D geometrical models can provide relevant information to many clinical applications such as surgical reconstructions improvement, mesh augmented repair, surgical training, among others.

1. Introduction

A wide range of animal models, such as rodents, domestic mammals or non-human primates, are used in experimental studies (Andersen and Winter, 2017). These animals are used in the testing of drugs, vaccines, and medical devices, mainly to determine the safety of medical product, and occasionally their efficacy (FDA, 2017). The use of animals allows the development of basic knowledge that supports pre-clinical and clinical studies. There are still many areas where animal testing is perceived to be necessary and non-animal testing is not always a scientifically valid or available option. Nevertheless, the Food and Drug Administration (FDA) as well as European authorities (find reference) are supporting and stimulating efforts to reduce animal testing. Several researchers are therefore doing efforts to reduce the need for animal testing, eventually even substituting them (FDA, 2017).

Sheep can mimic many human anatomical conditions. The sheep model is used in research areas, such as coronary surgery (Boumzebra et al., 2006), cardiovascular surgery (Katz et al., 2015), chronic lung disease (Gilmour et al., 1979), orthopedics (Martini et al., 2001), pelvic organ prolapse (POP) (Couri et al., 2012), brain injuries (Back et al., 2015), pregnancy and fetal growth (Vuguin, 2007; Barry et al., 2008). Our group and others have done a considerable effort to explore the use of sheep as a large animal model for pelvic floor disorders (Urbankova et al., 2017b; Urbankova et al., 2018).

This research will focus on the sheep used as a model to study the POP and the mesh augmented prolapse repair. Despite being a quadruped, the pelvic floor tissues and anatomy of sheep are comparable (relatively) in size and structure to humans (Abramowitch et al., 2009). It is possible to perform vaginal surgery with/without graft insertion (Urbankova et al., 2017a). There are some studies regarding the anatomy of the ovine pelvic floor (Urbankova et al., 2017b); however, mechanical loading conditions of pelvic soft tissues are not fully understood.

The complexity of pelvic surgeries promotes interdisciplinary research collaborations with technological fields such as engineering. A more recent trend is the use of in silico models, which could present a clear and understandable model combining multiscale parameters of the organs.

The purpose of this work was to create an *in silico* 3D geometrical model of the ovine pelvic floor organs, structures and soft tissues. The mechanical behavior of the main organs and structures was obtained, and a detailed morphological description was done in previous works (Rynkevic et al., 2017; Rynkevic et al., 2018). Combining 3D *in silico* model with already available experimental and histological data, may provide relevant information across disciplines, e.g. to improve surgical reconstructions. This 3D library of the ovine pelvic floor could be used as geometrical base model for numerical simulations, which eventually may lead to a reduction of the number of animals used in experimental studies.

2. Materials and methods

The 3D model of the ovine pelvic floor presented in this paper, is a more detailed and accurate version of the model used in previous investigations (Urbankova et al.,2017b). Nulliparous Swifter sheep underwent Magnetic Resonance (MR) imaging, on a 3 Tesla

MR device with a spinal coil (Magnetom Trio, Siemens, Erlangen, Germany) in the lateral recumbent position. Anatomic high-resolution T1 images were obtained with a slice thickness 0.9 mm and an interslice gap of 0mm (resolution 1.03 × 1.03 mm, TE 4.92 ms, TR 10 ms, the field of view 330 mm, bandwidth 446 Hz/pixel).

Sagittal and transversal scans were used to visualize pelvic floor anatomy and to create a 3D geometrical model using Mimics v17.0 software (Materialise NV, Leuven, Belgium). Based on MR images all individual parts of interest including bone structures (femur, pelvic bones and spine), organ walls (rectum, vagina, uterus, urethra, bladder), muscles (external anal sphincter, levator ani muscle, obturator externus muscle) and main blood vessels (ovarian and the internal iliac artery and inner pelvic vein and the caudal vena cava) were obtained and segmented. The bones and the pelvic organs were segmented using dynamic region growing and edited manually when necessary. The broad sacrotuberous ligament and the *levator ani* were defined by manual drawing splines on individual axial slices. The splines were exported to Matlab R2017b (MathWorks Inc., Natick, Massachusetts, U.S.A.) where a custom code generated a point cloud representing the structure of interest. The point cloud was then imported to the 3-Matic module of Mimics software to obtain a 3D geometrical model. Segmentation results were reconstructed into 3D geometrical models for each anatomical part. Artefact smoothing was made under guidance of gynecologists, while maintaining the integrity of the natural anatomic animal structure.

3. Results

Figure 1 represents the 3D model of the ovine pelvis. The bony pelvis serves as a protective shell for the pelvic organs (Figure 1**A)**. The sacrotuberous ligament forms a large trapezoidal sheet, it originates from the sacral vertebrae and inserts laterally on the opposite side on the ischial spine (Figure 1**B**). The levator ani is a paired muscle plate, inserted between the internal and external pelvic diaphragmatic fascia (Figure 1**B**). External anal sphincter has three parts; the proximal part is intimately associated with the levator ani muscle. The distal part is the strongest part with some fibres passing to the constrictor vulvae (Figure 1**B**).

The lower urinary tract, the uterus, and vagina are attached to the pelvic side wall by connective tissue that also contains the supplying vessels and nerves. The ovine reproductive tract consists of the ovaries, uterine tubes, the cervix and the vagina. The rectum is attached with the mesorectum to the dorsal wall of the pelvic cavity (Figure 1**C)**.

The pelvic floor and organs receive most of their blood supply via the ovarian and the internal iliac artery and its branches (Figure 1**D**). Venous drainage is through the inner pelvic vein and the caudal vena cava.

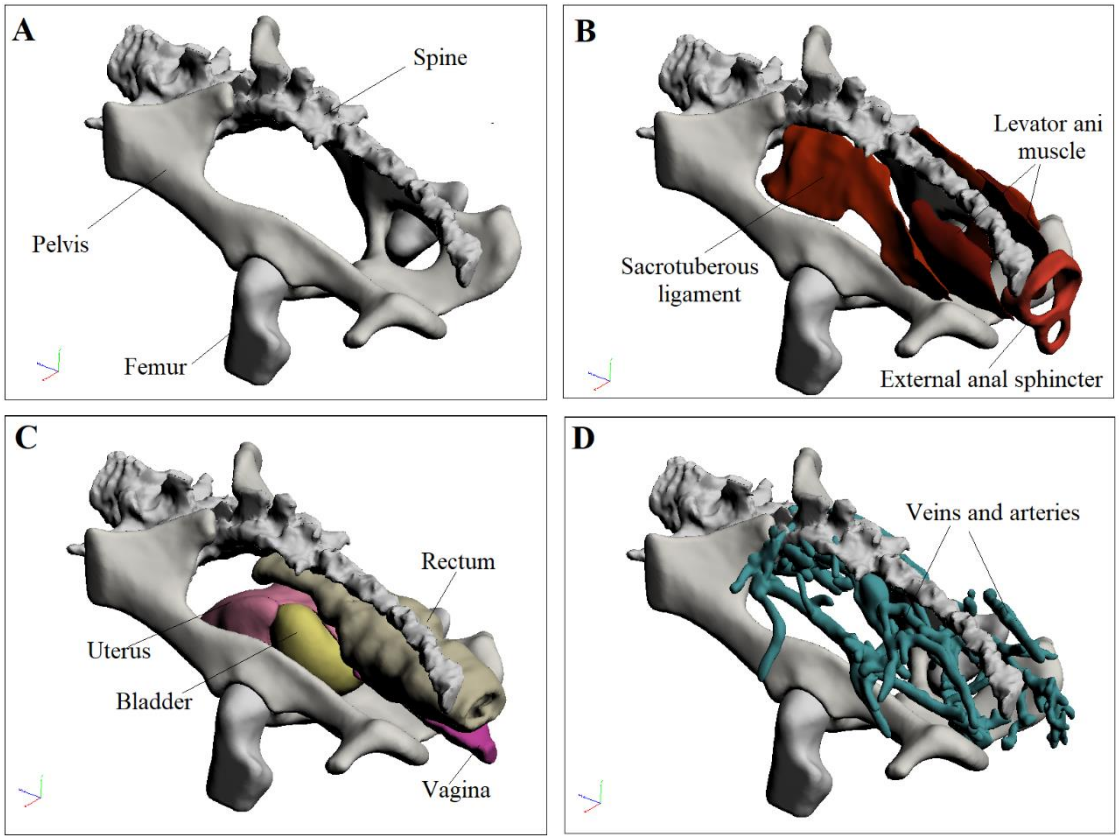

Fig. 5. 3D model of ovine pelvic floor. **A**: bony structure; **B**: muscles and ligaments; **C**: lower urinary tract and rectum; **D**: main arteries and veins.

4. Discussion

The results obtained from experimental pre-clinical and clinical studies, conducted on animals, are commonly used to test whether a medical device is suitable for human. Sheep is believed to be a representative experimental model for transvaginal surgeries (mesh augmented repair). Therefore a detailed study and description of the anatomical systems of interest (pelvic region) are needed to improve the investigations using this model.

Often scientists delving into the study of prolapse or urinary incontinence, study only specific organs, muscles or ligaments, and not all the structures and their complex relationships. Thus, there is insufficient information about the area under study (adjacent organs, their properties, structure and impact on the intervened organs organs). Such information could improve further research and knowledge (Chantereau et al., 2014; Rubod et al., 2012).

After a critical analysis, the authors believe this model can be successfully used not only as an auxiliary material for pre-clinical studies, but also in other areas such as biomedical engineering, material science, tissue engineering, veterinary medicine, etc. Creation of such models for other parts of the body: heart, circulatory system, brain, respiratory system, etc., may improve the quality of future investigations. Such virtual libraries could significantly reduce the number of experimental animals, by conducting in-silico simulations.

Conclusions

The proposed 3D geometrical model will be used to further advance the understanding of surgical solutions for pelvic floor repair using *in silico* simulation models (mainly finite element based). In the future these may come to substitute several *in vivo* animal models. Using the 3D geometrical model for finite element simulations, the dynamics of pelvic organs can be investigated. Hopefully these results will play a significant role in designing appropriate implant materials and whenever possible understand and/or predict undesired side effects such as graft related complications, ultimately leading to their prevention.

Conflict of interest statement

The authors do not have to disclose any financial or personal relationships with other people or organizations that could inappropriately influence (bias) their work.

Acknowledgment

This research has been supported by Fundação para a Ciência e a Tecnologia I.P. (FCT, Portugal) under the grand SFRH/BD/96548/2013, SFRH/BPD/111846/2015; UROSPHINX - Project 16842, COMPETE2020, through FEDER and FCT; and in part by a grant of the EC in the FP7-framework (Bip-Upy; NMP3-LA-2012-310389).

References

Abramowitch, S.D., Feola, A., Jallah, Z., Moalli, P.A., 2009. Tissue mechanics, animal models, and pelvic organ prolapse: Eur. J. Obstet. Gynecol. Reprod. Biol. 144, 146–158.

Andersen, M.L., Winter, L.M.F., 2017. Animal models in biological and biomedical research - experimental and ethical concerns. Anais da Academia Brasileira de Ciências, ISSN 1678-2690.

Back, S.A., Riddle, A., Roger Hohimer, A.R., 2015. The sheep as a model of brain injury in the premature infant. Animal Models of Neurodevelopmental Disorders. 104, 107-128.

Barry, J.S., Anthony, R.V., 2008. The pregnant sheep as a model for human pregnancy. theriogenology. 69, 55–67.

Boumzebra, D., Solem, J.O., Nakeeb, S., Halees, Z.A., 2006. The sheep as a model for coronary artery surgery experiments on beating heart. The Journal of Tehran University Heart Center. 1, 12-17.

Chantereau, P., Brieu, M., Kammal, M., Farthmann, J., Gabriel, B., Cosson, M,, 2014. Mechanical properties of pelvic soft tissue of young women and impact of aging. International Urogynecology Journal. 25, 1547–1553 .

Couri, B.M., Lenis, A.T., Borazjani, A., Paraiso, M.F.R., Damaser, M.S., 2012. Animal models of female pelvic organ prolapse: lessons learned.. Expert review of obstetrics & gynecology. 7, 249-260.

Gilmour, J.S., Jones, G.E., Rae. A.G., 1979. Experimental studies of chronic pneumonia of sheep.. Comp Immunol Microbiol Infect Dis. 1, 285-293.

Katz, M.G., Kendle, A.P., Fargnoli, A.S., Mihalko, K.L., Bridges, C.R., 2015. sheep (ovis aries) as a model for cardiovascular surgery and management before, during, and after cardiopulmonary bypass. Journal of the American Association for Laboratory Animal Science. 54, 7-8.

Martini, L., Fini, M., Giavaresi, G., Giardino, R., 2001. Sheep model in orthopedic research: a literature review. Comp Med. 51, 292-299.

Rubod, C., Brieu, M., Cosson, M., Rivaux, G., Clay, J.C., De Landsheere, L., Gabriel, B., 2012. Biomechanical properties of human pelvic organs. Urology. 79, 968.

Rynkevic, R., Martins, P., Hympanova, L., Almeida, H., Fernandes, A.A., Deprest, J., 2017. Biomechanical and morphological properties of the multiparous ovine vagina and effect of subsequent pregnancy. Journal of Biomechanics. 24, 94-102.

Rynkevic, R., Martins, P., Parente, M., Mascarenhas, T., Almeida, H., Fernandes, A.A., 2019. The effect of consecutive pregnancies on the ovine pelvic soft tissues: link between biomechanical and histological components. Ann Anat. 222, 166-172.

Urbankova, I., Callewaert, G., Sindhwani, N., Turri, A., Hympanova, L., Feola, A., Deprest, J., 2017a. Transvaginal mesh insertion in the ovine model. J Vis Exp, 27.

Urbankova, I., Vdoviakova, K., Rynkevic, R., Sindhwani, N., Deprest, D., Feola, A., Herijgers, P., Krofta, L., Deprest, J., 2017b. Comparative anatomy of the ovine and female pelvis. Gynecol Obstet Invest. 82, 582-591.

Urbankova, I., Callewaert, G., Blacher, S., Deprest, D., Hympanova, L., Feola, A., De Landsheere, L., Deprest, J. 2018. First delivery and ovariectomy affect biomechanical and structural properties of the vagina in the ovine model. Int Urogynecol J. 30, 455-464.

U.S. Food and Drug Administration, 2017. Why are animals used for testing medical products? https://www.fda.gov/AboutFDA/Transparency/Basics/ucm194932.htm [Accessed 24 01 2019].

Vuguin, P.M., 2007. Animal models for small for gestational age and fetal programing of adult disease. Hormone research. 68,. 113-123.

CHAPTER 10

GENERAL DISCUSSION

The overall objective of this thesis was to re-introduce underappreciated *in vitro* testing methods that may be relevant for the characterization of (novel) implants for the treatment of pelvic organ prolapse (POP) and urinary incontinence (UI), as well as the study of the mechanical behavior of pelvic floor soft tissues. These findings may be useful for the further application in *in silico* models.

In this thesis several implants were tested. Today the standard materials used are textile in nature, and typically based on the polymer polypropylene (PP). Those implants are used for the treatment of abdominal wall hernia, incisional hernia, the reconstruction of POP and treatment of UI. There is no implant today that matches the needs of all patients or indications. Meshes are "foreign bodies", per definition generating a host response. This process is physiologic and should integrate the mesh into the musculo-fascial complex, hence it needs to function together with these. Insufficient biocompatibility and inappropriate biomechanical properties may, among other surgical and patient factors, lead to graft related complications (GRCs) [1]. These GRCs include, yet are not limited to, mesh contraction (more often referred to as "shrinkage"), exposure (often referred to as "erosion"), pain, or mesh migration into adjacent viscera [2]. This thesis mainly involved the study of some mechanisms that are believed to be involved in complications and that have a mechanical origin. This could be due to mismatch between the mechanical properties of the mesh and tissue and the acting loads [3]. Again, GRCs may also be associated to an inappropriate host response to the implant material, patient, surgical and other yet to be defined factors.

Durable textile implants

The first PP meshes used for hernia repair caused complications such as infection, fistula, pain and exposure [4-5]. The complications were initially thought to be related to the pore size, i.e. when smaller than 10µm the risk of infection would be increased [5]. Microporous materials can harbor infections because of the inability of the native cells to access these areas. Another similar factor may be the nature of the filaments of the constituting mesh. Indeed, a different inflammation and foreign body response is generated to a monofilament and multifilament material [6]. In a multifilament mesh host cells often cannot penetrate between all filaments and fibers, because of the small gaps between fibers. As a consequence, the risk for infection would be lower in monofilament meshes [6].

Implant weight and density also may affect the host response [7]. Cobb et al. divided meshes based on their weight: heavy weight (>140 g/m^2), mid-weight (70-139 g/m^2), light weight (35-69g/m^2) and more recently ultra-lightweight meshes (<35g/m^2) [8]. Light weight meshes may increase the likelihood that they result in a more physiological

compliance of the host tissue after ingrowth. This would be because of a lesser load of foreign material into to the host, reducing scar formation and preserving the elasticity of the tissue [8]. Pore stability also plays an important role in tissue integration. When loaded, the initial pore size may be reduced (the pores "collapse") precluding proper tissue ingrowth [9].

Based on that it is believed that lighter weight, larger pore size, and monofilament type are associated with a better tolerability of the host and a reduced rate of complications. One of the more recent clinical implants is Restorelle mesh (Coloplast, Humlebaek, Denmark). It has properties which are theoretically advantageous, according to the above concepts [9]. This implant was often used as a reference synthetic textile mesh in this thesis. It is a knitted monofilament PP mesh, 300μm thick, weighing around 19 g/m², with a fiber diameter 80μm, pore size 1.6-2.0 mm and with stable pores [9].

Resorbable implants

One explanation for GRCs may be the permanent nature of the inflammatory reaction induced by durable materials. Therefore, one could consider using degradable scaffolds. Ideally, these should also be made with initial biomechanical properties close to that of the host tissue. These scaffolds eventually become integrated due to degradation and ingrowth of new tissue. The working life of such surgical meshes follows two periods: one is functional, and the other is passive. [10]. During the first (functional) period, the implant performs tissue functions. During the second period (passive) the implant is gradually substituted by ingrown tissue from the host. The newly formed tissue should be sufficiently strong to substitute the vanishing implant. That means that the rate of destruction of foreign material should not exceed the rate of recovery (regeneration). If that is not the case, the implant's mechanical or tissue function will be prematurely lost. In the past several resorbable textile implants, e.g. Dexton (polyglycolic acid) and Vicryl (polyglactin 910) have been developed. The degradation rate of these implants is between 90 and 180 days. These materials have the advantage that they can be used in an infected wound area, as a temporary support. Often however, there was mesh failure evidenced by herniation [11].

A novel generation of implants is made by electrospinning technology. Electrospinning enables the production of ultrafine fibers, assembled as a non-woven matrix-like structure, which can physically mimic the structure of the natural extracellular matrix of most connective tissues [12]. Such scaffolds have already been successfully used for tissue engineering for restoration of vessels, cartilage, bone, peripheral nerve, spinal cord and skin [13-15]. Through different electrospinning parameters, polymer choice, surface modifications and functionalization (bioactivation) customized implants could be developed.

The pipeline of testing implant materials

As a recommended step into the pipeline before the introduction of medical devices for prolapse surgery, the material properties should be obtained *via* mechanical testing [16]. Mechanical testing may simulate the working performance, the behavior and the

clinically relevant failure mechanisms of implants, under more or less complex loading conditions. In this work, besides standard testing methods (uniaxial tensile testing, isotropy testing, testing in wet and dry conditions) we performed *cyclic* tests, to mimic the effects of repetitive loading, similar to what is expected *in vivo*. Repetitive loadings were used to simulate and analyze the geometrical changes of a freshly implanted textile mesh under physiological load conditions during postoperative recovery [17-18]. Moreover, controlled *in vitro* degradation tests were conducted to mimic the biological environment and the action of its components on the implant material. Such studies may help us understand the changes in material properties as a result of the host response, already before the material is truly implanted. To simulate the normal and inflammatory response, neutral pH and acid media were used [19].

In this thesis several new materials were tested, as part of my own thesis and also other PhD students' projects. To demonstrate the relevance of my work we will discuss findings from this thesis as well as related studies I collaborated with, focused on two prototype materials: a non-degradable PP knitted macroporous ultra-lightweight implant (Restorelle, Coloplast), clinically used for POP treatment and UPy-PCL (ureidopyrimidinone-polycaprolactone) electrospun meshes with different fiber diameters (Chapter 3) and later on UPy-polycarbonate (Chapter 4), as well as a non-resorbable electrospun implants based on polyurethane fibers.

Based on uniaxial tensile testing all three UPy-PCL meshes had similar mechanical behavior and were less stiff (4-6 N/cm) than PP mesh (17 N/cm). It is believed that this is a beneficial feature, because it matches better with the properties of the native tissue of the host, which was in a range of 1N/cm-8N/cm according to another study (sheep vaginal tissue) [20]. A similar stress-strain curve was documented for other electrospun materials based on polylactic acid [21]. The tensile properties of the PP mesh were isotropic, whereas an anisotropic behavior was observed in UPy-PCL. Given that the predominant loading state *in vivo* is biaxial, anisotropy might be a useful feature [22].

We then conducted *in vitro* degradation testing and cyclic loading tests on Restorelle (19 g/m²) and UPy-PCL meshes from Chapter 3, but also on three other representative meshes (Chapter 2). One is Ultrapro - a partially absorbable mesh made from poliglecaprone and non-resorbable PP (28 g/m²), which our group has extensively tested [23]. This hybrid material allows the reduction of the amount of PP while maintaining surgical properties by adding a resorbable polymer. Another was Dynamesh Endolap, which is made from non-resorbable polyvinylidenefluoride (36 g/m²). Finally, we also used a heavy-duty PP mesh (Surgipro; 110 g/m²). *In vitro* degradation test on these clinically used meshes were carried out to supplement the already available in literature results [23-24].

Degradation induces significant mechanical property changes in *all* meshes. Electrospun meshes did not lose significantly weight, however implants were thinning progressively without measurable impact on the weight. This can be expected because PCL is degraded by hydrolysis, rather than it undergoes oxidation [25]. We cannot explain very well the change in thickness. Since those meshes were not analyzed under the electron microscope, we can only speculate that mesh became thinner due to fiber collapse. No degradation (weight and thickness loss) were observed in Restorelle mesh,

which contrasts sharply with that of the other meshes (Ultrapro, Dynamesh and Surgipro). For the first one that was logic, given the resorbable nature of one of its constituents (poliglecaprone). For Dynamesh there was a 4% weight loss in acid medium. For Surgipro there was only a reduction in thickness which probably more related to the nature of the multifilament structure.

Despite the different composition and architecture of the tested meshes, all underwent *permanent plastic deformation*. This may induce decreased mesh flexibility over time. Plastic deformation has been tied to the later occurrence of GRCs, for instance by restriction of the abdominal wall mobility [26]. Also, the borders of the Surgipro mesh were curling up during the cyclic loading test, which probably points to poor textile properties.

We then performed cyclic loading tests on meshes after the degradation phase (42 and 90 days). These were tested ex vivo, i.e. for 'dry' characteristics without ingrown tissue. We aimed to find out if our *in vitro* tests could predict mechanical behavior of the implants *in vivo*. Those in vivo tests were done in several animal models. Earlier implantation studies in a lower species were done by a colleague, in which full thickness abdominal wall defects were overplayed in rats (7 and 42 days) and rabbits (30 and 90 days) (Supplementary papers 1, 2). When using UPy-PCL meshes for abdominal wall defects reconstruction in rats and rabbits, the implants failed to induce sufficiently strong abdominal wall replacement. There was an approximately 50% herniation rate, whereas no herniation was observed in animals with PP implants. Samples for biomechanical testing (uniaxial tensile testing) were collected only from the animals without clinical reherniation and without graft related complications, as the latter ones were thought to be non-representative. Suitable UPy-PCL explants for testing were as compliant as native tissue, yet PP explants became stiffer, in both species. A similar material behavior was observed after *in vitro* tests. Restorelle PP mesh was stiffer at both degradation timepoints. Most of UPy-PCL mesh samples failed to withstand the cyclic loading tests after degradation. UPy-PCL meshes with thicker fiber thickness (2.0 μm) could sustain more than 100 cycles, while meshes with thicker fibers (2.3 μm and 2.6 μm) were failing at the first cycle. This may be because the overall density of the fibers was overall lower in the thicker meshes. Similar results were obtained in rabbits: the meshes with a thinner fiber diameter were closer to native tissue compliance. In conclusion a parallel between *in vivo* and *in vitro* results can be drawn; to some extent the *in vitro* tests might predict the mechanical behavior of the implants *in vivo*.

However, the high failure rate made us think about the modifications to electrospun material, i.e. changing the polymer to a slowly degradable, or perhaps to a non-degradable polymer. We used PU (electrospun non-degradable polyurethane) and UPy-PC (polycarbonate modified with Ureido-Pyrimidinone) for vaginal implantation in a sheep model (Chapter 4). In none of the sheep, obvious GRCs were observed. There was no difference in mechanical behavior among the PP, UPy-PCL and PU explants and native tissue repair specimens after vaginal wall reconstruction procedure. Pre-implantation 'dry' materials were subjected to a uniaxial cyclic test in dry and wet conditions. All meshes could sustained cyclic loading test and became less stiff under the wet conditions.

It was not possible to perform the *in vitro* degradation tests for PU and UPy-PC meshes, due to lack of resources at that time in this EU- framework program which was in its last year: we lacked material and time (180 days in a sheep model). It was neither possible to perform cyclic loading tests on the explants, because it was not possible to modify our testing equipment to a horizontal position and a water bath installation to prevent tissue drying.

Studies on pelvic floor tissues

During physiological life span events, such as pregnancy and childbirth, menopause or ageing, the vaginal wall, its support structures and pelvic floor organs undergo histological and mechanical changes. Epidemiologic studies show that a significant portion of women fail to recover completely from vaginal birth or become symptomatic when becoming [27]. Vaginal birth induced trauma appears to play an important role in the origin of POP [28]. To improve our knowledge on normal physiology, the effect of subsequent pregnancies, recovery following vaginal delivery, on the biomechanical and structural properties of the pelvic floor, we undertook several experiments in sheep at different time-point in their life cycle (Chapter 5 and Chapter 6). In that study we used pregnant ewes and sheep one year after their third vaginal delivery. Findings were compared to those in virgin ewes, as a reference. Our group previously described the gross anatomy of the ewe, as compared to the female pelvis [54] as well as gross anatomical changes during their life-span [30]. In this thesis a detailed comparative analysis of the biomechanical properties, histological and morphometric parameters of the proximal (upper third) and distal (distal third) vaginal wall was conducted. This included morphometry of all microscopic vaginal wall layers (squamous epithelium, lamina propria, muscularis and adventitia).

Significant regional differences of both biomechanical and histologic properties were observed. The upper vagina was stiffer than distal vagina, as was earlier demonstrated in post-menopausal sheep [31]. In our animals, a higher total collagen content coincided with a higher ultimate stress (further referred to as “strength”) and Young’s modulus on uniaxial tensiometry. The vaginal tissue of *pregnant* sheep was thinner and more extensible, which coincided with a significantly lower total collagen and higher elastin content. These results are in line with earlier studies in rats, where the stiffness and strength of vaginal tissues decreased during pregnancy [32]. Conversely, virgin sheep had the highest total collagen in their vaginal tissues. This coincided with higher strength. That tissue contained less elastin fibers, which may relate to the higher stiffness [30]. The biomechanical and structural properties of the vaginal tissue after pregnancy did not recover completely (to the virgin level), as earlier shown in rodents [32-33]. These mechanical properties are in concordance with the collagen and elastin levels demonstrated at the microscopic level.

The close anatomical relationship between the vaginal wall on the one hand, and the bladder and rectum on other hand, often contributes to the development of functional problems in these adjacent organs, leading to urinary incontinence, defecatory problems and sexual dysfunction. In line with the findings in the vagina, the external anal sphincter

and the levator ani muscle were more compliant in pregnancy. However, the bladder and rectum of pregnant ewes were stiffer and had a higher total collagen content compared to that of virgin or parous sheep one year after delivery. Mechanical properties of all pelvic organs assessed in parous sheep did not return to levels observed in virgin ewes. Also, the histologic findings were in line with that.

We used image analysis techniques, which allowed a detailed analysis of tissue structure. Without any doubt, biochemical analyses are the "gold standard" techniques used for precise total collagen and elastin content measurements [31]. However, image analysis techniques have earlier been shown to be adequate and can be used as a simple, rapid and low-cost technology for evaluating histological components [34-36]. We used only a Miller´s Elastica staining protocol, and that was enough to demonstrate the target constituents (total collagen, elastin and smooth muscle cells). Elastin, collagen and smooth muscle cells were evaluated on the same histological section. Although one may criticize that, conversely using *different* staining methods would imply the analysis of small samples over a broader region. Given the objectives of the work, any regional differences would introduce a significant bias relative content estimation.

In silico simulations

The characterization of vaginal tissue biomechanics is essential for a wide variety of applications, from the investigation into disease mechanisms, surgical procedures, development of medical devices or tissue engineering solutions such as implants and scaffolds. This research line aims to study the main stages of the mechanical characterization of biological soft tissues, starting from theoretical concepts based on hyperelastic models, followed by the determination of material-dependent parameters. We tried to link the observations on mechanical properties (experimental data) of the vaginal tissues and the material model predictions through histological data (Chapter 7). To obtain the nonlinear mechanical behavior of the vaginal tissue, the HGO (Holzapfel-Gasser-Ogden) model parameters [37] were fitted using a stochastic approach, namely the Simple Genetic Algorithm (SGA) [38]. The presented material model contains three parameters (μ, k_1 and k_2) that must be adjusted to obtain a reliable characterization of the tissue. The parameter μ is related to the matrix content, k_1 and k_2 reflect the fibers contribution. The SGA was able to fit the experimental data successfully. The results demonstrate a high correlation with the constituents' content where the resultant material parameters reflect the physiological state of the tested samples. We presented for the first time, the HM (Histologically-Motivated) coefficient, ξ, which connects the nonlinear mechanical behavior (tensile test) with the tissue morphology (histology). The coefficient ξ, is well correlated with histological data; the ratio increased linearly with increasing collagen content. Regarding the elastin and collagen contributions for tissue's load bearing, there is evidence that collagen fibers may play a dominant role. Collagen is largely responsible for soft tissue tensile strength, while elastin makes the tissue more compliant [39]. Factors such as collagen dispersion and orientation, undulation and orientation, type I:III ratio may contribute to the changes occurring during pregnancy or other events during the life span of women [31]. De Landsheere et al. [40] found less

collagen in pregnant vaginal tissue and no significant difference in collagen type III between pregnant, virgin and parous women. Collagen type I is largely responsible for the tissue's tensile strength [41]. Undoubtedly, elastin fibers play an important role in pelvic floor mechanics, however, alone they are unable to change the mechanical properties of the pelvic floor [28].

We used the HM coefficient, obtained from uniaxial tensile tests and histology, to characterize the multiaxial (ball burst) behavior of the sheep vaginal tissue, without direct mechanical measurements (Chapter 8). To verify the ball burst Finite Element Model (FEM) simulation-results, ball burst test experimental data from another study were used [30]. The predicted force and displacement values of the FEM simulation displayed a good correlation with the experimental testing results. In this way, the use of a HM coefficient offers a promising approach to predict macroscopic material behavior under multiaxial loading conditions. Nonetheless, more robust models should be addressed when dealing with tissues with more challenging microstructures. The HM-coefficient can be used as an 'inverse' (approximation method) to estimate the mechanical properties without direct experimental measurements, through basic histology. The presented methodology may work for other tissues (bladder and rectum) since the postulation of an HM-coefficient turns out to be transversal to the nature of the tissues.

We created a 3-dimentional (3D) geometrical model of the sheep pelvic floor cavity, using magnetic resonance (MR) images (Chapter 9). This model will be used in a future finite element model (FEM) simulations, applying the HM coefficient for tissue properties. Also, this model available in a 3D .pdf file could be used as an auxiliary material for pre-clinical studies [29], veterinary medicine, biomedical engineering, etc. Such virtual models could significantly reduce the number of experimental animals, by conducting *in silico* simulations.

FUTURE PERSPECTIVES

Basic science may improve clinical outcomes of pelvic floor dysfunction (PFD) through advances in different domains. First and foremost, there is much to learn to achieve an understanding of the basic mechanisms of these diseases. There is also a need for improved knowledge about the normal physiology, especially in a subject specific or individualized manner. In terms of the mechanical behavior of implants, there are significant knowledge gaps on the compatibility between tissue and implants that still remain open. Regarding the degradation of implants, our future research will focus on *in vitro* degradation experiments, by considering different additional simulated environments (i.e. oxidation and hydrolysis [25]) to correlate and predict in vivo events. Analysis of electron microscopy images will be used to characterize potential changes in mesh geometry and microstructure.

Another research avenue to be explored, consists of the mechanical testing of implants under cyclic loading. For a more realistic simulation of physiological processes, the cyclic loading tests will need to be performed in a 37°C bath. For future experiments on animal models, the strategy of using electrospun implants relative to textile implants

should be studied in more detail. Other biodegradable polymers, with a slower degradation rate or with bioactive peptides could be used to fasten the process of tissue remodeling.

The findings of this study were used to improve the current understanding of the morphological and mechanical changes in pelvic floor soft tissues due to pregnancy and during recovery after vaginal birth. However, experiments are to be conducted for missing time points such as primiparous or para-2 ewes, or sheep at advanced non-reproductive age. The study of the active biomechanical properties of the vaginal tissue as well as estrogen and other hormone level measurements as well as receptors, are planned as complements to the basic outcome measures used in our studies (histology and biomechanical testing).

We established a link between the morphological and biomechanical properties of pelvic floor soft tissues. If further explored properly, this may provide a new route for clinical diagnostics and for theoretical material modelling. The coefficient Histologically-Motivated (HM) was derived from experimental data and presented for the first time. It allowed a bridge between histological findings and theoretical models such as the HGO model (Holzapfel-Gasser-Ogden model). We used coefficients obtained from uniaxial tensile tests, as inputs for multiaxial loading simulations, with positive outcomes. Among other applications, these findings may play a significant role for conducting *in silico* simulations of biological tissues and structures. The coefficient could be used for advanced simulations of the pelvic floor tissues (i.e. different loading conditions, subsequent simulations of the explants, simulations of 3-D geometrical models of the sheep pelvic floor cavity (Chapter 9). In addition, our HM coefficient might be used as an 'inverse' method to estimate the mechanical behavior of the soft tissues without direct experimental measurements, using basic histology as the starting point. It may also be useful to create a database of histological analysis and biomechanical information combined with life cycle data. With adequate data mining resources this approach may pave the way to produce patient customized or personalized therapies (i.e lifestyle recommendations, surgery planning; prosthetics development, with mechanical properties tailored to individual requirements). The investigation of the biomechanics of the pelvic floor soft tissues through the application of *in silico* models (simulations), might complement or even come to substitute in some cases, subject specific *in vivo* experiments.

References

[1] Manodoro S Endo M, Uvin P, Albersen M, Vláčil J, Engels A, Schmidt B, De Ridder D, Feola A, Deprest J., "Graft-related complications and biaxial tensiometry following experimental vaginal implantation of flat mesh of variable dimensions.," *BJOG,* vol. 120, nº 2, pp. 244-250, 2013.

[2] A. R. Agrawal A., "Mesh migration following repair of inguinal hernia: a case report and review of literature," *Hernia,* vol. 10, pp. 79-82, 2006.

[3] Cobb W.S., Kercher K.W., Heniford B.T., "The argument for lightweight polypropylene mesh in hernia repair," *Surg. Innov,* pp. 63-69, 2005.

[4] Yildirim M, Engin O, Karademir M, Hoser A, Calik B., "Is repair of incisional hernias by polypropylene mesh a safe procedure?," *Med Princ Pract.,* vol. 19, nº 2, pp. 129-32, 2010.

[5] Falagas ME, Kasiakou SK., "Mesh-related infections after hernia repair surgery.," *Clin Microbiol Infect.* , vol. 11, nº 1, pp. 3-8., 2005.

[6] Klinge U, Junge K, Stumpf M, AP AP, Klosterhalfen B., "Functional and morphological evaluation of a low-weight, monofilament polypropylene mesh for hernia repair," *J Biomed Mater Res.,* vol. 63, nº 2, pp. 129-36, 2002.

[7] Bellón JM, Rodríguez M, García-Honduvilla N, Gómez-Gil V, Pascual G, Buján J., "Comparing the behavior of different polypropylene meshes (heavy and lightweight) in an experimental model of ventral hernia repair.," *J Biomed Mater Res B Appl Biomater.,* vol. 89, nº 2, pp. 448-55, 2009.

[8] Cobb WS, Burns JM, Peindl RD, Carbonell AM, Matthews BD, Kercher KW, Heniford BT., "Textile analysis of heavy weight, mid-weight, and light weight polypropylene mesh in a porcine ventral hernia model.," *J Surg Res.,* vol. 136, nº 1, pp. 1-7, 2006.

[9] Barone, W.R., Moalli, P.A., Abramowitch, S.D., "Textile properties of synthetic prolapse mesh in response to uniaxial loading.,," *Am. J. Obstet. Gynecol. (2016) 1–9,* vol. 215, nº 3, pp. 1-9, 2016.

[10] Guillaume O, Teuschl AH, Gruber-Blum S, Fortelny RH, Redl H, Petter-Puchner A., "Emerging Trends in Abdominal Wall Reinforcement: Bringing Bio-Functionality to Meshes.," *Adv Healthc Mater.,* vol. 4, nº 12, pp. 1763-89, 2015.

[11] Merril T. Dayton; Brentley A. Buchele; Siroos S. Shirazi; Lyle B. Hunt, "Use of an Absorbable Mesh to Repair Contaminated Abdominal-Wall Defects," *Arch Surg.* , vol. 121, nº 8, pp. 954-960, 1986.

[12] Indong Jun, Hyung-Seop Han,James R. Edwards,and Hojeong Jeon, "Electrospun Fibrous Scaffolds for Tissue Engineering: Viewpoints on Architecture and Fabrication," *Int J Mol Sci.,* vol. 19, nº 3, p. 745, 2018.

[13] Villarreal-Gómez L.J., Cornejo-Bravo J.M., Vera-Graziano R., Grande D.,, "Electrospinning as a powerful technique for biomedical applications: a critically selected survey," *J Biomater Sci Polym,* vol. 27, pp. 157-176, 2016.

[14] Glindtvad C,Chen M, Vinge Nygaard J, Wogensen L, Forman A, Danielsen CC, Taskin MB, Andersson KE, Axelsen SM, "Electrospun biodegradable microfibers induce new collagen formation in a rat abdominal wall defect model: A possible treatment for pelvic floor repair?," *J Biomed Mater Res B Appl Biomater,* vol. 106, nº 2, pp. 680-688, 2018 .

[15] Braghirolli DI, Steffens D, Pranke P., "Electrospinning for regenerative medicine: a review of the main topics.," *Drug Discov Today.,* vol. 19, nº 6, pp. 743-53, 2014.

[16] Slack M, Ostergard D, Cervigni M, Deprest J., "A standardized description of graft-containing meshes and recommended steps before the introduction of medical devices for prolapse surgery.," *Int Urogynecol J.,* nº 1, pp. s15-26, 2012.

[17] Sindhwani N, Liaquat Z, Urbankova I, Vande Velde G, Feola A, Deprest J., " Immediate postoperative changes in synthetic meshes - In vivo measurements.," *J Mech Behav Biomed Mater,* pp. 228-235, 2015.

[18] Patterson S, Ho YC, Wang WC,, "The Effect of Cyclic Loading on the Mechanical Performance of Surgical Mesh,"," *ICEM,* vol. 6, 2010.

[19] Galgut P, Waite I, Smith R., " Tissue reaction to biodegradable and non-degradable membranes placed subcutaneously in rats, observed longitudinally over a period of 4 weeks," *J. Oral Rehabil,* vol. 23, pp. 17-21, 1996.

[20] Rynkevic R, Martins P, Hympanova L, Almeida H, Fernandes AA, Deprest J, "Biomechanical and morphological properties of the multiparous ovine vagina and effect of subsequent pregnancy," *J Biomech,* vol. 57, pp. 94-102, 2017.

[21] Roman S, Mangir N, Bissoli J, MacNeil S., "Biodegradable scaffolds designed to mimic fascia-like properties for the treatment of pelvic organ prolapse and stress urinary incontinence," *Journal of Biomaterials Applications,* vol. 30, nº 10, pp. 1-11, 2016.

[22] Saberski ER, Orenstein SB, Novitsky YW,, " Anisotropic evaluation of synthetic surgical meshes.," *Hernia,* vol. 15, nº 1, pp. 42-52, 2011.

[23] Manfred M. Maurer, Barbara Röhrnbauer, Andrew Feola, Jan Deprest, and Edoardo Mazza, "Prosthetic Meshes for Repair of Hernia and Pelvic Organ Prolapse: Comparison of Biomechanical Properties," *Materials (Basel). ,* vol. 8, nº 5, p. 2794–2808, 2015.

[24] Pott PP, Schwarz ML, Gundling R, Nowak K, Hohenberger P, Roessner ED, "Mechanical properties of mesh materials used for hernia repair and soft tissue augmentation.," *PLoS One,* vol. 7, nº 10, p. e46978., 2012.

[25] Brugmans MCP, Söntjens SHM, Cox MAJ, Nandakumar A, Bosman AW, Mes T, Janssen HM, Bouten CVC, Baaijens FPT, Driessen-Mol A., "Hydrolytic and oxidative degradation of electrospun supramolecular biomaterials: In vitro degradation pathways," *Acta Biomater,* vol. 27, pp. 21-31, 2015.

[26] Müller M, Klinge U, Conze J, Schumpelick V. , "Abdominal wall compliance after Marlex® mesh implantation for incisional hernia repair,"," *Hernia,* vol. 2, pp. 137-117, 1998.

[27] Patel D.A., Xu X., Thomason A.D., Ransom S.B.,Ivy J.S., DeLancey J.O., ", "Childbirth and pelvic floor dysfunction: an epidemiologic approach to the assessment of prevention opportunities at deivery," *Am J Obstet Gynecol,* vol. 195, pp. 23-28, 2006.

[28] Rahn, D.D., Ruff, M.D., Brown, S.A., Tibbals, H.F., Word, R.A.,, "Biomechanical properties of the vaginal wall: effect of pregnancy, elastic fiber deficiency, and pelvic organ prolapse.," *Am J Obstet Gynecol. ,* vol. 198, pp. 1-6, 2008.

[29] Urbankova I, Vdoviakova K, Rynkevic R, Sindhwani N, Deprest D, Feola A, Herijgers P, Krofta L, Deprest J., "Comparative Anatomy of the Ovine and Female Pelvis," *Gynecol Obstet Invest.;82(6):,* vol. 82, nº 6, pp. 582-591, 2017.

[30] Urbankova I, Callewaert G, Blacher, Deprest D, Hympanova L, Feola , De Landsheere , Deprest J,, " First delivery and ovariectomy affect biomechanical and structural properties of the vagina in the ovine model.," *Int Urogynecol J,* 2018.

[31] Ulrich D, Edwards SL, Su K, White JF, Ramshaw JA, Jenkin G, Deprest J, Rosamilia A, Werkmeister JA, Gargett CE,, "Influence of reproductive status on tissue composition and biomechanical properties of ovine vagina.," *Publ. Lib. Sci,* p. 9, 2014.

[32] Alperin M, Feola A, Duerr R, Moalli P, Abramowitch S, "Pregnancy- and delivery-induced biomechanical changes in rat vagina persist postpartum," *Int Urogynecol J.,* vol. 21, nº 9, pp. 1164-1174, 2010.

[33] Drewes PG, Yanagisawa H, Starcher B, Hornstra I, Csiszar K, Marinis SI, et al., "Pelvic organ prolapse in fibulin-5 knockout mice: pregnancy-induced changes in elastic fiber homeostasis in mouse vagina," *Am J Pathol. American Society for Investigative Pathology,* vol. 170, pp. 578-589, 2007.

[34] Caetano, G.F., Fronza, M., Leite, M.N., Gomes, A., Frade, M.A.,, "Comparison of collagen content in skin wounds evaluated by biochemical assay and by computer-aided histomorphometric analysis.," *Pharm. Biol.,* vol. 14, pp. 1-5, 2016.

[35] De Landsheere L, Blacher S, Munaut C et al, "Changes in elastin density in different locations of the vaginal wall in women with pelvic organ prolapse.," *Int Urogynecol J ,* vol. 25, p. 1673–1681, 2014.

[36] De Landsheere, L., Brieu, M., Blacher, S., Munaut, C., Nusgens, B., Rubod, C., Noel, A., Foidart, J.M., Nisolle, M., Cosson, M.,, "Elastin density: Link between histological and biomechanical properties of vaginal tissue in women with pelvic organ prolapse?," *Int. Urogynecol. ,* vol. 27, pp. 629-635., 2016.

[37] Holzapfel, G.A., Gasser, T.C., Ogden, R.W., " A new constitutive framework for arterial wall mechanics and a comparative study of material models.," *J. Elasticity,* vol. 61, p. 1–48, 2000.

[38] Khalil, A.S., Bouma, B.E., Kaazempur Mofrad, M.R., " A combined FEM/genetic algorithm for vascular soft tissue elasticity estimation.," *Cardiovasc. Eng. ,* vol. 6, p. 93– 102., 2006.

[39] Fung, Y.C., , Biomechanics: Mechanical Properties of Living Tissues., New York: Springer, 1993.

[40] De Landsheere, L., Munaut, C., Nusgens, B., Maillard, C., Rubod, C., Nisolle, M., Cosson, M., Foidart, J.M.,, "Histology of the vaginal wall in women with pelvic organ prolapse: a literature review.," *International Urogynecology Journal,* vol. 24, pp. 2011-2020, 2013.

[41] Jackson, S., James, M,, Abrams, P., , "The effect of oestradiol on vaginal collagen metabolism in postmenopausal women with genuine stress incontinence.," *BJOG.,* vol. 109, pp. 339-44, 2002.

SUPPLEMENTARY MATERIAL 1

PHYSIOLOGIC MUSCULOFASCIAL COMPLIANCE FOLLOWING REINFORCEMENT WITH ELECTROSPUN POLYCAPROLACTONE-UREIDOPYRIMIDINONE MESH IN A RAT MODEL

Lucie Hympanova[1,2,3], Marina Gabriela Monteiro Carvalho Mori da Cunha[1,2], Rita Rynkevic[1,2,4], Manuel Zündel[5], Monica Ramos Gallego[6], Jakob Vange[6], Geertje Callewaert[1,2,7], Iva Urbankova[1,2,3], Frank Van der Aa[2,8], Edoardo Mazza[5,9], Jan Deprest[1,2,7]

[1] Centre for Surgical Technologies, KU Leuven, Leuven, Belgium
[2] Department of Development and Regeneration, KU Leuven, Leuven, Belgium
[3] Institute for the Care of Mother and Child, Charles University, Prague, Czech Republic
[4] INEGI, Faculdade de Engenharia da Universidade do Porto, Porto, Portugal
[5] Institute of Mechanical Systems, ETH Zurich, Zurich, Switzerland
[6] Coloplast A/S, Global R&D, Biomaterials, Holtedam, Humlebæk, Denmark
[7] Pelvic Floor Unit, University Hospitals KU Leuven, Leuven, Belgium
[8] Department of Urology, University Hospitals Leuven, Leuven, Belgium
[9] EMPA, Swiss Federal Laboratories for Materials Science and Technology, Dübendorf, Switzerland

Key words: pelvic organ prolapse, biomechanics, electrospun mesh, biocompatibility, hernia

Journal of the Mechanical Behavior of Biomedical Materials 74 (2017) 349–357

Contents lists available at ScienceDirect

Journal of the Mechanical Behavior of Biomedical Materials

journal homepage: www.elsevier.com/locate/jmbbm

Physiologic musculofascial compliance following reinforcement with electrospun polycaprolactone-ureidopyrimidinone mesh in a rat model

Lucie Hympanova[a,b,c], Marina Gabriela Monteiro Carvalho Mori da Cunha[a,b], Rita Rynkevic[a,b,d], Manuel Zündel[e], Monica Ramos Gallego[f], Jakob Vange[f], Geertje Callewaert[a,b,g], Iva Urbankova[a,b,c], Frank Van der Aa[b,h], Edoardo Mazza[e,i], Jan Deprest[a,b,g,*]

Published in Journal of Mechanical Behavior of Biomedical Materials (2017)

ABSTRACT

Purpose: Electrospun meshes may be considered as substitutes to textile polypropylene implants. We compared the host response and biomechanical properties of the rat abdominal wall following reinforcement with either polycaprolactone (PCL) modified with ureidopyrimidinone-motifs (UPy) or polypropylene mesh.

Methods: First we measured the response to cyclic uniaxial load within the physiological range both dry (room temperature) and wet (body temperature). 36 rats underwent primary repair of a full thickness abdominal wall defect with a polypropylene suture (native tissue repair) or reinforced with either UPy-PCL or ultra-light weight polypropylene mesh (n=12/group). Sacrifice was at 7 and 42 days. Outcomes were compliance of explants, mesh dimensions, graft related complications and semiquantitative assessment of inflammatory cell (sub) types, neovascularization and remodeling.

Results: Dry UPy-PCL implants are less stiff than polypropylene; both are more compliant in wet conditions. Polypropylene loses stiffness on cyclic loading. Both implant types were well incorporated without clinically obvious degradation or herniation. Exposure rates were similar (n=2/12) as well as mesh contraction. There was no reinforcement at low loads, while, at higher tension, polypropylene explants were much stiffer than UPy-PCL. The latter was initially weaker yet by 42 days it had a compliance similar to native abdominal wall. There were eventually more foreign body giant cells around UPy-PCL fibers yet the amount of M1 subtype macrophages was higher than in polypropylene explants. There were less neovascularization and collagen deposition.

Conclusion: Abdominal wall reconstruction with electrospun UPy-PCL mesh does not compromise physiologic tissue biomechanical properties yet provokes a vivid inflammatory reaction.

1. Introduction

Symptomatic pelvic organ prolapse decreases the quality of life of 11.4% women over 45 years (Slieker-ten Hove et al. 2009). Native tissue repair techniques have been considered suboptimal because of quoted reoperation rates of 30% (Olsen et al. 1997). In order to improve durability of repairs, synthetic meshes were introduced identical to those used in hernia repair. Though anatomical outcomes of mesh-augmented vaginal prolapse repairs are better, its introduction has coincided with the occurrence of more local complications and reinterventions (Maher et al. 2016). Consequently, current techniques in pelvic reconstruction surgery are being re-examined in an effort to find a mechanism to help improve long-term cure rates without increasing the risk of complications (SCENIHR 2015). Mesh placement is still recommended in specific cases. Nevertheless, the risk of graft related complications and their consequences should be assessed and compared with expected benefits.

Polypropylene (PP) is the most widely used polymer for weaving and knitting of durable implants. At present it is the main recommended polymer for manufacturing vaginal implants (SCENIHR 2015). Unfortunately, post-implantation complications such as pain, exposure or infection occur in up to 10% of operated women (Abed et al. 2011). These adverse effects are tied to a number of material aspects, such as preimplantation biomechanical mesh properties, its durable nature and subsequent host response, causing a chronic foreign body reaction and inappropriate compliance (Klinge et al. 1999). In an effort to reduce complications, lightweight macroporous mesh, which experimentally induce a more optimal host response, is currently being used (Kelly et al. 2016). This has not prevented complications from occurring. Given the severity of graft related complications, and difficulty to treat them, the search for better materials has been advocated (SCENIHR 2015; Mangera et al. 2012). An alternative to durable materials is to use non-textile scaffolds with a physiologic matrix structure as used in tissue engineering. Ideally, these would be synthetic, resorbable and should have the potential of being made bio-active. Synthetic materials are easier to obtain in larger quantities, cheaper and do not carry the risk of disease transmission compared to xeno- or allografts. Resorbable implants have the advantage of being eventually completely degraded, hence not maintaining a chronic inflammatory foreign body reaction, and all its related complications. Conversely, following degradation, the material is ideally replaced by neo-tissue that has functional properties as closely as possible to the original tissues without associated local complications (Roman et al. 2016). One strategy is to create implants by a process called electrospinning. This method uses electrostatic forces to draw charge threads of polymer solution to a collector (Morton 1902). These implants have a large surface, fiber and pore size of the extracellular matrix, which should facilitate cell adherence and their ingrowth (Cipitria et al. 2011). One innovative absorbable, supramolecular material that meets these criteria may be obtained from polycaprolactone modified with ureidopyrimidinone motifs (UPy-PCL). This polymer has received considerable attention as a suitable scaffold due to its elasticity, flexibility, and customizable degradation properties (Felfel et al. 2016). UPy-functionalized polymers have the ability to bind cell-adhesive peptides as one of tissue regeneration approaches

(Mollet et al. 2014). We have embarked into manufacturing such prototype implants. The primary objective of this study was to investigate the biomechanical properties of a primary repaired full-thickness abdominal wall defect reinforced with a novel hybrid UPy-PCL mesh types using a well-established rat model. Secondary objectives were to document biocompatibility and the host response to UPy-PCL as compared to polypropylene. We also aimed to compare these post-implantation mesh characteristics to those of the implant prior to implantation.

2. Materials and methods

2.1 Implants

Implants were fabricated either from polypropylene (PP, n = 12) or ureidopyrimidinone-polycaprolactone (UPy-PCL, n = 12), the UPy-PCL polymer was obtained from SupraPolix, Eindhoven, The Netherlands. The polypropylene implant used was a commercially available knitted Restorelle® (Coloplast, Humlebaek, Denmark), (Fig. 1B). Investigated UPy-PCL scaffold (Coloplast) was made by electro-spinning (Fig. 1A, see paragraph 2.2. for more details). Constituting fibers of UPy-PCL mesh are organized as a network-like structure with random in-plane orientation and fiber interspaces in the order of a few microns, whereas PP is composed of knitted filaments with a macroporous structure of 2.1 mm diameter and 230 μm interstitial pores (Ulrich et al., 2016).

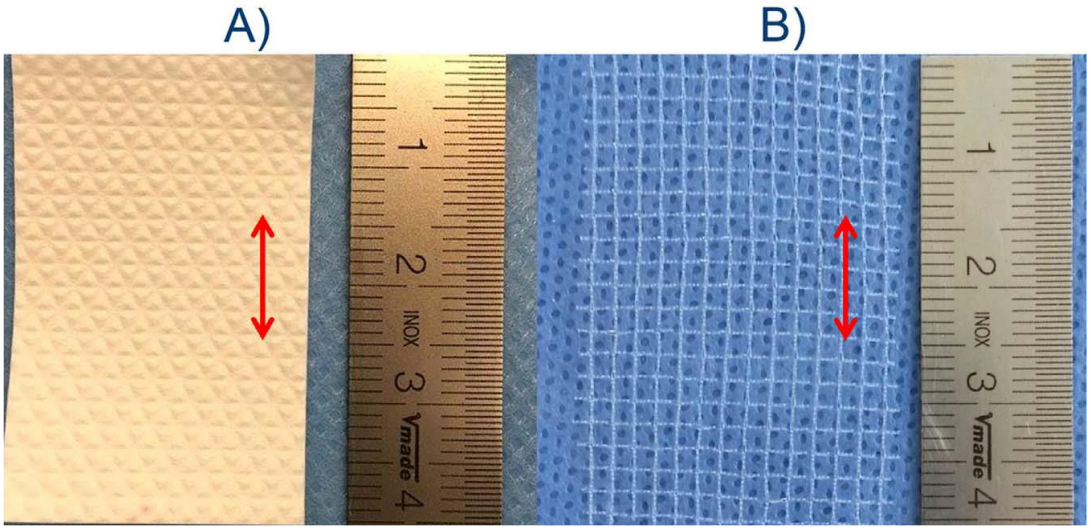

Fig. 1 Implanted materials: A: UPy-PCL electrospun and B: Restorelle®. Red arrows indicate the direction of loading for the ex vivo mechanical characterization of the implants under dry and wet conditions. (For interpretation of the references to colour in this figure legend, the reader is referred to the web version of this article.)

Investigated implants were from the same production lot, sterilized by electron beam irradiation (25 kGy) and packaged with a molecular sieve desiccant in an atmosphere of nitrogen. Main characteristics of polypropylene and UPy-PCL mesh are summarized in Table 1.

Table1. Implants characteristics.

	Polypropylene (Restorelle®)	**UPy-PCL**
Polymers	Polypropylene	Polycaprolactone modified with ureidopyrimidinone
Production method	Knitted monofilament	Electrospun
Durability	Non absorbable	Absorbable
Density (g/m2)	19.0	38.5–47.2
Fiber size (µm)	80	2
Porosity (pore size)	Macroporous (1.6–2.0 mm)	Microporous (6–16 µm)
Thickness (µm)	300	250–400

2.2 Electrospinning

Our electrospinning method employed a coaxial nozzle with the inner needle (17G) used to pump the polymer and outer (19G) for pure solvent. The purpose is to prevent clogging on the tip. The mesh was spun to an area density of 35–50 g/m2. After the spinning process, meshes were stored in a vacuum oven overnight at 45 °C/<1 mBar. Fiber size distribution was measured with scanning electron microscope. The mesh was cut to size and weighed to determine the exact area density. Fabrication parameters are in details depicted in Table 2.

Table2. UPy-PCL electrospun mesh fabrication process details. Geometry dimensions represent diameter and length.

Polymer solution properties		**Electrospinning process parameters**							
Polymer concentration	Solvent	Voltage (kV)		Flow rate (mL h^{-1})		Distance (cm)	Needle inner ø (gauge)	Target	
		Noozle	Drum	Polymer solution	Solvent			Geometry dimensions (cm)	Rotating speed (s^{-1})
13%wt UPy-PCL polymer	Chloroform metanol acetonitrile acetic acid	− 18.2	+ 5	5	0.5	22	19	25 × 50	3.0–3.1

2.3 Mechanical characterization of implant materials under dry and wet conditions (ex vivo)

Implants with a 4:1 aspect ratio were subjected to uniaxial tensile load in dry and wet conditions. Fig. 1 indicates the loading direction applied in the tests. The implant materials were characterized according to a standardized protocol that we previously used for textile meshes (Supplement 1) (Maurer et al. 2014).

2.4 Animals

Thirty six adult 12 weeks-old female Sprague Dawley rats (250–300 g) were randomly divided in three groups (n = 12/per group) based on power calculation: (1) native tissue primary repair, (2) reinforcement repair with UPy-PCL and (3) polypropylene. Animals were housed per four in cages with unrestricted access to the food, water and chew. They were treated in accordance with current national guidelines on animal welfare. The experimental protocol was approved by the Ethics Commission on Animal Experimentation of the Faculty of Medicine, KU Leuven.

2.5 Surgical procedure and study design

The anesthesia and surgical protocol were reported in detail in previous study (Supplement 2) (Ozog et al., 2009). Postoperatively, animals were allowed to move, eat and drink ad libitum. They were clinically examined daily the first week thereafter twice a week and all complications were noted. Harvesting was at 7 and 42 days (n =6 each group and time point).

2.6 Obduction

Under isoflurane anesthesia, rats were euthanized by intravenous administration of 0.2 mL of a mixture of embutramide 200 mg, mebezonium 50 mg and tetracaine hydrochloride 5 mg (T61; MSD Animal health BVBA; Brussels; Belgium) and underwent obduction. During gross anatomical examination we noted any herniation, fluid collections, infection or implant exposures (loss of epithelial integrity). Further the length and the width within the borders marked by the polypropylene sutures were measured and the contraction was calculated (explant/implant area* 100%). The former surgical area was resected 'en bloc' including 1 cm of the neighboring tissue. The presence of adhesions was scored using a scale of 0–3 (Toosie et al., 2000). The explant was cut into 10 mm wide strips, perpendicular to the long axis of the animal. The middle strip (10 × 30 mm) was kept in 0.9%NaCl saline solution at room temperature until biomechanically tested (< 2 h after sacrifice). Another specimen (10 × 10 mm) was fixed in 10% formalin solution for further histology (Supplement 3) to determine the host response. An additional strip (10 × 30 mm) from the contralateral side of the abdominal wall at exactly same location of the repair at the other side was harvested to be used as an internal control for tensiometry.

2.7 Uniaxial tensile load testing protocol of explants

Explants biomechanical testing was performed following previously used protocol (Supplement 3) (Ozog et al., 2011) Similarly to the ex vivo evaluation, the explants were characterized in terms of membrane stress and membrane stiffness. The latter was computed as tangent stiffness and evaluated for all repaired explants and their contralateral muscle at different level of elongations, up to 30% strain. To analyse the stiffening caused by the implanted reinforcement we determined the stiffness increase for each rat as the difference between the repaired and the contralateral control muscle explants.

2.8 Morphological study

Briefly histomorphometry and immunohistochemistry were done to obtain counts of myofibroblast, polymorphonuclear, endothelial or foreign body giant cells (FBGC), macrophages and their M1 and M2 subtypes (See Supplementary information 4). All morphometric analyses were performed by two investigators blinded to the treatment using ImageJ software (Schneider et al., 2012). Ten non-overlapping fields at the interface of the explant and the host tissue were assessed at 200× magnification. For the quantification of FBGC, cells were manually quantified using cell counter plugin. Furthermore, we measured collagen deposition on Masson's stain. The digital color

images were segmented (color deconvolution plugin) and further binarized in order to measure the percentage of the area stained in blue (Masson's Trichrome) or brown (immunostainings).

2.9 Statistics

Before the study groups were compared, each continuous variable was tested using the Kolmogorov-Smirnov test to verify the normality of distribution of continuous variables. One-way ANOVA followed by Tukey's post hoc test were used for data normally distributed. Kruskal-Wallis followed by Dunn's posttest were used for variables evaluated as not normally distributed. Data are reported as mean±SEM. Statistical significance level was defined as $p<0.05$. Statistical analysis was performed with Graphpad Prism 5.0 (GraphPad Software, Inc; La Jolla, USA).

3. Results

3.1 Mechanical properties of implant materials and explants

The cyclic response to uniaxial load (reported in Fig. 2A) is qualitatively similar for both materials, showing a strong inelastic deformation in the first cycle, followed by a fast stabilization. After ten cycles, both materials feature an approximately linear response within the measured strain range. Quantitatively however, there is a difference between the two materials, as displayed in Fig. 2B. In both dry and wet conditions, the stiffness of polypropylene mesh is higher than UPy-PCL, by a factor of 2.5–3.5 for their mean values. Experiments performed in wet conditions at 37 °C highlighted a loss of stiffness in the range of 30% for both materials when compared to the stiffness measured in dry environment. Interestingly, the stiffness of UPy-PCL implants does not display significant cyclic softening, contrary to the polypropylene implants which lose 25–30% of their stiffness within ten cycles.

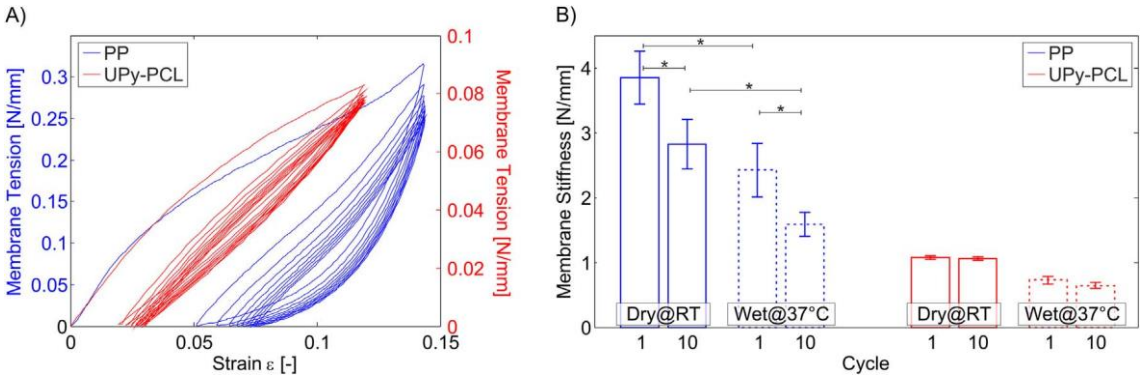

Fig. 2 Typical behavior of polypropylene (blue) and UPy-PCL (red) samples when subjected to a cyclic uniaxial tensile test. Note the different scales for the two materials. B) Tangent membrane stiffness of polypropylene (blue) and UPy-PCL (red) evaluated at the beginning of the loading curve in the first and the 10th load cycle for tests in dry conditions at room temperature and in distilled water at 37 °C. Reported is mean and standard deviation (N = 5 for polypropylene and N = 4 for UPy-PCL).

The mechanical response to uniaxial load of all explants after 7 and 42 days shows the J shape curve typical for biological tissues, resulting in a very compliant behavior in the unloaded configuration (zero strain) and progressively higher stiffness at larger strain. The stiffness of polypropylene reinforced explants at 25% strain region is significantly higher than all other explants at 7 days and remains at a similar level at 42 days (Figs. 3A and B). Conversely, the comparison of the native repair and the UPy-PCL reinforced samples reveals a temporal evolution of their mechanical behavior, resulting in a stiffness increase from 7 to 42 days. As a consequence, while at 7 days the UPy-PCL explants are more compliant than non-traumatized muscle, at 42 days they display a similar compliance as this control tissue. Interestingly, at 42 days the stiffness of the native repair muscle is comparable to the polypropylene reinforced explants.

The analysis of the stiffness difference between repaired and nontraumatized muscle of each rat is reported in Figs. 3C and D. The curves show that no reinforcement is present at low load for all explants, while the temporal evolution of the stiffening effect at larger strains depends on the reinforcement type. Polypropylene reinforces at a level comparable to its ex vivo stiffness at each time point. At 42 days, UPy-PCL explants also shows a stiffness increase comparable to the materials ex vivo stiffness, while their response at 7 days is much softer than the nontraumatized muscle tissue. Interestingly, the stiffness increase featured by the native repaired muscles is always larger than for the UPy-PCL reinforced tissue.

The measurement of the explant thickness (Supplementary figure 1) indicate that polypropylene reinforced explants at 42 days are significantly thinner than at 7 days and are slightly thinner than the contralateral muscles, while the UPy-PCL reinforced samples are on average 0.6 mm thicker.

3.2 Clinical findings and obduction

Three rats died one day after the surgery with initial wound dehiscence, eventually implant exposure and bowel perforation. That was most probably by mutilation. Survivors with polypropylene and UPy- PCL-implants had comparable exposure rates (16.6%; 2/12). We observed local fluid collection in three UPy-PCL rats (25%; 3/12) which persisted up to 7 days (Supplementary figure 2). This did not seem to irritate the animal; the area did not look inflamed neither any other local complication co-occurred. On percutaneous puncture done in one rat to elucidate this, it was serosanguinous fluid. By the later obduction in those animals nothing abnormal could be found. Clinical and necropsy details are displayed in Table 3. Both implant types were well incorporated with recognizable texture at 7 or 42 days (Supplementary figure 3). There were no herniation or obvious infection, neither was there any difference in mesh contraction at any time point. Adhesion scores were comparable.

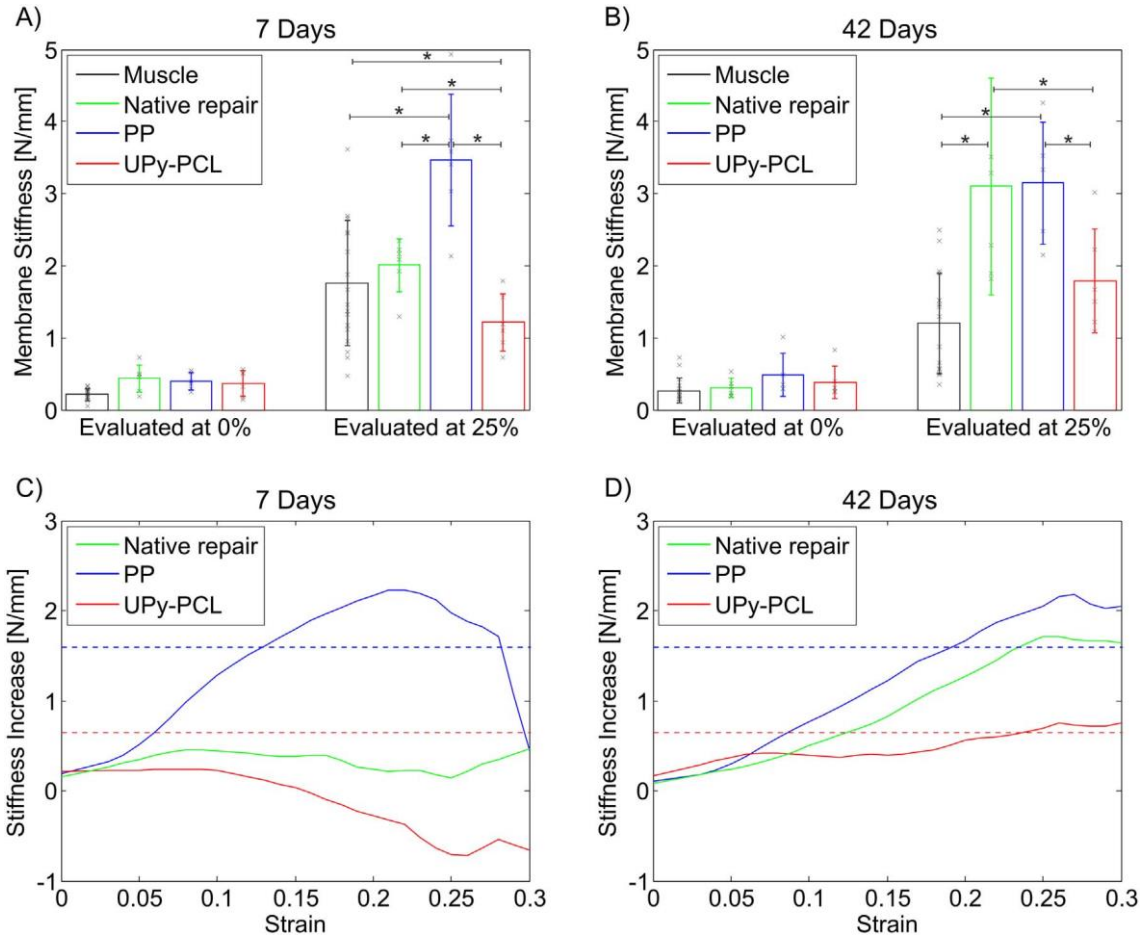

Fig. 3 Tangent membrane stiffness at 7 (A) and 42 days (B) of the explants evaluated at 0% and 25% strain. Reported is mean and standard deviation (N = 11 for muscle, N = 6 for native repair, N=5 for polypropylene and N=6 for UPy-PCL). Stiffness difference between the reinforced muscle and contralateral control muscle, evaluated independently for each rat for strains between 0% and 30% after C) 7 and D) 42 days. Results are reported as the mean line for polypropylene (blue), UPy-PCL (red) reinforced muscles and native repair (green). The horizontal dotted line represents the uniaxial stiffness measured after 10 cycles in wet conditions ex vivo (blue, polypropylene=1.59 N/mm, red, UPy-PCL=0.64 N/mm). Displayed data are the mean of the different rat groups (N = 6 for native repair, N = 5 for polypropylene, N=6 for UPy-PCL).

Table3. Clinical and necropsy findings in details.

Time point			**7 days**			**42 days**		
Group			Native repair	Polypropylene	UPy-PCL	Native repair	Polypropylene	UPy-PCL
Clinic	Fluid collection		0% (0/6)	0% (0/6)	33.3% (2/6)	0% (0/6)	0% (0/6)	16.7% (1/6)
	Exposure							
Obduction	Contraction (%)		0% (0/6)	33.3% (2/6)	16.7% (1/6)	0% (0/6)	0% (0/6)	16.7% (1/6)
			-	26.5± 12.9	26.6±6.4	-	24.7±12.25	27.4±8.31
	Adhesions	0	100%(6/6)	50% (3/6)	50% (3/6)	66.6% (4/6)	66.6% (4/6)	100% (6/6)
		1	0% (0/6)	33.3% (2/6)	33.3% (2/6)	33.3% (2/6)	33.3% (2/6)	0% (0/6)
		2		16.7% (1/6)	0% (0/6)	0% (0/6)	0% (0/6)	
		3		0% (0/6)	16.7% (1/6)	0% (0/6)	0% (0/6)	

3.3 Histology and immunohistochemistry

Microscopy readouts are displayed in Tables 4, 5 and Fig. 4. Initially there was polymorphonuclear infiltration in both mesh explants. By 42 days there were still polymorphonuclears, yet with lower counts in the UPy-PCL implants. Overall counts of macrophages did not differ between the two implanted groups. We further characterized this population. At 7 days, the polypropylene implanted animals had more M2a macrophages than the UPy-PCL animals. M1 cells were more abundant in the UPy-PCL rats at 42 days. There was no difference in M2c response.

Also, there were more FBGC in the UPy-PCL group than in the polypropylene animals. Connective tissue quantification using Masson's Trichrome showed a less intense in UPy-PCL implanted rats than the polypropylene, yet also less than in the primarily sutured animals without an implant ($p<0.001$). This was actually the case at both time points. There were more CD34 positive cells (an endothelial marker) in the polypropylene animals, yet less in the UPy-PCL rats. Native repair induced even less endothelial cells.

Table4. Badylak score of H & E stained histological slides, a,b,c are $p<0.05$ (Badylak et al., 2002).

Time point	**7 days**			**42 days**		
Group	Native repair	Polypropylene	UPy-PCL	Native repair	Polypropylene	UPy-PCL
FBGC	0.00±0.00a,b	0.60±0.12a,c	1.32±0.26b,c	0.00±0.00a	0.43±0.10a,b	2.25±0.25b
Polymorphonuclear	0.18±0.09a,b	2.47±0.23a	2.88±0.10b	0.00±0.00c	1.43±0.14c	0.60±0.08
Vascularity	0.78±0.26	1.07±0.24	1.08±0.10	0.36±0.16a	1.83±0.28a,b	0.75±0.20b

Table5. Summary of histological results. FBGC were counted as mean number of cells, other results as mean % area stained±SEM, a,b,c,d indicate significant differences ($p<0.05$) between the groups indicated by the respective letter.

Time point	**7 days**			**42 days**		
Group	Native repair	Polypropylene	UPy-PCL	Native repair	Polypropylene	UPy-PCL
Collagen amount	7.14±1.76	8.46±1.13	6.78±2.19	7.67±2.10a	21.95±5.27a,b	2.22±0.23b
α-SMA	0.04±0.02 a	8.11±1.12 a	3.34±0.73	0.01±0.01	0.44±0.42	0.08 ±0.03
FBGC	0.00±0.00	4.00±0.68 a	9.10±1.33 a	0.00±0.00	4.22±0.64 b	25.45±1.26 b
Total macrophages	0.03±0.02 a,b	3.70 ±1.43 a	2.91±1.07 b	0.01±0.08c,d	3.35±1.17c	4.25±1.25 d
Macrophage 1	5.40±3.85	32.78±14.4	25.77±8.13	0.56±0.56a	17.62±7.40	82.81±32.04a
Macrophage 2a	1.31±0.26 a	7.39±0.82 a,b	3.61±0.87 b	1.33±0.44c	4.96±0.68c	5.88±1.78
Macrophage 2c	2.30±0.72	5.68±2.52	3.00±0.49	1.10±0.42	2.62±0.81	0.62±0.26
Vascularity	2.23±0.50 a,b	7.00±1.39 a	6.32±0.39 b	2.57±0.54c	18.14±2.07c,d	6.15±1.20 d

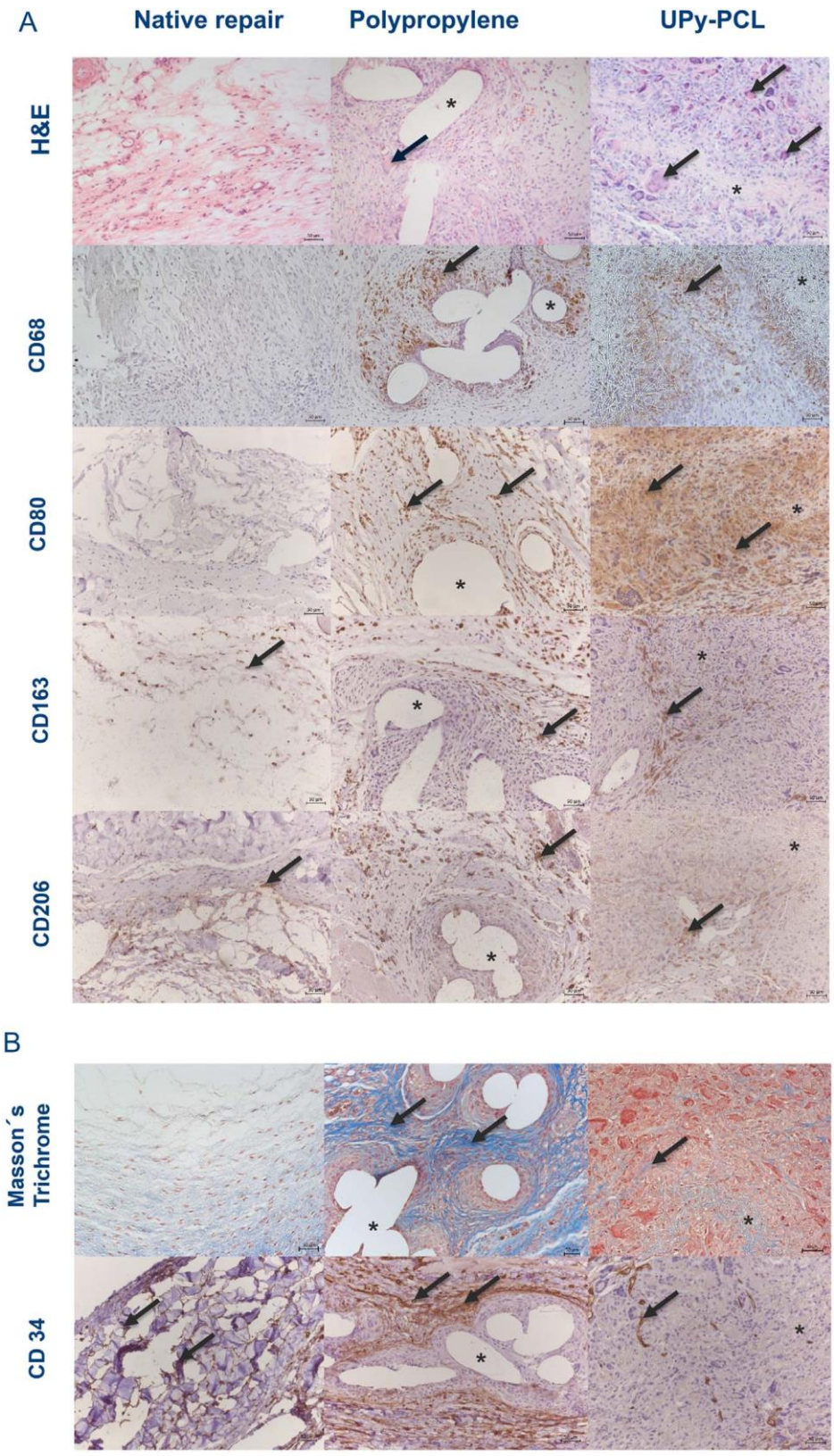

Fig. 4 Representative figures of histology and immunohistochemistry at 42 days, magnification 200×. A: Inflammation panel shows in UPy-PCL: higher counts of FBGC, comparable expression of CD68 as a marker for macrophages, high M1 stained by CD80, no difference in M2c (CD163), lower counts of M2a (CD206). B: Less connective tissues stained with blue in Masson's Trichrome in UPy-PCL, lower CD34 positivity, which visualize endothelial cell in vessels.

4. Discussion

There are many worries about how mesh reinforcement can influence the compliance, certainly within the comfort zone. We demonstrated that reinforcement of a suture-closed longitudinal defect with a novel UPy-PCL does not compromise the abdominal wall compliance, for deformations of 25% or less. This is not the case for a reconstruction with an ultra-light weight polypropylene. Also, we have shown that one can rationalize explant behavior based on preimplantation tensiometry in conditions simulating the in vivo situation.

Electrospun implants are new in the field of reconstructive surgery. It is important to remark that this manufacturing process allows generating fibrous materials that are very different from a textile mesh, such as Restorelle. In fact, the latter is made of thin knitted millimetre sized filaments with large pores while electrospun scaffolds are characterized by topological features (fiber diameters and pores) with sizes in the micrometer range. In this regard, the two implants differ not only in their mechanical properties, but also in the type of niche they offer to the cells when implanted. As we did for textile implants, we started by characterizing the materials using a standardized panel of tests (Maurer et al., 2014). Instead of the nonlinear, J-shaped tension-strain curve typical for biological tissues, both implant materials have a fairly linear loading response. Polypropylene shows larger inelastic deformations during the first loading cycle and more softening in wet conditions at body temperature, which should be representative for the in vivo situation.

UPy-PCL is clearly softer than polypropylene, exhibiting a stiffness which is comparable to that of unrepaired muscle tissue. It should be noted that the results of the mechanical characterization of implants and explants depends on the material orientation with respect to the loading axis. While the direction dependence of UPy-PCL scaffolds is not strong, due to their random fiber orientation, the polypropylene meshes exhibit strong anisotropy making this implant significantly more sensitive to misalignments in the implanted state. Fig. 3D demonstrates what the contribution of the implants is to the structural stiffness of the reconstructed area. In fact, the biomechanical response of the reinforced tissue can be understood as the combined mechanical contribution of the biological component (healing musclefascial tissue) and the reinforcing material acting in parallel (Röhrnbauer et al., 2013). The observation that there is at low strain no implant associated stiffness (Fig. 3D) demonstrates that the implant, at low strain, does nearly not contribute to the stiffness of the explant. At increasing strain, stiffness increases stabilize around 20–25% strain at the level of stiffness initially measured ex vivo. This was the case for both implants. The progressive engagement and support provided by the reinforcement is probably due to initial smaller mesh dimensions, which we interpret as a state of curling or undulation due to mesh contraction. In the unloaded situation the implants do not seem to contribute in a measurable way to the tissue stiffness. Yet with progressive stretching of the explant, the implant “uncurls” and increasingly contributes to the stiffness up to the level that the explant is extended past the contraction strain, from what point it starts to contribute with its entire stiffness. The agreement between the corresponding reinforcement levels of animal explants and the stiffness of implants measured ex vivo (Fig. 3D) suggests that the ex vivo characterization might be indicative

of the final reinforcement. This result is surprising in view of the complex mechanobiological processes involved in tissue remodeling leading to the measured mechanical response of the integrated implant. The results of the present study cannot be used to generalize the validity of this correlation for different implant types and configurations. To this end, a systematic investigation with comparable experiments is required.

By comparing the biomechanical properties of explants to a sutured native tissue repair we display what the effect of surgical reconstruction is on the healing process over time. Whereas we expected that after 42 days, the reinforcement of a sutured repair with UPy-PCL is more compliant than polypropylene, it was not expected that it would be more compliant than the sutured repair per se. However, this may not be entirely surprising. When the same analysis is done at 7 days, the native tissue repair is much more compliant and within the range of normal muscle. Over time there is apparently stiffening, which coincided with a trend for more collagen deposition, yet that did not reach significance.

The latter obviously may be due to the way the semi-quantitative score is made, using randomly selected locations, which may miss the scarred area within the explant. Also, collagen is not the only factor contributing to tissue stiffness. Anyway, the above demonstrates that in this model, the biomechanical properties, and thus tissue remodeling, are influenced by both, primary suture and implant material. The evolution of tissue compliance between 7 and 42 days further indicates that polypropylene can be considered as a relatively stiff and immediate effective reinforcement, which inhibits large strain of the underlying tissue at all time points. On the other hand, the reinforcement and support offered by the UPy-PCL mesh needs more time to fully develop but finally results in a collective stiffness which eventually is close to the physiological values, i.e. of unrepaired muscle. The stiffening effect in polypropylene explants was larger than the ex vivo stiffness of the dry polypropylene implant. This might indicate that the implant induces an increased density of load bearing components in the scarring tissue. An equal mechanism is suggested to explain the stiffness measured in the native tissue repair explants, where polypropylene sutures were used. One of the other, determinants of the biomechanical properties of explants is the host inflammatory response. Both materials provoke a comparable initial infiltration with predominantly polymorphonuclear cells, representing the acute phase of a foreign body reaction (Anderson, 2001). Later in the experiment, there was no difference in the number of macrophages as counted by the number of CD68 staining cells. CD68 is a membranous marker not expressed by FBGC. We did also stain for M2a (CD206) and M2c (CD163) markers, cells usually considered to play an anti-inflammatory role (Mantovani et al., 2004). Conversely UPy-PCL were massively surrounded by FBGC, as morphologically recognizable on hematoxylin and eosin stain. In an effort to differentiate the macrophages, we did immunohistochemistry yet those FBGC also expressed the CD80 epitope, which is typically expressed by M1 macrophages (Badylak et al., 2008), yet which can occasionally also has been described in FBGC (Palmer et al., 2014). Therefore CD80 staining did not allow us to estimate the magnitude of the M1 response. Given the abundancy of FBGC, immunohistochemistry staining does not permit to truly quantitate the number of mononuclear M1 cells. These

were higher at implanted groups compare to native repair. We do not want to over interpret these semi-quantative counts. To investigate this response it would be more interesting to document the cytokine profile produced by the inflammatory cells, using PCR. However, it might also be that the intense inflammation and the abundance of FBGC persisting at 42 days is part of the normal degradation process of the UPy-PCL implant (Cipitria et al., 2011; Felfel et al., 2016). Later on, it may be that this response will transit to a more M2 dominated infiltrate (Wynn and Barron, 2010). Polarization from M1 to M2 response is variable in period of days to weeks (Kim et al., 2016). PCL based implants are typically long lasting materials. In previous studies PCL persisted at least six months (Lam et al., 2008). In that respect we do not truly worry about the macrophage response observation, and would speculate this will go on until fully degraded. This should not be compared to the chronic fibrotic reaction that typically persists around non-resorbable polypropylene. Modification of the weight and structure of textile polypropylene has been earlier shown to modify the macrophage response, with proportionally lower M1 counts for lighter and more stable materials (Brown et al., 2015). Macrophages have an unique response to different biomaterials and we should keep that in focus (Wolf et al., 2015).

We acknowledge a number of limitations to this study. Given the implant is slowly degradable, additional time points hence longer term studies would be needed to examine the ultimate performance of the scaffold. Also, we could have expanded the outcome measures by molecular read outs. Further, we have used abdominal wall reconstruction, while our ultimate goal is vaginal implantation. The vagina is definitely a different surgical environment compared to abdominal wall, with its distinctive healing processes and its different biomechanical properties (Abramov et al. 2007). The effect of this difference will be further explored in more appropriate animal models, such as the sheep (Feola et al. 2015). We also saw a serosanguinous fluid collection in 25% of the rats early postoperatively, which we cannot truly explain. They did not persist, neither was they associated with local macroscopic signs of inflammation. Fluid collections also have been described with other matrix like implants, such as porcine small intestinal submucosa-derived matrix (Ozog et al., 2009). This local complication did not lead to exposures, which were anyway similar in both implanted groups. The latter coincided with apparent wound irritation and auto-mutilation.

Our study had also some specific strengths. First, we used two control groups, i.e. the contralateral muscle used for normalization, and the primary native tissue repair as a reference reconstruction method. Second, we first conducted detailed ex vivo characterization of the novel category of electrospun implants. We also compared to what is currently considered as one of the more sophisticated ultralight polypropylene meshes (Brown et al., 2015).

5. Conclusions

In the rat model, reinforcing a primary musculofascial repair by a novel UPy-PCL electrospun mesh does not compromise physiologic compliance. However, the novel implant material required longer time to provide adequate reinforcement. Forty-two days postoperatively, the material is not yet visibly degraded and the persisting inflammatory

process coincides with a vigorous M1-dominated local host response and many FBGC. Furthermore, although the cellular response to the used ultralight-weight polypropylene is rather M2-dominated, the associated biomechanical properties remain far from the physiological compliance of native tissue.

Funding

This work was supported by a grant of the European Commission in the FP7-framework (BiP-UPy; NMP3-LA-2012–310389) and Swiss National Science Foundation under Grant SNF 155918.

Ethical approval

KU Leuven P057/2014

Acknowledgement

We would like to thank to Rosita Kinnart and Ivan Laermans (Centre for surgical technologies, KU Leuven, Leuven, Belgium), Catherine Luyten and Petra Stevens (Department of Development and regeneration, KU Leuven) for the technical support during the experiment. We thank to Leen Mortier (University hospital Leuven) for help with manuscript management. We would like to thank also Tristan Mes and Anton Bosman (SupraPolix BV, Eindhoven, The Netherlands) for kindly providing the PCL-UPy material, Radoslaw Wach and Alicja Olejnik (TUL, Lodz, Poland) for material sterilization.

Appendix A. Supporting information

Supplementary data associated with this article can be found in the online version at http://dx.doi.org/10.1016/j.jmbbm.2017.06.032.

References

Abed, Husam, David D Rahn, Lior Lowenstein, Ethan M. Balk, Jeffrey L. Clemons, and Rebecca G. Rogers. 2011. "Incidence and Management of Graft Erosion , Wound Granulation , and Dyspareunia Following Vaginal Prolapse Repair with Graft Materials : A Systematic Review." *Int Urogynecol J* 22: 789. DOI 10.1007/s00192-011- 1384-5.

Abramov, Yoram, Barbara Golden, Megan Sullivan, Sylvia M. Botros, Jay-James R. Miller, Adeeb Alshahrour, Roger P. Goldberg, and Peter K. Sand. 2007. "Histologic Characterization of Vaginal vs. Abdominal Surgical Wound Healing in a Rabbit Model." *Wound Repair and Regeneration* 15: 80.

Anderson, James M. 2001. "Biological Responses To Materials." *Annu. Rev. Mater. Res* 31: 81–110. doi:10.1146/annurev.matsci.31.1.81.

Badylak, S, Klod Kokini, Bob Tullius, Abby Simmons-Byrd, and Robert Morff. 2002. "Morphologic Study of Small Intestinal Submucosa as a Body Wall Repair Device." *The Journal of Surgical Research* 103: 190. doi:doi:10.1006/jsre.2001.6349.

Badylak, S, J E Valentin, A. K Ravindra, G. P McCabe, and A. M Stewart-akers. 2008. "Macrophage Phenotype as a Determinant of Biologic Scaffold Remodeling." *Tissue Engineering. Part A* 14 (11): 1835–42. doi:10.1089/ten.tea.2007.0264.

Brown, Bryan N, Deepa Mani, Alexis L Nolfi, Rui Liang, Steven D Abramowitch, and Pamela A Moalli. 2015. "Characterization of the Host Inflammatory Response Following Implantation of Prolapse Mesh in Rhesus Macaque." *The American Journal of Obstetrics & Gynecology* 213 (5). Elsevier Inc.: 668.e1-668.e10. doi:10.1016/j.ajog.2015.08.002.

Cipitria, A., A. Skelton, T. R. Dargaville, P. D. Daltonac, and D. W. Hutmacher. 2011. "Design, Fabrication and Characterization of PCL Electrospun Scaffolds—a Review." *Journal of Materials Chemistry* 21: 9419. doi:10.1039/c0jm04502k.

Felfel, R.M., Leander Poocza, Miquel Gimeno-Fabra, Tobias Milde, Gerhard Hildebrand, Ifty Ahmed, Colin Scotchford, Virginie Sottile, David M Grant, and Klaus Liefeith. 2016. "In Vitro Degradation and Mechanical Properties of PLA-PCL Copolymer Unit Cell Scaffolds Generated by Two-Photon Polymerization." *Biomedical Materials* 11. IOP Publishing: 15011. doi:10.1088/1748-6041/11/1/015011.

Feola, Andrew, Masayuki Endo, Iva Urbankova, Thomas Deprest, Samantha Bettin, Bernd Klosterhalfen, and Jan Deprest. 2015. "Host Reaction to Vaginally Inserted Collagen Containing Polypropylene Implants in Sheep," no. 212: 1–8. doi:10.1016/j.ajog.2014.11.008.

Hopf, R., L. Bernardi, J. Menze, M. Zundel, E. Mazza, and A.E. Ehret. 2016. "Experimental and Theoretical Analyses of the Age-Dependent Large-Strain Behavior of Sylgard 184 (10:1) Silicone Elastomer." *Journal of the Mechanical Behavior of Biomedical Materials* 60: 425–37. doi:10.1016/j.jmbbm.2016.02.022.

Kelly, Michelle, Katherine Macdougall, Oluwafisayo Olabisi, and Neil McGuire. 2016. "In Vivo Response to Polypropylene Following Implantation in Animal Models: A Review of Biocompatibility." *International Urogynecology Journal and Pelvic Floor Dysfunction*. International Urogynecology Journal. doi:10.1007/s00192-016- 3029-1.

Kim, Yoon Kyung, Esther Y. Chen, and Wendy F. Liu. 2016. "Biomolecular Strategies to Modulate the Macrophage Response to Implanted Materials." *J. Mater. Chem. B* 4 (9). Royal Society of Chemistry: 1600–1609. doi:10.1039/C5TB01605C.

Klinge, U, B Klosterhalfen, M Müller, and V Schumpelick. 1999. "Foreign Body Reaction to Meshes Used for the Repair of Abdominal Wall Hernias." *The European Journal of Surgery = Acta Chirurgica* 165: 665.

Lam, Christopher X F, Dietmar W Hutmacher, Jan-Thorsten Schantz, Maria Ann Woodruff, and Swee Hin Teoh. 2008. "Evaluation of Polycaprolactone Scaffold Degradation for 6 Months in Vitro and in Vivo." *Journal of Biomedical Materials Research. Part A* 90 (3): 906–19. doi:10.1002/jbm.a.32052.

Maher, Christopher, Benjamin Feiner, Kaven Baessler, Corina Christmann-Schmid, Nir Haya, and Jane Marjoribanks. 2016. “Transvaginal Mesh or Grafts Compared with Native Tissue Repair for Vaginal Prolapse.”*Cochrane Database of Systematic Reviews*, no. 2. doi:10.1002/14651858.CD012079.

Mangera, Altaf, Anthony Bullock, Christopher Chapple, and Sheila MacNeil. 2012. “Are Biomechanical Properties Predictive of the Success of Prostheses Used in Stress Urinary Incontinence and Pelvic Organ Prolapse? A Systematic Review.” *Neurourology and Urodynamics* 30: 169. doi:10.1002/nau.21156.

Mantovani, Alberto, Antonio Sica, Silvano Sozzani, Paola Allavena, Annunciata Vecchi, and Massimo Locati. 2004. “The Chemokine System in Diverse Forms of Macrophage Activation and Polarization.” *Trends in Immunology* 25: 677. doi:10.1016/j.it.2004.09.015.

Maurer, M.M., B. Röhrnbauer, A. Feola, J. Deprest, and E. Mazza. 2014. “Mechanical Biocompatibility of Prosthetic Meshes: A Comprehensive Protocol for Mechanical Characterization.” *Journal of the Mechanical Behavior of Biomedical Materials* 40. Elsevier: 42–58. doi:10.1016/j.jmbbm.2014.08.005.

Mollet, Björne B., Marta Comellas-Aragonès, a. J. H. Spiering, Serge H. M. Sontjens, E. W. Meijer, and Patricia Y. W. Dankers. 2014. “A Modular Approach to Easily Processable Supramolecular Bilayered Scaffolds with Tailorable Properties.” *Journal of Materials Chemistry B* 2: 2483. doi:10.1039/c3tb21516d.
Morton, W J. 1902. “Method of Dispersing Fluids.” *US Patent 705,691*, 1.
Olsen, Ambre L, Vlxginla J Smith, John 0 Bergstrom, Joyce C. Colling, and Amanda L. Clark. 1997. “Epidemiology of Surgically Managed Pelvic Organ Prolapse and Urinary Incontinence.” *The American College of Obstetricians and Gynecologists* 89: 501.

Ozog, Y., M. L. Konstantinovic, E. Werbrouck, D De Ridder, E Mazza, and J Deprest. 2011. “Persistence of Polypropylene Mesh Anisotropy after Implantation: An Experimental Study.” *BJOG: An International Journal of Obstetrics and Gynaecology* 118: 1180–85. doi:10.1111/j.1471 0528.2011.03018.x.

Ozog, Y., Maja L. Konstantinovic, Sofie Verschueren, Federico Spelzini, Dirk De Ridder, and Jan Deprest. 2009. “Experimental Comparison of Abdominal Wall Repair Using Different Methods of Enhancement by Small Intestinal Submucosa Graft.” *International Urogynecology Journal and Pelvic Floor Dysfunction* 20: 435–41. doi:10.1007/s00192-008-0793-6.

Palmer, Jason A., Keren M. Abberton, Geraldine M. Mitchell, and Wayne A. Morrison. 2014. “Macrophage Phenotype in Response to Implanted Synthetic Scaffolds: An Immunohistochemical Study in the Rat.” *Cells Tissues Organs* 199 (2–3): 169–83. doi:10.1159/000363693.

Röhrnbauer, B., Y. Ozog, J. Egger, E. Werbrouckb, J. Deprest, and E. Mazza. 2013. “Combined Biaxial and Uniaxial Mechanical Characterization of Prosthetic Meshes in a Rabbit Model.” *Journal of Biomechanics* 46 (10). Elsevier: 1626–32. doi:10.1016/j.jbiomech.2013.04.015.

Roman, Sabiniano, Iva Urbánková, Geertje Callewaert, Flore Lesage, Christopher Hillary, Nadir I. Osman, Christopher R. Chapple, Jan Deprest, and Sheila MacNeil. 2016. “Evaluating Alternative Materials for the Treatment of Stress Urinary Incontinence and Pelvic Organ Prolapse: A Comparison of the In Vivo Response to Meshes Implanted in Rabbits.” *Journal of Urology* 196: 261–69. doi:http://dx.doi.org/10.1016/j.juro.2016.02.067.

SCENIHR. 2015. *Opinion on The Safety of Surgical Meshes Used in Urogynecological Surgery*. doi:10.2772/63702.

Schneider, Caroline A, Wayne S Rasband, and Kevin W Eliceiri. 2012. “NIH Image to ImageJ: 25 Years of Image Analysis.” *Nature Methods* 9. Nature Publishing Group: 671–75.

Slieker-ten Hove, Marijke C Ph, Annelies L Pool-Goudzwaard, Marinus J C Eijkemans, Regine P. M. Steegers-Theunissen, Curt W. Burger, and Mark E. Vierhout. 2009. “Symptomatic Pelvic Organ Prolapse and Possible Risk Factors in a General Population.” *American Journal of Obstetrics and Gynecology* 200: 184.e1-184.e7. doi:10.1016/j.ajog.2008.08.070.

Toosie, Katayoun, Kelly Gallego, Bruce E Stabile, Bethann Schaber, Samuel French, and Christian De Virgilio. 2000. “Fibrin Glue Reduces Intra-Abdominal Adhesions to Synthetic Mesh in a Rat Ventral Hernia Model.” *The American Surgeon* 66: 41–45.

Ulrich, Daniela, Sharon L. Edwards, David L J Alexander, Anna Rosamilia, Jerome A. Werkmeister, Caroline E. Gargett, and Vincent Letouzey. 2016. “Changes in Pelvic Organ Prolapse Mesh Mechanical Properties Following Implantation in Rats.” *American Journal of Obstetrics and Gynecology* 214 (2). Elsevier Inc.: 260e1-260e8. doi:10.1016/j.ajog.2015.08.071.

Wolf, Matthew T, Yoram Vodovotz, Stephen Tottey, Bryan N. Brown, and Stephen F. Badylak. 2015. “Predicting In Vivo Responses to Biomaterials via Combined In Vitro and In Silico Analysis.” *Tissue Engineering Part C: Methods* 21 (2): 148–59. doi:10.1089/ten.tec.2014.0167.

Wynn, Thomas, and Luke Barron. 2010. “Macrophages: Master Regulators of Inflammation and Fibrosis.”*Semin Liver Dis.* 30: 245. doi:10.1055/s-0030-1255354

Supplementary material 1

Rectangular samples with an aspect ratio of 4:1 (free length to width, polypropylene: 40mmx10mm and UPy-PCL: 16mm x 4mm) were cyclically loaded using a MTS 793 test rig (MTS Systems, Eden Prairie, USA). After the identification of the reference configuration by means of a force threshold (F=0.01N), the specimen was loaded to 15% nominal strain and successively unloaded down to the force threshold level, for a total of 10 cycles with a nominal strain rate of 0.2%/s. Strain in loading and transversal direction was quantified for the central region of the sample from images registered during the experiment with a CCD camera (Pike 100B Allied Vision Technologies GmbH) and successively analyzed using a custom algorithm to track optical features on the sample surface. Tests were performed either in dry conditions at room temperature or in distilled water at 37°C (Hopf et al. 2016). Measured response was characterized in terms of membrane tension (i.e. force divided by initial sample width) and membrane stiffness values (in N/mm) were determined as the tangent at the membrane tension versus strain curve at a strain of 0%.

Supplementary material 2

Anesthesia was induced in a chamber with 5% of isoflurane (Iso-Vet®; Piramal Healthcare UK Ltd; Morpeth; United Kingdom) and maintained with a combination of ketamine (65mg/kg; Nimatek®; Eurovet Animal Health B.V.; Bladel; Nederland) and xylazine (10mg/kg Xyl -M®; VMD; Arendonk; Belgium). Surgery was carried out in sterile conditions. The paramedian longitudinal incision, way from the future defect, was created in the right hemi-abdomen and skin flap was raised. Using a ruler, a longitudinal full-thickness defect (30 × 5 mm) was created in the left anterior abdominal wall, consisting of fascia, muscle and peritoneum. This was subsequently primarily closed with a continuous polypropylene 4/0 suture (Prolene, Ethicon, Dilbeek, Belgium) at an interrun distance of 5 mm. In animals from the mesh reinforcement groups (2) and (3), a 40x25mm strip of mesh was laid over the primarily sutured defect. The mesh was fixed by interrupted polypropylene 4/0 stitches at the corners and half way each side, followed by a running suture with interrun distance 5mm of 4/0 poliglecaprone (Monocryl, Ethicon), essentially fixing the implant in a tension free fashion. The subcutaneous layer and skin were closed with continuous resorbable 4/0 and 3/0 Monocryl, respectively. The wound was sprayed with aluminum. Elizabethan collars were placed for 24 hours to prevent auto-mutilation. Rats were kept on a heating pad until recovery from anesthesia.

Supplementary material 3

We used a vertical uniaxial Zwick tensiometer with a 200 N cell load set up (Zwick GmbH & Co. KG, Ulm, Germany) (Ozog et al. 2011). Explants (10x30mm) were clamped tension free and tested immediately after explantation. The zero elongation was defined as clamp-to-clamp distance at preload (0.1 N) reached with a constant elongation of 10mm/min. Here, cross-sectional dimensions were measured at three parts of the specimen using an analogue caliper (accuracy 0.05mm; Horex, Helios Preisser, Gammertingen, Germany). Afterwards, specimen was elongated with a speed 10mm/min

up to the failure defined as 60% drop of the load. Strain was calculated by dividing the elongation by the clamp-to clamp distance and membrane tension dividing force by the initial sample width.

Supplementary information 4

Formalin-fixed specimens were embedded in paraffin and cut into 5μm thick slices. Slides stained with hematoxylin and eosin (H&E) were used for Badylak score of inflammation and vascularization (Badylak et al. 2002). Due to vigorous foreign body giant cells (FBGC) reaction we performed also the real number counting of FBGC. The amount of collagen at the interface of the explant were assessed semi-quantitatively using Masson's Trichrome staining. Immunostainings were used for more accurate quantification of presented cells and vessels. Alpha smooth muscle actin (α-SMA) was used to further investigate the nature of the fibrotic reaction, to detect myofibroblasts, CD34 for endothelial cells, CD68 for total amount of macrophages (M), CD80 stains macrophage subtype M1, CD206 and CD163 are markers of subtypes M2a and M2c respectively. In detail after deparaffinization, endogenous peroxidase activity was blocked with 0.5% H2O2 in PBS for 20 min at room temperature. Sections were then heated at 98°C for 1 hour in citrate buffer (10mmol/L, pH 6) to enhance antigen retrieval or digested with pepsin. Non-specific binding was minimized by incubating sections in 1% BSA and 2% milk in PBS-0.1% tween 80 for 30 min. Sections were then incubated overnight at 4°C with the primary polyclonal antibodies against α-smooth muscle actin at 1:100 dilution (α-SMA- clone 1A4, DAKO, Heverlee, Belgium; myofibroblast marker), CD34 at 1/1000 (EP373Y, ab81289, Abcam, Cambridge, UK; endothelial marker), CD163 at 1/300 (MCA342R, AbD Serotec, Puchheim, Germany; M2c marker), CD206 at 1/300 (sc34577, Santa Cruz, Heidelberg, Germany; M2a marker), CD68 at 1/200 (MCA 341R, AbD Serotec; macrophage marker) and CD80 at 1/ 100 (sc-9091, Santa Cruz; M1 marker). Negative controls included buffer alone. Specific labeling was detected with EnVision/HRP Detection Kit (DAKO). The color reaction was developed with 3,3'-diaminobenzidine (Sigma-Aldrich, Diegem, Belgium) and sections were counterstained with Mayer hematoxylin. Sections were then dehydrated through graded ethanol, cleared in xylene, and mounted in dePex (BDH, vWR international, Haasrode, Belgium).

Supplementary figures

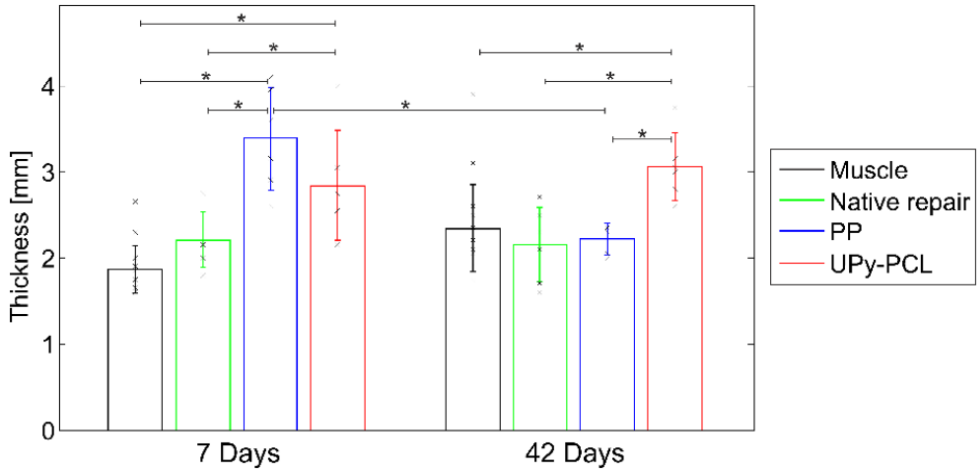

Supplementary figure 1. Measured thickness of the explant samples at 7 and 42 days. Reported is mean and standard deviation (N=11 for muscle, N=5 for polypropylene, N=6 for UPy-PCL and N=6 for native repair)

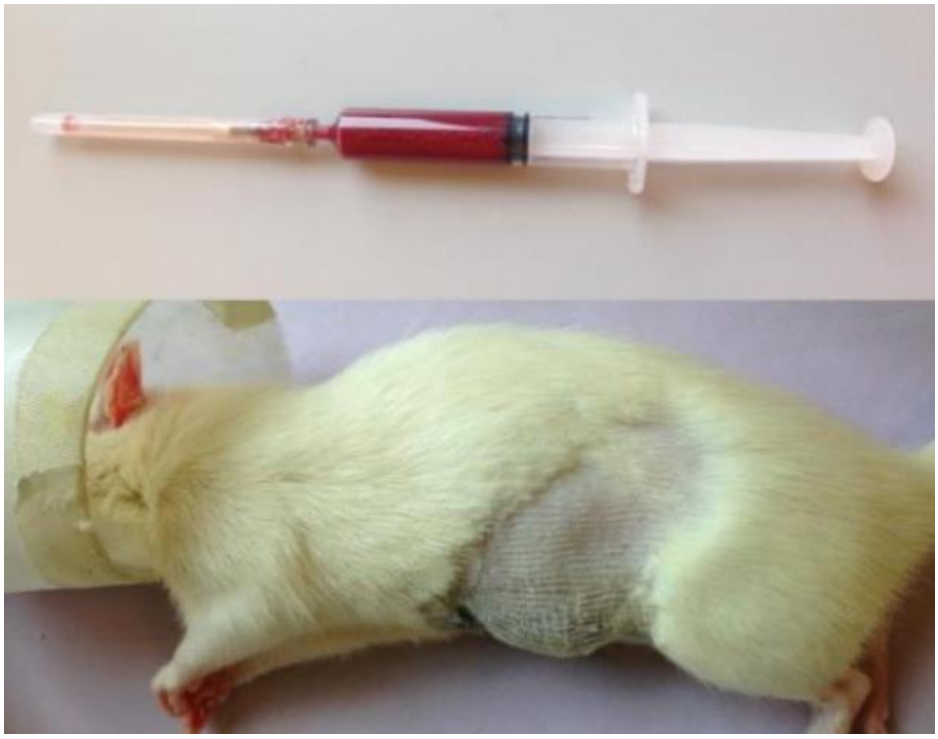

Supplementary figure 2. Sero-sanguinolent fluid collection punctured and collected in syringe in one of UPy-PCL rats.

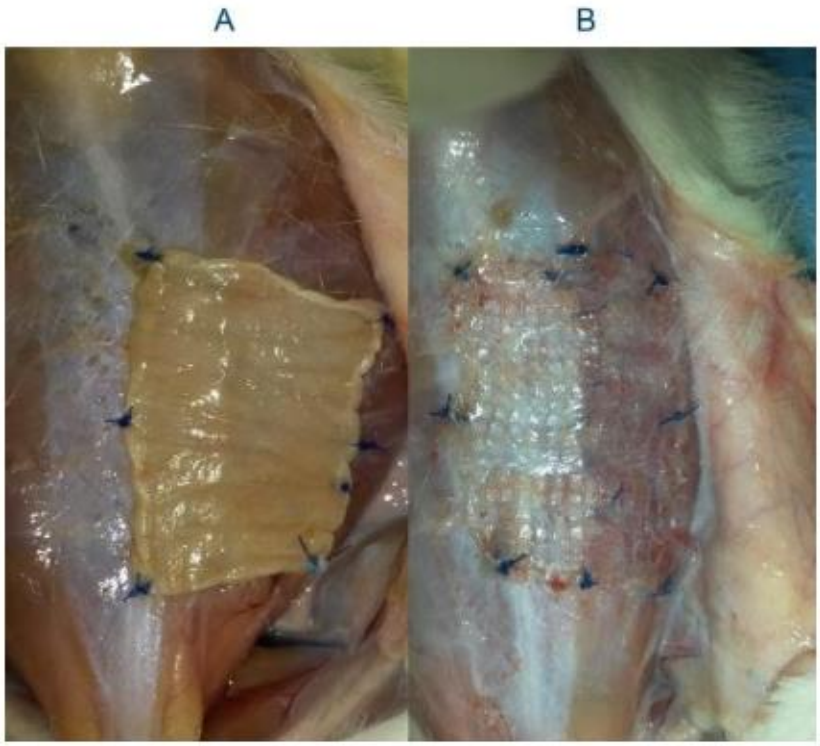

Supplementary figure 3. Implanted meshes after 42 days: A: UPy-PCL electrospun and B: Restorelle®.

SUPPLEMENTARY MATERIAL 2

EXPERIMENTAL RECONSTRUCTION OF AN ABDOMINAL WALL DEFECT WITH ELECTROSPUN POLYCAPROLACTONE UREIDOPYRIMIDINONE MESH CONSERVES COMPLIANCE YET MAY HAVE INSUFFICIENT STRENGTH

Lucie Hympanova [a,b,c,*], Marina Gabriela Monteiro Carvalho Mori da Cunha [a,b,*], Rita Rynkevic [a,b,e], Radoslaw A. Wach [f], Alicja K. Olejnik [f], Patricia Y.W. Dankers [g], Boris Arts [g], Tristan Mes [h], Anton W. Bosman [h], Maarten Albersen [i], Jan Deprest [a,b,d]

[a] Centre for Surgical Technologies, Group Biomedical Sciences, KU Leuven, Leuven, Belgium
[b] Department of Development and Regeneration, Woman and Child, Group Biomedical Sciences, KU Leuven, Leuven, Belgium
[c] Institute for the Care of Mother and Child, Third Faculty of Medicine, Charles University, Prague, Czech Republic
[d] Pelvic Floor Unit, University Hospitals KU Leuven, Leuven, Belgium
[e] INEGI, Faculdade de Engenharia da Universidade do Porto, Universidade do Porto, Porto, Portugal
[f] Institute of Applied Radiation Chemistry, Faculty of Chemistry, Technical University of Lodz, Lodz, Poland
[g] Laboratory of Macromolecular and Organic Chemistry, Eindhoven University of Technology, Eindhoven, The Netherlands
[h] SupraPolix BV, Horsten 1, 5612 AX Eindhoven, The Netherlands
[i] Department of Urology, University Hospitals Leuven, Leuven, Belgium
*first two authors contributed equally

Key words: hernia, biomechanics, electrospun mesh, biocompatibility, polypropylene

Experimental reconstruction of an abdominal wall defect with electrospun polycaprolactone-ureidopyrimidinone mesh conserves compliance yet may have insufficient strength

Lucie Hympanova[a,b,c,1], Marina Gabriela Monteiro Carvalho Mori da Cunha[a,b,1], Rita Rynkevic[a,b,e], Radoslaw A. Wach[f], Alicja K. Olejnik[f], Patricia Y.W. Dankers[g], Boris Arts[g], Tristan Mes[h], Anton W. Bosman[h], Maarten Albersen[i], Jan Deprest[a,b,d,*]

Published in Journal of Mechanical Behavior of Biomedical Materials (2018)

ABSTRACT

Purpose: Electrospun meshes mimic the extracellular matrix, which may improve their integration. We aimed to compare polycaprolactone (PCL) modified with ureidopyrimidinone (UPy) electrospun meshes with ultra-lightweight polypropylene (PP; Restorelle) reference textile meshes for *in vivo* compliance. We chose UPy-PCL because we have shown it does not compromise biomechanical properties of native tissue, and because it potentially can be bioactivated

Methods: We performed ex vivo biomechanical cyclic loading in wet conditions and in vivo overlay of full-thickness abdominal wall defects in rats and rabbits. Animals were sacrificed at 7, 42 (rats; n=6/group) and 30 and 90 days (rabbits; n=3/group). Outcomes were herniation, mesh degradation and mesh dimensions, explant compliance and histology. High failure rates prompted us to provide additional material strength by increasing fiber diameter and mesh thickness, which was further tested in rabbits as a biomechanically more challenging model.

Results: Compliance was tested in animals without herniation. In both species, UPy-PCL-explants were as compliant as native tissue. In rats, PP-explants were stiffer. Contraction was similar in UPy-PCL and PP-explants. However, UPy-PCL-meshes macroscopically degraded from 30 days onwards, coinciding with herniation in up to half of animals. Increased fiber and mesh thickness did not improves outcome. Degradation of UPy-PCL is associated with an abundance of foreign body giant cells until UPy-PCL disappears.

Conclusion: Abdominal wall reconstruction with electrospun UPy-PCL meshes failed in 50%. Degradation coincided with a transient vigorous foreign body reaction. Non-failing UPy-PCL-explants were as compliant as native tissue. Despite that, the high failure rate forces us to explore electrospun meshes based on other polymers.

1. Introduction

Abdominal wall hernia is common with a lifetime prevalence of over 30% [1]. It is usually operated electively, and today a tension-free mesh repair technique is recommended by the European Hernia Society [2]. Mesh reconstructions have a lower recurrence rate than sutured repair without an increase in postoperative pain [3]. However, the use of meshes may lead to complications including infection, exposure, migration, adhesions, occasionally persistent pain and a potential effect on fertility in men [4,5]. Mesh complications are believed to be caused by persistence of the material, chronic inflammation, contraction and a high stiffness [4,6]. Textile meshes, typically made of polymer polypropylene (PP), are the most commonly used implants in general surgery and gynecology, and this is therefore also used in this study. Depending on the weight and textile fabric, PP may cause an adverse host response [4,6]. To reduce the risk for that, clinicians have moved towards light-weight macroporous polypropylene constructs with better properties [4]. Despite that, there might still be complications [7].

Development of novel meshes has been advocated to decrease graft-related complications [8]. A mesh used to repair a structural defect should be strong enough under tension and flexible at rest. As an implant, it needs to be biocompatible and induce an appropriate host response. Durable materials cause a chronic inflammatory reaction, which obviously could be avoided by using degradable polymers. The pace of degradation should be chosen such that the mesh remains supportive, until newly formed tissue can resist the forces. An alternative to knitted textile meshes is the use of an electrospun matrix. Those matrices have been widely used in tissue engineering for restoration of vessels, cartilage, bone, peripheral nerve, spinal cord and skin [9]. Through different electrospinning parameters, polymers, surface modifications and functionalization (incorporation of biomolecules) one can determine biomechanical properties and the ultimate host response. Electrospinning permits the production of extracellular-matrix-like three-dimensional structures with nano-scale fibers [10]. The nano-fibrous architecture can improve cell-material interactions [11]. Electrospun matrices have been shown to support cell adhesion (fibroblasts), production of connective tissue [12] and a nanofibrous surface can temper the inflammatory response at the interleukin level [13]. One example of a slowly degradable (6-7months) three-dimensional synthetic web on the market is Gore Bio A (William Gore, Flagstaff, Arizona, USA). Gore Bio A is composed of poly(ethylene terephthalate)/chitosan and manufacturing utilizing a melt-spinning technique. This material was tested in animal model as a subcutaneous implant [14], as a reinforcement of a sutured defect [15,16], yet to our knowledge no yet to bridge a defect. Clinical uncontrolled studies in inguinal, hiatal and ventral hernia repair have been done [17–19], and one controlled trial on ventral hernia repair is ongoing [20].

We decided to electrospun a UPy-PCL scaffold, i.e. polycaprolactone (PCL) polymer modified by dimerizing quadruple hydrogen bonding 2-ureido-4[1H]-pyrimidinone (UPy) moieties. PCL is one of the many polymers that can be used as a backbone for electrospinning. It has been used in research for bone and vessels regeneration guidance [21,22]. *Ex vivo* it has sufficient biomechanical strength [23] and induces a minimal foreign body response [24]. When UPy is bound to PCL it impacts *in vitro* degradation:

UPy-PCL degrades mainly via an oxidative pathway compared to PCL alone, which is sensitive to enzymatic and hydrolytic degradation [25]. UPy-modification of polymers is a novel approach, which allows to bind e.g. bioactive peptides to the electrospun matrix. It allows a modular approach to gain control over cellular behavior and activity [26–28]. By functionalization of a matrix it may be possible to create e.g. a bilayered scaffold with adhesive and antiadhesive surface on each side [29]. UPy-hydrogels have also been shown to be a slow-release drug-carrier to the myocardium in a porcine model of myocardial infarction [30]. We earlier showed that UPy-PCL explants have biomechanical properties comparable to that of native tissue [31]. Herein we aimed to test their in vivo performance in appropriate models for abdominal wall hernia surgery. Initial screening was on the rat model and further longer term testing was on rabbits [32]. When shown reasonably effective, our next step would be to bind bioactive peptides that may improve tissue ingrowth (cell adhesion, proliferation, extracellular matrix production) or reduce infections.

2. Materials and methods

2.1 Meshes

Ureidopyrimidinone-polycaprolactone (UPy-PCL) polymer was obtained from SupraPolix BV (Eindhoven, the Netherlands) and electrospun by Coloplast A/S (Humlebaek, Denmark). Details about polymers, spinning and sterilization are described in Supplement 1. Meshes were characterized for fiber size distribution and directionality by scanning electron microscopy (Supplementary figure 1). Based on initial clinical results the fiber diameter or mesh thickness was increased and tested in rabbits (Table 1). Standard textile ultra-lightweight polypropylene meshes (Restorelle®; Coloplast A/S) were used as controls. Rectangular mesh samples were weighed and measured to establish density and underwent ex vivo cyclic uniaxial loading for 10 cycles in wet conditions for determination of comfort zone stiffness values (Supplement 2, Table 1).

Table1. Characteristics of the materials used in this study. * and # represent a significant difference between groups ($p < 0.05$), † the rats were euthanized earlier than the scheduled 90 days, due to failure of the implant. The comfort zone stiffness UPy-PCL data were not normally distributed.

	Macroporous polypropylene (Restorelle®)	**Electrospun polycaprolactone modified with ureidopyrimidinone (UPy-PCL)**		
		Standard	Thicker mesh	Thicker fiber
Mesh thickness (µm)	300	250-400	500-800	250-400
Fiber size (µm)	80.0	1.8-3.2	1.8-3.2	3.6-6.4
Density (g/m^2)	19.0	38.5 - 47.2	59.6 – 72.3	46.6-63-6
Comfort zone stiffness (N/mm)	1.58 ± 0.19*	0.66 ± 0.02 *, #	1.70 ± 0.10 #	0.90 ± 0.07
Number of implants in rats (7, 42, and 56 † days)	12	18	0	0
Number of implants in rabbits (30 and 90 days)	12	12	6	6

2.2 Animals and study design

Thirty rats and eighteen rabbits were randomly divided into groups with a size based on a power calculation as in Supplement 3. The timeline and design of the experiment are illustrated in Figure 1. In the initial experiment in rats, two groups (UPy-PCL and

polypropylene) were implanted for 7 and 42 days. These time points were chosen as representative of the inflammatory and regenerative phase of the healing response. Since initially no complications were observed in rats, identical meshes were implanted in the biomechanically more challenging rabbit model [32] for 30 and 90 days, with a later time point chosen mainly to study the effects of degradation. Yet because of failures observed in half of the rabbits at 30 days, we added a 90 days time point to the rat study, to closer study the effects of degradation. In these rats all reconstructions failed around 54±4 days, and the experiment with that particular implant type was aborted at that point. To provide additional strength to UPy-PCL meshes, implants were modified, either by using a thicker mesh or thicker fibers. Those materials were again implanted in rabbits to stay up to 90 days.

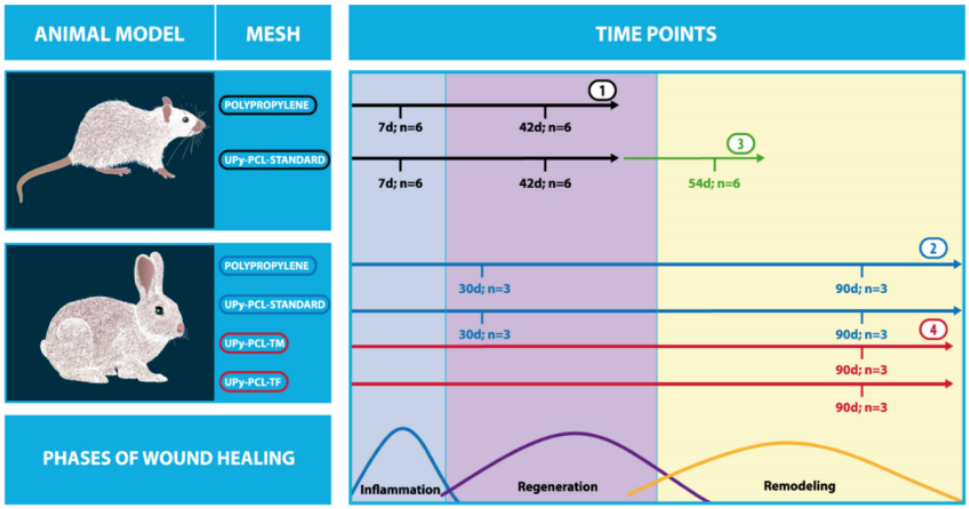

Fig. 1 Study design. 1) Experiments were performed consecutively, first in rats (black arrows) up to 42 days to study short-term effects. 2) Then we implanted these for a longer period in rabbits (blue arrows). 3) Given insufficient strength, the degradation process was documented by prolonging the rat experiments well in to the remodeling phase (green arrow). 4) The material was adjusted by thicker fibers (TF) and thicker mesh (TM) and evaluated in the rabbit (red arrows). n = number of animals used in the study. Phases of wound healing (bottom line) according to Yoseph et al., 2015.

2.3 Experimental surgery and obduction

We earlier reported in detail about the anesthesia, surgical protocol and pain relief for rat and rabbit studies [33,34]. Briefly, in rats one full thickness defect measuring 15x30mm was created in the left hemi-abdominal wall. In rabbits, two identical abdominal defects were created per animal, one in the right lower and one in the left upper quadrant. The defects were not primarily sutured, yet overlaid with an oversizing mesh (25x40mm), which was fixed tension free with separate polypropylene 4/0 sutures at the corners and additionally one half way in between corners. Further, a poliglecaprone 25 (Monocryl; Ethicon, Dilbeek, Belgium) 4-0 was placed in a continuous fashion around the implant (Figure 2 and 3). The mesh dimensions at the end of the surgery were measured, for future reference following which the subcutis and skin were closed.

At obduction 10 mm wide explant strips taken parallel to the body axis were cut for biomechanical testing, additional samples were used for histological documentation of the host response (Supplement 4) and for gel permeation chromatography (GPC) to study degradation (Supplement 5) [21]. Non-operated abdominal wall samples were used as a control for biomechanics. Other outcome measures were herniation, local complications, adhesion score [35] and mesh contraction (%). Further details on animals, anesthesia, surgical protocols, euthanasia and obduction are described in Supplement 6.

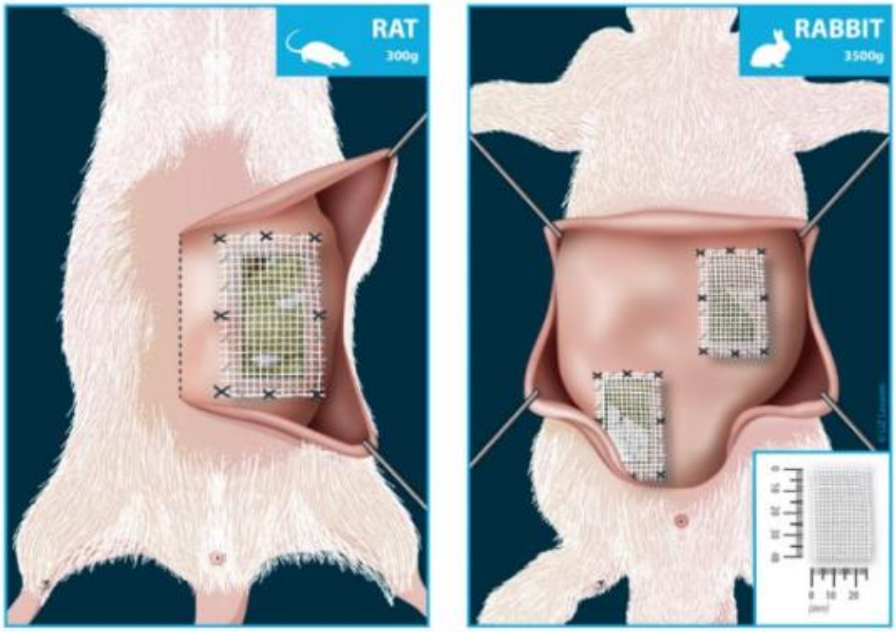

Fig. 2 Schematic representation of surgical procedures in the rat and rabbit. After raising skin flaps, a full-thickness abdominal wall defect was created and overlaid with the implant.

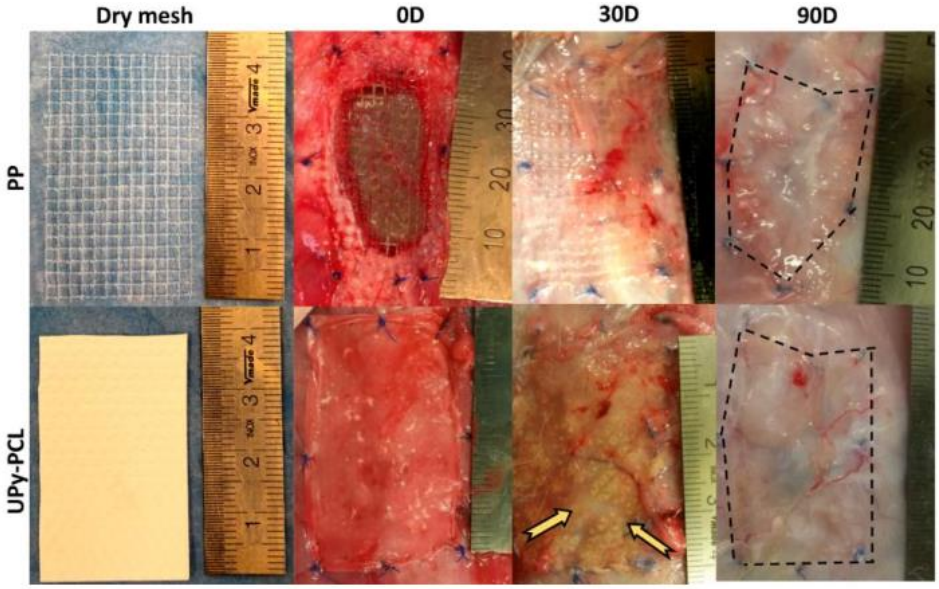

Fig. 3 PP and UPy-PCL dry mesh prior to implantation (left); immediately after implantation (0d) and 30 and 90 days after implantation in the rabbit. The implanted UPy-PCL mesh and its texture is still recognizable at 30 days, however a few cracks (yellow arrows) are already visible. No macroscopically visible mesh can be observed at 90 days (bottom right).

2.4 Biomechanical testing of explants

Biomechanical testing of explants in animals without herniation was performed following a previously used protocol [36] on a uniaxial Zwick tensiometer with a 200 N cell-load set-up (Zwick GmbH & Co. KG, Ulm, Germany) without cyclic preconditioning. Explants (10x30mm) were clamped tension free, with the interface within the clamps, so that the tissue-implant complex was tested as a whole. The zero elongation was defined as the clamp-to-clamp distance at preload (0.1 N). Cross-sectional dimensions were measured at three sections through the specimen using an analog caliper. Afterwards, the specimen was elongated with a speed of 10mm/min up to failure. The strain was calculated by dividing the elongation by the clamp-to-clamp distance and stress dividing force by the cross-sectional area.

2.5 Statistics and ethics

Comparison of the groups was performed with an unpaired t-test for normally distributed data and Mann-Whitney for not normally distributed data. For comparison of more groups, one-way ANOVA followed by Tukey's post hoc test was used for normally distributed data. Kruskal-Wallis followed by Dunn's post test were used for not normally distributed data. Normally distributed data are reported as mean ± SD, not normally distributed as median ± SEM. Statistical significance level was defined as $p < 0.05$ (details in Supplement 3). Experiments were approved by the Ethics Committee on Animal Experimentation of the Faculty of Medicine, KU Leuven. Animals were treated in accordance with current national guidelines on animal welfare.

3. **Results**

3.1 Ex vivo characterization of investigated materials

Standard UPy-PCL meshes were less stiff than polypropylene. Electrospun meshes with thicker fibers had a stiffness comparable to standard UPy-PCL. The thicker mesh was stiffer and similar to polypropylene (Table 1).

3.2 Local complications and obduction

Necropsy details are displayed in Table 2. No exposures were observed. There were fluid collections in 6/18 UPy-PCL and 1/12 polypropylene rats persisting for up to 7 days, as observed before (Supplementary Figure 2a) [31]. These did not look infected and disappeared spontaneously. At 7 and 42 days all UPy-PCL meshes were partially integrated into the tissues covering and neighboring the implant, yet still maintaining a recognizable texture. Herniations however occurred beyond 50 days (Figure 4a), so that the experiment was terminated to avoid suffering of the animals (day 54). Contraction at 7 days was about 30% without differences between groups, and that was similar at 42 days. In UPy-PCL animals explanted later on and not having herniation, mesh dimensions were larger.

In rabbits, we did not observe exposures or fluid collections. Mesh degradation was macroscopically visible as cracks at 30 days (Figure 3) until complete disappearance of

the mesh material. From 30 days onwards visible herniations (Figure 4a) were observed at different time points in one third of UPy-PCL rabbits, yet none in polypropylene animals, except one. In that rabbit, there was local separation of the mesh between polypropylene sutures not causing obvious symptoms (Supplementary Figure 2b). Change of fiber and mesh thickness of UPy-PCL meshes did not affect the rate of herniation. There was significant mesh contraction in the PP groups at both time points.

Table2. Obduction results. * represents a significant difference between mesh area at the time of implantation and explantation ($p<0.05$)

RAT						
Time point	7 days		42 days		54 days	
Group	PP	UPy-PCL Standard	PP	UPy-PCL Standard	UPy-PCL Standard	
Hernia	0%(0/6)	0%(0/6)	0%(0/6)	0%(0/6)	50%(3/6)	
Macroscopic degradation	0%(0/6)	0%(0/6)	0%(0/6)	0%(0/6)	50%(3/6)	
Expansion (+) Contraction(-) (%)	-35.5±8.3*	-32.6±1.0*	-17.5±15.5*	-30.2±4.4*	+ 22.4±14.6	
Adhesions 0	0%(0/6)	16.7%(1/6)	0%(0/6)	0%(0/6)	0%(0/6)	
Adhesions 1	0%(0/6)	0%(0/6)	0%(0/6)	66.6%(4/6)	66.6%(5/6)	
Adhesions 2	50%(3/6)	33.3%(2/6)	33.3%(2/6)	33.3%(2/6)	16.7%(1/6)	
Adhesions 3	50%(3/6)	50%(3/6)	66.6%(4/6)	0%(0/6)	0%(0/6)	
RABBIT						
Time point	30 days		90 days			
Group	PP	UPy-PCL Standard	PP	UPy-PCL Standard	UPy-PCL Thicker mesh	UPy-PCL Thicker fiber
Hernia	0%(0/6)	50%(3/6)	16.7%(1/6)	16.7%(1/6)	33.3%(2/6)	33.3%(2/6)
Macroscopic degradation	0%(0/6)	100%(6/6)	0%(0/6)	100%(6/6)	100%(6/6)	100%(6/6)
Expansion (+) Contraction (-) (%)	-20.9±15.6*	-12.0±19.7	-15.0±12.8*	-25.2±26.3	+4.8 ± 2.6	+8.3 ± 24.7
Adhesions 0	16.7%(1/6)	16.7%(1/6)	0%(0/6)	50%(3/6)	33.3%(2/6)	16.7%(1/6)
Adhesions 1	0%(0/6)	0%(0/6)	0%(0/6)	0%(0/6)	16.7%(1/6)	16.7%(1/6)
Adhesions 2	0%(0/6)	16.7%(1/6)	0%(0/6)	0%(0/6)	16.7%(1/6)	16.7%(1/6)
Adhesions 3	83.3%(5/6)	66.6%(4/6)	100%(6/6)	50%(3/6)	33.3%(2/6)	50%(3/6)

3.3 Uniaxial tensile testing

In rats, measurements on UPy-PCL explants were in the range of that of native tissue (Table 3). Polypropylene rat explants were significantly stiffer in the comfort zone compared to UPy-PCL yet also to contralateral native tissue (Figure 5a). Conversely, in rabbits without herniation, there were no differences. In other words, all non-degraded UPy-PCL and polypropylene explants were within the range of native tissue (Figure 5b).

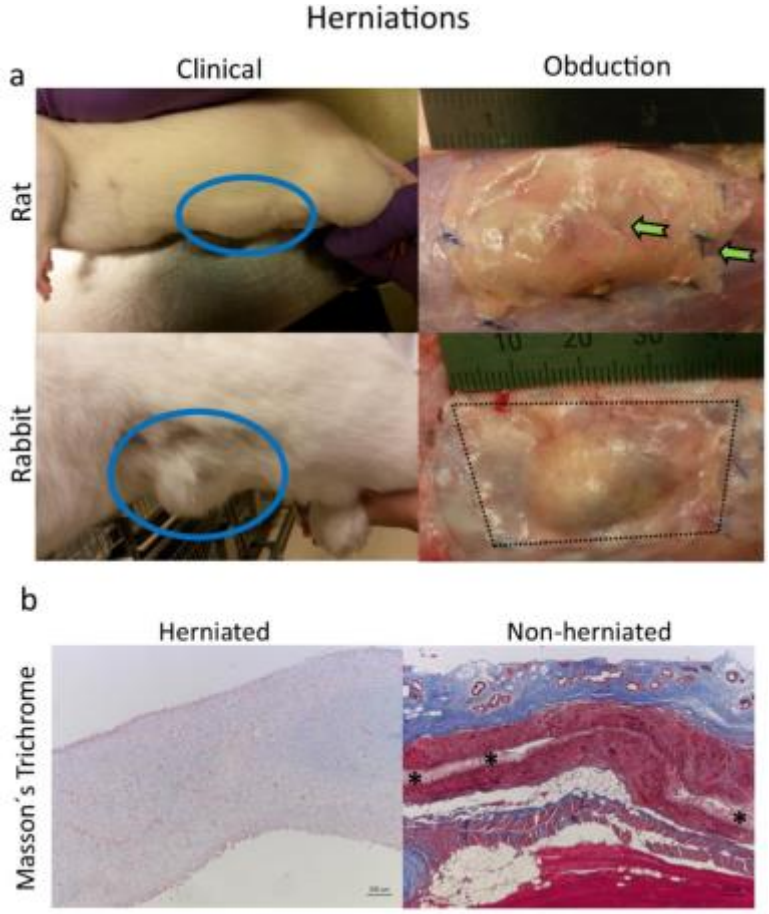

Fig. 4 a - Representative figures of herniations in rats and rabbits. Clinically, a bulge in the implanted area could be observed. At obduction, cracks and signs of degradation were observed in rats at 54 days after implantation (green arrows). The implant was completely degraded in rabbits by 90 days after implantation (black dotted line). b – Masson´s Trichrome staining of representative tissue of herniated (left) and non-herniated (right) rabbits implanted with UPy-PCL thicker fibers (50x magnification). Mesh fibers are still visible in non-herniated animals (asterisk); connective tissue is thicker (blue) and has a more aligned collagen fibres.

Table3. Young's modulus of explants measured in the comfort and stress zone (Ozog, 2011). # points to a significant difference compared to internal control (contralateral abdominal wall). * means significant difference between groups at the same time point ($p<0.05$). Not normally distributed data were: rats contralateral abdominal wall in the stress zone and rabbits UPy-PCL standard at 30 days in the comfort and stress zone, UPy-PCL -TM and UPy-PCL-TF in the comfort and stress zone.

RAT							
Time point		Contralateral abdominal wall	7 days		42 days		54 days
Group			PP	UPy-PCL Standard	PP	UPy-PCL Standard	UPy-PCL Standard
Young's modulus (N/mm^2)	Comfort zone	0.29±0.15#	0.70±0.33#,*	0.32±0.18*	1.67±0.95#,*	0.34±0.15*	0.19±0.01
	Stress zone	1.00±0.22#	1.32±0.46	0.75±0.37	4.10±1.31#,*	1.18±0.46*	0.42± .35

RABBIT								
Time point		Contralateral abdominal wall	30 days		90 days			
Group			PP	UPy-PCL Standard	PP	UPyPCL Standard	UPy-PCL TM	UPy-PCL TF
Young's modulus	Comfort zone	0.19±0.09	0.25±0.23	0.12±0.02	0.50±0.41	0.45±0.30	0.40±0.12	0.47±0.12

(N/mm^2)	Stress zone	1.18±0.62	1.15±1.02	1.33±0.37	2.08±0.96	2.39±0.92	0.89±0.41	2.93±0.65

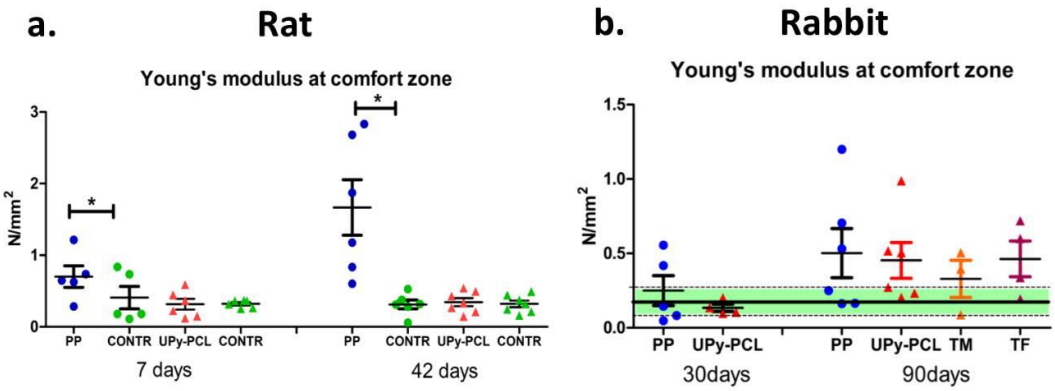

Fig. 5 a - Individual observations in rats at 7 and 42 days. Measurements of UPy-PCL animals were comparable to measurements of contralateral abdominal wall tissue in the same rat (CONTR). b - Individual observations in rabbits at 30 and 90 days. Individual measurements on native tissue in external controls are not displayed, yet the line refers to the mean and ± 1 SD (dotted line). PP – polypropylene, TM – thicker UPy-PCL mesh, TF – thicker fiber UPy-PCL mesh.

3.4 Degradation assay

In rats there was enough UPy- PCL retrieved in all samples at 7 days, in five at 42 days, yet at 54 days the polymer was not measurable with this method. There was a progressive drop in the number and the weight average molecular weight (Mn/Mw) from preimplantation specimens, which was not significant by 7 days, yet by 42 days these parameters dropped by around 24.5% (Mn)/20.3% (Mw) from baseline (Table 4). In none of the rabbit explants UPy-PCL could be detected.

Table4. Molecular weight of UPy-PCL as measured by GPC. A significant difference from baseline (#) or from 7 days (*). Mn data at 42 days and data from non-implanted meshes were not normally distributed.

Standard UPy-PCL	**non-implanted mesh**	**Rat 7 days**	**Rat 42 days**
Mn (kDa)	14.3 ± 0.0#	13.4 ± 0.3*	10.8 ± 0.7*,#
Mw (kDa)	34.5 ± 0.0#	34.7 ± 2.8*	27.4 ± 6.8*,#

3.5 Morphological study

First, morphometric scores were made on explants from non-herniating animals. On hematoxylin & eosin (H&E) stain, the area of the mesh was easily recognized. At closer look a microfiber structure was visible, surrounded by inflammatory cells. At 7 days these were on the surface of the mesh, and few cells were apparently fused into foreign body giant cells (FBGC) (Figure 6b). At the later time points, cells were found deeper over the entire width of the mesh (Figure 6d). Also, visually it seems that the mesh was degrading, evidenced by increasingly scarcer and thinner or even disconnected islands of remnant material, surrounded by FBGC (Figure 7b, d). In between fibers also fibroblasts and

infiltrating vessels were visible. At 90 days small islets and single fibers were surrounded by large FBGC. In some rabbit samples, we could not identify any mesh fibers anymore however there was fibrous tissue visible on the place where the mesh used to be. The numbers of FBGC and the amount of connective tissue are displayed in Table 5. There was no difference in FBGC numbers between the three UPy-PCL meshes, yet cell counts were much higher than in polypropylene explants. In rabbits, the number of macrophages was higher in UPy-PCL at 30 days compared to polypropylene, yet without differences at 90 days. Counts of myofibroblasts were comparable between polypropylene and UPy-PCL in both species at any time point. Vessels were seen on the mesh surface at 7 days, yet at later time points vessels were present deeper into the UPy-PCL scaffold (Figure 8). Connective tissue quantification using Masson's Trichrome indicated less collagen in standard UPy-PCL implanted animals at 30 days (rabbits, Figure 7f) or 42 days (rats, Figure 6h) compared to polypropylene, however at 90 days (rabbits) the collagen content was similar in nonherniating animals. The amount of collagen was higher in the thicker fiber group. In summary, in UPy-PCL explants over time there was increasing connective tissue deposition, vascularization and disappearance of FBGC. Around polypropylene filaments there was a limited inflammatory reaction with less FBGC and the spaces in between were infiltrated by connective tissue and vessels (Figure 6,7). We also looked at sections from herniating animals. Some sparse filaments could be recognized in a few samples. Inflammatory cells were in that case present exclusively around those filaments. The herniation sac was composed mainly of connective tissue (Figure 4b).

Table5. FBGC counts and amount of collagen in explants. Collagen is semi-quantitatively estimated as a percentage area stained blue by Masson's Trichrome. Significant differences ($p<0.05$) between groups are marked with *and #. PP- rat FBGC data at 7 days, PP and UPy-PCL-TF collagen amount data at 90 days were not normally distributed.

RAT						
Time point	7 days		42 days		54 days	
Group	PP	UPy-PCL Standard	PP	UPy-PCL Standard	UPy-PCL Standard	
FBGC	2.00 ± 0.84*	10.67 ± 5.35*	4.56 ± 3.24*	26.28±12.62*	39.60 ± 10.21	
Collagen amount	13.42 ± 4.84	10.59 ± 2.10	33.08 ±3.55*	10.24 ± 2.65*	11.30 ± 6.10	
RABBIT						
Time point	30 days		90 days			
Group	PP	UPy-PCL Standard	PP	UPy-PCL Standard	UPy-PCL TM	UPy-PCL TF
FBGC	1.97 ± 0.78*	34.17±18.91*	2.21 ± 1.06	10.83±17.28	8.25 ± 9.10	5.83 ± 6.09
Collagen amount	15.68 ± 4.85*	5.77 ± 1.76*	13.15 ±1.18*	10.74 ± 4.41#	38.57± 6.61	48.44±0.04*,#

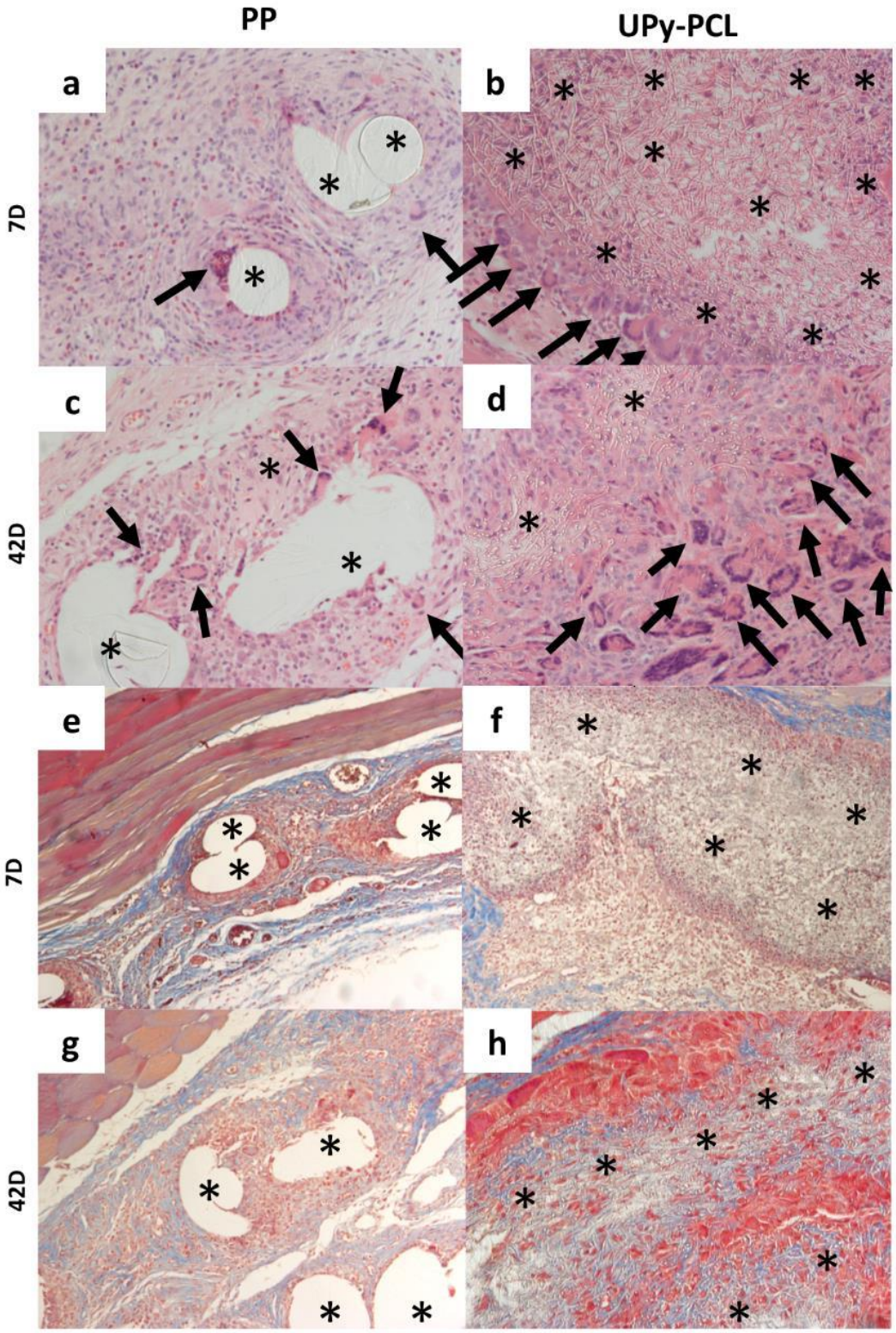

Fig. 6 Representative images of hematoxylin and eosin (H&E; a-d, 200X) and Masson´s trichrome stains (e-h, 100X) of PP and UPy-PCL explants in rats. Mesh fibers are indicated by asterisks and foreign body giant cells (FBGC) by black arrows. Connective tissue lights up as blue (e-h). On H&E: at 7 days, PP fibers (a) and UPy-PCL mesh (b) are surrounded by inflammatory cells and few FBGC. Later on, at 42 days, more FBGC are evident around PP fibers (c) and deeper over the entire width of the UPy-PCL mesh (d). Masson´s trichrome: The spaces in between implant material are infiltrated by connective tissue (e, g).

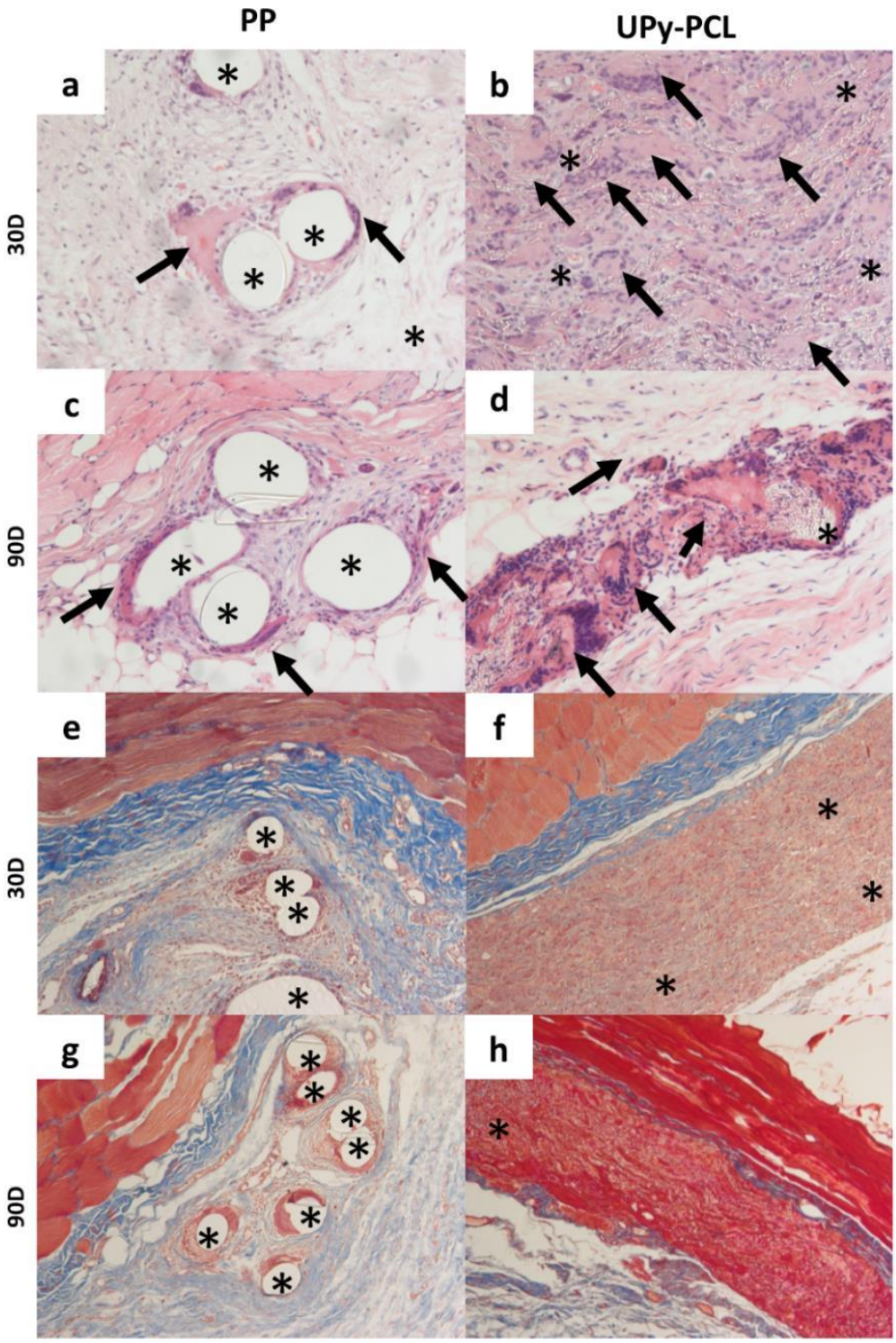

Fig. 7 Representative images of hematoxylin and eosin (a-d, 200X) and Masson´s trichrome stain (e-h, 100X) of PP and UPy-PCL explants in rabbits. Mesh fibers are indicated by asterisks and foreign body giant cells (FBGC) by black arrows. At 30 days, FBGC are visible around the PP fibers (a) and deeper over the entire width of the UPy-PCL mesh (b). Later on, more FBGC are evident around PP fibers (c). At 90 days, only a few clusters of UPy-PCL fibers are visible microscopically and less FBGC compared to 30 days. Connective tissue was observed on Masson's trichrome (blue). PP explants showed more collagen at 30 (e) and 90 (g) days compared to UPy-PCL (e, h). In UPy-PCL explants, the mesh is replaced by newly formed tissue with few collagen (blue) (h).

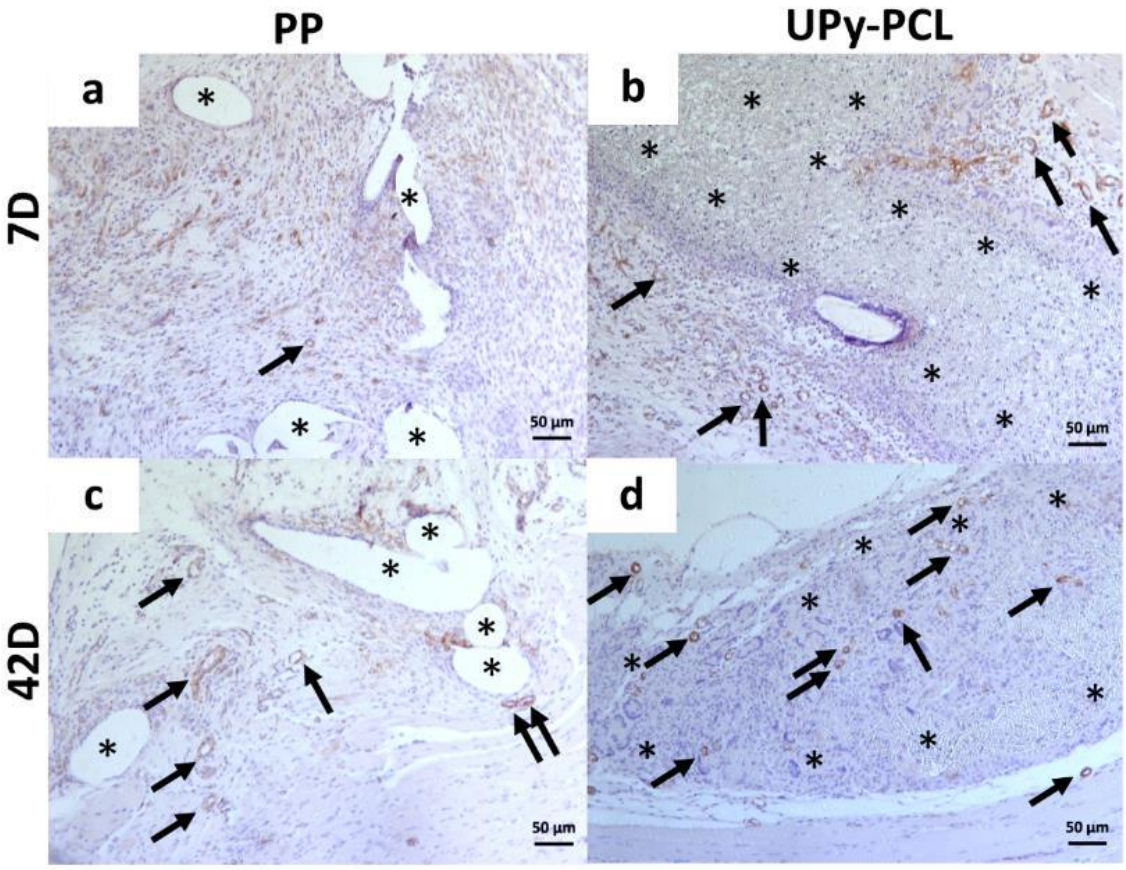

Fig. 8 Representative images of α- SMA stains of rat explants. The pores of PP mesh are located between open areas where the PP has been dissolved (marked with an asterisk) (a, c). The relatively larger pores of PP mesh are infiltrated by tissue and vessels (arrows). At 7 days vessels (arrows) are restricted to the UPy-PCL mesh surface (b), yet at later time-points vessels are present deeply into the UPy-PCL scaffold (d). Clusters of the UPy-PCL mesh fibers are marked with an asterisk.

4. Discussion

The primary goal of this experiment was to measure compliance of the abdominal wall reconstructed with novel electrospun UPy-PCL. Passive biomechanical tests identify the force at disruption and compliance over different areas along the force-elongation curve. In contrast to polypropylene, UPyPCL had a disruption problem, clinically translating in herniation in 50% of the animals, irrespective of the amount of polymer used. In the other half of animals, the explants seem to perform well with a compliance in the physiologic range. Visible degradation of the material was paralleled with a vigorous foreign body reaction fading out as the material was being degraded.

Electrospinning enables customizing a variety of parameters and create a microstructure supporting cell adherence, interactions and creation of an auxiliary environment. Rather than a passive support of textile meshes, these matrices can stimulate tissue regeneration, both by their three-dimensional structure and/or bioactivation [29]. We looked into the use of PCL as this polymer is biocompatible and yields a mild inflammatory response [24]. When electrospun into matrices, it facilitates cell infiltration

and integrates well into the host, without signs of encapsulation, which eventually may reduce graft-related complications [21,37]. Thanks to the versatility of electrospinning, implants may be tailored so that they mimic the biomechanical properties of native tissue. We showed in a previous study that the tested UPy-PCL mesh when used in rats with reinforced abdominal wall repairs preserve on the short term a stiffness similar to that of non-injured abdominal wall [31]. This apparently on the longer term and with a more challenging defect is still so yet there is problem of failure. Polypropylene is non-degradable and is known to provoke a chronic inflammatory process, which in rats coincided with stiffening as widely demonstrated before [6]. Unfortunately, the strategy of using a degradable polymer resulted in surgical failure in half of the animals. UPy-PCL is locally predominantly degraded by enzyme accelerated oxidative pathways [25]. When partially degraded it undergoes intracellular digestion by inflammatory cells, including FBGC [38,39]. We confirmed a vigorous inflammatory response to UPy-PCL as reported earlier [31]. We hypothesized that herniation was due to a too fast degradation process, yet we could not overcome that by increasing the polymer load. Probably, because its degradation mechanism is a combination of surface and bulk erosion [25]. PCL was earlier shown to persist for six months without remarkable decrease of mass loss in rabbit bone reconstruction [21], so we assumed it would be suitable for abdominal wall repair, allowing plenty time for constructive remodeling and proper connective tissue maturation. In contrast, in our study degradation was already macroscopically visible from 30 days onwards. Faster degradation compared to what was reported in the literature could be due to the UPy linker. This could modify the host response, change the degradation pathway and accelerate degradation. Additionally, its use as a substitute for the abdominal wall rather than cortical bone replacement, which obviously are completely different biomechanical conditions [21]. Other possible explanation is the variable characteristics of electrospun meshes in different spinning conditions which end in different surface and inter-fibre spaces. We admit that we could not quantify the degradation process in detail. First, in animals with herniation we could not study degradation until full degradation, as animals had to be sacrificed earlier given potential suffering. Second, we used a chemical assay, which is apparently not sensitive enough in vivo, as it did not detect any UPy-PCL anymore from 30 days in rabbits, whereas microscopically elements of UPy-PCL fibers were persisting up to 90 days.

Late persistence of the polymer does apparently not prevent mechanical failure as the construct loses its strength. We interpret these findings as if the remodeling process coinciding with degradation is not able to sufficiently reconstitute new tissue strong enough in the timeframe defined by the speed of polymer degradation. We observed faster UPy-PCL mesh degradation in rabbits compared to rats. This may be due to a variety of reasons, such as differences in the immune system and/or extracellular matrix metabolism. Obviously also another factor has played a role, since the same implant dimensions were used in both species, hence a higher material/body mass ratio was used in rats therefore proportionally more material was to be degraded in the rat. Additionally, there are different loading conditions in both animals, all playing a role in the degradation [40]. In UPy-PCL explants, there was a vigorous inflammatory reaction with abundant FBGC around a dense fiber network. The intensity of the inflammatory reaction to the

simple PCL material is reported to be limited [24], whereas when linked with UPy obviously it provokes a more vigorous reactions, for as far unrelated experiments can be compared [31].

In our control animals implanted with polypropylene, we observed that in rats PP-explants were stiffer than native tissue, yet in rabbits the compliance fell in the normal range. In most of our previous experiments, polypropylene had an adverse effect on compliance, the magnitude of it determined by the porosity, weight, or other mesh characteristics [41]. Restorelle is one of the polypropylene textile implants associated with a milder host response in several animal models [42], yet still in rats the abdominal wall compliance was not in the normal range. Our experiment was not designed to explore why this is so different in both animal models. However we plan to look deeper into this, using biochemical and/or molecular techniques e.g. to quantify collagen types and amounts, more quantitative morphometry, measuring secondary effects of stress shielding, or others. Obviously, that research may still not discount for the essential differences between two animal models, such as intraabdominal pressure, the different proportion of the surface of the implant to the entire abdominal wall, to name only a few. We also observed faster degradation of UPy-PCL in rabbits than in rats. For degradation, next to size and pressure differences, also the difference in inflammatory response between species may play a role.

We acknowledge limitations in our study, some already addressed above. Further, biaxial biomechanical testing would have been more relevant, however the limited sample dimensions forced us to use uniaxial testing. A sham procedure with a non-repaired open defect was not possible, since it would lead to immediate herniation and suffering of animals. Also, the low number of non-herniated specimens compromised the statistical power. Neither did we compare mesh with and without UPy motifs, nor did we yet explore other UPy-polymers – an endeavor we meanwhile undertook using UPy modified polycarbonate, which is more resistant to degradation. From our preliminary in vitro studies, we opt for further testing UPy modified polycarbonate which had longer lasting in vitro. On the other hand, this study investigates for the first time UPy-PCL mesh to reconstruct an abdominal wall defect. Faster degradation and herniation in rabbits proved species diversity and/or the importance of using different models. We compared our results to normal healthy tissue and also light-weighted polypropylene which has become the reference polymer in textile meshes. We determined that doubling the fiber diameter and mesh thickness did not improve outcomes. We confirmed degradation, visually, by microscopy and GPC. When the material is completely degraded there was no inflammatory reaction anymore. At last, when the implant and reconstruction do not fail, the biomechanical properties of explants were equal to native tissue.

5. Conclusions

We evaluated the performance of degradable UPy-PCL-electrospun meshes for repairing abdominal wall defects. In half of the animals in whom the repair was effective, UPy-PCL explants were as compliant as native tissue. Unfortunately, the other half of animals had visible herniation. We think this was mainly due to fast degradation.

Degradation histologically coincided with the presence of FBGC. We aimed to prolong endurance by increasing the amount of material, however in vain.

Acknowledgement

We thank the European Commission for supporting this research via the framework program 7 (BiP-UPy; NMP3-LA-2012-310389). Rosita Kinnart, Ivan Laermans (Centre for surgical technologies, KU Leuven, Leuven, Belgium), Catherine Luyten, Petra Stevens (Department of Development and Regeneration, KU Leuven) and Leen Mortier (University Hospitals Leuven) are thanked for logistic support. Manuel Zündel and Edoardo Mazza (Institute of Mechanical Systems, ETH Zurich, Zurich, Switzerland; EMPA, Swiss Federal Laboratories for Materials Science and Technology, Dübendorf, Switzerland) are thanked for earlier biomechanical characterization of the mesh. Monica Ramos Gallego and Jakob Vange (Coloplast A/S, Global R&D, Biomaterials, Holtedam, Humlebæk, Denmark) are thanked for mesh spinning and SEM characterization.

Funding

This work has been entirely supported by a grant from the European Commission: Seventh framework program (BiP-UPy; NMP3-LA-2012-310389). LH, MC, RR, RW, AO, PD, BA, TM, AB, JD report grant support from the European Commission: Seventh framework program (BiP-UPy; NMP3-LA-2012-310389) during the conduct of the study. The research program of JD has received support in the research period via service agreements handled by the transfer office “Leuven Research and Development” from Clayton Utz (Australia). MA has no conflict of interest.

Ethical approval

KU Leuven P064/2013

Appendix A. Supplementary material

Supplementary data associated with this article can be found in the online version at doi:10.1016/j.jmbbm.2018.08.026.

References

[1] Primatesta, P., Goldacre, M.J., Inguinal hernia repair: incidence of elective and emergency surgery, readmission and mortality., Int. J. Epidemiol. 25 (1996) 835–839. doi:10.1093/ije/25.4.835.

[2] Simons, M.P., Aufenacker, T., Bay-Nielsen, M., Bouillot, J.L., Campanelli, G., Conze, J., de Lange, D., Fortelny, R., Heikkinen, T., Kingsnorth, A., Kukleta, J., Morales-Conde, S., Nordin, P., Schumpelick, V., Smedberg, S., Smietanski, M., Weber, G., Miserez, M., European Hernia Society guidelines on the treatment of inguinal hernia in adult patients, Hernia. 13 (2009) 343–403. doi:10.1007/s10029-009-0529 7.

[3] Grant, A., Go, P., Fingerhut, A., Kingsnorth, A., Merello, J., O'Dwyer, P., Payne, J., Repair of groin hernia with synthetic mesh: meta-analysis of randomized controlled trials., Ann. Surg. 235 (2002) 322–332. doi:10.1097/00000658-200203000-00003.

[4] Brown, C.N., Finch, J.G., Which mesh for hernia repair?, Ann. R. Coll. Surg. Engl. 92 (2010) 272–278. doi:10.1308/003588410X12664192076296.

[5] Peeters, E., Spiessens, C., Oyen, R., De Wever, L., Vanderschueren, D., Penninckx, F., Miserez, M., Sperm motility after laparoscopic inguinal hernia repair with lightweight meshes: 3-Year follow-up of a randomized clinical trial, Hernia. 18 (2014) 361–367. doi:10.1007/s10029-012-1028-9.

[6] Cobb, W.S., Kercher, K.W., Heniford, B.T., The argument for lightweight polypropylene mesh in hernia repair., Surg. Innov. 12 (2005) 63–69. doi:10.1177/155335060501200109.

[7] Mukthinath, G., Shankar, K., Bhaskaran, A., A comparative study of postoperative complications of lightweight mesh and conventional prolene mesh in Lichtenstein hernia repair, 4 (2016) 2130–2134.

[8] Bringman, S., Conze, J., Cuccurullo, D., Deprest, J., Junge, K., Klosterhalfen, B., Parra-Davila, E., Ramshaw, B., Schumpelick, V., Hernia repair: The search for ideal meshes, Hernia. 14 (2010) 81–87. doi:10.1007/s10029-009-0587-x.

[9] Braghirolli, D.I., Steffens, D., Pranke, P., Electrospinning for regenerative medicine : a review of the main topics, Drug Discov. Today. 19 (2014) 743–753. doi:10.1016/j.drudis.2014.03.024.

[10] Boudriot, U., Dersch, R., Greiner, A., Wendorff, J.H., Electrospinning Approaches Toward Scaffold Engineering — A Brief Overview, Artif. Organs. 30 (2006) 785–792.

[11] Woo, K.M., Chen, V.J., Ma, P.X., Nano-fibrous scaffolding architecture selectively enhances protein adsorption contributing to cell attachment, J. Biomed. Mater. Res. - Part A. (2003).

[12] Vashaghian, M., Ruiz-Zapata, A.M., Kerkhof, M.H., Zandieh-Doulabi, B., Werner, A., Roovers, J.P., Smit, T.H., Toward a New Generation of Pelvic Floor Implants With Electrospun Nanofibrous Matrices: A Feasibility Study, Neurourol. Urodyn. 36 (2017) 565–573. doi:10.1002/nau.

[13] Andersson, A.-S., Backhed, F., Euler, A. Von, Richter-dahlfors, A., Sutherland, D., Kasemo, B., Nanoscale features influence epithelial cell morphology and cytokine production, Biomaterials. 24 (2003) 3427–3436. doi:10.1016/S0142-9612(03)00208-4.

[14] Yeo, K.K., Park, T.H., Park, J.H., Chang, C.H., Kim, J., Seo, S.W., Histologic Changes of Implanted Gore BioA in an Experimental Animal Model, 2014 (2014).

[15] Peeters, E., Barneveld, K.W.Y. Van, Schreinemacher, M.H., Hertogh, G. De, Ozog, Y., Bouvy, N., Miserez, M., One-year outcome of biological and synthetic bioabsorbable meshes for augmentation of large abdominal wall defects in a rabbit model, J. Surg. Res. 180 (2013) 274–283. doi:10.1016/j.jss.2013.01.025.

[16] Lopez-Cano, M., Armengol, M., Quiles, M.T., Biel, A., Velasco, J., Huguet, P., Gil, X., Mestre, A., Delgado, L.M., Gil, F.X., Arbo, M.A., Preventive midline laparotomy closure with a new bioabsorbable mesh : An experimental study, 1 (2013) 0–9. doi:10.1016/j.jss.2012.05.041.

[17] Symeonidis, D., Efthimiou, M., Koukoulis, G., Athanasiou, E., Mamaloudis, I., Tzovaras, G., Open inguinal hernia repair with the use of polyglycolic acid / trimethylene carbonate absorbable mesh : a critical update of the long-term results, (2013) 85–87. doi:10.1007/s10029-012-1016-0.

[18] Agrusa, A., Romano, G., Frazzetta, G., De Vita, G., Silvia, D.G., Chianetta, D., Di Buono, G., Sorce, V., Gulotta, G., Case Report Hiatal Hernia Repair with Gore Bio-A Tissue Reinforcement : Our Experience, 2014 (2014). doi:10.1155/2014/851278.

[19] Rosen, M.J., Bauer, Ã.J.J., Harmaty, M., Carbonell, A.M., Cobb, W.S., Matthews, B., Goldblatt, M.I., Selzer, D.J., Poulose, B.K., Hansson, Ã.Ã.B.M.E., Rosman, C., Chao, J.J., Jacobsen, G.R., Multicenter , Prospective , Longitudinal Study of the Recurrence , Surgical Site Infection , and Quality of Life After Contaminated Ventral Hernia Repair The COBRA Study, 265 (2017) 205–211. doi:10.1097/SLA.0000000000001601.

[20] López-cano, M., Pereira, J.A., Lozoya, R., Feliu, X., Villalobos, R., Navarro, S., Antonia, M., Armengol-carrasco, M., PREBIOUS trial : A multicenter randomized controlled trial of PREventive midline laparotomy closure with a BIOabsorbable mesh for the prevention of incisional hernia : Rationale and design, Contemp. Clin. Trials. 39 (2014) 335–341. doi:10.1016/j.cct.2014.10.009.

[21] Lam, C.X.F., Hutmacher, D.W., Schantz, J.-T., Woodruff, M.A., Teoh, S.H., Evaluation of polycaprolactone scaffold degradation for 6 months in vitro and in vivo., J. Biomed. Mater. Res. A. 90 (2008) 906–919. doi:10.1002/jbm.a.32052.

[22] Mrówczynski, W., Mugnai, D., Valence, S. De, Porcine carotid artery replacement with biodegradable electrospun poly-e-caprolactone vascular prosthesis, (2013) 210–219. doi:10.1016/j.jvs.2013.03.004.

[23] Chakroff, J., Kayuha, D., Henderson, M., Johnson, J., Development and Characterization of Novel Electrospun Meshes for Hernia Repair, SOJ Mater. Sci. Eng. 2 (2015) 1–9. https://www.researchgate.net/profile/Jed_Johnson/publication/276291238_Development_and_Characterization_ of_Novel_Electrospun_Meshes_for_Hernia_Repair/links/5556158a08aeaaff3bf5ed09.pdf.

[24] Palmer, J.A., Abberton, K.M., Mitchell, G.M., Morrison, W.A., Macrophage phenotype in response to implanted synthetic scaffolds: An immunohistochemical study in the rat, Cells Tissues Organs. 199 (2014) 169–183. doi:10.1159/000363693.

[25] Brugmans, M.C.P., S, S.H.M., Cox, M.A.J., Nandakumar, A., Bosman, A.W., Mes, T., Janssen, H.M., Bouten, C.V.C., Baaijens, F.P.T., Driessen-mol, A., Hydrolytic and oxidative degradation of electrospun supramolecular biomaterials : In vitro degradation pathways, 27 (2015) 21–31. doi:10.1016/j.actbio.2015.08.034.

[26] Kieltyka, R.E., Bastings, M.M.C., Van Almen, G.C., Besenius, P., Kemps, E.W.L., Dankers, P.Y.W., Modular synthesis of supramolecular ureidopyrimidinone–peptide conjugates using an oxime ligation strategy, Chem. Commun. 48 (2012) 1452–1454. doi:10.1039/c1cc14728e.

[27] Dankers, P.Y.W., Adams, P.J.H.M., Löwik, D.W.P.M., Van Hest, J.C.M., Meijer, E.W., Convenient solid-phase synthesis of ureido-pyrimidinone modified peptides, European J. Org. Chem. 2007 (2007) 3622–3632. doi:10.1002/ejoc.200700191.

[28] De Feijter, I., Goor, O., Hendrikse, S., Comellas-Aragonès, M., Söntjens, S., Zaccaria, S., Fransen, P., Peeters, J., Milroy, L.-G., Dankers, P., Solid-Phase-Based Synthesis of Ureidopyrimidinone–Peptide Conjugates- for Supramolecular Biomaterials, Synlett. 26 (2015) 2707–2713. doi:10.1055/s-0035-1560520.

[29] Mollet, B.B., Comellas-Aragonès, M., Spiering, a. J.H., Söntjens, S.H.M., Meijer, E.W., Dankers, P.Y.W., Sontjens, S.H.M., Meijer, E.W., Dankers, P.Y.W., A modular approach to easily processable supramolecular bilayered scaffolds with tailorable properties, J. Mater. Chem. B. 2 (2014) 2483. doi:10.1039/c3tb21516d.

[30] Bastings, M.M.C., Koudstaal, S., Kieltyka, R.E., Nakano, Y., Pape, A.C.H., Feyen, D.A.M., Van Slochteren, F.J., Doevendans, P.A., Sluijter, J.P.G., Meijer, E.W., Chamuleau, S.A.J., Dankers, P.Y.W., A

fast pH-switchable and self-healing supramolecular hydrogel carrier for guided, local catheter injection in the infarcted myocardium, 3 (2014) 70–78. doi:10.1002/adhm.201300076.

[31] Hympanova, L., Mori da Cunha, M.G.M.C., Rynkevic, R., Zündel, M., Gallego, M.R., Vange, J., Callewaert, G., Urbankova, I., Van der Aa, F., Mazza, E., Deprest, J., Physiologic musculofascial compliance following reinforcement with electrospun polycaprolactone-ureidopyrimidinone mesh in a rat model, J. Mech. Behav. Biomed. Mater. 74 (2017) 349–357. doi:https://doi.org/10.1016/j.jmbbm.2017.06.032.

[32] Ozog, Y., Konstantinovic, M.L., Werbrouck, E., De Ridder, D., Mazza, E., Deprest, J., Shrinkage and biomechanical evaluation of lightweight synthetics in a rabbit model for primary fascial repair, Int Urogynecol J. (2011) 1099–1108. doi:10.1007/s00192-011-1440-1.

[33] Konstantinovic, M.L., Lagae, P., Zheng, F., Verbeken, E.K., De Ridder, D., Deprest, J., Comparison of host response to polypropylene and non-cross-linked porcine small intestine serosal-derived collagen implants in a rat model, BJOG An Int. J. Obstet. Gynaecol. 112 (2005) 1554–1560. doi:10.1111/j.1471-0528.2005.00688.x.

[34] Claerhout, F., Verbist, G., Verbeken, E., Konstantinovic, M., De Ridder, D., Deprest, J., Fate of collagen-based implants used in pelvic floor surgery: A 2-year follow-up study in a rabbit model, Am. J. Obstet. Gynecol. 198 (2008). doi:10.1016/j.ajog.2007.05.032.

[35] Toosie, K., Gallego, K., Stabile, B.E., Schaber, B., French, S., De Virgilio, C., Fibrin glue reduces intra-abdominal adhesions to synthetic mesh in a rat ventral hernia model, Am. Surg. 66 (2000) 41–45.

[36] Ozog, Y., Konstantinovic, M.L., Werbrouck, E., Persistence of polypropylene mesh anisotropy after implantation: An experimental study, BJOG An Int. J. Obstet. Gynaecol. 118 (2011) 1180–1185. doi:10.1111/j.1471- 0528.2011.03018.x.

[37] Gomes, S.R., Rodrigues, G., Martins, G.G., Roberto, M. a., Mafra, M., Henriques, C.M.R., Silva, J.C., In vitro and in vivo evaluation of electrospun nanofibers of PCL, chitosan and gelatin: A comparative study, Mater. Sci. Eng. C. 46 (2015) 348–358. doi:10.1016/j.msec.2014.10.051.

[38] Anderson, J.M., McNally, A.K., Biocompatibility of implants: Lymphocyte/macrophage interactions, Semin. Immunopathol. 33 (2011) 221–233. doi:10.1007/s00281-011-0244-1.

[39] Woodruff, M.A., Hutmacher, D.W., The return of a forgotten polymer - Polycaprolactone in the 21st century, Prog. Polym. Sci. 35 (2010) 1217–1256. doi:10.1016/j.progpolymsci.2010.04.002.

[40] Li, Y., Chu, Z., Li, X., Ding, X., Guo, M., Zhao, H., Yao, J., Wang, L., Cai, Q., Fan, Y., The effect of mechanical loads on the degradation of aliphatic biodegradable polyesters, Regen. Biomater. 4 (2017) 179–190. doi:10.1093/rb/rbx009.

[41] Röhrnbauer, B., Ozog, Y., Egger, J., Werbrouckb, E., Deprest, J., Mazza, E., Combined biaxial and uniaxial mechanical characterization of prosthetic meshes in a rabbit model, J. Biomech. 46 (2013) 1626–1632. doi:10.1016/j.jbiomech.2013.04.015.

[42] Brown, B.N., Mani, D., Nolfi, A.L., Liang, R., Abramowitch, S.D., Moalli, P.A., Characterization of the host inflammatory response following implantation of prolapse mesh in rhesus macaque, Am. J. Obstet. Gynecol. 213 (2015) 668.e1-668.e10. doi:10.1016/j.ajog.2015.08.002

Supplementary figures

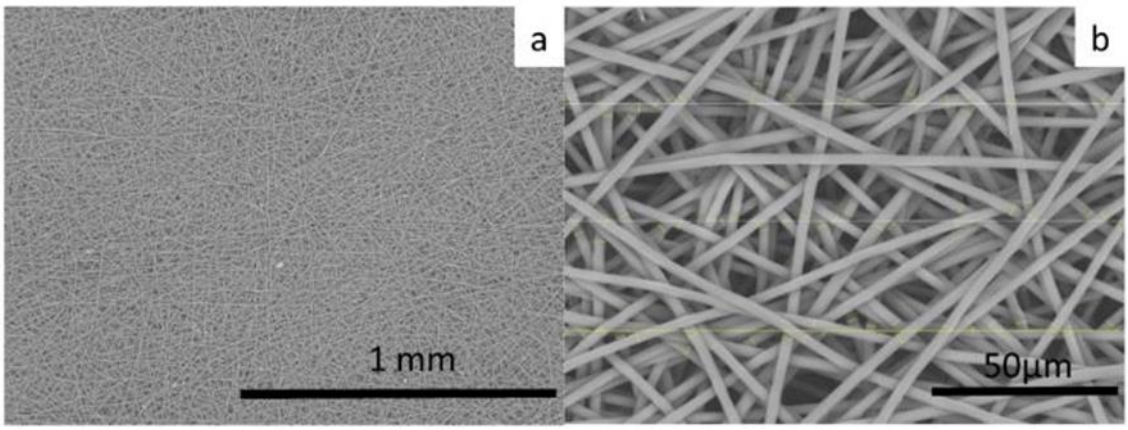

Supplementary figure 1. (a) UPy-PCL electrospun mesh under scanning electron microscope with random fiber orientation (100x magnification) and (b) example of fiber size measurement (1200x magnification).

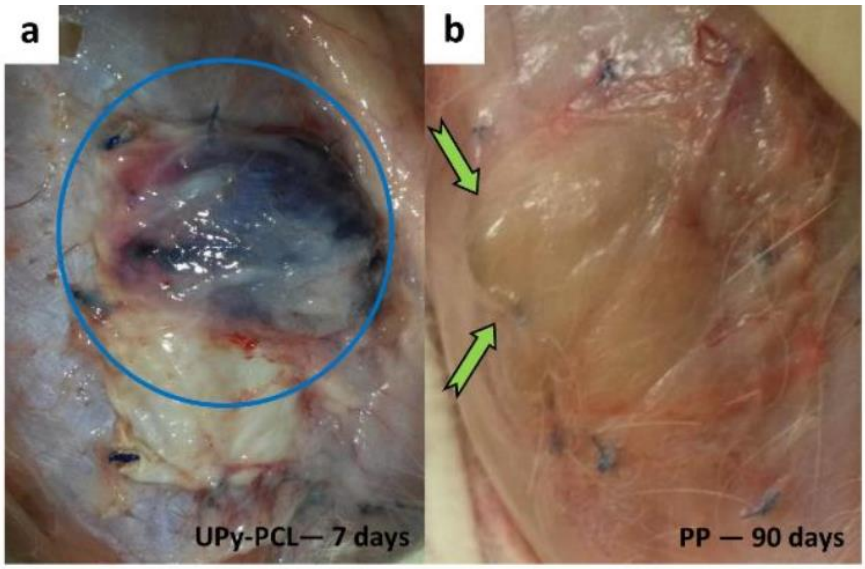

Supplementary figure 2. (a) Serosanguinolent fluid collection (blue circle) in a rat 7 days after UPy-PCL implantation. There were no arguments for infection. (b) Subclinical herniation in polypropylene group (arrow) bulging laterally in between two sutures (90 days).

CHAPTER 11

SUMMARY

Pelvic floor disorders (PFD), including Pelvic Organ Prolapse (POP), can have a significant negative impact on a woman's daily activities and quality of life. Many surgical techniques to correct vaginal prolapse have been proposed but their long-term benefits have been poorly evaluated. To improve the currently perceived poor anatomical outcomes of native tissue repairs, surgeons have turned to mesh-augmented repairs. However, the vaginal insertion of mesh has been associated with a high rate of graft related complications (GRCs). It therefore seems that the ideal implant has not been developed yet. To do so, proper knowledge of the mechanical properties of vaginal tissue and candidate implants, that would match the host tissue as closely as possible, seems required.

The herein presented research consists of three parts: two experimental parts (*in vitro* as well as *ex vivo*) and one computational (*in silico*) part. In the first *in vitro* part we characterized the mechanical properties of novel electrospun implants *via* mechanical testing (Chapter 2 and Chapter 3). Electrospun implants are a new strategy for augmenting repairs. They mimic the extracellular matrix, and this should improve integration into the host. In the second *in vivo* part we evaluate the host-response to these electrospun implants in representative animal models (rats, rabbits and sheep) (Chapter 4 and Supplementary paper 1 and 2). In those studies, we use a clinical light weight synthetic durable textile polypropylene implant, i.e. Restorelle®, Coloplast as a control. To document how vaginal wall and pelvic floor soft tissues recover one year after vaginal birth, comprehensive biomechanical and histological analysis was conducted on sheep pelvic floor soft tissues (Chapter 5, Chapter 6). Finally, in the third part of the work, the experimental data obtained in previous chapters, was used to create an adequate material model for the *in silico* simulations, which are intended to simulate *ex vivo* experiments in an *in silico* environment (Chapter 7, Chapter 8). Finally, using magnetic resonance (MR) images a 3-dimensional geometrical model of the ovine pelvic floor cavity was created (Chapter 9) for further *in silico* simulations.

The mechanical behavior of novel prototype electrospun implants made from supramolecular polymers based on Ureido-Pyrimidinone (UPy)-moieties and a poly(ε-caprolactone) (PCL) backbone with different fiber diameters (2.0, 2.3 and 2.6 µm) were investigated under different conditions. An *in vitro* degradation process and repetitive loadings were used to evaluate their mechanical performance. For this part of the study, a wider range of meshes used for hernia surgery and POP repair were tested. The results showed that novel electrospun implants had a similar mechanical behavior, despite differences in fiber diameter. They were more compliant than the reference PP mesh Restorelle®. Also they became more compliant in wet conditions and had an anisotropic behavior. As expected, the behavior of PP meshes was pH independent. However, degradation induced significant mechanical property changes in all UPy-PCL and other

tested meshes. Also, all meshes underwent permanent plastic deformation, which has been previously named as a potential cause of GRCs.

Further, the novel implants were used in preclinical *in vivo* experiments. Rats were used for initial screening purposes, followed by rabbits, because of their dimensions and higher intra-abdominal pressure. The latter may be more representative from a biomechanical perspective. Finally, sheep were used, which permit vaginal and abdominal surgery. Explants and native tissue samples (taken from the opposite side of the abdominal wall) were tested using uniaxial tensile testing (rats and rabbits) and larger specimens by ball burst testing (sheep). Outcome measures were stiffness and elongation, obtained from load elongation curves. The primary outcome in the small animal models was the occurrence of re-herniation (considered as surgical failure). Samples for further biomechanical testing were collected only from the animals without clinical reherniation, and without graft related complications.

Explants from *rats* implanted with electrospun UPy-PCL mesh to reinforce a primarily sutured defect in the abdominal wall, harvested 7 and 42 days later, were more compliant than polypropylene-augmented (Restorelle®) explants and primary sutured repair. At 42 days Restorelle® and native tissue primary repair explants became stiffer compared to native unoperated abdominal wall muscles. UPy-PCL abdominal explants were as compliant as native tissue. On histology a vigorous inflammatory reaction was observed.

UPy-PCL and PP Restorelle® implants were also used in a gap-bridging model, which is closer to an incisional type of hernia. Large full thickness defects were created and overlaid with mesh in rats (7, 42d after implantation) and rabbits (with a longer implantation period of 30 and 90 days). With this challenging model we saw high herniation rates, i.e. in almost one out of three to two animals. Because of this high failure rate, we additionally made alternative PCL-electrospun implants. They had thicker fiber diameters or were thicker on itself, in order to provide additional material strength. However, this was in vain: herniation rates remained as high. In the ones not failing, early stage compliance, both in rats and rabbits, of UPy-PCL and PP abdominal explants were in the range of native tissue. However, at late stages in rats, PP explants became stiffer than UPy-PCL explants and native tissue. Again, because of the poor strength, which we tied to the fast degradation process, we considered to use electrospun implants based on other slower resorbable polymers, e.g. polycarbonate (PC), and as an alternative strategy, also *non-resorbable* polyurethane electrospun implants.

With those we moved to the sheep model and reinforced the posterior vaginal wall and assessed outcomes at 60 and 180 days. Reference material was again the PP Restorelle® mesh. Further non-absorbable polyurethane (PU) and a polycarbonate modified with Ureido-Pyrimidinone (UPy-PC) electrospun meshes were used. In none of the sheep, there were GRCs after vaginal implantation. Therefore, all vaginal explants could be used for mechanical testing. Both electrospun meshes (PU and UPy-PC) were as compliant as native tissue at both timepoints. Restorelle® PP explants were stiffer than native tissue at 60 days, yet at 180 days explants were again as compliant as native tissue.

Vaginal birth induced trauma plays an important role in the origin of POP. The close anatomical relationship between the vaginal wall on the one hand, and the bladder and

rectum on the other hand, often contributes to the simultaneous development of functional problems in these adjacent organs, leading to urinary incontinence, defecatory problems and sexual dysfunction. This part of the research includes observations on how the vaginal wall and pelvic floor soft tissues change during pregnancy, and how they recover one year after vaginal delivery when being compared to findings in virgin sheep.

Correlations between mechanical parameters and histological analysis were analyzed. Outcome measures of the mechanical properties were the Young's modulus, ultimate stress and elongation, as obtained from stress-strain curves. Further for histological analysis we measured tissue thickness, total collagen (%), elastin (%), and smooth muscle (%) contents. All pelvic floor soft tissues undergo profound histologic and mechanical changes, particularly during pregnancy and do not recover to original levels one year after vaginal delivery. Significant regional differences were identified in the ovine vaginal wall. The proximal vagina was stiffer than the distal, irrespective of the reproductive status. The pregnant sheep vagina was more compliant than the vagina of parous or virgin sheep, coinciding with lower total collagen and higher elastin levels and a higher amount of smooth muscle cells. Yet parous sheep vaginal tissue was less compliant than that of virgins. The cervix in pregnant sheep was more compliant than that of virgin or parous sheep. In contrast, the bladder and rectum became stiffer. Bladder and rectum contained more total collagen, less elastin fibers and less smooth muscle cells. One year after vaginal delivery the uterus was more compliant than in virgin sheep. The Young's moduli in the comfort and stress zones differed significantly. Compared to virgin ewes, the parous sheep uterus contained less total collagen and more elastin fibers. Their rectum and bladder had a higher ultimate stress, elastin fibers and smooth muscle cell counts were significantly lower in these tissues, yet the total collagen content was higher which is in agreement with a reduced compliance. Given the obvious correlation between histologic features and mechanical properties for the pelvic floor soft tissues tested, we concluded that collagen is largely responsible for soft tissue tensile strength and elastin for tissue elasticity.

The results obtained in the sheep vaginal specimens were used to create a realistic material model for further simulations. In this study a strategy to correlate tensile testing experiments with a material model capable to capture the nonlinear response over a large strain range was proposed. Simpler versions of the HGO model (Holzapfel-Gasser-Ogden) were used to describe the mechanical behavior of the samples under uniaxial load, where constant parameters μ (shear modulus, related to the matrix content), k_1 and k_2 (reflect the fibers contribution) define the mechanical response. For convenience, we defined the dimensionless ratio ξ as a suitable regulator for the matrix and fiber contributions. We called it the Histologically-Motivated (HM) coefficient as it is well correlated with histological data, linking the nonlinear mechanical behavior (tensile test) with the tissue morphology (histology). The HM coefficient from uniaxial data was applied for multiaxial loading simulations. Therefore, the mechanical properties of the ball burst specimens were predicted through basic histology, without direct mechanical measurements under those loading conditions. A 3D geometrical model of the ovine pelvic floor cavity was created, using MR images and can now be used for future dynamic simulations of the pelvic floor soft tissues applying HM coefficient for the soft tissues.

In conclusion, this project made several important observations. First, the mechanical behavior of novel electrospun meshes under different conditions was comparable to that of native tissues, in terms of compliance and anisotropy. *In vivo*, degradable UPy-PC and durable PU electrospun meshes did not cause graft related complications after vaginal reconstruction in sheep. Both induce a biomechanical behavior comparable to that of native tissue. The ovine vaginal wall and pelvic floor soft tissues undergo significant histologic and mechanical changes during pregnancy and do not recover to original levels one year after. A parallel between mechanical properties of the soft tissues and histological features was established. Finally, we presented a Histologically-Motivated coefficient which may be very promising in estimating the mechanical properties of the tissue *via* histological information. The HM coefficient reflects the pathophysiological state of the soft tissues and can therefore be used in complex simulation environments.

SAMENVATTING

Bekkenbodemdysfuncties (Pelvic Floor Disoders, PFD), inclusief vaginale verzakking (Pelvic Organ Prolapse, POP), hebben een aanzienlijke negatieve impact op de dagelijkse activiteiten en levenskwaliteit van een vrouw. Er zijn veel chirurgische technieken die gebruik maken van natief weefsel om POP te corrigeren, maar de langetermijns resultaten zijn niet erg goed. Om die verbeteren grepen chirurgen naar implantaten (ook “matjes” genoemd), omdat die bij liesbreukherstel de uitkomsten verbeteren. Wanneer dit type implantaten echter vaginaal ingebracht worden lokken ze vaker dan gewenst complicaties uit (graft related complications; GRCs). Dit is in zeker mate te wijten aan de aard van het implantaat. Het heeft er alles van dat het ideale implantaat nog niet is ontwikkeld. Om dit te mogelijk te maken, is vooreerst een goede kennis van de mechanische eigenschappen van zowel het vaginaal weefsel als die van het mogelijkse implantaat, nodig, en zijn die bij voorkeur op elkaar afgestemd.

Ons onderzoek bestaat uit drie delen: twee delen zijn experimenteel (*in vitro* evenals *ex vivo*) en één is computationeel (*in silico*). In het eerste *in vitro* deel karakteriseerden we de mechanische eigenschappen van een nieuw type elektrisch gesponnen implantaat door middel van mechanische testen (hoofdstukken 2 en 3). Elektrisch gesponnen implantaten bootsen de natieve extracellulaire matrix na, want de integratie van het implant in de gastheer zou moeten verbeteren. In het tweede experment evalueerden we de *in vivo* gastheer-respons op dit type implantaten in representatieve diermodellen (ratten, konijnen, evenals schapen) (hoofdstuk 4 en supplementaire publicaties 1 en 2). In deze studies gebruikten we als referentie product een klinisch lichtgewicht synthetisch, niet-resorbeerbaar, textiel polypropyleen implantaat (Restorelle ®, Coloplast). Wij voerden in hoofdstuk 5 en 6 uitvoerige biomechanische en histologische studies uit om de karakteristieken van de vaginawand en bekkenbodemorganen te bepalen, dit één jaar na normale vaginale bevalling. Tenslotte worden in het derde deel van deze thesis de experimenteel verkregen gegevens uit vorige hoofdstukken, gebruikt om een in silico model te ontwikkelen, waarop dan de ex en in vivo experimenten op te simuleren (Hoofdstuk 7 en 8). In hoofdstuk 9 creëerden we een 3-dimensionaal geometrisch model op basis van magnetische resonantie (MR) beelden van de bekkenbodem van schapen, voor latere *in silico* simulaties.

Het mechanische gedrag van deze nieuwe elektrisch gesponnen implantaten gemaakt van supramoleculaire polymeren op basis van Ureïdo-pyrimidinone (UPy) - en poly-ε-caprolactone (PCL) met verschillende vezeldiameters (2,0, 2,3 en 2,6 μm) werden onderzocht onder verschillende omstandigheden. *In vitro* werd het afbraakproces en repetitieve belastingen gesimuleerd en het effect ervan op hun mechanische eigenschappen. Voor dit deel van de studie werd een meerdere meshes die gebruikt worden voor hernia- en POP- herstel getest. Nieuwe elektrisch gesponnen implantaten vertoonden een gedrag dat vergelijkbaar was aan dat van natief weefsel, ongeacht de fiber-diameter. Ze waren complianter dan het referentie-PP-netje

Restorelle ® . In vochtige toestand ware nog complianter en ze waren bovendien anisotroop. Zoals verwacht waren de eigenschappen van PP meshes pH onafhankelijk. Voor UPy-PCL matjes daarentegen leidde degradatie echter tot significante veranderingen in de biomechanische eigenschappen. Bovendien ondergingen alle netjes blijvende plastische vervorming, een fenomeen dat eerder in verband is gebracht met het ontwikkelen van GRCs.

Verder werden de nieuwe implantaten ook gebruikt in preklinische *in vivo* experimenten . In eerste instantie werden de matjes gescreen op ratten waarna ze ook bij konijnen ingplant, dit omwille van hun grotere gestalte en intra-abdominale druk, wat de implantaten biomechanisch meer op de proef stelt. Tenslotte werden ze ook bij schapen gebruikt, waarop vaginale en abdominale chirurgie mogelijk is. Explantaten en natieve weefselmonsters die gepreleveerd werden aan de tegenoverliggende zijde van de buikwand, werden getest met behulp van uniaxiale trekproeven (ratten en konijnen) en wat grotere monsters met behulp van de zogenaamde “ball burst-test” (schapen). Uitkomstmaten waren compliantie en uitrekking. De primaire uitkomst bij de kleinere diermodellen was chirurgisch falen, zijnde het optreden van littekenbreuken. Biomechanische testen werd alleen uitgevoerd bij dieren zonder klinische littekenbreuken of GRCs.

Bij ratten met een primair overhecht defect, afgedekt met Upy-PCL, bleken de explantaten 7 en 42 dagen na de ingreep, complianter dan bij reconstructies met PP (Restorelle®). Restorelle®-explantaten en een natief weefsel herstel bleken stijver vergeleken met natief, niet geopereerd buikwandweefsel. UPy-PCL-abdominale explantaten hadden een compliantie in “range” van wat bij natief weefsel werd geobserveerd. Bij histologisch onderzoek werd in de Upy-PCL een zeer uitgesproken vreemd weefsel reactie vastgesteld.

De UPy-PCL en PP Restorelle®- implantaten werden ook gebruikt in een zogenaamd “gap-bridging”-ratten-model , daarbij simulerend wat bij een incisie-type hernia gebeurt . Ratten (7, 42 d na implantatie) en konijnen (iets langere implantatieperiode, zijnde 30 en 90 dagen) bleken toch littekenbreuken te vertonen bij één op de twee tot drie dieren. Omwille van dit hoge percentage mislukkingen, hebben we een alternatief implantaat gemaakt van PCL, met dikkere vezeldiameters of dikker opzelf, om extra materiaalsterkte te verschaffen. Dit was echter tevergeefs: het aantal litteenbreuken bleef hoog en bij de andere dieren waren de explantaten (zowel bij ratten als bij konijnen) initieel even compliant als natief weefsel. Later waren bij ratten de Upy-PCL explanten even compliant als natief weefsel, maar PP waren de stijver. Het is echter omwille van de de zwakke treksterkte, overeenkomend met het hoge aantal littekenbreuken dat we een ander polymeer gebruikt om nieuwe, hopelijks sterkere electrisch gesponnen matjes te maken. Daarvoor gebruikten we in eerste instantie het resorbeerbare polycarbonaat (PC) maar ook het *niet-resorbeerbare* polyurethaan (PU). Uiteindelijk testen we zowel het Upy-PC en PU om de achterste vaginawand te herstellen. Treksterkte, compliantie en GRCs werden gemeten 60 en 180 d na implantatie. Het referentiemateriaal was wederom de PP Restorelle-®mesh. Bij geen van de schapen waren er locale complicaties, en de vaginawand van schapen geïmplanteerd met zowel PU als Upy-PC elektrisch gesponnen netjes was even compliant als natief

weefsel. Restorelle® PP -explantaten waren aanvankelijk (60 d) iets stijver, maar na 180 dagen was de compliantie als die van natief weefsel.

Het trauma en de weefselveranderingen na vaginale geboorte draagt in belangrijke mate bij tot het ontstaan van POP. De nauwe anatomische relatie tussen de vaginawand aan de ene kant, en de blaas en het rectum aan de andere kant, heeft als gevolg dat functionele problemen in deze aangrenzende organen zich vaak samen voordien, zoals daar zijn urine-incontinentie, defecatieproblemen en seksuele disfunctie. Daarom waren we geinteresseerd wat de karakterisitieken zijn van de vaginawand en bekkenbodem bij schapen tijdens de zwangerschap, één jaar na vaginale bevalling in vergelijking met die van jonge “maagdelijke” schapen.

Verder werden correlaties tussen de mechanische parameters en histologische analyse van de weefsels gemaakt. Biomechanisch gebruikten we de zogenaamde Young's modulus, de treksterkte en “rek”, als voorheen. Anatomisch maten we de weefseldikte, het totaal collageen (%), het elastine (%) en gladde spier (%) vezels. Alle zachte weefsels van de bekkenbodem bleken ingrijpende histologische en mechanische veranderingen te ondergaan tijdens de zwangerschap, die niet helemaal blijken te herstellen één jaar na de bevalling. Significante regionale verschillen werden vastgesteld in de vagina, waarbij de proximale vagina stijver bleek dan de distale, ongeacht de reproductiestatus. De vagina van reeds bevallen schapen was complianter dan die bij maagdelijke schapen. Dit viel samen met een lager totaal collageen en hoger elastine en glad spierweefsel. In de zwangerschap was de vagina complianter dan bij “maagdelijk” schapen. Ook andere organene werden gemeten: in zwangerschap neemt de compliantie van de baarmoederhals af, terwijl de blaas en het rectum stijver worden. Blaas en rectum bleken ook meer totaal collageen, minder elastinevezels en minder gladde spiercellen te bevatten. Een jaar na de bevalling bleef de baarmoeder nog steeds complianter dan bij maagdelijke schapen. Er waren aanzienlijke verschillen in de Young's modulus in de comfort- en stresszones van de trekcurve. Opnieuw bleek dit overeen te komen met minder totaal collageen en meer elastinevezels. Het rectum en de blaas bleken stijver en hadden hoge treksterte. Histologisch kwam dat overeen met minder elastine vezels en gladde spiercellen, maar meer collageen, zoals te verwachten is bij een grotere stijfheid. De duidelijke correlatie tussen histologische kenmerken en mechanische eigenschappen is volgens ons vooral gemedieerd door het collageen en elastine gehalte.

De aldus verkregen resultaten lieten ons toe een realistisch materiaal model te creëren voor verdere simulaties, dat de niet lineaire respons van de weefsels over een langer trektraject kan bevatten. Een eenvoudige versie is het HGO-model (Holzapfel-Gasser-Ogden) waarbij het mechanisch gedrag van weefsels onder uniaxiale belasting wordt beschreven, met als constante parameters μ (afschuifmodulus, die functie is van het matrixgehalte), k_1 en k_2 (reflecteert de bijdrage van de weefselvezels). Voor het gemak definieerden we de dimensieloze verhouding ζ als een coëfficient die de matrix- en vezelbijdrage aan de observaties goed beschrijft. We noemden dit de Histologisch Gemotiveerde of Verantwoorde (HM)-coëfficiënt, die dus de weefselmorfologie en het niet-lineaire mechanische gedrag (treksterkte) beschrijft. De HM-coëfficiënt van de uniaxiale gegevens werd dan ook toegepast voor multiaxiale belastingssimulaties. Op die wijze voorspelden we bio-mechanische karakteristieken zoals door “ball burst testing”

gemeten. Aansluitend is een 3D-geometrisch model van de bekkenbodem van schapen gemaakt met behulp van MR-afbeeldingen. Dit kan nu verder worden gebruikt voor dynamische simulaties van de zachte weefsels van de bekkenbodemorganen, gebruik maken van hun HM-coëfficiënt.

Samenvattend heeft dit project enkele belangrijke zaken gerealiseerd. Ten eerste werden de biomechanische karakteristieken van nieuwe elektrisch gesponnen matjes onder verschillende omstandigheden *ex vivo* vergeleken met die van natief weefsel. *In vivo* blijken afbreekbare UPy-PC en niet afbreekbare PU elektrisch gesponnen matjes geen locale complicaties te veroorzaken, noch in ratten, konijnen of schapen. Beide matjes induceren in het explant een biomechanisch gedrag dat vergelijkbaar is dat van natief of eigen weefsel. Verder blijken de vaginale wanden en de bekkenorganen van de ooi belangrijke morfologische en biomechanische veranderingen te ondergaan tijdens de zwangerschap, die niet helemaal herstellen in het eerste een jaar na de bevalling. Verder konen we een parallel tussen de mechanische eigenschappen van de zachte weefsels en de histologische kenmerken vaststellen, en werd een zogenaamde histologische gemotiveerde coëfficiënt geïntroduceerd. Deze laat toe om vanuit de microscopische bevindingen de biomechanische eigenschappen te voorspellen. Deze kan gebruikt worden in complexe simulaties.

RESUMO

As disfunções do pavimento pélvico (DPP), incluindo o prolapso dos órgãos pélvicos, podem ter um impacto negativo significativo sobre as atividades diárias e a qualidade de vida de uma mulher. Foram propostas muitas técnicas cirúrgicas para a correção do prolapso vaginal, mas os seus benefícios a longo prazo ainda não foram devidamente avaliados. Atualmente as reconstruções anatómicas que envolvem somente os tecidos da paciente, são consideradas como insatisfatórias. Para as melhorar, os cirurgiões recorrem a intervenções que incluem redes de reforço (implantes). No entanto, a inserção por via vaginal da rede, tem sido associado a uma elevada taxa de complicações cirúrgicas. Aparentemente o implante ideal ainda não foi desenvolvido. Para fazê-lo, é necessário um bom conhecimento das propriedades mecânicas do tecido vaginal e do potencial implante. Tal conhecimento permitirá estabelecer a melhor correspondência possível entre as propriedades dos dois materiais.

A investigação aqui apresentada composta por três partes: duas experimentais (*in vitro* e *ex vivo*) e uma computacional (*in silico*). Na primeira parte, *in vitro*, são caracterizadas as propriedades mecânicas dos novos implantes produzidos por electrospinning através de ensaios mecânicos (Capítulos 2 e 3). Os implantes produzidos por electrospinning são uma abordagem recente para melhorar a eficácia das cirurgias em que se usam redes. Estes implantes tentam mimetizar a matriz extracelular, o que melhora a integração do implante no hospedeiro. Na segunda parte, *in vivo*, é avaliada a resposta do hospedeiro aos implantes produzidos por electrospinning, recorrendo a modelos animais representativos (ratos, coelhos e ovelhas) (Capítulo 4 e Artigo suplementar 1 e 2). Nesses estudos, foi usados um implante de polipropileno têxtil durável, sintético e leve como controle – o implante Restorelle ® da empresa Coloplast. Para documentar como os tecidos moles da parede vaginal e do pavimento pélvico recuperam um ano após o parto vaginal, foi efetuada uma análise biomecânica e histológica abrangente, realizada em tecidos moles do pavimento pélvico de ovelha (Capítulo 5, Capítulo 6). Finalmente, na terceira parte do trabalho, os dados experimentais obtidos nos capítulos anteriores, foram utilizados na criação de um modelo de comportamento material (constitutivo), adequado à criação de modelos *in silico*. Estes modelos destinam-se a simular as experiências *ex vivo* num ambiente *in silico* (Capítulo 7, Capítulo 8). Finalmente, usando imagens de ressonância magnética (MR) foi criado um modelo geométrico tridimensional da cavidade pélvica da ovelha (Capítulo 9) para posterior utilização em simulações *in silico.*

O comportamento mecânico de protótipos dos novos implantes produzidos por electrospinning, feitos a partir de polímeros supramoleculares de base Ureido-Pirimidinona (UPy) com estrutura de poli (ε-caprolactona) (PCL) com fibras de diferentes diâmetros (2.0, 2.3 e 2.6 μm), foram investigadas para diferentes condições. Para avaliar o seu desempenho mecânico, foram submetidos a um processo de degradação *in vitro* e a carregamentos cíclicos. Para esta parte do estudo, foi testada uma gama mais ampla de redes usadas em cirurgias de hérnia e correção de prolapso. Os resultados mostraram que os novos implantes produzidos por electrospinning tiveram um comportamento mecânico semelhante, apesar das diferenças no diâmetro da fibra. Apresentam maior "compliance"

do que a rede de PP Restorelle ®, usado como referência. Também se tornaram mais "compliance" quando molhados e revelaram um comportamento anisotrópico. Como esperado, o comportamento das redes de PP não foi influenciado pelo pH. No entanto, a degradação induziu mudanças significativas nas propriedades mecânica em todas as redes de UPy-PCL, bem como nas redes ensaiadas. Além disso, todas as redes sofreram deformação plástica permanente, que foi previamente identificada como uma potencial causa de complicações relacionadas com implantes.

Os novos implantes foram ainda utilizados em experiências pré-clínicas realizadas *in vivo*. A triagem inicial foi efetuada usando ratos e posteriormente foram usados coelhos, devido às suas maiores dimensões e pressão intra-abdominal. Os últimos serão um modelo mais representativo do ponto de vista biomecânico. Por fim, foram utilizadas ovelhas, que permitem a cirurgia vaginal e abdominal. Implantes removidos e amostras de tecidos nativos (retirados do lado oposto da parede abdominal) foram ensaiados usando testes de tração uniaxial (ratos e coelhos) e amostras maiores foram ensaiados por "*ball burst*" (ovelha). À partir destes ensaios foi calculado a rigidez e a deformação, obtidas a partir de curvas de carga e deslocamento. O resultado principal dos modelos animais pequenos foi a ocorrência de reherniação (considerada como falha cirúrgica). As amostras para ensaios biomecânicos adicionais, foram recolhidas apenas em animais sem reherniação clínica, e sem complicações relacionadas com implantes.

Os explantes de ratos implantados com redes UPy-PCL para reforço de defeitos da parede abdominal previamente suturados, colhidos entre os sete e 42 dias pós implantação, exibiram mais "compliance" do que os explantes reforçados com polipropileno (Restorelle®) e previamente suturados. Após 42 dias os explantes de reparação primária de Restorelle® e de tecido nativo tornaram-se mais rígidos quando compara com os a músculos da parede abdominal nativa não operada. Os explantes abdominais UPy-PCL eram tão "compliance" quanto o tecido nativo. Através da análise histológica foi observada uma vigorosa reação inflamatória.

Os implantes UPy-PCL e PP Restorelle® foram também usados num modelo de "*gap-bridging*", que se aproxima mais de uma hérnia incisional. Foram provocados grandes defeitos, através de toda a espessura da parede abdominal, e preenchidos com as redes, para diferentes períodos, em ratos (7 e 42 dias de implantação) e em coelhos com um período de implantação mais longo (30 e 90 dias). Com este modelo mais exigente, observaram-se altas taxas de herniação, ou seja, aproximadamente em um de cada três animais. Devido a esta elevada taxa de insucessos, foram produzidos por electrospinning implantes de PCL alternativos. Estes implantes tinham diâmetros de fibra superiores ou eram mais espessos, por forma a conferir uma robustez adicional ao implante. No entanto, este esforço foi em vão dado que as taxas de herniação permaneceram elevadas. Nos casos de sucesso, a "compliance" inicial dos explantes de UPy-PCL e PP da parede abdominal, era da mesma ordem de grandeza do tecido nativo, tanto para os ratos como para os coelhos. No entanto, para os ratos os explantes de PP tornaram-se mais rígidos do que os explantes de UPy-PCL e o tecido nativo, em etapas mais tardias. Mais uma vez este resultado ficou a dever-se à insuficiente resistência do implante, o que nós consideramos ser uma consequência do rápido processo de degradação. Considerámos por isso produzir implantes por electrospinning, baseados em outros polímeros cuja reabsorção fosse mais

lenta, por exemplo policarbonato (PC), e como uma estratégia alternativa, também foram considerados implantes produzidos com polímeros não-reabsorvíveis como o poliuretano. Com estes novos implantes, o modelo usado foi a ovelha, procedendo-se ao reforço da parede posterior da vagina, sendo os resultados avaliados ao fim de 60 e 180 dias. O material usado como referência foi novamente a rede PP Restorelle®. Para além deste material, foram também usadas redes de poliuretano (PU) não-absorvível e em policarbonato modificado com Ureido-Pirimidina (UPy-PC), produzidas por electrospinning. Nenhuma das ovelhas apresentou complicações na sequência do implante vaginal. Assim, todos os explantes vaginais puderam ser usados para realizar ensaios mecânicos. As redes produzidas por electrospinning (PU e UPy-PC) revelaram-se tão complacentes como o tecido nativo após os dois períodos de implantação considerados. Os explantes de Restorelle® PP eram mais duros que o tecido nativo após 60 dias de implantação, mas aos 180 dias os explantes estavam novamente em conformidade com o tecido nativo.

O trauma induzido pelo parto vaginal tem um papel importante no aparecimento do prolapso. A íntima relação anatómica entre a parede vaginal, por um lado, e a bexiga e o reto, por outro lado, contribuem frequentemente para o desenvolvimento simultâneo de problemas funcionais nesses órgãos adjacentes, levando à incontinência urinária, problemas defecatórios e disfunção sexual. Esta parte da investigação inclui a observação de como os tecidos moles da parede vaginal e do pavimento pélvico são modificados durante a gravidez, e de como recuperam um ano após o parto vaginal, quando comparados com os resultados obtidos em ovelhas virgens.

A correlação entre as propriedades mecânicas e a análise histológica foi estudada. As propriedades mecânicas consideradas foram o módulo de Young, a tensão de rutura e a elongação, diretamente obtidas a partir das curvas de tensão-deformação. Para além da análise histológica, foram medidas a espessura do tecido, o conteúdo total de colagénio (%), de elastina (%) e de músculo liso (%). Todos os tecidos moles do pavimento pélvico sofrem profundas alterações histológicas e mecânicas, particularmente durante a gravidez e não recuperam para os níveis originais um ano após o parto vaginal. Foram identificadas diferenças regionais significativas na parede vaginal ovina. A vagina proximal era mais rígida que a distal, independentemente do status reprodutivo. A vagina da ovelha grávida era mais "compliance" do que a vagina de ovelhas com parto ou virgens, coincidindo com menor quantidade de colagénio total e maiores níveis de elastina e uma maior quantidade de células musculares lisas. No entanto, o tecido vaginal das ovelhas com parto foi menos complacente do que o das virgens. O colo do útero em ovelhas grávidas era mais complacente do que o de ovelhas virgens ou com parto. Em contraste, a bexiga e o reto ficam um pouco mais rígidos. A bexiga e o reto continham mais colagénio (total), menos fibras de elastina e menos células musculares lisas. Um ano após o parto vaginal, o útero foi mais complacente do que nas ovelhas virgens. Os módulos de Young nas zonas de conforto e de stresse diferiram significativamente. Comparado com o das ovelhas virgens, o útero das ovelhas com parto contem menos colagénio total e mais fibras de elastina. O reto e a bexiga apresentaram uma tensão de rotura mais elevada, as fibras de elastina e a contagem de células musculares lisas foram significativamente menores nesses tecidos,

mas o conteúdo total de colagénio foi maior, o que é coerente com a redução de "compliance" observada.

Dada a óbvia correlação entre as características histológicas e as propriedades mecânicas observada nos tecidos moles do pavimento pélvico testados, é possível concluir que para estes tecidos o colagénio é largamente responsável pela resistência à tração e a elastina pela elasticidade do tecido. Os resultados obtidos pela análise dos espécimes vaginais colhidos de ovelhas foram usados na criação de um modelo material realista a ser usado em outras simulações. Neste estudo foi proposta uma estratégia para correlacionar resultados experimentais de ensaios de tração com um modelo de material capaz de capturar a resposta não linear num grande intervalo de tensão. Uma versão simplificada do modelo HGO (Holzapfel-Gasser-Ogden) foi usada para descrever o comportamento mecânico de amostras sob carga uniaxial, os parâmetros do modelo, μ (módulo de cisalhamento, relacionado com o conteúdo da matriz do tecido), k_1 e k_2 (refletem a contribuição das fibras) definem a resposta mecânica. Por conveniência, definimos a razão adimensional ξ como um regulador adequado para as contribuições de matriz e fibra. Chamamos-lhe coeficiente Histologicamente-Motivado (HM), pois correlaciona-se significativamente com os dados histológicos, ligando o comportamento mecânico não linear (ensaios de tração) com a morfologia do tecido (histologia). O coeficiente HM foi aplicado em simulações aplicadas a estados de tensão multiaxiais, em modelos de tecido vaginal. As propriedades mecânicas de tecidos cujas, amostras foram testadas por "*ball burst*" foram previstas através de histologia básica, sem medições mecânicas diretas para essas condições de carga. Um modelo geométrico 3D da cavidade do pavimento pélvico ovino foi criado, usando imagens ressonância magnética e pode agora ser usado para futuras simulações dinâmicas dos tecidos moles do pavimento pélvico, aplicando o coeficiente HM para os tecidos moles.

Em conclusão, este projeto permitiu várias observações importantes. Em primeiro lugar, o comportamento mecânico das novas redes produzidas por electrospinning, sob diferentes condições, foi comparável ao dos tecidos nativos, em termos de conformidade e anisotropia. *In vivo*, tanto as redes biodegradáveis UPy-PC como as redes não-degradáveis de PU produzidas por electrospinning não causaram complicações relacionadas com o implante após a sua aplicação na reconstrução vaginal em ovelhas. Ambas induzem um comportamento biomecânico comparável ao do tecido nativo. Os tecidos moles da parede vaginal e do pavimento pélvico sofrem alterações histológicas e mecânicas significativas durante a gravidez e não recuperam os níveis originais um ano pós-parto. Foi estabelecido um paralelismo entre propriedades mecânicas dos tecidos moles e características histológicas. Por último, apresenta-se um coeficiente Histologicamente-Motivado que pode ser muito promissor para estimar as propriedades mecânicas do tecido *através da* informação histológica. O coeficiente de HM reflete o estado fisiopatológico dos tecidos moles e, portanto, pode ser usado em ambientes complexos de simulação.

CURRICULUM VITAE

PERSONAL INFORMATION

Name: Rita Rynkevic

Address: Rua de Ramos 955- 2 dto, 4410-246, Vila Nova de Gaia, Portugal

Email: r.rynkevic@gmail.com

Date and place of Birth: 23/06/1987, Neustrelitz, Germany

Nationality: Lithuanian, Russian

EDUCATION AND TRAINING

09/2006–06/2010
Bachelor Degree in Biomechanics, VGTU (Vilnius Gediminas Technical University), Vilnius (Lithuania)
Dissertation title: Design of a bar for the manufacture of orthopedic inserts

09/2010–10/2012
Master Degree in Computing and Medical Instrumentation Engineering, ISEP (Instituto Superior de Engenharia do Porto), Porto (Portugal)
Dissertation title: Biomechanical Modeling and Simulation of Spider Crab

01/2013–Present
Doctoral Program in Occupational Safety and Health, FEUP (Faculdade de Engenharia da Universidade do Porto), Porto (Portugal)
Dissertation title: In vivo models and in silico simulations of mesh augmented prolapse repair

05/2014–Present
Doctoral Programme generic Track, Biomedical Science, KU Leuven, Leuven (Belgium)
Dissertation title: In vivo models and in silico simulations of mesh augmented prolapse repair

02/2012–03/2012
Intensive program in Energy development, ISEP (Instituto Superior de Engenharia do Porto), Porto (Portugal)

WORK EXPERIENCE

04/2009–09/2010
Engineer, "Ortopedijos Technika"L. Asanavičiūtės g. 27a, LT — 04318 Vilnius (Lithuania) http://www.ortopedija.lt.
Individual manufacturing of orthopedic inserts, breast prostheses. Prosthesis, orthesis, and rehabilitation technique production.

01/2012-01/2014
Trainee, INESC TEC, Campus da FEUP, Porto (Portugal)
ROBIS project

03/2013–06/2013
Reseacher, DMEC-Polo FEUP, Porto (Portugal).
Investigation project: "Bio-computational study of tinnitus, PTDC/SAUBEB/ 104992/2008"

11/2012–12/2014
Reseacher, DMEC-Polo FEUPCampus da FEUP, Rua Dr. Roberto Frias, 404, Porto (Portugal).
Modelling, simulations and analysis using Finite Element Method

01/2015–Present
Researcher INEGI, Porto (Portugal)

ADDITIONAL INFORMATION ON EDUCATION:

2015- Course on Laboratory Animal Science for persons that carry out experiments or take part in them, KU Leuven, Belgium

2015- Scientific paper writing, KU Leuven, Belgium

LANGUAGE SKILLS:

Russian, English, Lithuanian, Portuguese, Belorussia

THESIS RELATED PUBLICATION ACTIVITY

1. Rynkevic R, Martins P, Hympanova L, Almeida H, Fernandes AA, Deprest J., "Biomechanical and morphological properties of the multiparous ovine vagina and effect of subsequent pregnancy" *J Biomech*., vol. 57, pp. 94-102, 2017.

2. Rynkevic R, Martins P, Pereira F., Ramião N, and Fernandes AA, "*In vitro* study of the mechanical performance of hernia mesh under cyclic loading" *Journal of Materials Science: Materials in Medicine*, vol. 28 (11), 2017.

3. Cunha M, Hympanova L, Rynkevic R, Gallelo M, Wach R, Olejnik A, Mes T, Bosman A, Vange J, Callewaert G, Deprest J, "Ureidopyrimidinone-polycaprolactone electrospun MESH reinforce rabbit abdominal wall incisional hernia maintains physiological compliance" *European Journal of Obstetrics & Gynecology and Reproductive Biology*, vol. 211 (232), 2017.

4. Hympanova L, Cunha M, Rynkevic R, Zündel M, Gallego M, Vange J, Callewaert G, Urbankova I, Van der Aa F, Mazza E, Deprest J, "Physiologic musculofascial compliance following reinforcement with electrospun polycaprolactone-ureidopyrimidinone mesh in a rat model" *J Mech Behav Biomed Mater*., vol. 27 (74), pp. 349-357, 2017.

5. Hympánová L**,** Rynkevic R, Román S, Mori da Cunha MGMC, Mazza E, Zündel M, Urbánková I, Gallego MR, Vange J, Callewaert G, Chapple C, MacNeil S, Deprest J. "Assessment of Electrospun and Ultra-lightweight Polypropylene Meshes in the Sheep Model for Vaginal Surgery", *Eur Urol Focus*. 2018.

6. Hympanova L, Mori da Cunha MGMC, Rynkevic R, Wach RA, Olejnik A, Dankers P, Arts B, Mes T, Bosman A, Albersen M, Deprest J, "Experimental reconstruction of an abdominal wall defect with electrospun polycaprolactoneureidopyrimidinone mesh conserves compliance yet may have insufficient strength" *J Mech Behav Biomed Mater*., 2018.

7. Rynkevic R, Ferreira J, Martins P, Parente M, Fernandes AA, "Linking hyperelastic theoretical models and experimental data of vaginal tissue through histological data" *Journal of Biomechanics*, vol. 82, 271-279, 2019.

8. Rynkevic R, Martins P, Parente M, Andre D, Mascarenhas T, Fernandes AA, "The effect of consecutive pregnancies on the ovine pelvic soft tissues: link between biomechanical and histological components" *Annals of Anatomy*, vol. 222, 166-172, 2018.

9. Rynkevic R, Martins P, Joyeux L, Engels A, Almeida H, Fernandes AA, Deprest J, "Microstructural Vaginal Tissue Transformations In Virgin, Pregnant And Postpartum Ewes" *Neurourology and Urodynamics*, vol. 35, nº 3, pp. 150-152, 2016.

10. Rynkevic R, Martins, Mascarenhas T, Fernandes AA, Deprest J, "Pregnancy induced changes of pelvic floor soft tissues: the relationship between biomechanical and histological parameters" *Neurourology and Urodynamics*, vol.36, 546-548, 2017.

OTHER PUBLICATIONS

1. Rynkevic R, Silva M, Marques A, "Biomechanical modeling and simulation of the spider crab (maja brachydactyla)" *IEEE*, 2013. DOI: 10.1109/ENBENG.2013.6518429.

2. Rynkevic R, Martins P, Parente M, Natal R, Barros M, Santos D, "Implant shape influence on the mechanical behavior of breast implants. Application to PIP implants" *IEEE* 2013. DOI: 10.1109/ENBENG.2013.6518409.

3. Rynkevic R, Silva M, Marques A, "Biomechanical Study of the Spider Crab as Inspiration for the Development of a Biomimetic Robot" *Biomaterials and Biomechanics in Bioengineering* 2 (4), pp.249-269, 2015.

4. Ramião N, Martins P, Rynkevic R, Fernandes A, Barroso M, Santos D, "Biomechanical properties of breast tissue, a state-of-the-art review" *Biomech Model Mechanobiol*, vol. 15(5),1307-23, 2016.

5. Engels A, Bauters D, Rynkevic R, Pranpanus S, Richter J, van Mieghem T, Hoylaerts MF, Deprest J, "Thrombin Generation by Fetoscopic Trauma to the Fetal Membranes: An in vivo and in vitro Study" *Fetal Diagn Ther*.: vol. 39(4), 261-8, 2016.

6. Urbankova I, Vdoviakova K, Rynkevic R, Sindhwani N, Deprest D, Feola A, Herijgers P, Krofta L, Deprest J, "Comparative Anatomy of the Ovine and Female Pelvis" *Gynecol Obstet Invest.*, 2017.

7. Urbankova I, Sindhwani N, Callewaert G, Turri A, Rynkevic R, Hympanova L, Feola A, Deprest J, "*In vivo* documentation of shape and position changes of MRI-visible mesh placed in t rectovaginal septum" *J Mech Behav Biomed Mater*, vol. (75), 379 –389, 2017.

8. Eastwood MP, Daamen WF, Joyeux L, Pranpanus S, Rynkevic R, Hympanova L, Pot MW, Hof DJ, Gayan-Ramirez G, van Kuppevelt TH, Verbeken E, Deprest J, "Providing Direction Improves Function: Comparison of a Radial Pore Orientated Acellular Collagen Scaffold to Clinic Alternatives in a Surgically Induced Rabbit Diaphragmatic Tissue Defect Model" *J Tissue Eng Regen Med*. 2018.

9. Hympanova L, Mori da Cunha MGMC, Rynkevic R, Zündel M, Gallego MR, Vange J, Callewaert G, Urbankova I, Van der Aa F, Mazza E, Deprest J, "Morphological and Functional Changes in the Vagina following Critical Lifespan Events in the Ewe" *Gynecol Obstet Invest*. vol. 11, 1-9, 2019.

10. Mori da Cunha MGMC, Hympanova L, Rynkevic R, Mes T, Bosman AW, Deprest J., "Biomechanical Behaviour and Biocompatibility of Ureidopyrimidinone-Polycarbonate Electrospun and Polypropylene Meshes in a Hernia Repair in Rabbits" *Materials (Basel)*. 2019 Apr 10;12(7).

THESIS RELATED CONFERENCES AND PRESENTATIONS

1. Rynkevic R, Martins P, Parente M, Fernandes AA, "Application of in silico models instead of in vivo models in a pelvic organ prolapse studies" *Mechanical Engineering Conference (CEM 2016)*, Porto, Portugal, 1-3 of June 2016.

2. Rynkevic R, Martins P, Hympanova L, Fernandes AA, Deprest J, "Virgin ovine vaginal tissue biomechanical properties and regional differences" *Internacional Urogynecology annual meeting (IUGA)*, Cape Town, South Africa, August 2016.

3. Hympanova L, Cunha M, Rynkevic R, Gallelo M, Wach R, Olejnik A, Mes T, Bosman A, Vange J, Callewaert G, Deprest J, "Physiologic compliance of rat abdominal wall incisional hernia reinforced with electrospun ureidopyrimidone mesh" *41 Internacional Urogynecology annual meeting*, Cape Town, South Africa, 2-6 August, 2016.

4. Rynkevic R, Hympanova L, Cunha M, Gallelo M, Wach R, Olejnik A, Mes T, Bosman A, Vange J, Callewaert G, Deprest J, "The effect of cyclic loading on the mechanical performance of novel electrospun meshes for pelvic organ prolapse repair" *9th EUGA Annual Congress*, Amsterdam, Netherlands, November 2016.

5. Rynkevic R, Martins P, Ramião N, Fernandes AA, "Mechanical performance of meshes used in hernia surgery following in-vitro degradation test*" 7º Congresso Nacional de Biomecânica (CNB2017)*, Guimarães, Portugal., 10-11 of February 2017.

6. Rynkevic R, Martins P, Fernandes AA, "In-vitro degradation test and effect of freezing on mechanical performance of meshes used in hernia surgery" *Second Doctoral Congress Engineering (DCE2017)*, Porto, Portugal., 8th-9th of June 2017.

7. Rynkevic R, Martins P, Fernandes AA, Deprest J, "Effect of multiple deliveries on biomechanical properties of pelvic organ tissues.," *42 International Urogynecology annual meeting (IUGA2017)*, Vancouver, Canada., 20-24 of June 2017.

8. Hympanova L, Cunha M, Rynkevic R, Zündel M, Gallego M, Vange J, Callewaert G, Urbankova I, Van der Aa F, Zaccaria S, Deprest J, "Comparable vaginal wall biomechanical properties following electrospun polycarbonate- ureidopyrimidone mesh implantation and simulated native tissue repair in sheep" *42 Internacional Urogynecology annual meeting*, Vancouver, Canada, June, 2017.

9. Cunha M, Hympanova L, Rynkevic R, Gallelo M, Wach R, Olejnik A, Mes T, Bosman A, Vange J, Callewaert G, Deprest J, "C-rgd bioactivation moderates the inflammatory response to upy-polucarbonate e-spun mesh in rat" *42 Internacional Urogynecology annual meeting (IUGA)*, Vancouver, Canada, June, 2017.

10. Rynkevic R, Martins P, Fernandes AA, Mascarenhas T, "Pregnancy induced changes of pelvic floor soft tissues: the relationship between biomechanical and histological parameters" *ICS Annual Meeting*, Florence, Italy, 2017.

11. Rynkevic R, Martins P, Ferreira J, Parente M, Mascarenhas T, Fernadess AA, "Accurate in silico simulation of the ovine bladder based on mechanical and histological data" *V MIPS Annual Meeting at Rome*, Italy, May 2018.

12. Rynkevic R, Martins P, Ferreira J, Parente M, Mascarenhas T, Fernadess AA, "A histological basis for the nonlinear behavior of pelvic tissues" *43 Internacional Urogynecology annual meeting (IUGA)*, Viena, Austria, June, 2018.

13. Rynkevic R, Martins P, Ferreira J, Parente M, Mascarenhas T, Fernadess AA, "Simulations of vaginal tissue: application of histologically motivated coefficient to multiaxail loading conditions" *V MIPS Annual Meeting at Barcelona*, Spain, April 2019.

OTHER CONFERENCES AND PRESENTATIONS

1. Rynkevic R, Silva M, Marques A, "Simulation and Control of a Spider Crab Biomechanical Model" *International Association of Science and Technology for Development (IASTED) MIC*, Innsbruck, Austria, February 2013. DOI: 10.2316/P.2013.794-029.

2. Rynkevic R, Silva M, Marques A, "Biomechanical modeling and simulation of the spider crab (maja brachydactyla)" *Bioengineering (ENBENG), 2013 IEEE 3rd Portuguese Meeting in Bioengineering*, Braga, Portugal, February, 2013. DOI: 10.1109/ENBENG.2013.6518429.

3. Rynkevic R, Martins P, Parente M, Natal R, Barros M, Santos D, "Implant shape influence on the mechanical behavior of breast implants. Application to PIP implants" *Bioengineering (ENBENG), 2013 IEEE 3rd Portuguese Meeting in Bioengineering*, Braga, Portugal, February 2013. DOI: 10.1109/ENBENG.2013.6518409.

4. Rynkevic R, Martins P, Parente M, Natal R, Barros M, Santos D, "Mechanical Behaviour of the PIP Breast Implants Under Compression" *Congresso Nacional de Biomecânica, (CNB)*, Espinho, Portugal, 2013.

5. Rynkevic R, Martins P, Parente M, Natal R, Barros M, Santos D, "Mechanical behaviour of the breast implants using hyperelastic material models" *Congress on Numerical Methods in Engineering*, Bilbao, Spain, June, 2013.

6. Rynkevic R, Martins P, Parente M, Natal R, Barros M, Santos D, "Mechanical behaviour of the pip breast implant during a static compression test" *6th Portuguese Congress on Biomechanics*, Monte Real, Leiria, Portugal, 2015.

AWARDS AND ACHIEVEMENTS

Awarded the Abstract Winner Award at the *V MIPS Annual Meeting at Rome*, May 2018.

Rynkevic R, Martins P, Ferreira J, Parente M, Mascarenhas T, Fernandes AA "*Accurate in silico simulation of the ovine bladder based on mechanical and histological data"*.

PERSONAL ACKNOWLEDGEMENT

This thesis is respectfully presented to the University of Leuven through its Rector, Prof. Luc Sels, to the Faculty of Medicine through its dean Prof. Paul Herijgers and to the University of Porto through its Rector Prof. Antonio Sousa Pereira, to the Faculty of Engineering of the University of Porto through its Dean Prof. João Falcão e Cunha.

I would like to thank the jury members Prof. Frank Van der Aa, Prof. Hans Van Oosterwyck, Prof. Renato Natal Jorge, Prof. Julius Griškevičius, Prof. Ladislav Krofta and Dr. Baptiste Pierrat for spending some of their precious time reading and amending this manuscript.

I am very grateful to my promoter in KU Leuven Prof. Dr. Jan Deprest, who taught me a lot. Thank you for your patience, for your advices, for your time and for teaching me. Thanks to my promoter in University of Porto Prof. Antonio Augusto Fernandes, for his support in all beginnings, for advises, for guidance and understanding. I am very grateful to my co-promoter in Portugal Prof. Pedro Martins, for the continuous support, spent endless hours during manuscript writing and for his lessons. I appreciate your advises; our scientific discussions and personal talks supported me during PhD. I would like to thank Prof. Marco Parente for his patience and time. Thanks to Prof. Nele Famaey for her remarks and ideas.

I also want to thank my colleagues form KULeuven and Porto University, my relatives and friends all over the world, who were helping me, were supporting me and wishing me luck during PhD.

Special words I would like to tell my family, for their support in this life stage. I would like to dedicate this manuscript to them. To my baby-boys Zacarias and Isaac, who changed me for the better, who forced me to improve and keep up with everything. To my husband Marlon, who traveled with me, supported me in everything and were always listening. To my parents for their precious advises, limitless support, understanding and patience; and for giving me this opportunity to study where I wanted.

Sincerely,

Rita

Personal contribution: Personal contribution is identified in each chapter. I designed the study experiments under the supervision of my promoters Prof. Jan Deprest and Prof. Antonio Augusto Fernandes and co-promoter Dr. Pedro Martins. The majority of experiments was carried out and evaluated by myself, with the collaboration of the research fellows quoted as co-authors in the chapters and laboratory technicians. I have written all the manuscripts included in the thesis as well as the introduction and discussion. My promoters, co-promoters and co-authors edited the manuscript and individual chapters.

Scientific acknowledgment: Scientific acknowledgments are stated in each chapter.

Conflict of interest: Conflicts of interest are quoted for each chapter. Funding agencies did not interfere with study designs, data collection or data interpretation. All contracts were handled by the transfer office of the KU Leuven.